CONTROL AND SAFETY OF FULLY ACTUATED AND UNDERACTUATED NONLINEAR SYSTEMS: FROM ADAPTATION TO ROBUSTNESS TO OPTIMALITY

A Dissertation
Presented to
The Academic Faculty

By

Vahid Azimi

In Partial Fulfillment
of the Requirements for the Degree
Doctor of Philosophy in the
School of Electrical and Computer Engineering

Georgia Institute of Technology

May 2020

CONTROL AND SAFETY OF FULLY ACTUATED AND UNDERACTUATED NONLINEAR SYSTEMS: FROM ADAPTATION TO ROBUSTNESS TO OPTIMALITY

Approved by:

Dr. Seth Hutchinson, Advisor
School of Interactive Computing
Georgia Institute of Technology

Dr. Erik Verriest
School of Electrical and Computer Engineering
Georgia Institute of Technology

Dr. Fumin Zhang
School of Electrical and Computer Engineering
Georgia Institute of Technology

Dr. Chaouki T. Abdallah
School of Electrical and Computer Engineering
Georgia Institute of Technology

Dr. Panagiotis Tsiotras
School of Aerospace Engineering
Georgia Institute of Technology

Date Approved: April 06, 2020

The world is a mountain, in which your words are echoed back to you

Rumi

To my parents.

ACKNOWLEDGEMENTS

Foremost, I would like to express my sincere gratitude to my advisor Prof. Seth Hutchinson for the continuous support of my Ph.D. study and related research, for his patience, motivation, and immense knowledge. His guidance helped me in all the time of research and writing of this dissertation. I could not have imagined having a better advisor and mentor for my Ph.D. study.

Besides my advisor, I would like to thank the rest of my dissertation committee members: Prof. Chaouki Abdallah, Prof. Panagiotis Tsiotras, Prof. Erik Verriest, and Prof. Fumin Zhang for their insightful comments and encouragement, but also for the hard question which incented me to widen my research from various perspectives.

I am indebted to my former advisor Prof. Dan Simon for his continued support and encouragement. He convincingly guided and encouraged me to be professional and do the right thing even when the road got tough. Without his persistent help, the goal of obtaining my Ph.D. would not have been realized. Many thanks also to Prof. Daniel Munther and Prof. Alenka Zajic for their support, encouragement, and supervisory roles towards my career goals. My thanks also go to Prof. Aaron Ames, who provided me an opportunity to join his laboratory as a Visiting Student. I am grateful to Prof. Mark Spong and Prof. Girish Chowdhary for enlightening me at the first glance of this research.

I would also like to thank my current and past fellow labmates, peers, and friends for many interesting adventures and discussions we have had together. Last but not the least, I would like to thank my entire family for their constant support and unconditional love.

TABLE OF CONTENTS

LIST OF TABLES

LIST OF FIGURES

LIST OF ACRONYMS

ACC	Adaptive cruise control
AG	Asymptotic gain
AMI	Approximate model inversion
BGF	Bounded-gain forgetting
CARE	Continuous algebraic Riccati equation
CB	Control bound
CBF	Control barrier function
CL	Concurrent learning
CLF	Control Lyapunov function
DoA	Degrees of actuation
DoF	Degrees of freedom
eCBF	Exponential control barrier function
eCLF	Exponential control Lyapunov function
eDE	Exponential disturbance-to-error
eDES	Exponential disturbance-to-error stable
eDES-LF	Exponential disturbance-to-error stable-Lyapunov function
eDSSs-ZCBF	Exponential disturbance-to-state safe zeroing control barrier function
eISS	Exponential input-to-state stable
eISS-LF	Exponential input-to-state stable-Lyapunov function
eISSs-ZCBF	Exponential input-to-state safe zeroing control barrier function
EoM	Equations of motion
eTVRZCBF	Exponential time-varying robust zeroing control barrier function
eZCBF	Exponential zeroing control barrier function
FCL	Filtering-based concurrent learning
FL	Feedback linearization
IRCLF	Intelligent robust control Lyapunov function
KF	Kalman filter
LK	Lane keeping
LS	Least-squares
MIMO	Multi-input multi-output
MRAC	Model reference adaptive control
NN	Neural network
NNCL	Neural network concurrent learning
OFPS	Optimal fixed-point smoother

PE	Persistent excitation
PEB	Prediction error-based
PRR	Prismatic-revolute-revolute
PWMNC ..	Pointwise min-norm control
QP	Quadratic program
QP-ARCLF	Quadratic program-adaptive robust control Lyapunov function
QPARCLBF	Quadratic program-adaptive robust control Lyapunov-control barrier function
QP-CLBF ..	Quadratic program-based control Lyapunov-control barrier function
QSE	Quasi-static equilibrium
RBFNN ...	Radial basis function neural network
RCBF	Robust control barrier function
RCLF	Robust control Lyapunov function
RMSE	Root mean square error
SHL	Single hidden layer
SISO	Single-input single-output
TEB	Tracking-error based
TVRCBF ..	Time-varying robust control barrier function
TVRCLF ..	Time-varying robust control Lyapunov function
UUB	Uniform ultimate boundedness
ZCBF	Zeroing control barrier function
ZS	Zero stable

SUMMARY

The state-of-the-art quadratic program-based control Lyapunov-control barrier function (QP-CLBF) is a powerful control approach to balance safety and stability in a pointwise optimal fashion. However, under this approach, modeling inaccuracies may degrade the performance of closed-loop systems and cause violation of safety-critical constraints. This thesis extends the recently-developed QP-CLBF through the derivation of five novel robust quadratic program-based adaptive control approaches for fully actuated and underactuated nonlinear systems with a view toward adapting to unknown parameters, being robust to unmodeled dynamics and disturbances, ensuring the system remains in safe sets, and being optimal with respect in a pointwise fashion. The proposed control strategies are formulated for five different problems: (i) control of fully actuated nonlinear systems with structured uncertainties, (ii) control and safety of fully actuated nonlinear systems with unstructured uncertainties, (iii) active space control of underactuated systems, (iv) passive space control and safety of underactuated systems, and (iv) exponential control and safety of fully actuated nonlinear systems with parametric uncertainties and unknown control coefficient.

To achieve the above-mentioned goals, we begin by developing adaptation mechanisms, incorporated in the inner layer of the control structure, to estimate unknown nonlinear dynamics. The adaptive laws use historical data concurrently with instantaneous data to achieve an accurate estimation. A robust term robustifies closed-loop systems to disturbances and uncanceled uncertainties. A three-term control law, including feed-forward, adaptive, and stabilizing terms, is suggested whose latter term is generated in a pointwise optimal fashion by synthesizing a quadratic program (QP) in the outer layer, subject to three inequality constraints: a robust control Lyapunov function (RCLF), a robust control barrier function (RCLF), and control bounds. The unified two-layer control techniques can significantly improve control objectives and safety performance over the baseline QP-CLBF when applying to all above-mentioned problems. The boundedness / convergence of all system signals is proven using Lyapunov stability arguments. The performance of proposed control schemes are validated on different fully actuated and underactuated nonlinear

systems in each problem.

Simulation and quantitative results demonstrate the superiority of proposed approaches over the baseline methods. These benefits are five-folds: (i) accurate estimation of unknown nonlinear dynamics, (ii) convergence of error trajectories to a smaller neighborhood of the origin, (iii) converge of the barrier violation to a smaller neighborhood of the origin, (iv) formal stability analysis of closed-loop systems showing boundedness / convergence, and (v) establishment of robustness to modeling error, unmodeled dynamics, and time-varying disturbances.

CHAPTER 1

INTRODUCTION AND LITERATURE SURVEY

In this section, the notion of quadratic program-based control Lyapunov function (QP-CLF), history of different adaptive control approaches, and safety using control barrier functions (CBFs) are studied. The advantages and related limitations to these methods are then highlighted.

1.1 Stabilization using control Lyapunov functions (CLFs)

Lyapunov stability analysis is a widely-used tool for assessing stabilization of closed-loop systems. In particular, control synthesis using Lyapunov theory leads to the creation of CLFs for stabilizing nonlinear control systems [1, 2]. CLFs are an effective online strategy when incorporating QP as part of the control synthesis step, resulting in QP-CLF control design [3, 4]. QP is a powerful optimization tool for balancing multiple control specifications at the same time. Thus, joint use of a CLF approach with a QP leads to a pointwise optimal controller with the desired control Lyapunov properties. The QP-CLF method provides good trade-off between control optimality, stabilization performance, and other physical constraints. In the recent years, QP-CLF controllers have been widely applied on different applications to find an optimal solution between system stability and control optimality [5, 4].

In [6, 7], a pointwise optimal control strategy combining CLF and QP with impedance control was presented for a bipedal robot platform in simulation and a prosthesis device walking in experiment. As the general design procedure of QP-CLF controllers, by defining tracking error $e = y - y^d$ with actual y and desired y^d outputs, the system dynamics are first transformed into the error dynamics. By utilizing a general feedback linearization controller, error dynamics are linearized by a main control signal u, which is a function of virtual control input μ and model information. Then, by employing a QP, the virtual control input as a pointwise local optimal control input is computed. In [6, 7], however, due to the lack of model information, instead of substituting

μ into u, μ was directly considered as u. In other words, QP only focused on the tracking error while not caring about the model information. This strategy was called "model-free QP-CLF".

However, some works were designed with the assumption of perfect knowledge about system dynamics. In [8, 3], a QP has been used as a pointwise optimal control synthesis method for minimizing control effort while establishing system stability through a CLF approach. In those papers, linear error dynamics were first created using an input-output feedback linearization approach. Then, the convex optimization problem QP was employed to compute the virtual input while a set of inequality constraints were enforced. The CLF and bounds on the control signals were considered as the constraints. Above-mentioned QP-CLF approaches suffer from several shortcomings. (i) They are designed in a model-ignoring manner or with the assumption of fully-known system dynamics. It implies that model uncertainty is not considered in the stability analysis. (ii) They are not robust against unmodeled dynamics and external disturbances. These shortcomings deliver QP-CLF controllers that provide convergence of error trajectories to a neighborhood of the origin whose size is a function of uncompensated modeling errors.

In order to solve the aforementioned issues, baseline QP-CLF controller was modified under parameter uncertainty in some recent works [9, 10]. In [9], a unified QP-CLF controller and least-squares (LS) estimation was presented under parameter uncertainty for achieving exponential convergence of fully-actuated nonlinear systems. That paper suffers from several drawbacks. The main one is that the controller requires system acceleration and inversion of the mass matrix. The LS estimation also needs an inversion, which causes the singularity issue and computational cost. The approach is not also robust against the external disturbances and unmodeled dynamics. In [10], parameter to state stability of CLF approach was presented for underactuated robots. In that paper, the parameter uncertainty was only measured to quantify the affect of it on the performance of system while no any estimation method was used to identify the unknown dynamics.

Since it is often that the mathematical model of a system is a simplified version of the real system, system dynamics are not fully known and the approximated description contains model uncertainties. On the other hand, with the aim of having a formal stability analysis and using the model information in the controller structure, a model-based controller is desired to design. Under these circumstances, an adaptive controller should be employed to estimate the missing dynamical information.

1.2 Adaptive control approaches

Adaptive controllers can solve this problem by providing estimates of system dynamics for use in QP-CLF. Adaptive control is able to implement learning and adaptation using an online parameter estimation in the control structure. Various instantaneous data-based adaptive controllers such as tracking-error based (TEB) and tracking error-based / prediction error-based (TEB/PEB) exist to estimate the unknown system dynamics [11, 12, 13, 14].

The direct adaptive controller is one of the most widely-used adaptive approaches whose adaptation mechanism only uses instantaneous tracking error. In [15], a direct adaptive controller was proposed for a manipulator in which parameter adaptation is derived by motion tracking error. The controller presented in that paper has two parts. The first part is responsible for full dynamic compensation and attempts to provide the joint dynamic torques necessary to make the desired motions. The second part is simply a PD feedback. In [11], a robust adaptive sliding mode controller was designed for nonlinear systems. The control law developed in that paper includes two parts. The first part is an adaptive term to handle uncertain parameters. For the adaptive term, a TEB adaptation law was used which extracts information about the parameters from only the tracking error. A boundary layer trajectory was incorporated in the adaptation mechanism to prevent unfavorable parameter drift when tracking errors are small and due mostly to noise and disturbances. On the other hand, this trajectory balances control chatter and performance. The second part is a robust term that compensates for external disturbances and non-parametric uncertainties. Under that controller, tracking error trajectory converges to boundary layers and robustness to non-parametric uncertainties is established. Under the above-mentioned controllers, although asymptotic convergence of tracking error is ensured, system parameters may not be properly identified.

The composite adaptive controller can provide more accurate parameter estimation based on an update law which uses both tracking and prediction errors [16, 12, 17]. Since tracking errors in the joint displacements and prediction error in the joint torques are influenced by parameter uncertainties, composite adaptive controller uses a TEB/PEB adaptation, whereby, parameter adaptation is derived by using both tracking and prediction errors. In turn, it provides more accurate estimation of system parameters. In [12], a composite adaptive controller (TEB/PEB) with bounded-gain forgetting (BGF) was designed for parameter estimation. To avoid the need for joint acceleration in the adaptation structure, model regressor was filtered by a first-order stable filter. To benefit from data forgetting and to avoid unboundedness, composite adaptation law also benefited from an exponential forgetting least-squares gain update along with BGF method. Under that method, more accurate estimation of system parameters results in a better knowledge of system model, and in turn, the controller achieves better tracking performance over TEB-based controllers. Other modern methods in adaptive control improve parameter estimation through transient response and strong parametric convergence properties [18].

However, to guarantee parameter convergence, all above-mentioned methods require *persistent excitation* (*PE*) conditions for the system states, which is not always guaranteed nor feasible to check. So in other words, the aforementioned adaptive controllers require *PE* conditions to achieve asymptotic/exponential converge of the system parameters. Approaches that dispense of the need for *PE* have been designed [19, 20], one of which is the concurrent learning (CL) approach. The CL adaptive approach has been recently proposed in which instantaneous data along with the recorded data are concurrently used for adaptation [21, 22]. CL is able to guarantee the exponential convergence of system parameters without requiring *PE*, when the system has been observed to be exciting over a finite time interval [21]. It uses current and recorded data for the adaptation mechanism so exponential convergence of system parameters can be achieved under assumption of linear independence of some recorded history stack [22].

In [21], an approximate model inversion-based model reference adaptive control (AMI-MRAC) was formulated for a class of nonlinear systems with structured uncertainty. In that method, for convergence of the system outputs y to the output of the reference model y^d, a pseudo-control input v (desired acceleration) was designed to find the main control signal u so that the system is transformed into the form $\ddot{x} = v - \Delta$ with Δ as modeling uncertainty. The pseudo-control input v has three terms: a PD feedback, a feed-forward term, and an adaptive term. To update system parameters, a CL adaptation law was used that uses both recorded and instantaneous data. That paper ensures that if system states are exciting over finite intervals (rich data can be recorded online), exponential convergence of tracking error and parameter estimation error can be achieved, so *PE* is not required. An online algorithm for recording data points was also proposed based upon the maximizing minimum singular value of a matrix that shows up in the derivative of the Lyapunov function. In [22], a CL-based MRAC approach was designed for systems with unstructured uncertainties and validated on flight test. The AMI-MRAC was formulated and a three-term control law was synthesized. A single hidden layer NN was employed for adaptive term while the NN weights were updated using a CL adaptation law. Results showed that the method guarantees exponential convergence of the NN parameters to a compact ball around the true values without the *PE* requirements.

In general, the above-mentioned CL model-based MRAC involves a two-part control law, where a linear feedback part with constant gains (PD controller) stabilizes and controls the system, and a CL adaptive part is in charge of identifying the system uncertainties, which altogether is able to provide good reference model tracking performance. However, CL-MRAC suffers from several shortcomings: (i) it is not robust to control coefficient uncertainty, unmodeled dynamics, and disturbances; (ii) it is not optimal in terms of control signal; and (iii) the required control bounds cannot be enforced to this controller.

1.3 Safety using control barrier functions (CBFs)

Control barrier functions (CBFs) are widely-used in the control literature because of their relationship with Lyapunov-like functions, their ability to create the safety and avoidance properties, and their performance in multi-objective control [5, 23]. CBFs are the extension of BFs in the control systems whose conditions are affine in control signal and can be formulated as constraints in the

QPs. Similar to the CLFs, in CBFs, a set of inequality constraints is enforced on the derivative of a candidate CBF (reciprocal or zeroing) to search for a class of control inputs that provides forward invariance of a safe set. Thus, QPs can be synthesized subject to CBF and CLF constraints to meet stability and safety performance at the same time, whereby, creating multi-objective control systems. In QPs, stability objective can be viewed as a soft constraint and safety as a hard one. These objectives may not be thus achievable at the same time to have a feasible control signal from the QP optimization. Barrier functions can be categorized in two different types. (i) *Reciprocal* barrier functions $B(x)$, which are unbounded in the set boundary $\partial\mathcal{C}$ ($B(x) \longrightarrow \infty$ as $x \longrightarrow \partial\mathcal{C}$), require $\dot{B} \leq \alpha(1/B)$ with a class-$\mathcal{K}$ function α. (ii) *Zeroing* barrier functions $h(x)$ are vanished in the set boundary $\partial\mathcal{C}$ ($h(x) \longrightarrow 0$ as $x \longrightarrow \partial\mathcal{C}$) and require $\dot{h} \geq -\alpha(h)$ [5]. For both types, if $B(x)$ or $h(x)$ meet the Lyapunov-like conditions, set $\mathcal{C}$ is then forward invariant.

CBFs are commonly-used to define safety conditions in control applications. In [5], CBFs were unified with CLFs in the context of a QP (QP-CLBF) to achieve safety and control objectives. The method was applied to adaptive cruise control (ACC) and lane keeping (LK). That work relies on the perfect knowledge of system dynamics to construct the inequality constraints CBF and CLF. However since system dynamics usually contain parametric or/and unstructured uncertainties, under such controller, barrier functions may exceed the safe set and tracking performance is degraded. To mitigate these issues, in [24], a robust QP-CLBF controller was designed to handle modeling uncertainty, and to guarantee stability and safety. In [25], robustness of CBFs was studied under modeling perturbation, and input-to-state stability conditions for forward invariance were provided in the presence of disturbances. Although the above works investigate the robustness of QP-CLBF controllers, they do not take the estimation of unknown dynamics into consideration to provide better performance and more accurate safety.

Motivated by the shortcomings above and the desire of developing new multi-objective controllers, this thesis formulates five different robust quadratic program-based adaptive control approaches to satisfy a large and diverse set of objectives for different fully actuated and under-actuated nonlinear systems. The proposed controllers are developed to leverage the complementary strengths of baseline existing QP-CLBFs under which the control objectives and safety performance of systems with modeling inaccuracies and disturbances are degraded. Simulations and comparisons to existing QP-CLBFs on different real-world fully actuated and underactuated robotic applications are carried out to validate the benefits of the proposed techniques. The thesis is outlined as follows. Control and safety of fully actuated nonlinear systems with structured and unstructured uncertainties are investigated in Chapter 2. Active space control of underactuated robotic systems is formulated in Chapter 3. Passive space control and safety of underactuated robotic systems are presented in Chapter 4. A method for exponential control and safety of fully actuated nonlinear systems with parameter uncertainties and unknown control coefficients is suggested in Chapter 5. Finally, conclusions and future works are discussed in Chapter 6.

CHAPTER 2

CONTROL AND SAFETY OF NONLINEAR SYSTEMS WITH STRUCTURED AND UNSTRUCTURED UNCERTAINTIES

In this chapter, we begin by presenting basics of control Lyapunov function (CLF) and zeroing control barrier function (ZCBF), and then highlight associated drawbacks of baseline QP-CLF and QP-CBF controllers in the presence of modeling error and disturbances. Proposed solutions to improve the baseline methods are suggested. Problem statement is then described for systems with structured and unstructured uncertainties. Finally, proposed controllers are introduced and simulations are carried out to validate the benefits of our approaches over the baseline methods.

2.1 Basic background

2.1.1 Quadratic program-control Lyapunov function (QP-CLF)

Consider a general affine form of nonlinear systems as

$$\dot{x} = f(x) + g(x)u + \Delta(x) \tag{2.1}$$

with $x \in \Re^n$ and $u \in \Re^m$ such that $f(x)$ and $g(x)$ are locally Lipschitz continuous, and $\Delta(x)$ is a bounded modeling error.

Definition 1. A continuously differentiable function $V(x) : \Re^n \to \Re$ is an exponentially stabilizing control Lyapunov function (eCLF) for the system (2.1) with $\Delta(x) = 0$ if there exist a set of controls $\mathcal{U}$ and positive scalars $\gamma, a_1, a_2 > 0$ such that [4]

$$a_1\|x\|^2 \leq V(x) \leq a_2\|x\|^2, \tag{2.2}$$

$$\inf_{u \in \mathcal{U}} [\mathcal{L}_f V(x) + \mathcal{L}_g V(x)u] \leq -\gamma V(x),$$

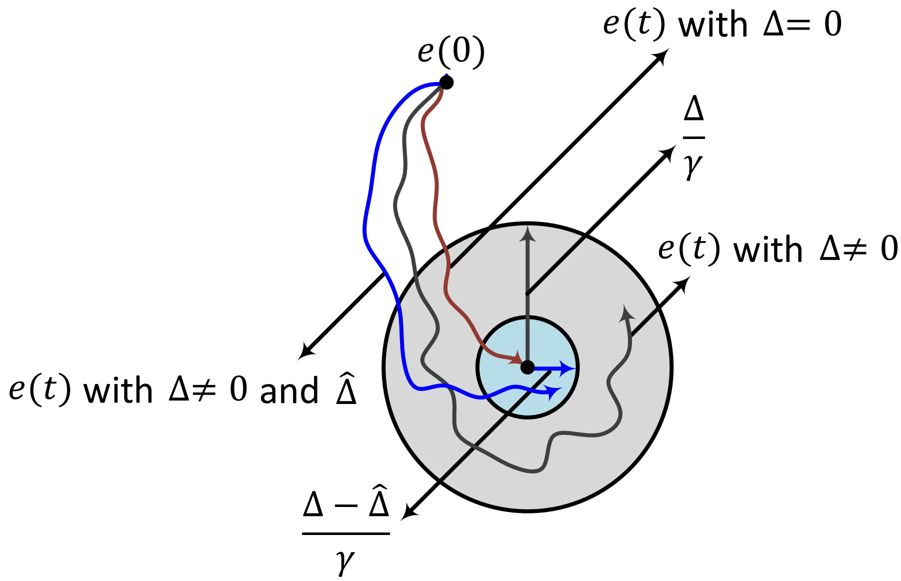

(a) Convergence of $e(t)$

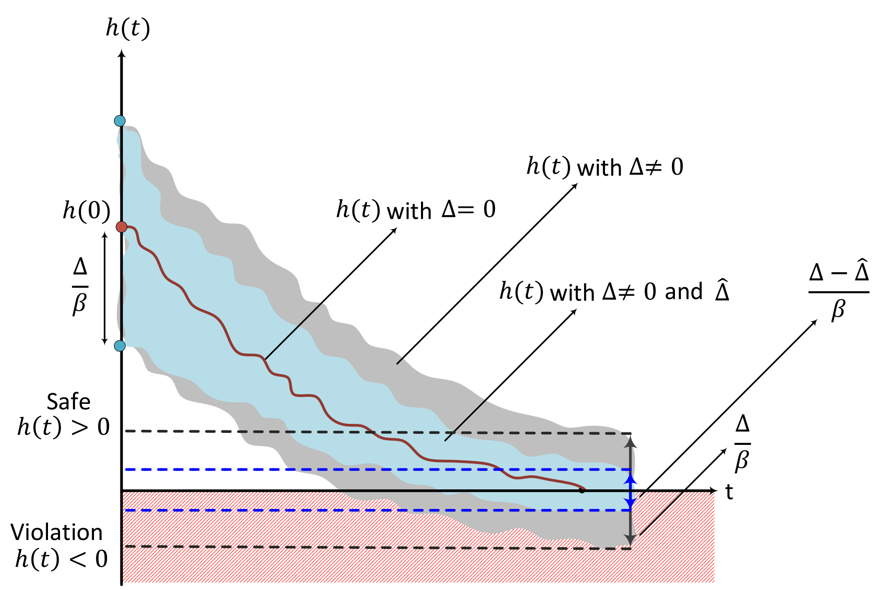

(b) Convergence of $h(t)$

Figure 2.1: Convergence of (a) the error trajectory $e(t)$ and (b) the barrier function $h(t)$, both in the presence of the modeling error Δ

where $\mathcal{L}_f V(x) = \frac{\partial V(x)}{\partial x} f$ and $\mathcal{L}_g V(x) = \frac{\partial V(x)}{\partial x} g$ are the Lie derivatives of $V(x)$ with respect to f and g, respectively.

CLF guarantees stability of nonlinear systems. We aim to design a family of controllers that satisfies (2.2). In terms of error dynamics, this implies picking the control u for the system (2.1) to achieve exponential convergence of the tracking error e to zero, where $e = x - x_d$ with x_d as a desired trajectory for x. Based on Definition 1, to achieve this convergence, a control Lyapunov certificate like one presented in (2.2) must hold, which renders $V(e) \leq e^{-\gamma t} V(0)$ (due to Comparison lemma [26] (Lemma 3.4)). In the absence of the modeling error Δ and under a CLF-based controller, $V(t)$ starts from $V(0)$ and exponentially converges to zero at the convergence rate γ. However, in the presence of the modeling error, $\dot{V} \leq 0$ if $\|e\| \geq \frac{\Delta}{\gamma}$, resulting in the boundedness of e in a neighborhood of the origin with size $\frac{\Delta}{\gamma}$. To shrink down the size of the neighborhood and provide better convergence, one might think of is to increase the parameter γ. However, this may result in more control effort and unfavorable system solutions. Without loss of generality, if the control u is computed by a QP subject to the inequality constraint (2.2) (resulting in QP-CLF), the system trajectory is uniformly ultimately bounded (UUB) in a neighborhood around the origin in the presence of modeling error.

Solution 1: To avoid increasing the parameter γ which results in higher control effort, estimating Δ and compensating for the modeling error is suggested. By doing so, the proposed controller/estimator renders convergence of the system trajectory to a smaller neighborhood of size $\frac{\Delta - \hat{\Delta}}{\gamma}$ without increasing the convergence rate (shown in Fig. 2.1(a)). Solution 1 will be formulated later in this chapter through the derivation of two proposed adaptive approaches.

2.1.2 Quadratic program-control barrier function (QP-CBF)

Zeroing control barrier function (ZCBF) guarantees the forward invariance of a set so if the system starts inside the set, it remains in the set for all time [5]. Defining the set

$$\mathcal{C} = \{x \in \Re^n : h(x) \geq 0\}, \tag{2.3}$$

we aim to compute a family of controls to ensure the forward invariance of the set $\mathcal{C}$.

Definition 2. A continuous function $\alpha : [0, a) \longrightarrow [0, \infty)$ for $a > 0$ belongs to a class-$\mathcal{K}$ function if it is strictly increasing and $\alpha(0) = 0$.

Definition 3. A continuously differentiable function $h(x) : \Re^n \to \Re$ is a zeroing control barrier function (ZCBF) for the system (2.1) with $\Delta(x) = 0$ and the set $\mathcal{C}$ if there exist a set of controls $\mathcal{U}$ and a class-$\mathcal{K}$ function α such that [4]

$$\sup_{u \in \mathcal{U}} [\mathcal{L}_f h(x) + \mathcal{L}_g h(x) u] \geq -\alpha(h(x)), \tag{2.4}$$

where $\mathcal{L}_f h(x) = \frac{\partial h(x)}{\partial x} f$ and $\mathcal{L}_g h(x) = \frac{\partial h(x)}{\partial x} g$ are the Lie derivatives of $h(x)$ with respect to f and g, respectively.

We aim to pick the control u for the system (2.1) such that the set $\mathcal{C}$ is forward invariant, which requires holding the barrier certificate. Applying the Comparison lemma, the barrier certificate renders $h(x) \geq e^{-\gamma t} h(0)$, which results in $h(x) \geq 0$ for $t \geq 0$. With no modeling uncertainty, $\Delta = 0$, $h(t)$ starts from $h(0)$ and vanishes in the set boundary ∂C ($h(x) \longrightarrow 0$ as $x \longrightarrow \partial C$). However, since the exact system model is not available, the barrier convergence for the system (2.1) will be affected by the modeling error Δ. Under this condition and by picking $\alpha(h(x)) = \beta h(x)$ with $\beta > 0$, we have $\dot{h}(x) \geq -\beta h(x) + \Delta$, which results in $h(x) \geq e^{-\beta t} h(0) + \frac{\Delta}{\beta}$. It implies that $h(t)$ starts from $h(0) + \frac{\Delta}{\beta}$ and converges to a ball of size $\frac{\Delta}{\beta}$ around zero. Here, two cases can be considered. (i) Increasing the parameter β decreases the effect of the modeling error and provides smaller barrier violation, but resulting in more control effort. (ii) Decreasing the parameter β boosts the effect of Δ and renders higher barrier violation. In this case, x may/may not hit ∂C depending on the nature of system and desired trajectory that x has to follow. Without loss of generality, for any h, any function α, and using a QP-based controller, the variable of interest may exceed the safe set in the presence of the modeling error.

Solution 2: To avoid increasing the parameter β which causes more control effort, estimating Δ and compensating for the modeling error is suggested. This way, the barrier certificate under the proposed controller/estimator renders $h(x) \geq e^{-\beta t} h(0) + \frac{\Delta - \hat{\Delta}}{\beta}$. This implies that $h(t)$ starts from a neighborhood around $h(0)$ and converges to a smaller ball of size $\frac{\Delta - \hat{\Delta}}{\beta}$ as shown in Fig. 2.1 (b). Solution 2 will be formulated later in this chapter through the derivation of a proposed adaptive control approach.

2.2 Problem statement

In this section, we aim to formulate Solutions 1 and 2 through the derivation of two robust quadratic program-based adaptive controllers for nonlinear systems with structured and unstructured uncertainties. Consider the following 2D nonlinear system of the form

$$\begin{aligned} \dot{x}_1 &= x_2 \\ \dot{x}_2 &= f(x) + bu + d, \end{aligned} \tag{2.5}$$

where $x = [x_1 \quad x_2]^T$; the dynamics $f(x)$ are unknown; b is an unknown control coefficient; u is the control signal; and d is an unknown bounded disturbance such that $\|d\| \leq \bar{d}$.

Assumption 1. Assume that $b = b_0 + \Delta b$, where b_0 is our best estimate with the same sign as b, and Δb is the uncertainty. Though b_0 is constant, Δb can have bounded state dependence.

Assumption 2. Assume that $u = u^* + \Delta u$, where u^* is the commanded input, and Δu is a bounded control defect stemming from any input constraints.

Define the output $y = x_1$ and its desired trajectory as y_d, where boundedness of y_d for all time is presumed. A three-term pointwise optimal adaptive control law will be synthesized

$$u^* = \frac{1}{b_0}(\ddot{y}_d - v_{opt} - v_{ad}), \tag{2.6}$$

where the control law u^* uses the known part of the b; $\ddot{y}_d$ is the feed-forward term; v_{opt} represents the pointwise optimal signal (which will be presented later in this chapter); and v_{ad} is the adaptive signal that will be introduced in the next two subsections.

2.2.1 System with structured uncertainty

The unknown dynamics are linearly parameterized by known basis functions $\Phi(x) = [\phi_1(x), ..., \phi_r(x)]^T \in \Re^r$ and true parameter vector $\theta^* \in \Re^r$,

$$f(x) = \theta^{*^T}\Phi(x), \tag{2.7}$$

where r is number of the unknown parameter vector elements. The adaptive component v_{ad} is defined as

$$v_{ad} = \hat{\theta}^T\Phi(x), \tag{2.8}$$

where $\hat{\theta}$ denotes the estimate of θ^*. Assume that $d = 0$. The tracking error dynamics follow from Eqs. (2.5)-(2.8),

$$\ddot{e} = v_{opt} + \epsilon_e - \epsilon_b - \epsilon_u, \quad \text{for} \quad e = y_d - y, \tag{2.9}$$

where the last three terms arise from the uncertainty and input constraint

$$\begin{aligned} \epsilon_e =& v_{ad} - f(x) = \tilde{\theta}^T\Phi(x) \quad \text{for} \ \tilde{\theta} = \hat{\theta} - \theta^*, \\ \epsilon_b =& \Delta b\, u, \quad \text{and} \\ \epsilon_u =& b\, \Delta u, \end{aligned} \tag{2.10}$$

where ϵ_b and ϵ_u show the control error and the defect error, respectively. For bounded control signal and bounded control defect, the control error and defect error are then bounded i.e., $|\epsilon_b| \leq \bar{\epsilon}_b$ and $|\epsilon_u| \leq \bar{\epsilon}_u$. The estimation error ϵ_e is bounded if $v_{ad} - f(x)$ lies in a ball of radius $\bar{\epsilon}_e$.

To formulate the Solution 1 for systems with structured uncertainty, using adaptive control synthesis, an update law for $\hat{\theta}$ will be designed so that $\hat{\theta} \to \theta^*$ in the ideal case, implying that $v_{ad} \to f(x)$, and therefore that $|\epsilon_e| \leq \bar{\epsilon}_e$ in the non-ideal case. Consequently, the error dynamics (2.9) represent stable linear evolution with three bounded disturbances ϵ_e, ϵ_u, and ϵ_b. Concurrent learning (CL) adaptive approach is used to achieve an accurate parameter estimation and in turn smaller ϵ_e.

The other disturbances ϵ_u and ϵ_b are compensated by a robust term. The adaptive, optimal, and robust components are then unified to create the main control signal (2.6) to provide better stability of the system with less control effort. Lyapunov arguments will establish UUB with exponential convergence to the ultimate bound. The next section describes the controller components leading up to the proposed approach to provide convergence of the solutions to small balls of the origin.

2.2.2 System with unstructured uncertainty

The system dynamic $f(x)$ is assumed to be structurally unknown. The error dynamics are

$$\begin{aligned}\ddot{e} &= \ddot{y}_d - f(x) - bu - d = \ddot{y}_d - f(x) - b(u^* + \Delta u) - d \\ &= \ddot{y}_d - f(x) - b\Delta u - u^*(b_0 + \Delta b) - d = -G(x, u^*) + D(d, \Delta u) - b_0 u^* + \ddot{y}_d,\end{aligned} \quad (2.11)$$

where $G(x, u^*) = f(x) + u^*\Delta b$ contains unstructured uncertainties depending on measurable variables x and u^*; and $D(d, \Delta u) = -(b\Delta u + d)$ is the part with unmeasurable variables d and Δu. In this case, v_{ad} will be constructed by a neural network (NN) later in this chapter to compensate for $G(x, u^*)$.

Substituting the control law into (2.11) gives

$$\ddot{e} = v_{opt} + \epsilon_e + D(d, \Delta u), \quad (2.12)$$

where $\epsilon_e = v_{ad} - G(x, u^*)$ represents the estimation error.

Using the control law (2.6), the nonlinear system (2.5) turns into the linear system (2.12) with input v_{opt}, and the bounded disturbances D and ϵ_e. To address Solutions 1 and 2 for systems with unstructured uncertainty, a NN adaptive approach is designed to estimate the unknown dynamics and provide smaller ϵ_e. A robust term is designed to compensate for the term D. The adaptive and optimal terms are then incorporated into the main control signal to provide better stability with less control effort. UUB of system solutions are finally guaranteed using Lyapunov arguments. The next section describes the controller components leading up to the proposed neuro-adaptive approach to provide convergence of the ZCBF and tracking error to smaller neighborhoods of the origin over non-adaptive baseline approaches.

2.3 Proposed robust quadratic program-based adaptive controllers

In this section, adaptive controllers are designed to improve the convergence of barrier function (safety performance) and error trajectory (tracking performance) over baseline non-adaptive controllers in the presence of modeling error and disturbances. The proposed control approaches meet multiple design specifications such as control optimality, tracking performance, dynamic estimation, safety performance, and robustness to unmodeled dynamics. To provide context for the proposed controllers, Fig. 2.2 illustrates their structures. The traditional QP-CLF and QP-CLBF approaches act as an outer layer, synthesizing a stabilizing pointwise optimal control signal. Though it works well empirically, performance is impacted by model uncertainty. The aim is to incorporate an adaptive inner layer through the inclusion of a concurrent learning (CL) adaptive control strategy.

We propose to incorporate the CL adaptive control component in the inner layer of the baseline controllers. In the outer layer, v_{opt} is optimized by the QP subject to robust RCLF (RCLF) and CBF constraints, and control bounds. In the inner layer, the CL adaptive part identifies unknown dynamics through the use of historical data plus the current instantaneous performance. The identification rate is exponential. The optimal and adaptive signals v_{opt} and v_{ad} are unified with a feed-forward term to provide the main control signal u for the system. We formulate a QP using an optimization problem to minimize the pointwise optimal signal part v_{opt}, and in turn u. System stability is maintained via a RCLF constraint. Following that, the CL approach is added so the estimation error ϵ_e converges to zero or at least remains bounded by a small positive number. Stability analysis of the system will be carried out using the Lyapunov argument.

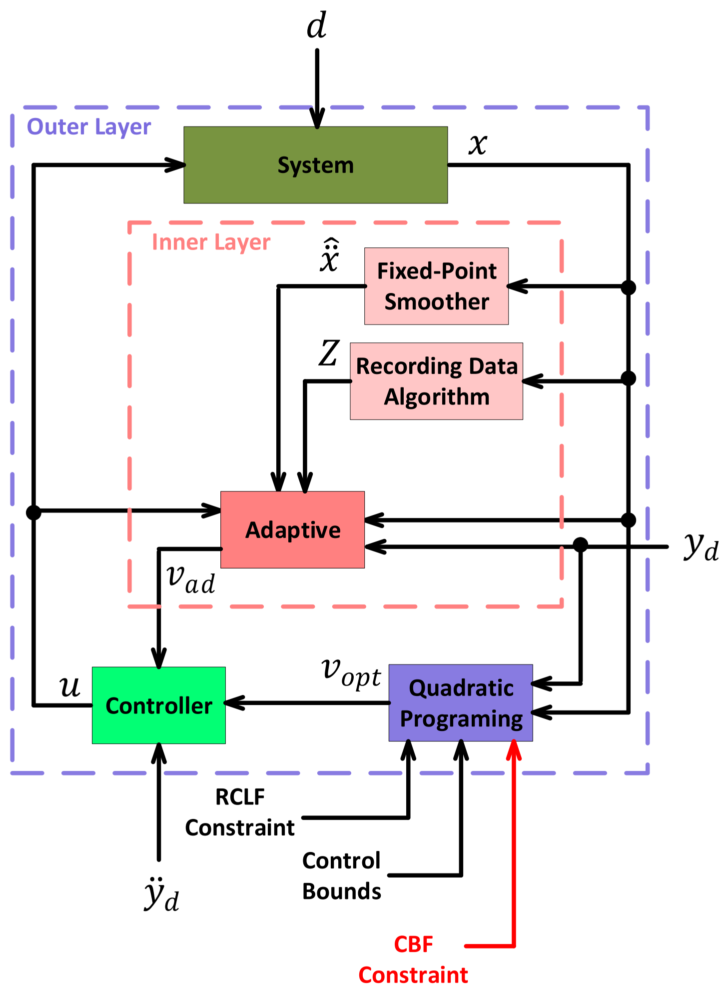

Figure 2.2: Proposed robust quadratic program-based adaptive control structure. The figure shows the structure of QP-adaptive robust CLF (QP-ARCLF), while for QP-adaptive robust CLBF (QP-ARCLBF), system is unstructured, adaptive part has a NN-based structure, and the CBF constraint shown in red is incorporated in the QP formulation.

2.3.1 Robust control Lyapunov function (RCLF) and pointwise min-norm control (PWMNC) law

With the aim of designing RCLF-based controllers for the system (2.5), this section provides an overview of basic definitions for RCLF and PWMNC law for the problem of state-feedback design for time-invariant systems [27].

Definition 4. Consider the time-invariant system

$$\dot{x} = f(x, u, w), \tag{2.13}$$

where $f : \mathcal{X} \times \mathcal{U} \times \mathcal{W} \rightarrow \mathcal{X}$ is a continuous function with the state variable $x \in \mathcal{X}$, the control input $u \in \mathcal{U}$, and the disturbance input $w \in \mathcal{W}$. A continuously differentiable function $V(\mathcal{X}) : \mathcal{X} \rightarrow \Re_+$ is a RCLF for such system if and only if there exist a $c_v \in \Re_+$ and a function $\alpha_v(x)$ such that $V(x) > c_v$ and

$$\inf_{u \in \mathcal{U}(x)} \sup_{w \in \mathcal{W}(x,u)} [\mathcal{L}_f V(x, u, w) + \alpha_v(x)] < 0. \tag{2.14}$$

Definition 5. Given a RCLF $V(\mathcal{X}) : \mathcal{X} \rightarrow \Re_+$ for the system (2.13), a lower semilcontinuous set $K : \mathcal{X} \rightarrow \mathcal{U}$ with nonempty convex values on $V^{-1}(c_v, \infty)$ is defined at points $V(x) = c_v$ as

$$K(x) := \{u \in U(x) : \; D(x, u) < 0\} \tag{2.15}$$

with the control constraint U and the continuous function $D : \mathcal{X} \times \mathcal{U} \rightarrow \Re$ as

$$D(x, u) := \max_{w \in \mathcal{W}(x)} \left[\mathcal{L}_f V(x, u, w) + \alpha_v(x)\right]. \tag{2.16}$$

It follows that for all $x \in V^{-1}(c_v, \infty)$, the nonempty closed convex set

$$\overline{K(x)} = U(x) \cap \{u \in \mathcal{U} : \; D(x, u) \leq 0\} \tag{2.17}$$

has a unique element of minimum norm. To achieve the minimal selection of $\overline{K(x)}$ on $V^{-1}(c_v, \infty)$, the following function is picked

$$m(x) = \text{ arg min} \left\{ \|u\| : u \in \overline{K(x)} \right\}. \tag{2.18}$$

Definition 6. Consider the time-invariant system

$$\dot{x} = f(x) + g(x)u + h(x)w \tag{2.19}$$

with continuous functions $f(x)$, $g(x)$, and $h(x)$. In view of (2.15), the set K can be defined for

$$D(x,u) = \Psi_0(x) + \Psi_1^T(x)u \tag{2.20}$$

with

$$\begin{aligned} \Psi_0(x) &:= \nabla V(x).f(x) + \alpha_v(x) + \|\nabla V(x).h(x)\| \\ \Psi_1(x) &:= [\nabla V(x).g(x)]^T . \end{aligned} \tag{2.21}$$

Definition 7. Given the set $\overline{K(x)}$ and the minimal selection $m(x)$ from (2.17) and (2.18), the following PWMNC law is applied for the system (2.19) for all $x \in V^{-1}(c_v, \infty)$

$$m(x) = \begin{cases} -\frac{\Psi_0(x)\Psi_1(x)}{\Psi_1^T(x)\Psi_1(x)} & \text{if } \Psi_0(x) > 0 \\ 0 & \text{if } \Psi_0(x) \leq 0 \end{cases} \tag{2.22}$$

whose denominator never goes to zero as the set $K(x)$ is *nonempty* when $x \in V^{-1}(c_v, \infty)$.

Remark 1. The PWMNC law (2.22) for the system (2.19) can be equivalently implemented by the following QP optimization problem as claimed in [8, 5]

$$\begin{aligned} u = \ & \text{argmin} \quad u^T u \\ & \text{s.t.} \quad D(x,u) \leq 0 \end{aligned} \tag{2.23}$$

which results in a QP-based RCLF controller.

Remark 2. Every RCLF can be also a CLF if $c_v = w = 0$. It implies that a continuously differentiable *radially unbounded* function $V(x)$ is a CLF for the system $\dot{x} = f(x, u)$ if

$$x \neq 0 \ \rightarrow \ \inf_{u \in \mathcal{U}} \ \mathcal{L}_f V(x, u) < 0. \tag{2.24}$$

2.3.2 QP-adaptive robust CLF (QP-ARCLF) for systems with structured uncertainties

In this section, QP-ARCLF is designed for systems with structured uncertainty to address the Solution 1. Through this design, we aim to improve the tracking performance of the baseline non-adaptive controllers which are deigned based on the CLF constraint. Using an adaptive controller incorporated in the inner layer of the control structure, the unknown system dynamics are identified and the estimates are sent to the outer layer (baseline CLF-based controller) to provide better tracking performance in the presence of modeling error. This way, the size of convergence ball will be decreased over the baseline methods via estimation of the unknown dynamics and compensation for the disturbances.

A. Outer layer design

Define $\xi = [e \quad \dot{e}]^T$ so that Eq. (2.9) becomes

$$\dot{\xi} = F\xi + Gv_{opt} + G\epsilon_e - G\epsilon_b - G\epsilon_u \tag{2.25}$$

with

$$F = \begin{bmatrix} 0 & I \\ 0 & 0 \end{bmatrix}, \quad G = \begin{bmatrix} 0 \\ I \end{bmatrix}. \tag{2.26}$$

To achieve a rapidly exponentially stabilizing RCLF for the system, we begin by defining $\xi_\gamma = [e/\gamma \quad \dot{e}]^T$ and Riccati equations [4, 7]

$$F^T P_\gamma + P_\gamma F - \frac{1}{\gamma} P_\gamma G G^T P_\gamma + \frac{1}{\gamma} D_\gamma Q D_\gamma = 0, \tag{2.27}$$

where Q is a symmetric positive-definite matrix; γ is the tracking convergence rate; $P_\gamma = D_\gamma P D_\gamma$ such that $P = P^T > 0$ solves the continuous algebraic Riccati equation (CARE) $F^T P + PF - PGG^T P + Q = 0$; and D_γ is defined as $D_\gamma = \text{diag}(I/\gamma, I)$. All three disturbances ϵ_e, ϵ_u, and ϵ_b are matched with v_{opt} acting on the system (2.25). Therefore all the disturbances are compensated for, in the RCLF structure, via v_{opt}.

The following positive-definite Lyapunov function in the exponentially stabilizing RCLF framework [4]

$$V_\gamma(\xi) = \xi^T P_\gamma \xi \tag{2.28}$$

satisfies the inequality conditions

$$\alpha_1 \|\xi\|^2 \leq V_\gamma(\xi) \leq \frac{\alpha_2}{\gamma^2}\|\xi\|^2. \tag{2.29}$$

Take derivative of (2.28) and substitute (2.25) into it to obtain

$$\dot{V}_\gamma(\xi) = \xi^T(P_\gamma F + F^T P_\gamma)\xi + 2\xi^T P_\gamma G(v_{opt} + \epsilon_e - \epsilon_u - \epsilon_b). \tag{2.30}$$

On the other hand, the derivative of (2.28) can be written

$$\dot{V}_\gamma(\xi) = \frac{\partial V_\gamma(\xi)}{\partial \xi}\dot{\xi} = L_F V_\gamma(\xi) + L_G V_\gamma(\xi)(v_{opt} + \epsilon_e - \epsilon_u - \epsilon_b), \tag{2.31}$$

where $L_F V_\gamma(\xi) = \frac{\partial V_\gamma(\xi)}{\partial \xi} F\xi$ and $L_G V_\gamma(\xi) = \frac{\partial V_\gamma(\xi)}{\partial \xi} G$ are the Lie derivatives of $V_\gamma(\xi)$ with respect to F and G, respectively.

Comparing (2.30) and (2.31), one has

$$L_F V_\gamma(\xi) = \xi^T(P_\gamma F + F^T P_\gamma)\xi, \;\; L_G V_\gamma(\xi) = 2\xi^T P_\gamma G. \tag{2.32}$$

Exponential convergence of the error trajectory ξ requires satisfying

$$\dot{V}_\gamma(\xi) + \frac{\alpha_3}{\gamma} V_\gamma(\xi) \leq 0, \tag{2.33}$$

where $\alpha_3 = \frac{\lambda_{min} Q}{\lambda_{max} P}$, and $\lambda_{min}(.)$ and $\lambda_{max}(.)$ denote the minimum and maximum eigenvalues of a matrix, respectively. In doing so, the error signal satisfies

$$\|\xi\| \leq \frac{1}{\gamma}\sqrt{\frac{\alpha_2}{\alpha_1}} e^{-\frac{\alpha_3}{2\gamma}} \|\xi(0)\|. \tag{2.34}$$

The pointwise optimal control signal v_{opt} can be found as

$$v_{opt}(\xi) = \{v_{opt} : \Psi_0(\xi) + \Psi_1^T(\xi) v_{opt} \leq 0\}, \tag{2.35}$$

where the RCLF constraint

$$\Psi_0(\xi) + \Psi_1^T(\xi) v_{opt} \leq 0 \tag{2.36}$$

satisfies the constraint (2.33). Using Eqs. (2.31), (2.32), and (2.33), $\Psi_0(\xi)$ and $\Psi_1(\xi)$ are found to be

$$\begin{aligned} \Psi_0(\xi) =& L_F V_\gamma(\xi) + \frac{\alpha_3}{\gamma} V_\gamma(\xi) + R(\xi) \\ \Psi_1(\xi) =& L_G V_\gamma(\xi), \end{aligned} \tag{2.37}$$

where the robust term

$$R(\xi) = K_r \|L_G V_\gamma(\xi)\| \tag{2.38}$$

compensates for the effects of ϵ_u and ϵ_b for a proper selection of the gain $K_r > 0$.

Due to Definition 7, the following PWMNC law provides an open-loop solution to Eq. (2.35)

$$v_{opt}(\xi) = \begin{cases} -\frac{\Psi_0(\xi)\Psi_1(\xi)}{\Psi_1^T(\xi)\Psi_1(\xi)} & \text{if } \Psi_0(\xi) > 0 \\ 0 & \text{if } \Psi_0(\xi) \leq 0 \end{cases} \tag{2.39}$$

for all $\xi \in V_\gamma^{-1}(c_v, \infty)$ based upon Definitions 4, 5, 6, and 7. Note that the law (2.39) never divides by zero as the set (2.35) is *nonempty* for $\xi \in V_\gamma^{-1}(c_v, \infty)$. In other words, the law (2.39) is implementable and the RCLF constraint (2.36) could be satisfied through $\Psi_1(\xi)$ *whenever* $V_\gamma(\xi) > c_v$ [27].

Due to Remark 1, the following QP is synthesized subject to the RCLF and control bound constraints as

$$\begin{aligned} v_{opt} = &\text{argmin} \quad v_{opt}^T v_{opt} + ld^2 \\ &\text{s.t.} \quad \Psi_0(\xi) + \Psi_1^T(\xi) v_{opt} \leq d \\ &\qquad + v_{opt} \leq b_0 u_{max} + u_s \\ &\qquad - v_{opt} \leq b_0 u_{max} - u_s \end{aligned} \tag{2.40}$$

where $u_s = -v_{ad} + \ddot{y}_d$. The QP problem (2.40) bounds u through a relaxation of the RCLF constraint associated to the penalty coefficient l. The last two constraints bound the main control signal u such that $-u_{max} \leq u \leq u_{max}$.

Remark 3. Since in the above optimization problem, the RCLF constraint guarantees stability in the presence of ϵ_e, ϵ_u, and ϵ_b, the proposed QP-ARCLF is robust against control coefficient uncertainty.

Remark 4. When control limit constraints are not actively enforced, the system will have the desired convergence properties. When actively enforced, there will be a control defect, $\Delta u = u - u^*$, and tracking performance may degrade.

B. Inner layer design

The CL adaptive control inner layer aims to estimate/recover the true system dynamics $f(x)$ using both recorded and instantaneous information of the system states. The reasons for CL adaptive control are two-fold: (i) it guarantees exponential convergence of parameter vector and (ii) it does not require the *PE* condition to always hold (but to have held at some point in time). Estimating v_{ad} from Eq. (2.8) involves updating the parameter vector θ. The modified form of the CL adaptive law [21, 28] will be:

$$\dot{\hat{\theta}} = -\eta_a \Phi(x)\xi^T P_\gamma G - \eta_b \sum_{i=1}^{m} \Phi(x_i)\hat{\epsilon}_{ei}^T, \tag{2.41}$$

where m is the number of recorded data points kept; and η_a and η_b are the adaptation convergence coefficients for the current (first term) and recorded (second term) adaptation parts, respectively. For the recorded part, $\Phi(x_i)$ and ϵ_{ei} are realized for i-th recorded data, where $i \in [1, 2, ..., m]$. Since θ^* is not known, a proxy for it is estimated from the closed-loop system dynamics. In particular, an estimate for ϵ_{ei} is obtained from

$$\hat{\epsilon}_{ei} = \hat{\theta}^T \Phi(x_i) - \hat{f}(x_i) \ \text{ with } \ \hat{f}(x_i) = \dot{\hat{x}}_2 - v_i, \tag{2.42}$$

where $v = b_0 u$ (v_i is the i-th recorded data) and $\dot{x}_2$ can be estimated using a fixed-point smoother algorithm [29, 30].

Remark 5. Recording data points [22]: Define the history stack $Z = [\Phi(x_i), ..., \Phi(x_m)] \in \Re^{r \times m}$ whose acceptance policy requires storing points that are sufficiently different from the last point stored. The minimum cardinality required is the basis function dimension r, while a larger m provides a richer, over constrained recorded data stack. If y_d is exciting over a finite interval ($\Phi(x)$ is exciting), Z will have r linearly independent columns (rank$Z$ = r), and in turn exponential convergence of the unknown parameter vector θ is guaranteed. There is no need to require the *PE* condition of the $\Phi(x)$. In case that the history stack gets full, a data point remover algorithm removes one point and adds another one to maximize the minimum singular value of the history stack $\sigma_{min}(Z)$, which increases the rate of the estimation convergence. Note that the $\sigma_{min}(Z)$ may be more maximized if a larger maximum number of stored data m_{max} is chosen. Also, the minimum number of the stored data m_{min} should be equal to the basis function dimension r.

C. Stability analysis

This section is devoted to perform stability analysis for the proposed joint controller QP-ARCLF. The candidate Lyapunov function will be a function of both trajectory error ξ and the parameter estimation error $\tilde{\theta}$ with ϵ_b seen as an exogenous input and ϵ_u due to the control defect. Consider the following candidate Lyapunov function

$$V(\tilde{\theta}, \xi) = \frac{1}{2}\tilde{\theta}^T \eta^{-1} \tilde{\theta} + \frac{1}{2}\xi^T P_\gamma \xi, \tag{2.43}$$

where for simplicity $\eta = \eta_a = \eta_b$; see Eq. (2.41).

Theorem 1. *Assume that $|\epsilon_b| \leq \bar{\epsilon}_b$, $|\Delta u| \leq \bar{\epsilon}_u$ over the time domain of interest, and y_d is exciting over a finite interval. Given the Lyapunov function (2.43), the QP optimization (2.40) subject to the RCLF constraint, and the CL adaptation control law (2.41), if rank$(Z) = r$, then $(\xi, \tilde{\theta})$ is UUB with exponential convergence rate for all unknown b, unknown $\theta \in \Re^r$, and any $x(0)$ [31].*

Proof. Taking the time derivative of (2.43) gives

$$\dot{V}(\tilde{\theta}, \xi) = \tilde{\theta}^T \eta^{-1} \dot{\tilde{\theta}} + \xi^T P_\gamma \dot{\xi}. \tag{2.44}$$

Substituting (2.10), (2.25), and (2.41) into (2.44) yields

$$\begin{aligned} \dot{V}(\tilde{\theta}, \xi) = & - \tilde{\theta}^T \Phi(x) \xi^T P_\gamma G - \tilde{\theta}^T \sum_{i=1}^{m} \Phi(x_i) \Phi(x_i)^T \tilde{\theta} \\ & + \xi^T P_\gamma F \xi + \xi^T P_\gamma G (v_{opt} + \tilde{\theta}^T \Phi(x) - \epsilon_u - \epsilon_b) \end{aligned} \tag{2.45}$$

for which utilizing

$$2\gamma P_\gamma F = \left(P_\gamma G G^T P_\gamma - D_\gamma Q D_\gamma\right), \tag{2.46}$$

one has

$$\begin{aligned}\dot{V}(\tilde{\theta}, \xi) =& -\tilde{\theta}^T \sum_{i=1}^{m} \Phi(x_i)\Phi(x_i)^T \tilde{\theta} - \frac{1}{2\gamma}\xi^T D_\gamma Q D_\gamma \xi \\ &+ \frac{1}{2\gamma}\xi^T \left(P_\gamma G G^T P_\gamma\right)\xi + \xi^T P_\gamma G v_{opt} - \xi^T P_\gamma G(\epsilon_u + \epsilon_b).\end{aligned} \tag{2.47}$$

Case 1: $\Psi_0(\xi) > 0$

The PWMNC law v_{opt} is determined from the first condition of (2.39) for which incorporation of (2.32) and (2.37), one can write

$$v_{opt} = -\frac{\xi^T(P_\gamma F + F^T P_\gamma)\xi + \frac{\alpha_3}{\gamma}\xi^T P_\gamma \xi + K_r \|2\xi^T P_\gamma G\|}{2\xi^T P_\gamma G}. \tag{2.48}$$

Substituting v_{opt} into (2.47) and using (2.46) yields

$$\begin{aligned}\dot{V}(\tilde{\theta}, \xi) =& -\tilde{\theta}^T \sum_{i=1}^{m} \Phi(x_i)\Phi(x_i)^T \tilde{\theta} - \frac{1}{2\gamma}\xi^T D_\gamma Q D_\gamma \xi + \frac{1}{2\gamma}\xi^T \left(P_\gamma G G^T P_\gamma\right)\xi - \xi^T P_\gamma G(\epsilon_u + \epsilon_b) \\ &- \frac{1}{2}\xi^T \left(\frac{1}{\gamma}P_\gamma G G^T P_\gamma - \frac{1}{\gamma}D_\gamma Q D_\gamma\right)\xi - \frac{\alpha_3}{2\gamma}\xi^T P_\gamma \xi - K_r\|\xi^T P_\gamma G\|.\end{aligned} \tag{2.49}$$

Canceling the similar terms and bounding the control defect gives

$$\dot{V}(\tilde{\theta}, \xi) = -\tilde{\theta}^T \sum_{i=1}^{m} \Phi(x_i)\Phi(x_i)^T \tilde{\theta} - \xi^T P_\gamma G(\epsilon_u + \epsilon_b) - \frac{\alpha_3}{2\gamma}\xi^T P_\gamma \xi - K_r\|\xi^T P_\gamma G\| \tag{2.50}$$

which further reduces to

$$\dot{V}(\tilde{\theta}, \xi) \leq -\lambda_{min}\Big(\sum_{i=1}^{m} \Phi(x_i)\Phi(x_i)^T\Big)\|\tilde{\theta}\|^2 - \frac{\alpha_3}{2\gamma}\lambda_{min}(P_\gamma)\|\xi\|^2 - \|\xi^T P_\gamma G\|\left(K_r - (\bar{\epsilon}_b + \bar{\epsilon}_u)\right). \tag{2.51}$$

Define $H = \sum_{i=1}^{m} \Phi(x_i)\Phi(x_i)^T = ZZ^T$. According to Remark 5, as soon as the history stack Z becomes full rank, H is positive definite. Selection of the gain K_r determines the type of system stability such that (i) if $K_r = \bar{\epsilon}_b + \bar{\epsilon}_u$, the system would be exponentially stabilizing, (ii) if $K_r > \bar{\epsilon}_b + \bar{\epsilon}_u$, the system is asymptotically stable, and (iii) if $K_r < \bar{\epsilon}_b + \bar{\epsilon}_u$, the system is concluded to be UUB. Note that in the absence of control saturation, Δu vanishes and in turn, smaller ultimate bound may be established.

Case 2: $\Psi_0(\xi) \leq 0$

From (2.37), $\Psi_0(\xi) \leq 0$ implies that

$$\xi^T(P_\gamma F + F^T P_\gamma)\xi + \frac{\alpha_3}{\gamma}\xi^T P_\gamma \xi + K_r\|2\xi^T P_\gamma G\| \leq 0. \tag{2.52}$$

Utilizing (2.52) to simplify (2.45), recalling that if $\Psi_0(\xi) \leq 0$, then $v_{opt} = 0$, and following the same steps results in (2.51), implying that the same results are obtained. $\square$

Remark 6. Proof of Theorem 1 shows that the system solutions are bounded inside the following compact balls B_ξ and $B_{\tilde{\theta}}$ if $K_r < \bar{\epsilon}_b + \bar{\epsilon}_u$

$$\begin{aligned} \|\xi\| &\leq B_\xi\Big(\tilde{\theta}, K_r - (\epsilon_b + \epsilon_u), \gamma\Big) \\ \|\tilde{\theta}\| &\leq B_{\tilde{\theta}}\Big(\xi, K_r - (\epsilon_b + \epsilon_u), \lambda_{min}(H)\Big). \end{aligned} \tag{2.53}$$

This shows that the error trajectory converges to a neighborhood of the origin with size B_ξ that depends on the parameter estimation performance, disturbance compensation by the robust term, and the convergence coefficient γ. It implies that with a proper dynamic estimation and disturbance attenuation, there is no need to increase the parameter γ to achieve a nice tracking performance. Hence, under the same convergence rate, the proposed controller could outperform the baseline QP-CLF with regard to the tracking performance and control effort.

2.3.3 QP-adaptive robust CLBF (QP-ARCLBF) for systems with unstructured uncertainties

In this section, the second controller QP-ARCLBF is formulated for systems with unstructured uncertainties to address the Solutions 1 and 2. Through this design, the error trajectory and the barrier violation converge to smaller neighborhoods of the origin over baseline non-adaptive methods under dynamic estimation and disturbance attenuation. This section presents the proposed controller, which consists of a high level control synthesis method and a low-level adaptive component. The low-level part, neural network concurrent learning (NNCL), provides an estimate of the unknown plant to the high-level controller, which generates a pointwise optimal control signal via a QP-RCLBF. Control and safety constraints are enforced during the pointwise optimal control synthesis. First, the general setup of the optimizing control is described with regards to expected stabilization performance via a RCLF, where the added robust term compensates for $D(d, \Delta u)$ and other modeling error terms. The barrier constraints are then formulated to create desired safe sets. Since model uncertainty impacts both of these, the NNCL adaptive is deigned to estimate the unknown dynamics. These components are all unified and UUB of tracking and estimation signals is proven.

A. Control Lyapunov function (CLF) and pointwise min-norm control (PWMNC)

Utilize $\xi = [e, \dot{e}]^T$ to write (2.12) as

$$\dot{\xi} = F\xi + B(\epsilon_e + D + v_{opt}) \tag{2.54}$$

for which using the same Lyapunov function (2.28) and the CLF condition (2.33), the error trajectory ξ converges to zero with convergence rate $\frac{\alpha_3}{2\gamma}$, when ϵ_e and D vanish. To satisfy the CLF condition, the PWMNC law (2.39) can be applied with same $\Psi_0(\xi)$ and $\Psi_1(\xi)$ from (2.37), and the robust term $R(\xi) = K_r \|L_B V_\gamma(\xi)\|$ to compensate for unmeasurable disturbance $D(d, \Delta u)$. Using the PWMNC law (2.39), the RCLF condition (2.36) holds for sufficiently small $\epsilon_e + D$, relative to $R(\xi)$.

B. Zeroing control barrier function (ZCBF)

To impose a velocity constraint for the system at the moment a disturbance encountered, control barrier functions can be applied [23]. According to Definition 3, a controller is sought keeping the state within the super level-set

$$\mathcal{C} = \{x \in \Re^{n_s} : h(x) \geq 0\}, \tag{2.55}$$

where $h(x) : \Re^{n_s} \to \Re$ is a continuously differentiable ZCBF if

$$\dot{h}(x) + \alpha_4 h(x) \geq 0 \tag{2.56}$$

on the set Int$(\mathcal{C}) = \{x \in \Re^{n_s} : h(x) > 0\}$ for $\alpha_4 > 0$. Then, if the initial velocity starts in the set $\mathcal{C}$, it will stay in set $\mathcal{C}$ for all $t \geq 0$ (i.e., $\mathcal{C}$ is forward invariant). Here, a velocity constraint is desired to hold even in the presence of a disturbance. When a disturbance is encountered, the system velocity must be remained between a maximum velocity v_{max} and a minimum velocity v_{min} such that $v_{min} \leq x_2 \leq v_{min}$.

For this purpose, the associated positive ZCBFs are

$$h_1(x) = x_2 - v_{min} \geq 0 \quad \text{and} \qquad h_2(x) = v_{max} - x_2 \geq 0 \tag{2.57}$$

for which the equivalent ZCBF conditions to Eq. (2.56) are

$$\begin{aligned} &- v_{opt} + (\ddot{y}_d - v_{ad} + G - D) + \alpha_{4_1} h_1(x) \geq 0 \\ &v_{opt} - (\ddot{y}_d - v_{ad} + G - D) + \alpha_{4_2} h_2(x) \geq 0, \end{aligned} \tag{2.58}$$

where $\alpha_{4_i} > 0$ for $i = 1, 2$. Since G and D are unknown, the ZCBF conditions (2.58) are not realizable. To solve this issue, let us define $\epsilon_e = v_{ad} - (G - D)$ to obtain

$$\begin{aligned} -v_{opt} + \ddot{y}_d + \alpha_{4_1} h_1(x) &\geq \ \epsilon_e \\ v_{opt} - \ddot{y}_d + \alpha_{4_2} h_2(x) &\geq -\epsilon_e. \end{aligned} \tag{2.59}$$

In view of (2.59), with a proper estimation of G and compensation for D, the ZCBF constraints will be bounded in a neighborhood of size ϵ_e. The following section covers the design of the NNCL in conjunction with a fixed-point smoother to generate v_{ad} for the main control signal u and the ZCBF conditions (2.59) to be implementable.

C. Neuro-CL adaptive control (NNCL)

Here, a single hidden layer (SHL) perceptron NN serves as the universal approximator for the unknown part $G(x, u^*)$ [32, 33]. Thus, the adaptive part v_{ad} can be defined as

$$v_{ad}(\hat{W}_1, \hat{W}_2, x, u^*) = \hat{G}(x, u^*) = \hat{W_2}^T \sigma(Z), \tag{2.60}$$

where $Z = \hat{W_1}^T z \in \Re^{n_h}$; $z = [b_{in}, x, u^*]^T \in \Re^{(n_s+n_u+1)}$ is the input vector with bias $b_{in} \geq 0$ to the NN ; $\hat{W}_1 \in \Re^{(n_s+n_u+1)\times n_h}$ and $\hat{W}_2 \in \Re^{(n_h+1)}$ are NN weight matrices for the input later to hidden layer and hidden layer to output layer, respectively; n_s, n_u, and n_h are the number of the control, number of the states, and number of the hidden layer neurons, respectively; $\sigma(Z) = [b_\sigma, \sigma_1(Z_1), ..., \sigma_{n_h}(Z_{n_h})]^T \in \Re^{(n_h+1)}$ with bias $b_\sigma \geq 0$; and $\sigma_i(Z_i) = \frac{1}{1+e^{-a_i Z_i}}$ is the sigmoid activation function for $i = 1, ..., n_h$.

To achieve the best approximation of $G(x, u^*)$ (e.g., smallest bounded outcome $v_{ad} - G(x, u^*)$), the following CL adaptation laws update the weight matrices $\hat{W}_1$ and $\hat{W}_2$ [34]

$$\dot{\hat{W}}_1 = -\eta_{a1}\xi^T P_\gamma B z \hat{W}_2{}^T \dot{\sigma}(\hat{W}_1^T z) - \eta_{a1}\eta_e\|\xi\|\hat{W}_1 - \eta_{b1}\sum_{i=1}^{m} \hat{\epsilon}_{ei} z_i \hat{W}_2^T \dot{\sigma}(\hat{W}_1^T z_i) \tag{2.61}$$

$$\begin{aligned}\dot{\hat{W}}_2 =& -\eta_{a2}\xi^T P_\gamma B \left(\sigma(\hat{W}_1^T z) - \dot{\sigma}(\hat{W}_1^T z)\hat{W}_1^T z\right) - \eta_{a2}\eta_e\|\xi\|\hat{W}_2 \\ & - \eta_{b2}\sum_{i=1}^{m} \hat{\epsilon}_{ei}\left(\sigma(\hat{W}_1^T z_i) - \dot{\sigma}(\hat{W}_1^T z_i)\hat{W}_1^T zi\right),\end{aligned}$$

where η_{a1}, η_{a2}, η_{b1}, and η_{b2} are the adaptation convergence coefficients; and $\hat{\epsilon}_{ei}$ can be computed as follows

$$\hat{\epsilon}_{ei} = v_{ad_i} - \hat{M}(x_i, u_i^*, d, \Delta u) \text{ with } \hat{M} = \dot{\hat{x}}_2 - v_i, \tag{2.62}$$

where $\hat{M} = G - D$; $v = b_0 u^*$; and a fixed-point smoother computes $\hat{x}_2$ [30].

Remark 7. In the absence of the control defect and disturbance, $\hat{M} = G$ and in turn $\hat{\epsilon}_{ei} = v_{ad_i} - G$.

Remark 8. The violation of system velocity from the safe set $\mathcal{C}$ is bonded by ϵ_e whose estimated value is $\hat{\epsilon}_e = v_{ad} - \hat{M}$.

Remark 9. Recording data points: To achieve the best convergence of v_{ad} to G, the candidate point should be sufficiently different from the last point recorded to be eligible for storing. This way the history stack $H = [z_1, ..., z_m]$ will have at least $n_s + n_u + 1$ linearly independent columns (rank$(H) = n_s + n_u + 1$) and in turn provide full-rank updates in Eq. (2.61) for exponential convergence.

D. Unified controller

The PWMNC law (2.39) resolves the RCLF condition. This section formulates an online closed-loop QP to satisfy the RCLF condition (2.36), and to apply control bounds and velocity constraints (2.59) to the system. Meanwhile, $G(x, u)$ is estimated by the NNCL adaptive part and $D(d, \Delta u)$ is compensated by the robust part $R(\xi)$. The main control signal u is enforced to be bounded by two control bounds (CBs), such that $CB_1 : u \leq u_{max}$ and $CB_2 : -u_{max} \leq u$. Due to

Remark 1, the QP with the above design requirements can be formulated as

$$
\begin{aligned}
\mathbf{v_{opt}} = & \underset{(\mathbf{d},\mathbf{v_{opt}})\in\Re^{nu+1}}{\text{argmin}} \quad \mathbf{v_{opt}}^T\mathbf{v_{opt}} + l\mathbf{d}^2 \\
\text{s.t.}\ & \text{RCLF}:\ -\mathbf{d} + \Psi_1^T(\xi)\mathbf{v_{opt}} \le -\Psi_0(\xi) \\
& \text{ZCBF}_1:\ +\mathbf{v_{opt}} \le \alpha_{4_1} h_1(x) + (\ddot{y}_d - \hat{\epsilon}_e) \\
& \text{ZCBF}_2:\ -\mathbf{v_{opt}} \le \alpha_{4_2} h_2(x) - (\ddot{y}_d - \hat{\epsilon}_e) \\
& \text{CB}_1:\ +\mathbf{v_{opt}} \le b_0 u_{max} + u_s \\
& \text{CB}_2:\ -\mathbf{v_{opt}} \le b_0 u_{max} - u_s,
\end{aligned}
\tag{2.63}
$$

where $u_s = -v_{ad} + \ddot{y}_d$ and l is a penalty coefficient to relax the RCLF constraint when the CB and ZCBF are applied.

Remark 10. The control bounds (CBs) and the velocity bounds (ZCBFs) may not be jointly realizable when an external disturbance is encountered even if the RCLF constraint is highly relaxed (small l). Feasibility of the optimization problem (2.63) depends on (i) the underlying nonlinear control system, (ii) the magnitude of the disturbance, (iii) the state of the system at its onset, and (iv) whether the CBs and ZCBFs are in conflict. Under this circumstance, a priority should be made by the engineer to determine which constraint is more important; the other constraint should be dropped or relaxed.

E. Stability analysis

This section provides a unified stability analysis of the QP controller, NNCL adaptive estimator, and RCLF part. Consider the following candidate Lyapunov function

$$
V(\tilde{W}_1, \tilde{W}_2, \xi) = \frac{1}{2}\text{tr}\left(\tilde{W}_1^T \eta_1^{-1} \tilde{W}_1\right) + \frac{1}{2}\tilde{W}_2^T \eta_2^{-1} \tilde{W}_2 + \frac{1}{2}\xi^T P_\gamma \xi, \tag{2.64}
$$

where tr$(.)$ stands for trace of a matrix. To simplify the stability analysis, let $\eta_1 = \eta_{a1} = \eta_{b1}$ and $\eta_2 = \eta_{a2} = \eta_{b2}$.

Theorem 2. *Assume both disturbance d and control defect Δu are bounded, and y_d is exciting over a finite interval. Given the Lyapunov function (2.64), the QP program (2.63), and the adaptation mechanism (2.61), if rank$(H) = n_s + n_u + 1$, then $(\xi, \tilde{W})$ is UUB for unknown b, unstructured dynamics $f(x)$, and any $x(0)$ [35].*

Proof. Define $\tilde{W}_1 = \hat{W}_1 - W_1^*$ and $\tilde{W}_2 = \hat{W}_2 - W_2^*$. Taking the derivative (2.64) gives

$$\dot{V} = \text{tr}\left(\tilde{W}_1^T \eta_1^{-1} \dot{\hat{W}}_1\right) + \tilde{W}_2^T \eta_2^{-1} \dot{\hat{W}}_2 + \xi^T P_\gamma \dot{\xi}. \tag{2.65}$$

Substituting the error dynamics (2.12) into (2.65) yields

$$\dot{V} = \xi^T P_\gamma F \xi + \xi^T P_\gamma B(v_{opt} + v_{ad} - G + D) + \text{tr}\left(\tilde{W}_1^T \eta_1^{-1} \dot{\hat{W}}_1\right) + \tilde{W}_2^T \eta_2^{-1} \dot{\hat{W}}_2. \tag{2.66}$$

Using (2.27), the first term of (2.66) is given as

$$\begin{aligned}\dot{V} =& \frac{1}{2\gamma}\xi^T \left(P_\gamma B B^T P_\gamma\right)\xi - \frac{1}{2\gamma}\xi^T D_\gamma Q D_\gamma \xi + \xi^T P_\gamma B(v_{opt} + v_{ad} - G + D) \\ &+ \text{tr}\left(\tilde{W}_1^T \eta_1^{-1} \dot{\hat{W}}_1\right) + \tilde{W}_2^T \eta_2^{-1} \dot{\hat{W}}_2.\end{aligned} \tag{2.67}$$

Case 1: $\Psi_0(\xi) > 0$

For this case, incorporating the first condition of (2.39) instead of v_{opt} into (2.67) gives

$$\begin{aligned}\dot{V} =& \frac{1}{2\gamma}\xi^T \left(P_\gamma B B^T P_\gamma\right)\xi - \frac{1}{2\gamma}\xi^T D_\gamma Q D_\gamma \xi + \xi^T P_\gamma B(v_{ad} - G + D) + \text{tr}\left(\tilde{W}_1^T \eta_1^{-1} \dot{\hat{W}}_1\right) \\ &+ \tilde{W}_2^T \eta_2^{-1} \dot{\hat{W}}_2 - \frac{1}{2}\xi^T \left(P_\gamma F + F^T P_\gamma\right)\xi - \frac{\alpha_3}{2\gamma}\xi^T P_\gamma \xi - K_r \|\xi^T P_\gamma G\|.\end{aligned} \tag{2.68}$$

Substituting $P_\gamma F + F^T P_\gamma$ from (2.27) into (2.68) and canceling the similar terms yields

$$\dot{V} = -\frac{\alpha_3}{2\gamma}\xi^T P_\gamma \xi + \text{tr}\left(\tilde{W}_1^T \eta_1^{-1} \dot{\hat{W}}_1\right) + \tilde{W}_2^T \eta_2^{-1} \dot{\hat{W}}_2 - K_r \|\xi^T P_\gamma B\| + \xi^T P_\gamma B(v_{ad} - G + D). \tag{2.69}$$

Substitution of the NNCL adaptation laws (2.61) into (2.69) and noting that

$$v_{ad} - G = \hat{W_2}^T \sigma(\hat{W}_1^T z) - W_2^{*T} \sigma({W_1}^{*T} z) \tag{2.70}$$

gives

$$\begin{aligned}
\dot{V} =& \xi^T P_\gamma B \left(\hat{W_2}^T \sigma(\hat{W}_1^T z) - W_2^{*T} \sigma({W_1}^{*T} z) \right) - \tilde{W}_2^T \xi^T P_\gamma B \left(\sigma(\hat{W}_1^T z) - \dot{\sigma}(\hat{W}_1^T z) \hat{W}_1^T z \right) \\
& - \tilde{W}_2^T \sum_{i=1}^{m} \hat{\epsilon}_{ei} \left(\sigma(\hat{W}_1^T z_i) - \dot{\sigma}(\hat{W}_1^T z_i) \hat{W}_1^T zi \right) - \tilde{W}_2^T \eta_e \|\xi\| \hat{W}_2 - \text{tr} \left(\eta_e \tilde{W}_1^T \|\xi\| \hat{W}_1 \right) \\
& - \text{tr} \left(\tilde{W}_1^T \xi^T P_\gamma B z \hat{W_2}^T \dot{\sigma}(\hat{W}_1^T z) \right) - \text{tr} \left(\tilde{W}_1^T \sum_{i=1}^{m} \hat{\epsilon}_{ei} z_i \hat{W}_2^T \dot{\sigma}(\hat{W}_1^T z_i) \right) \\
& - \frac{\alpha_3}{2\gamma} \xi^T P_\gamma \xi - K_r \|\xi^T P_\gamma B\| + \xi^T P_\gamma B D.
\end{aligned} \tag{2.71}$$

Utilizing the first-order Taylor approximation of $\sigma({W_1}^{*T} z)$ about the weight W_1 as [22]

$$\sigma({W_1}^{*T} z) = \sigma(\hat{W}_1^T z) - \dot{\sigma}(\hat{W}_1^T z) \tilde{W}_1^T z, \tag{2.72}$$

the first line of Eq. (2.71) can be written as

$$\begin{aligned}
\hat{W_2}^T \sigma(\hat{W}_1^T z) - W_2^{*T} \sigma({W_1}^{*T} z) =& \tilde{W}_2^T \sigma(\hat{W}_1^T z) + \hat{W}_2^T \dot{\sigma}(\hat{W}_1^T z) \tilde{W}_1^T z \\
& - \tilde{W}_2^T \dot{\sigma}(\hat{W}_1^T z) \hat{W}_1^T z + \tilde{W}_2^T \dot{\sigma}(\hat{W}_1^T z) {W_1}^{*T} z
\end{aligned}$$

whose substitution into (2.71) and canceling similar terms gives

$$\dot{V} = -\tilde{W}_2^T \sum_{i=1}^{m} \hat{\epsilon}_{ei} \left(\sigma(\hat{W}_1^T z_i) - \dot{\sigma}(\hat{W}_1^T z_i)\hat{W}_1^T zi \right) - \text{tr}\left(\tilde{W}_1^T \sum_{i=1}^{m} \hat{\epsilon}_{ei} z_i \hat{W}_2^T \dot{\sigma}(\hat{W}_1^T z_i) \right) + \xi^T P_\gamma B D \tag{2.73}$$

$$- \tilde{W}_2^T \eta_e \|\xi\| (\tilde{W}_2 + W_2^*) - \text{tr}\left(\eta_e \tilde{W}_1^T \|\xi\| (\tilde{W}_1 + W_1^*) \right)$$
$$- \frac{\alpha_3}{2\gamma} \xi^T P_\gamma \xi - K_r \|\xi^T P_\gamma B\| + \xi^T P_\gamma B \tilde{W}_2^T \dot{\sigma}(\hat{W}_1^T z) {W_1^*}^T z,$$

where $\hat{\epsilon}_{ei}$ can be written as

$$\hat{\epsilon}_{ei} = v_{ad_i} - \hat{G}(x_i, u_i^*) = v_{ad_i} - G(x_i, u_i^*) + \epsilon_{si} = \hat{W}_2{}^T \sigma(\hat{W}_1^T z_i) - {W_2^*}^T \sigma({W_1^*}^T z_i) + \epsilon_{si} \tag{2.74}$$

such that $\epsilon_s = G - \hat{G}$ is the estimation error of the fixed-point smoother.

Utilizing the first-order Taylor approximation of $\sigma({W_1^*}^T z_i)$ about the weight W_1 (similarly as Eqs. (2.72) and (2.73)), Eq. (2.74) can be written as

$$\hat{\epsilon}_{ei} = \tilde{W}_2^T \sigma(\hat{W}_1^T z_i) + \hat{W}_2^T \dot{\sigma}(\hat{W}_1^T z_i)\tilde{W}_1^T z_i - \tilde{W}_2^T \dot{\sigma}(\hat{W}_1^T z_i)\hat{W}_1^T z_i + \tilde{W}_2^T \dot{\sigma}(\hat{W}_1^T z_i){W_1^*}^T z_i + \epsilon_{si}. \tag{2.75}$$

By adding and subtracting $\sum_{i=1}^{m} \hat{\epsilon}_{ei}\hat{\epsilon}_{ei}^T$ in (2.73), substituting (2.75) into it, and canceling the similar terms, (2.73) can be written as

$$\begin{aligned} \dot{V} = & -\frac{\alpha_3}{2\gamma} \xi^T P_\gamma \xi - K_r \|\xi^T P_\gamma B\| + \xi^T P_\gamma B \left(\tilde{W}_2^T \dot{\sigma}(\hat{W}_1^T z){W_1^*}^T z + D \right) \\ & - \sum_{i=1}^{m} \hat{\epsilon}_{ei}\hat{\epsilon}_{ei}^T + \sum_{i=1}^{m} (\tilde{W}_2^T \dot{\sigma}(\hat{W}_1^T z_i){W_1^*}^T z_i + \epsilon_{si})\hat{\epsilon}_{ei}^T - \tilde{W}_2^T \eta_e \|\xi\| (\tilde{W}_2 + W_2^*) \\ & - \text{tr}\left(\eta_e \tilde{W}_1^T \|\xi\| (\tilde{W}_1 + W_1^*) \right) \end{aligned} \tag{2.76}$$

from which one has

$$\dot{V} \leq -\frac{\alpha_3}{2\gamma}\lambda_{min}(P_\gamma)\|\xi\|^2 - K_r\|\xi^T P_\gamma B\| + \|\xi^T P_\gamma B\|\left(\|\tilde{W}_2^T\dot{\sigma}(\hat{W}_1^T z){W_1^*}^T z\| + |D|\right) \tag{2.77}$$
$$-\sum_{i=1}^{m}\|\hat{\epsilon}_{ei}\|^2 + \sum_{i=1}^{m}\|\hat{\epsilon}_{ei}\|(\|\tilde{W}_2^T\dot{\sigma}(\hat{W}_1^T z_i){W_1^*}^T z_i\| + |\epsilon_{si}|) - \eta_e\|\xi\|\left(\|\tilde{W}_2\|^2 + \|\tilde{W}_1\|^2\right)$$
$$+\eta_e\|\xi\|\left(\|\tilde{W}_2\|\|W_2^*\| + \|\tilde{W}_1\|\|W_1^*\|\right).$$

Let

$$\begin{aligned}
&\|\hat{\epsilon}_{ei}\| \leq \bar{\epsilon}_{ei} \\
&|\epsilon_{si}| \leq \bar{\epsilon}_{si} \\
&\|\tilde{W}_2^T\dot{\sigma}(\hat{W}_1^T z){W_1^*}^T z\| \leq Q_1 \\
&\|\tilde{W}_2^T\dot{\sigma}(\hat{W}_1^T z_i){W_1}^{*T} z_i\| \leq Q_2 \\
&|D| \leq \bar{D} \\
&\tilde{W} = [\|\tilde{W}_1\|, \|\tilde{W}_2\|]^T \\
&W^* = [\|W_1^*\|, \|W_2^*\|]^T
\end{aligned} \tag{2.78}$$

with $Q_1, Q_2, \bar{\epsilon}_{ei}, \bar{\epsilon}_{si}, \bar{D} > 0$ to obtain

$$\dot{V} \leq -\frac{\alpha_3}{2\gamma}\lambda_{min}(P_\gamma)\|\xi\|^2 - \|\xi^T P_\gamma B\|\left(K_r - Q_1 - \bar{D}\right) - \sum_{i=1}^{m}\bar{\epsilon}_{ei}^2 + \sum_{i=1}^{m}\bar{\epsilon}_{ei}(Q_2 + \bar{\epsilon}_{si})$$
$$-\eta_e\|\xi\|\|\tilde{W}\|^2 + \eta_e\|\xi\|\|\tilde{W}\|\|W^*\|. \tag{2.79}$$

Choosing $K_r = \alpha_5 + Q_1 + \bar{D}$ with $\alpha_5 > 0$ and assuming that $\|W^*\| \leq \bar{W}^*(\bar{W}^* > 0)$, Eq. (2.79) reduces to

$$\dot{V} \leq -\frac{\alpha_3}{2\gamma}\lambda_{min}(P_\gamma)\|\xi\|^2 - \alpha_5\|P_\gamma B\|\|\xi\| - \sum_{i=1}^{m}\bar{\epsilon}_{ei}^2 + \sum_{i=1}^{m}\bar{\epsilon}_{ei}(Q_2 + \bar{\epsilon}_{si}) \tag{2.80}$$
$$- \eta_e\|\xi\|\|\tilde{W}\|^2 + \eta_e\bar{W}^*\|\xi\|\|\tilde{W}\|.$$

For a sufficiently large convergence rate γ and robust gain α_5, $\dot{V} \leq 0$ outside of the following balls:

$$\|\xi\| \geq \frac{C_1 + \sqrt{C_1^2 + \frac{2\alpha_3}{\gamma}\lambda_{min}(P_\gamma)C_2}}{\frac{\alpha_3}{\gamma}\lambda_{min}(P_\gamma)} : B_\xi \tag{2.81}$$
$$\|\tilde{W}\| \geq \frac{C_3 + \sqrt{C_3^2 + 4\eta_e\|\xi\|C_4}}{\eta_e\|\xi\|} : B_{\tilde{W}},$$

where

$$C_1 = \eta_e\bar{W}^*\|\tilde{W}\| - \eta_e\|\tilde{W}\|^2 - \alpha_5\|P_\gamma B\| \tag{2.82}$$
$$C_2 = \sum_{i=1}^{m}\bar{\epsilon}_{ei}(Q_2 + \bar{\epsilon}_{si}) - \sum_{i=1}^{m}\bar{\epsilon}_{ei}^2$$
$$C_3 = \eta_e\bar{W}^*\|\xi\|$$
$$C_4 = C_2 - \left(\frac{\alpha_3}{2\gamma}\lambda_{min}(P_\gamma)\|\xi\|^2 + \alpha_5\|P_\gamma B\|\|\xi\|\right).$$

Case 2: $\Psi_0(\xi) \leq 0$

In this case, $\Psi_0(\xi) \leq 0$ implies that

$$L_F V_\gamma(\xi) \leq -\frac{\alpha_3}{\gamma}V_\gamma(\xi) - R(\xi) = -\frac{\alpha_3}{\gamma}\xi^T P_\gamma \xi - 2K_r\|\xi^T P_\gamma G\|. \tag{2.83}$$

Since $\xi^T P_\gamma F\xi = \frac{1}{2}L_F V_\gamma(\xi)$, we have

$$\xi^T P_\gamma F\xi \leq -\frac{\alpha_3}{2\gamma}\xi^T P_\gamma \xi - K_r\|\xi^T P_\gamma G\|. \tag{2.84}$$

Now, substituting $v_{opt} = 0$ and (2.84) into (2.66), and following the same steps results in the same balls presented in (2.81). $\square$

Remark 11. Theorem 2 shows that in both cases I and II, all system solutions are UUB. It implies that the unified proposed controller renders the bounded solution for the tracking error trajectories and estimation errors to the compact balls B_ξ and $B_{\tilde{W}}$, respectively. The boundedness of system solutions to these balls are only guaranteed under the assumption of boundedness of $D(d, \Delta u)$ i.e., both disturbance and control defect are bounded.

Remark 12. Proof of the Theorem 2 shows that the system solutions are bounded inside the compact balls B_ξ and $B_{\tilde{W}}$ as

$$\|\xi\| \leq B_\xi(\tilde{W}, K_r - D, \gamma) \quad \text{and} \quad \|\tilde{W}\| \leq B_{\tilde{W}}(\xi, K_r - D, \eta_e). \tag{2.85}$$

This shows that with a good dynamic estimation and compensation of D, the error trajectory converges to a smaller neighborhood of the origin compared with baseline non-adaptive QP-CLBF, while no high value of γ is needed. In addition, convergence of the barrier function to a smaller ball is guaranteed. Thus, the proposed controller performs better with regard to the tracking performance and control effort with the same convergence coefficient as used for non-adaptive baseline method.

2.4 Simulation results for QP-ARCLF and QP-ARCLBF

2.4.1 Improved results of QP-ARCLF over baseline QP-CLF

To show the performance of the proposed approach QP-ARCLF, we apply our controller to an illustrative nonlinear system example. We then compare the proposed method with the baseline QP-CLF regarding to the control optimality, tracking performance, and robustness to the system parameter and control coefficient uncertainties.

Design parameters of the controllers are tuned as $\gamma = 2$, $u_{max} = 3$, $l = 100$, $\eta_a = \eta_b = 1$, and

$m_{max} = 5$. Consider the following nonlinear second-order inverted pendulum system as:

$$\dot{x}_1 = x_2 \qquad (2.86)$$
$$\dot{x}_2 = \sin(x_1) - x_2|x_2| + u,$$

where $x = [x_1, x_2]^T$ is the vector of angular position and angular velocity; u is the joint torque; $\Phi(x) = [\sin(x_1), x_2|x_2|]^T \in \Re^2$, $\theta^* = [1, -1]^T \in \Re^2$, and $b = 1$.

A. Evaluation of the proposed controller

Fig. 2.3 shows tracking performance of both position and velocity of the inverted pendulum for the proposed controller QP-ARCLF. It can be seen that the system states accurately track the desired trajectories with a root mean square error (RSME) of 0.016 rad for position tracking and 0.022 rad/s for velocity tracking. Fig. 2.3 also shows the joint torque u and the optimal control signal v_{opt}, which are optimized by the QP framework (2.40). It is seen that v_{opt} is minimized to zero, when the history stack becomes full rank (rank(Z)=2) and in turn the system dynamics are fully identified by the adaptation mechanism.

Fig. 2.4 demonstrates estimation performance for the parameter vector $\hat{\theta}$ using the CL adaptation mechanism (2.41). As expected from Theorem1, the estimated parameters exponentially converge to a compact ball around their true values when rank(Z)=2. Fig. 2.4 illustrates estimation performance of the unknown dynamics $f(x)$ and convergence of its estimation error $\hat{\epsilon}_{ei}$ for $i = 1, ..., m_{max} = 5$. It can be observed that after getting the rank condition satisfied, $f(x)$ is accurately identified. This figure also shows convergence of all $\hat{\epsilon}_{ei}$, which implies that estimated stored unknown dynamics converge to the current estimate of the unknown dynamics for all relating columns of the history stack. It shows that $\hat{f}(x)$ in (2.42) converges to a compact ball around $f(x)$.

B. Performance comparison with baseline QP-CLF

To test robustness and control optimality of the proposed controller QP-ARCLF, a robustness

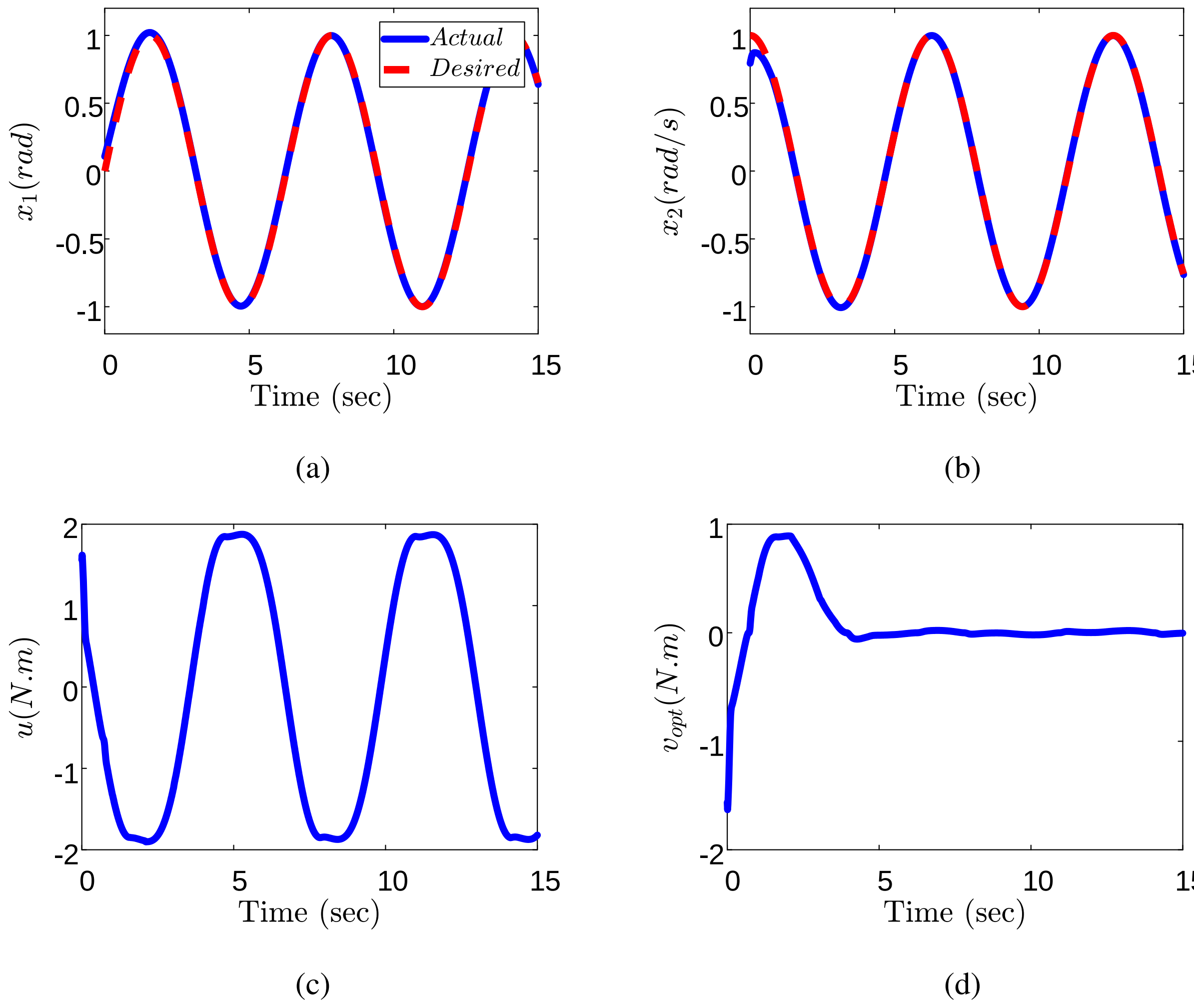

Figure 2.3: Results of QP-ARCLF: tracking performance and control effort. The control v_{opt} vanishes when the system is identified.

test is performed over the baseline QP-CLF controller. In this test, the system parameters θ and the control coefficient b are perturbed so the uncertainties $\Delta\theta$ and Δb are iteratively changed with a resolution of 10% from -50% to +50%. Fig. 2.5 shows that the tracking performance $\mathrm{RMSE_x}$ of the proposed controller remains unchanged and consistent for positive values of $\Delta\theta$ while the baseline QP-CLF controller has increasing tracking error. An increasing trend is observed on $\mathrm{RMSE_x}$ for both controllers as Δb increases for negative values of $\Delta\theta$. However, tracking performance of the proposed controller is still better than the baseline controller. Fig. 2.5 also shows that although the control cost $\mathrm{RMSE_u}$ of the proposed controller is lower than the one for the baseline controller,

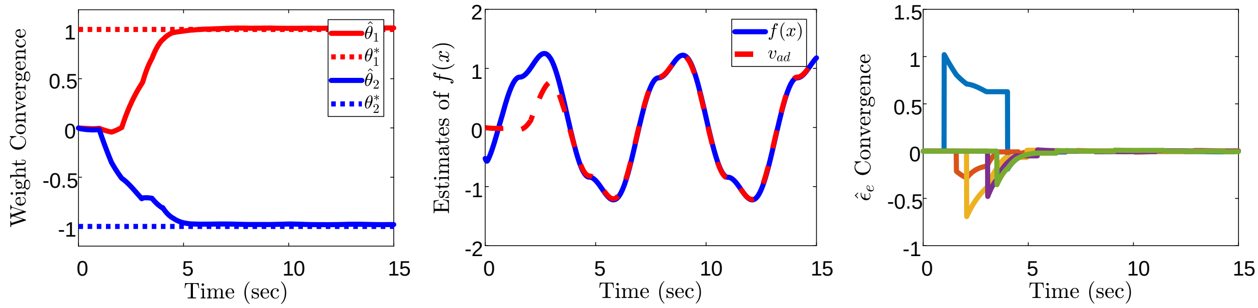

Figure 2.4: Results of QP-ARCLF: the left figure shows weight convergence, the middle figure shows estimation performance of the unknown dynamics $f(x)$, and the right figure shows convergence of its estimation error $\hat{\epsilon}_{ei}$ for $i = 1, ..., m_{max}$.

both controllers perform similarly regarding the control effort for perturbed parameters. This figure in general shows that the surfaces of $\mathrm{RMSE_x}$ and $\mathrm{RMSE_u}$ for the proposed controller remain always below the baseline controller, implying better tracking performance and control optimality of the proposed approach over the baseline method.

Fig. 2.6 illustrates RMSE values of weight convergence and $\hat{\epsilon}_e$ convergence in the presence of $\Delta\theta$ and Δb. It is seen that although the error values increase as the parameter uncertainties increase, the RMSE values are bounded in small balls around the origin.

2.4.2 Improved results of QP-ARCLBF over baseline QP-CLBF

In this section, the effectiveness of QP-ARCLBF is shown by performing simulation studies on the same inverted pendulum, which is now affected by an unknown disturbance d. In the simulation, θ and $\dot{\theta}$ are the position and velocity of the pendulum, and the system dynamics are assumed to be structurally unknown. The controller parameters chosen are (i) dynamic estimation: $\eta_{a1} = \eta_{a2} = \eta_{b1} = 1$, $\eta_{b2} = 5$, $\eta_e = 1$ (adaptation convergence rate), $b_\sigma = b_{in} = 1$ (network bias), $m = 5$ (number of recorded data), $n_u = 1$ (input number), $n_s = 2$ (state number), $n_h = 8$ (hidden layer number); (ii) safety constraint: $\alpha_{4_1} = \alpha_{4_2} = 100$; (iii) control constraint: $u_{max} = 2$; (iv) tracking error convergence rate: $\gamma = 1$; (v) robust gain: $K_r = 1.2$; and (vi) relaxing coefficient of RCLF constraint: $l = 20$.

A. Tracking and estimation performances

In this section, the main control signal u should not exceed from $\pm$ 2 N.m. The tracking performance and control effort of the proposed controller QP-ARCLBF are illustrated in Fig. 2.7. From Figs. 2.7(a) and 2.7(b), it can be seen that both position and velocity of the inverted pendulum can accurately track the desired trajectories even when the initial value of the states and references are different from each other. Fig 2.7(c) shows that the error trajectories of the system remain uniformly ultimately bounded based on what we claimed through Theorem 2. In other words, the error trajectories certainly lie inside the ball B_ξ derived in the proof. Fig 2.7(d) shows the main control torque u and the internal signal v_{opt} from the high-level controller. It is observed that solution of the proposed optimization-based controller i.e., v_{opt} is minimized when the unknown dynamics are identified and the error signals enter the compact ball.

Figs 2.8(a) and 2.8(b) show that the NN weights $\hat{W}_1$ and $\hat{W}_2$ get settled when the history stack H meets the rank condition i.e., rank$(H) = n_s + n_u + 1 = 4$. This implies that the weight estimation error definitely converges to the ball $B_{\tilde{W}}$ around its true value as expected from the proof of Theorem 2. In turn, $\hat{G}$ converge to a compact ball around G as observed from Fig 2.8(c). Fig 2.8(d) shows that $v_{ad} - \hat{M}$ converges when rank$(H) = 4$, which implies convergence of the NN output to the estimated unknown dynamics for different stored data of the history stack.

B. Performance comparison with baseline QP-CLBF

In this section, superiority of the proposed QP-ARCLBF over the baseline QP-CLBF is shown via a robustness test. Simulation is carried out with perturbed system parameters and control coefficient for different values of disturbance d and barrier coefficient β to evaluate performance of the controllers with regard to tracking performance, control optimality, and velocity violation Δ_v form the safe set. Here, the velocity constraints are actively enforced to see how different controllers react at the moment when the disturbance (unexpected push) encountered. For the sake of a fair comparison, design parameters of the controllers are chosen to be same. The velocity constraints are formulated as ZCBF: -1 rad/s $\leq \dot{\theta} \leq 1$ rad/s. In the simulation, system parameters

p and control coefficient b are both perturbed by +50$\%$ from their nominal values, while different values of $d(t)$ are applied to the system each time at $t = 30sec$. The applied disturbance takes different values $d = 3, 4, 5, 6$ N.m.

Figure 2.9 demonstrates barrier violation, tracking performance, and control cost in the presence of the perturbed parameters over different values of d and β for the proposed and baseline controllers. Fig 2.9(a) shows that the barrier violation Δ_v under the proposed controller remains unchanged and consistent during the variations of β and d. However, when the baseline controller is used, Δ_v is variable and increases as d increases and/or β decreases. It shows that the proposed controller is robust against different values of d and β. However, the baseline controller is sensitive to the parameters β and d such that barrier violation significantly decreases as β increases. Thus, to achieve a good and robust safety permanence, the proposed controller does not require a high value of β, which may cause higher control effort and peak torque on the system.

Figure 2.9(b) demonstrates that the $\mathrm{RMSE_x}$ surface of the proposed controller is always below the surface of the baseline one, showing better robustness of QP-ARCLBF over variations of d and β. Figs 2.9(c) and (d) show that the proposed controller requires less average control effort $\mathrm{RMSE_u}$ and peak torque u_{max} for different values of β and d when the system parameters are perturbed by 50$\%$. From the robustness tests, the conclusion that can be drawn is that the proposed controller generates the lower values of Δ_v, $\mathrm{RMSE_x}$, $\mathrm{RMS_u}$, and u_{max} for different values of β and d, showing that the proposed approach improves safety performance, control optimality, and robustness over the non-adaptive baseline QP-CLBF.

2.5 Conclusions and next chapter

This chapter presented two robust QP-based adaptive control approaches for nonlinear systems with structured and unstructured uncertainties. The unified multi-objective controllers were able to estimate the unknown nonlinear dynamics and robustify the closed-loop system in the presence of unmodeled dynamics and disturbances in an optimal control fashion. UUB of all system's solutions was proven through Theorems 1 and 2 by using Lyapunov arguments. Simulations and comparisons to baseline controllers (QP-CLF and QP-CLBF) on an illustrative nonlinear example confirmed the benefits of our approaches with regard to safety performance, tracking accuracy, and robustness to disturbances. While the presented approaches can be applied to a wide range of uncertain fully actuated nonlinear systems, their applications to underactuated systems have to be taken into consideration. This naturally encourages us to extend the presented approaches for the active control of underactuated systems in the presence of modeling error and disturbances; this will be formulated in the next chapter.

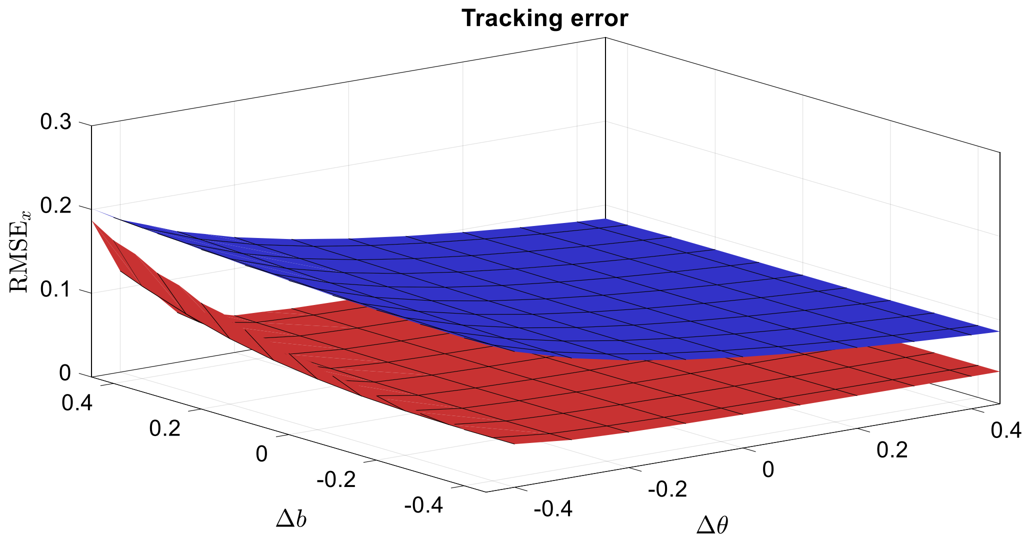

(a) Tracking performance

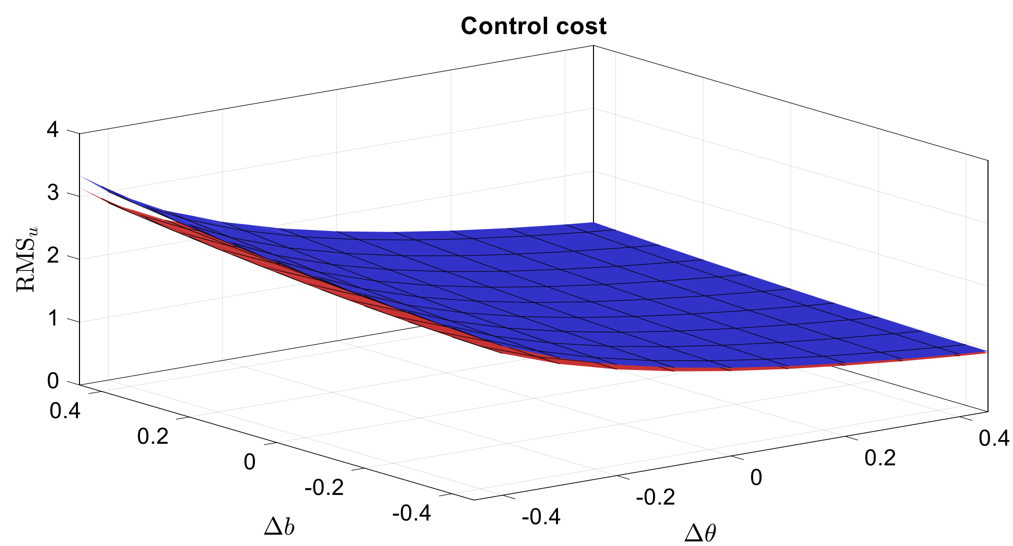

(b) Control optimality

Figure 2.5: Performance of different controllers in the presence of $\Delta\theta$ and Δb; red surface shows the behavior for the proposed controller QP-ARCLF and the blue one is for the baseline controller QP-CLF.

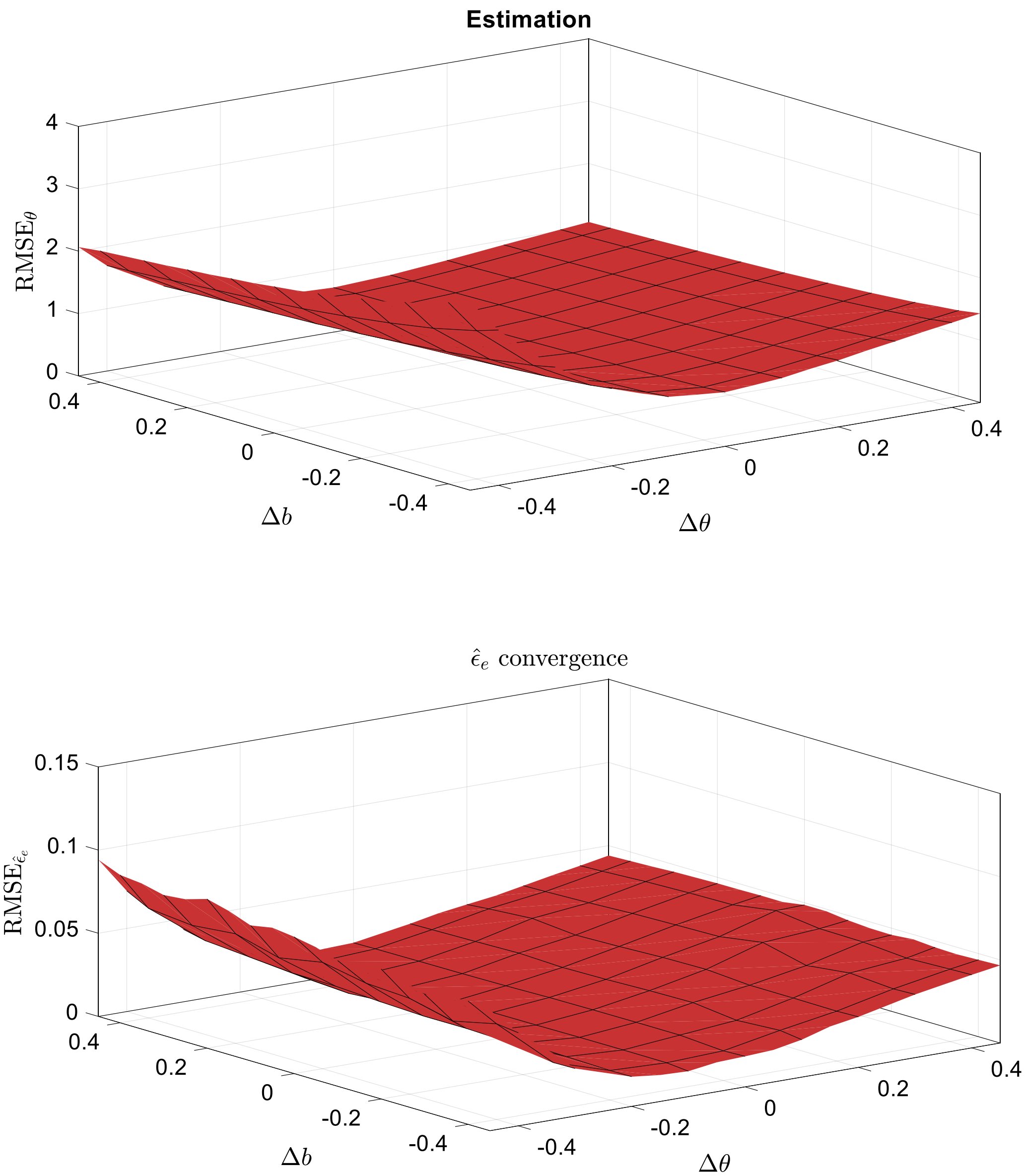

Figure 2.6: Performance of the proposed controller in the presence of $\Delta\theta$ and Δb.

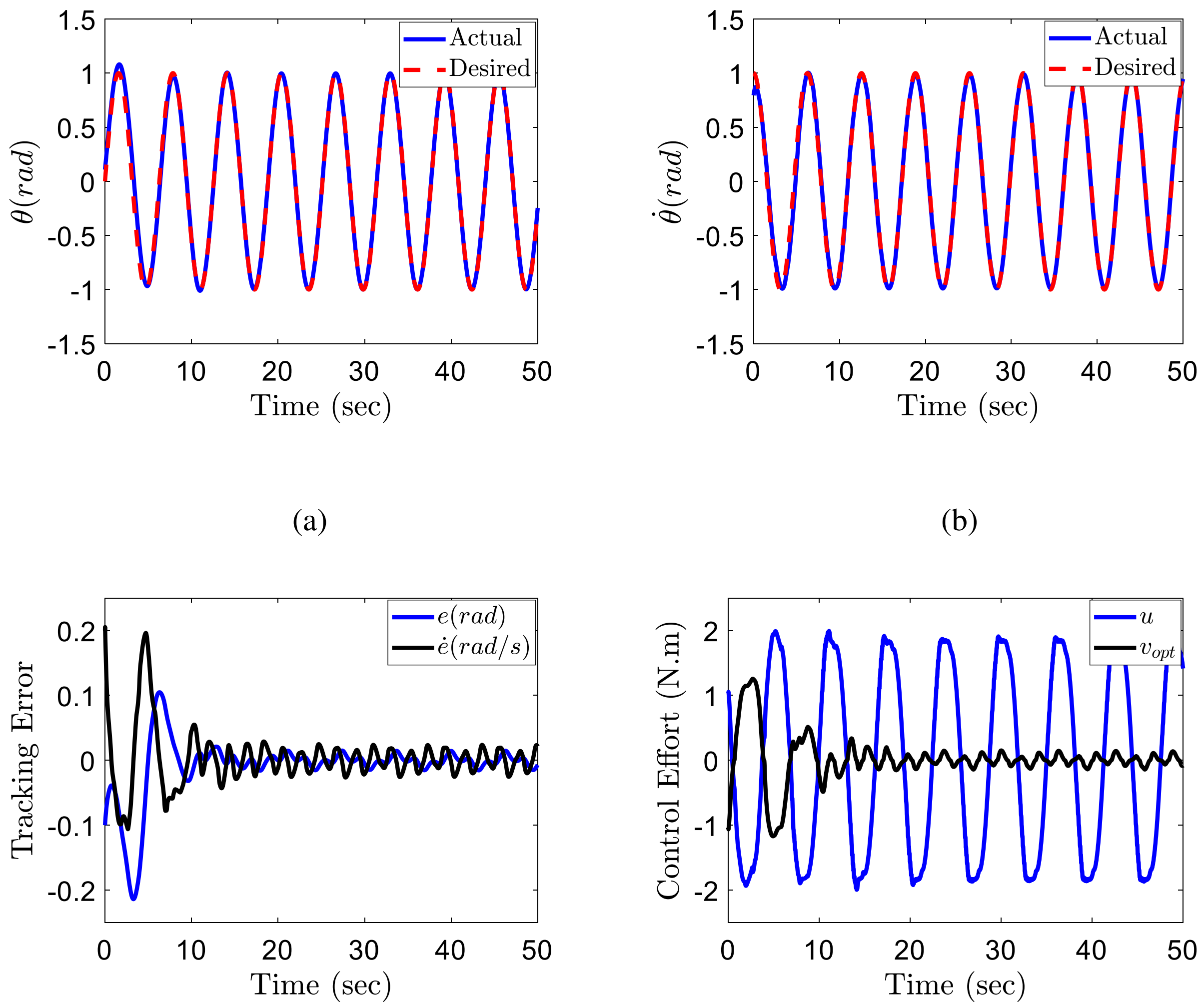

(a) (b) (c) (d)

Figure 2.7: Results of QP-ARCLBF: tracking performance and control effort

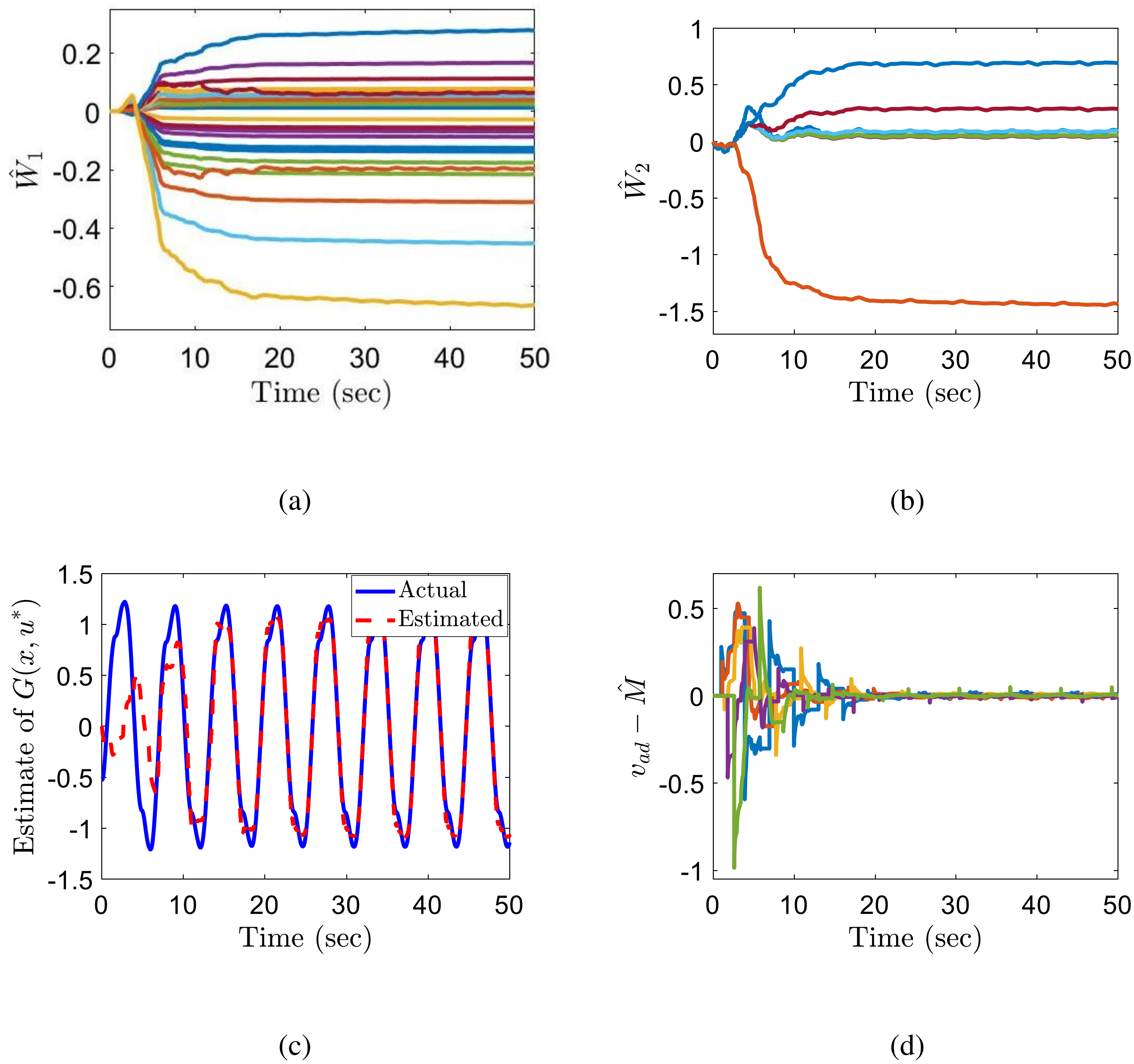

(a) (b)

(c) (d)

Figure 2.8: Results of QP-ARCLBF: estimation performance

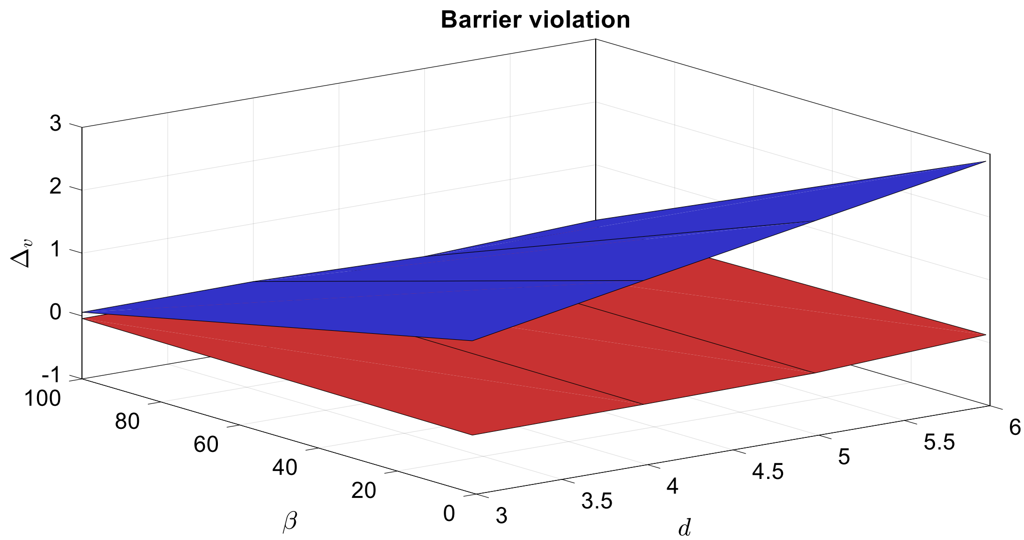
Barrier violation
3
2
1
0
-1
Δ_v
100
80
60
40
20
0
β
3
3.5
4
4.5
5
5.5
6
d

(a)

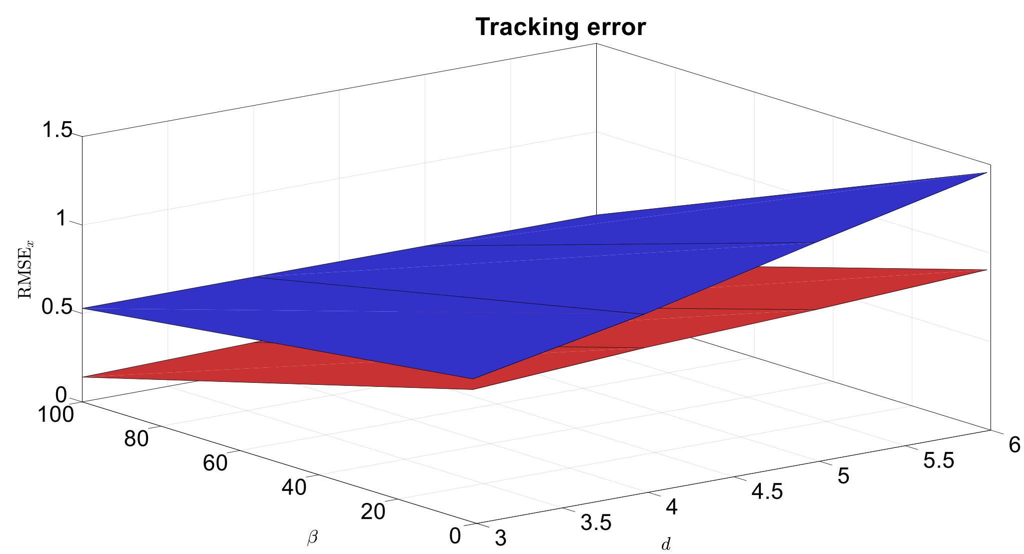
Tracking error
1.5
1
0.5
0
RMSE_x
100
80
60
40
20
0
β
3
3.5
4
4.5
5
5.5
6
d

(b)

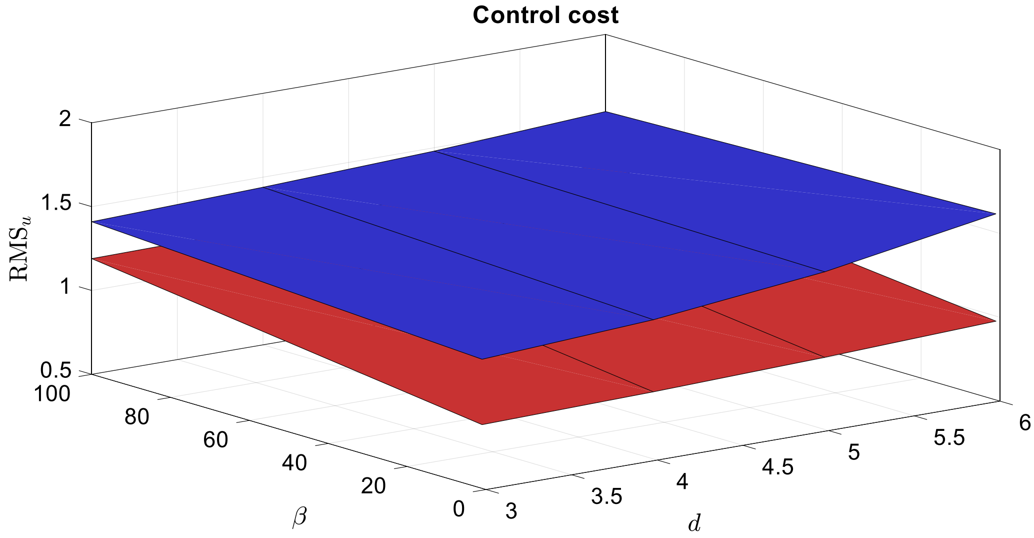

(c)

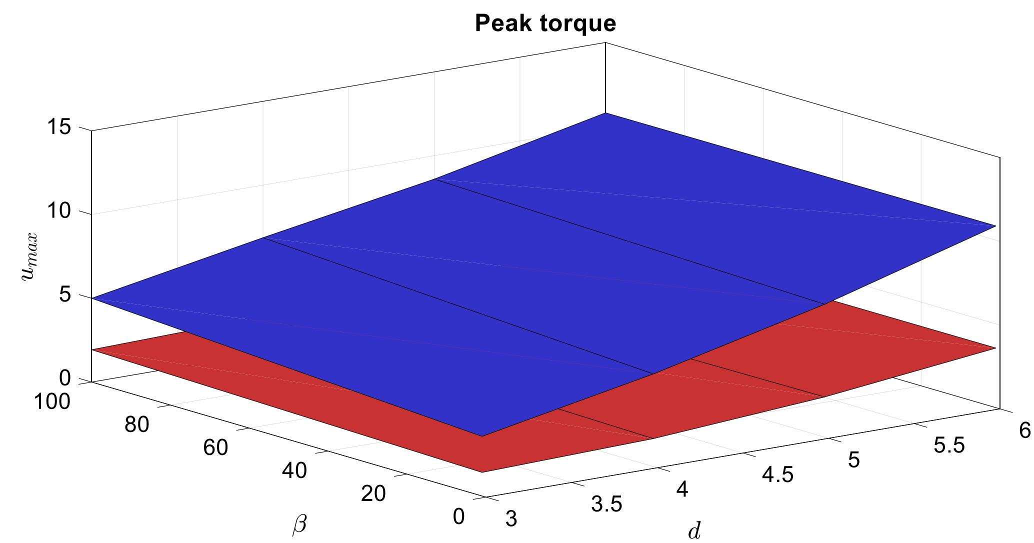

(d)

Figure 2.9: Barrier violation, tracking performance, and control cost in the presence of the perturbed parameters Δp=50% and Δb=50% over different values of d and β for the proposed QP-ARCLBF and baseline QP-CLBF. Red surface shows the behavior for the proposed controller and the blue one is for the baseline controller.

CHAPTER 3

ACTIVE (COLLOCATED) SPACE CONTROL OF UNDERACTUATED SYSTEMS

This chapter develops a controller for the active space control of underactuated robotic systems with a view toward adapting to unknown parameters, being robust to unmodeled dynamics and disturbances, and being optimal with respect in a pointwise fashion. To achieve the goals of this chapter, the model dynamics are first partitioned into active and passive spaces. As a remedy for nonlinear coupling between these spaces, the system's acceleration is estimated for use in the control algorithm. The modeling uncertainty associated with both unknown system parameters and unknown control map is then estimated. An online QP is synthesized utilizing an intelligent robust control Lyapunov function (IRCLF) constraint to ensure the system stability with minimal control effort, while using the estimates of the unknown dynamics. The IRCLF is designed to automatically compensate for acceleration estimation error, unmodeled dynamics, and disturbances without the need for their bounds a *priori*. Convergence / UUB of all system signals is proven using Lyapunov stability arguments and the Barbalat lemma. The performance of the proposed control scheme is validated on two different underactuated systems: a foot-leg model on the deformable ground and the overhead crane system. Simulation results show the benefits of our controller against the baseline QP-RCLF and an adaptive QP-RCLF regarding the control optimality, tracking accuracy, dynamic estimation performance, and robustness to disturbances.

In the last two decades there has been increased emphasis on designing control algorithms for underactuated systems; herein underactuated systems mean systems that have fewer degrees of actuation (DoA) than degrees of freedom (DoF). This is, in part, due to the multiple applications such as manipulators operating on dynamic platforms [36], aircraft [37], brachiating robots [38, 39, 40], bat robots [41, 42], and walking robots [43, 44]. This has been coupled with large body of work on control strategies for fully-actuated systems [45, 46, 47, 48, 49, 50, 51, 52]. However, the techniques that have been already designed for fully-actuated systems cannot be directly applied for underactuated systems. This, coupled with the desire to develop new multi-objective control schemes for underactuated robotic systems motivates the study of such systems.

3.1 Background

Underactuated systems often can be partitioned to two different subspaces: the active (actuated) subspace and the passive (unactuated) subspace. Active and passive subspaces are also called *collocated* and *non-collocated* subspaces, respectively [53]. The active space is the subsystem, often achieved with a coordinate transformation, with the same dimension as the number of control inputs while the remaining components of the system are the passive space, i.e., the component of the system that cannot be actuated directly. Partial feedback linearization is a classic method wherein normal form renders the system into the active and passive spaces, this has a variety of applications [53, 54, 55, 56]. Additionally, a variety of other methods have been developed for the control of underactuated systems. Energy-based approach is a popular control technique that has been extensively studied for very important underactuated systems such as Pendubot [57], pendulums [58], robot manipulators [59], and biped locomotion [60]. Torque optimality is another design specification that should be taken into account in the control design problems. To have the optimal energy consumption, optimal control has been also recently applied on several underactuated applications such as bipedal robot, spacecraft, snake robots, wheeled inverted pendulum, cable-driven robot, etc [44, 61, 62, 63, 64].

Since the theoretical model of an underactuated system is almost approximated version of the actual system, the derived model may contain modeling inaccuracies. Thus, the control design of underactuated systems has to take model uncertainties into account. Sliding mode control is one of the most popular approaches to compensate for the modeling issues and provide stability of the closed-loop system in their presence [65, 66, 67, 68, 69, 70, 71, 72]. Adaptive control is able to implement learning and adaptation using an online parameter estimation in the control structure. Over the years, an enormous amount of research has been carried out in an attempt of applying different adaptive controllers for underactuated robotic systems [73, 74, 75, 76].

For underactuated systems, controlling all degrees of freedom is almost impossible or at least a very problematic task. Thus, the control problem of such systems reduces to stabilization of either the active or passive spaces. However, nonlinear coupling between the active and passive spaces adds complexity to control the underactuated systems. Thus, to control the active joints, as targeted in this chapter, the acceleration information of the passive joints can be provided for the control algorithm. One approach is to directly measure the acceleration [77], which is called *direct measurement* method. However, in practice, the joint acceleration measurements are not available, or if are, very noisy and not convenient for real-time implementation. To mitigate this issue, the acceleration equations of the passive space could be substituted into the active space, i.e., the *substitution* method (which refers to the well-known partial feedback linearization approach). However, the result is that the active space may not be linearly parametrized, which requires much more complexity in the controller structure, particularly for systems with high dimensions. Modeling uncertainty associated with underactuated systems makes the control problem even more complex. The existence of the unmodeled dynamics and external time-varying disturbances may also degrade the closed-loop performance or even lead to instability. Meanwhile, the control of underactuated systems should also take optimality of the controller and the required control bounds into consideration.

3.2 Contributions

The goal of this chapter is to design a robust quadratic program-based adaptive controller that accounts for all of the aforementioned challenges in the control of underactuated systems. The main contributions of this chapter are as follows:

1. The design of a multi-objective robust quadratic program-based adaptive control scheme for application to underactuated robotic systems that is able to achieve simultaneous objectives: active space control, system identification, and point-wise control optimality in the presence of unmodeled dynamics and disturbances

2. The estimate of system's accelerations as an alternative to the *direct measurement* and *substitution* methods for use in the control algorithm

3. The estimate of system dynamics and unknown control map simultaneously

4. The design of an intelligent robust component to automatically compensate for acceleration estimation error, unmodeled dynamics, and disturbances without the need for their bounds a *priori*

5. The formal proof of the convergence / UUB of all system solutions

6. Validation of the proposed controller on two illustrative underactuated systems: a foot-leg system on deformable ground and the overhead crane system

In this chapter, we begin by partitioning the underactuated system into the active and passive spaces. With the aim of the stabilization of the active state space, an affine form of this space is derived. As an alternative for the *direct measurement* and *substitution* methods, in this chapter, the system's accelerations are estimated for use in the proposed control algorithm. By doing so, the direct acceleration measurements are not required and the active space retains the property of linear parameterization. To estimate the unknown system dynamics, associated with both parameter uncertainties and unknown control map, this chapter extends and encompasses the CL adaptive approach, which was recently developed for fully actuated systems.

As explained earlier, CL is able to achieve exponential convergence of parameter and tracking errors without requiring the *PE* conditions while simultaneously using instantaneous and recorded data. However, to date, scant attention has been paid to extend the CL technique for underactuated systems while simultaneous estimation of system parameters and control map is desired. As also discussed, QP-CLF controller is able to find the optimal solution between system stabilization and control effort, whereby to date, has been widely applied for different applications. However, the previous chapter provided ample evidence regarding the performance degradation of such controllers under modeling inaccuracies. Recall that although the robust QP-CLF controllers [9, 10, 78] are able to robustify the system against parameter uncertainties, the first work [9] requires the measurement of the system's acceleration and the last two ones [10, 78] do not include any estimation method to identify the unknown system dynamics.

In this chapter, we basically extend and robustify the QP-CLF controller to underactuated systems with model inaccuracies. With the goal of achieving boundedness of the active error trajectories in a pointwise optimal fashion, a QP is synthesized w.r.t. a robust CLF (RCLF). The resulting QP-RCLF simultaneously uses the estimates of system dynamics derived by the proposed adaptive controller, and a robust component that can automatically compensate for unmodeled dynamics, acceleration estimation error, and disturbances only when they negatively impact the system's stability (in a pointwise optimal manner).

The appeal of the proposed QP-RCLF is that the gain of the robust component is updated using an adaptation mechanism which removes the need for knowing the bounds of the aforementioned unknown terms. Unlike the robust controllers with constant gains, our method renders better control optimality and stronger robustness in the presence of unexpected time-varying external disturbances. The convergence / UUB of all system solutions is finally proven by Lyapunov stability arguments and the Barbalat lemma. Simulations and comparisons to two of existing strategies, the baseline QP-RCLF and a model-based adaptive QP-RCLF [31], on two underactuated systems: a foot-leg model on deformable ground and the overhead crane system, are carried out to validate the soundness of the proposed scheme.

The chapter is organized as follows. Section 3.3 presents the system's model and the problem statement. Section 3.4 formulates the proposed controller. Section 3.5 presents simulation results. Section 3.6 concludes this chapter and discusses the need for the next chapter.

3.3 System description and problem statement

In this section, we begin by describing a general form of the underactuated systems and then present the problem statement. Consider the following equations of motion of the n DoF robot that can be derived by using the Euler-Lagrange formula:

$$M(q)\ddot{q} + C(q,\dot{q})\dot{q} + \Phi(q) = \tau + d(t), \tag{3.1}$$

where $q = [q_1, ..., q_n]^T \in \Re^n$ is a vector of generalized coordinates; $\tau \in \Re^n$ is the control torque vector; $M(q)$ and $C(q,\dot{q})$ are the $n \times n$ inertia matrix, and the $n \times n$ Coriolis and Centripetal matrix respectively; $\Phi(q) \in \Re^n$ is a vector that consists of the gravity effects and elastic forces; and $d(t) \in \Re^n$ is the vector of bounded disturbances.

For an underactuated system, $M(q)$, $C(q,\dot{q})$, $\Phi(q)$, τ, $d(t)$, and q of the above system can be partitioned as the following "lower actuated" form

$$M = \begin{bmatrix} M_{uu} & M_{ua} \\ M_{au} & M_{aa} \end{bmatrix}, C = \begin{bmatrix} C_u \\ C_a \end{bmatrix}, \Phi = \begin{bmatrix} \Phi_u \\ \Phi_a \end{bmatrix}, \tau = \begin{bmatrix} 0 \\ u \end{bmatrix}, d = \begin{bmatrix} d_u \\ d_a \end{bmatrix}, q = \begin{bmatrix} q_u \\ q_a \end{bmatrix}, \tag{3.2}$$

where subscripts "u" and "a" stand for unactuated (passive) and actuated (active) subspaces, respectively; and u is the vector of the torque inputs acting on the active subspace. The system (3.1) along with the partitioned components in Eq. (3.2) yields a lower actuated system for which the first l coordinates are unactuated and the remaining $n-l$ coordinates are actuated such that $q_u = [q_{u_1}, ..., q_{u_l}]^T \in \Re^l$ and $q_a = [q_{a_1}, ..., q_{a_{n-l}}]^T \in \Re^{n-l}$. It implies that the system has $n-l$ DoA. Note that if control constraints are actively enforced, then there will be a control defect such that

$$u = \begin{cases} u^* & \text{if} \quad |u^*| \leq \bar{u} \\ u^* + \Delta u & \text{if} \quad |u^*| > \bar{u} \end{cases}, \tag{3.3}$$

where u^* is the commanded input and Δu is the control defect when u^* hits $\bar{u}$.

Assumption 3 (Bounded disturbance and control defect)**.** The time-varying disturbance $d(t)$ and the control defect Δu are uniformly bounded such that $d(t), \Delta u \in \mathcal{L}_\infty$.

The following properties of the model (3.1) are assumed when developing the proposed algorithms:

Property 1. The inertia matrix $M(q)$ is symmetric, positive definite, and uniformly bounded.

Property 2. The matrix $\dot{M} - 2C$ is skew-symmetric, i.e., $x^T(\dot{M} - 2C)x = 0 \;\; \forall x \in \Re^n$.

Property 3. The Coriolis and centripetal matrix C has the property that $|C(q, \dot{q})| \leq \kappa|\dot{q}|$ for some $\kappa > 0$.

Property 4. The system dynamics (3.1) is expressed linearly in terms of the unknown parameter vector $P_G \in \Re^{r_G \times 1}$ such that

$$M(q)\ddot{q} + C(q, \dot{q})\dot{q} + \Phi(q) = Y_G(q, \dot{q}, \ddot{q})P_G, \tag{3.4}$$

where $Y_G(q, \dot{q}, \ddot{q}) \in \Re^{n \times r_G}$ is a known model regressor matrix.

We aim to extend and encompass both QP-CLF controller and CL technique to underactuated robotic systems. The control problem is to design a robust quadratic program-based adaptive controller for the underactuated system (3.1) to achieve multiple design specifications: active state space stabilization, pointwise control optimality, dynamic estimation, and robustness to unknown disturbances. Under the proposed controller, the boundedness of all system signals is desired. In the next section, a new multi-objective robust quadratic program-based adaptive controller is designed to meet the above objectives.

3.4 Proposed robust quadratic program-based adaptive controller

This section is organized into three distinct subsections. Subsection 3.4.1 describes an affine control form of the active state space of the underactuated system (3.1) while the system's acceleration is estimated for use in the controller formulation. Subsection 3.4.2 formulates the proposed controller through five distinct parts. The UUB of all system solutions is finally proven using Lyapunov stability frameworks and the Barbalat lemma in Subsection 3.4.3.

3.4.1 Affine representation of the active space

With the aim of partial control of the active state space, the last $n-l$ equations of (3.1) can be written as the following affine control form

$$\ddot{q}_a = f(q, \dot{q}, \ddot{q}) + Bu^* + B\Delta u + Bd_a(t), \tag{3.5}$$

where $\ddot{q}_a = [\ddot{q}_{a_1}, ..., \ddot{q}_{a_{n-l}}]^T \in \Re^{n-l}$ and $u^* = [u_1^*, ..., u_{n-l}^*]^T \in \Re^{n-l}$ are the vectors of the accelerations and the commanded torques of the active space, respectively; $B \in \Re^{n-l\times n-l}$ is the control map; $d_a(t) \in \Re^{n-l}$ and $\Delta u \in \Re^{n-l}$ are the vectors of the bounded disturbances and the control defects acting on the active space, respectively; and $f \in \Re^{n-l}$ is a vector of unknown nonlinear functions whose elements are given as

$$f_i = -\frac{1}{M_{aa_{ii}}}\left(M_{au_i}^T\ddot{q}_u + M_{aa_i}^T K_i\ddot{q}_a + C_{a_i}^T\dot{q} + \Phi_{a_i}\right), \tag{3.6}$$

where $M_{au_i} \in \Re^l$, $M_{aa_i} \in \Re^{n-l}$, $C_{a_i} \in \Re^n$, and $\Phi_{a_i} \in \Re$ denote the i^{th} row of M_{au}, M_{aa}, C_a, and Φ_a respectively for $i = 1, ..., n-l$; the scalar $M_{aa_{ii}}$ stands for the i^{th} diagonal element of M_{aa} with $i = 1, ..., n-l$; $K_i \in \Re^{n-l\times n-l}$ with $i = 1, ..., n-l$ represents an identity matrix whose i^{th} element is zero; and the control map is defined as $B = \text{diag}(\frac{1}{M_{aa_{ii}}}) \in \Re^{n-l\times n-l}$ with $i = 1, ..., n-l$.

Let us define $M_{aa_{ii}}(q) = b_{1_i} + b_{2_i}\mathscr{F}_i(q)$ such that b_{1_i} and b_{2_i} are two positive constants associated with system parameters, and $\mathscr{F}_i(q)$ is a position-dependent function. This follows that $\frac{1}{M_{aa_{ii}}} = \frac{1}{b_{1_i}} - \frac{b_{2_i}\mathscr{F}_i(q)}{b_{1_i}M_{aa_{ii}}}$ using which one obtains

$$f_i = \bar{f}_i + \Delta_{f_i}(\mathscr{F}_i(q)) \quad \text{with} \quad \bar{f}_i = -\frac{1}{b_{1_i}}\left(M_{au_i}^T\ddot{q}_u + M_{aa_i}^T K_i\ddot{q}_a + C_{a_i}^T\dot{q} + \Phi_{a_i}\right), \tag{3.7}$$

where $\bar{f}_i$ can be expressed linearly with respect to the system's parameters, but $\Delta_{f_i}(\mathscr{F}_i(q))$ does not necessarily hold this property. Hence, the vector $\bar{f}$ including the elements $\bar{f}_i$ can be linearly parametrized by a regressor matrix $Y \in \Re^{n-l\times r}$ and a parameter vector $P \in \Re^{r}$ such that the control affine model (3.5) can be rewritten as

$$\ddot{q}_a = Y(q, \dot{q}, \ddot{q})P + Bu^* + B\Delta u + Bd_a(t) + \Delta_f(\mathscr{F}(q)), \tag{3.8}$$

where the nonparameterizable term $\Delta_f(\mathscr{F}(q)) \in \Re^{n-l}$ includes $\Delta_{f_i}(\mathscr{F}_i(q))$ for $i = 1, ..., n-l$.

As seen from Eq. (3.8), the regressor matrix Y contains the acceleration information of the active and passive subspaces, and cannot be directly utilized in the controller structure. Because one of the goals of this work is to develop a control scheme which does not require the system's acceleration, we estimate this information as an alternative to the direct measurement and direct substitution of the acceleration equations. For this purpose, a Kalman filter (KF) [30] is employed to estimate the system's acceleration $(\widehat{\ddot{q}}_u, \widehat{\ddot{q}}_a)$ while assuming that the measurements of position q and velocity $\dot{q}$ of both active and passive subspaces are available.

Remark 13 (Acceleration estimation)**.** To estimate the acceleration information, the KF algorithm [30] is applied for the following linear system which is constructed based upon the measurements of q and $\dot{q}$:

$$\dot{z} = Az \quad \text{and} \;\; A = \begin{bmatrix} 0_{2n\times n} & I_{2n\times 2n} \\ 0_{n\times n} & 0_{n\times 2n} \end{bmatrix} \in \Re^{3n\times 3n}, \tag{3.9}$$

where $z = [q, \dot{q}, \ddot{q}]^T \in \Re^{3n}$. The KF algorithm only requires available noisy measurements of q and $\dot{q}$, while there is no need for any knowledge of the system dynamics.

Property 5 (Bounded acceleration estimation error)**.** The acceleration estimation error of the KF algorithm is bounded under certain conditions if the initial estimation error, control input u, disturbance $d_a(t)$, control defect Δu, and the nonparameterizable term $\Delta_f(\mathscr{F}(q))$ are all bounded [79, 80].

3.4.2 Controller structure

Utilizing the system's acceleration estimated from the previous subsection, this subsection is devoted to formulate the proposed controller. This subsection is comprised of five distinct parts. Part A is dedicated to derive a control law in which the estimation of model uncertainties associated with both system parameters and control map is targeted. Part B revisits CLF-based controllers and discusses the impact of uncertainties on their performance. Part C presents an intelligent robust CLF-based controller to ensure robustness against model uncertainties. Part D presents a parameter adaptation mechanism to provide simultaneous estimation of system parameters and control map. Finally, Part E unifies design components through a QP to construct a multi-objective controller.

A. Main control law

With the acceleration estimation of the previous subsection in hand, one may think of choosing the following control law

$$u^* = B^{-1}(\ddot{q}_a^d - v_{opt} - v_{ad}), \tag{3.10}$$

where $\ddot{q}_a^d = [\ddot{q}_{a_1}^d, ..., \ddot{q}_{a_{n-l}}^d]^T \in \Re^{n-l}$ is the vector of desired active space acceleration; $v_{opt} \in \Re^{n-l}$ represents the pointwise optimal signal that will be computed by the QP controller; and $v_{ad} = Y(q, \dot{q}, \widehat{\ddot{q}}_u, \widehat{\ddot{q}}_a)\widehat{P} \in \Re^{n-l}$ is the adaptive component with $\widehat{P}$ as the estimates of P.

However since the elements of matrix B (i.e., $M_{aa_{ii}}$) are unknown, the control law (3.10) is not implementable, and one may think of estimating the matrix B. However, (i) simultaneous estimation of the parameter vector P and the control map B adds more complexity to the controller design and (ii) this may pose the singularity issues for $\hat{B}^{-1}$. To mitigate the above-mentioned obstacles, the control design in this part avoids to estimate the matrix B by itself, but alternatively, the estimation of uncertainty associated with matrix B is aimed.

For this purpose, the system (3.8) can be rewritten as

$$\ddot{q}_a = YP + U\Delta B + B_0 u^* + B\Delta u + Bd_a(t) + \Delta_f(\mathscr{F}(q)), \tag{3.11}$$

where B is split into the constant matrix $B_0 = \text{diag}(\frac{1}{b_{1_i}}) \in \Re^{n-l\times n-l}$ and the state-dependent vector $\Delta B(q) \in \Re^{n-l}$ including the elements $-\frac{b_{2_i}\mathscr{F}_i(q)}{b_{1_i}M_{aa_{ii}}}$ for $i = 1, ..., n-l$; and $U = \text{diag}(u_i) \in \Re^{n-l\times n-l}$ for $i = 1, ..., n-l$. Since vector ΔB is unknown and we have access to the control signal measurements, augmenting ΔB and U with the regressor matrix Y and the parameter vector P respectively yields

$$\ddot{q}_a = \Psi\Upsilon + B_0 u^* + B\Delta u + Bd_a(t) + \Delta_f(\mathscr{F}(q)), \tag{3.12}$$

where $\Psi = [Y, U] \in \Re^{(n-l)\times(r+n-l)}$ is the augmented regressor matrix; and $\Upsilon = [P, \Delta B]^T \in \Re^{r+n-l}$ is the augmented parameter vector.

Lemma 1 (Boundedness of $\dot{\Upsilon}$)**.** The derivative of the unknown part ΔB is bounded, which in turn results in the boundedness of $\dot{\Upsilon}$ by a positive scalar such that $\|\dot{\Upsilon}\| \leq \overline{\Upsilon}$.

Proof. The kinetic energy of the system (3.1) can be expressed as

$$T = \frac{1}{2}\dot{q}^T M(q)\dot{q}, \tag{3.13}$$

using which the Lagrangian's equation can be derived as

$$\frac{d}{dt}\frac{\partial T}{\partial \dot{q}} - \frac{\partial T}{\partial q} = M\ddot{q} + \dot{M}\dot{q} - \frac{1}{2}\left(\frac{\partial M}{\partial q}\dot{q}\right)^T \dot{q} = \mathcal{Q}, \tag{3.14}$$

where j^{th} column of the matrix $\frac{\partial M}{\partial q}\dot{q}$ is defined as $\sum_{i=1}^{n} \frac{\partial (M)_i}{\partial q_j}\dot{q}_i$ with $(M)_i$ denoting the i^{th} column of the matrix M; and $\mathcal{Q}$ represents the vector of generalized forces. Rewriting the equations of motion (3.1) as $M(q)\ddot{q} + C(q,\dot{q})\dot{q} = \mathcal{Q}$ and comparing it with (3.14) results in the following relationship between $\dot{M}$ and C

$$C\dot{q} = \dot{M}\dot{q} - \frac{1}{2}\left(\frac{\partial M}{\partial q}\dot{q}\right)^T \dot{q}. \tag{3.15}$$

Given Property 3, in view of (3.15), one obtains

$$\|\dot{M}\dot{q} - \frac{1}{2}\left(\frac{\partial M}{\partial q}\dot{q}\right)^T \dot{q}\| \leq \|C\dot{q}\| \leq \kappa\|\dot{q}\|^2 \tag{3.16}$$

wherein it follows that all terms on the left-hand side of (3.16) are bounded for bounded velocities of the system. Consequently, $\dot{M}$ and in turn its diagonal elements associated with the active space, $\dot{M}_{aa_{ii}}$ with $i = 1, ..., n-l$, are bounded. This in turn implies that the derivatives of the matrices B and ΔB, and consequently, the derivative of the vector Υ are all bounded. To meet the demands of the stability analysis in Subsection 3.4.3, we consider $\overline{\Upsilon} > 0$ as an upper bound for $\|\dot{\Upsilon}\|$. □

Based upon the system (3.12), the following three-term control law is suggested

$$u^* = B_0^{-1}(\ddot{q}_a^d - v_{opt} - v_{ad}), \tag{3.17}$$

where $v_{ad} = \widehat{\Psi}\widehat{\Upsilon}$ represents the adaptive component with $\widehat{\Upsilon}$ as the estimation of Υ. Note that here, the constant matrix B_0 with positive diagonal elements $\frac{1}{b_{1_i}}$ is always invertible. With the structure of the main control law (3.17) in hand, the next part will review CLF-based controllers and discuss how such controllers can be negatively impacted by model uncertainties.

B. CLF-based controller

With the goal of active state space stabilization, let us define the tracking error vector of the active coordinates as $e = q_a^d - q_a \in \Re^{n-l}$. Substituting the control law (3.17) into the dynamics (3.12) yields

$$\ddot{e} = -\Psi\Upsilon + \widehat{\Psi}\widehat{\Upsilon} + v_{opt} - B\Delta u - Bd_a(t) - B\Delta_f. \tag{3.18}$$

Let define $\widetilde{\Upsilon} = \widehat{\Upsilon} - \Upsilon$ and $\widetilde{\Psi} = \Psi - \widehat{\Psi}$ to have

$$\ddot{e} = v_{opt} + \epsilon_\Upsilon - \epsilon_\Psi - \Delta u^B - d_a^B - \Delta_f^B, \tag{3.19}$$

where $\epsilon_\Upsilon = \widehat{\Psi}\widetilde{\Upsilon} \in \Re^{n-l}$ and $\epsilon_\Psi = \widetilde{\Psi}\Upsilon \in \Re^{n-l}$ stem from the estimation error and the acceleration estimation error, respectively; and $\Delta u^B = B\Delta u$, $d_a^B = Bd_a(t)$, and $\Delta_f^B = B\Delta_f$. Note that for bounded acceleration estimation error (Property 5) and bounded dynamic estimation error (i.e., if v_{ad} converge to a small neighborhood of $\Psi\Upsilon$), signals ϵ_Υ and ϵ_Ψ are bounded such that $\|\epsilon_\Upsilon\| \leq \bar{\epsilon}_\Upsilon$ and $\|\epsilon_\Psi\| \leq \bar{\epsilon}_\Psi$. In addition, since B, Δu, $d_a(t)$, and Δ_f are all bounded, then Δu^B, d_a^B, and Δ_f^B are bounded such that $\|\Delta u^B\| \leq \overline{\Delta u}$, $\|d_a^B\| \leq \bar{d}$, and $\|\Delta_f^B\| \leq \overline{\Delta_f}$ with $\overline{\Delta u}, \bar{d}, \overline{\Delta_f} > 0$.

Let us define $\zeta = [e, \dot{e}]^T \in \Re^{2(n-l)}$ to rewrite the error dynamics (3.19) as

$$\dot{\zeta} = F\zeta + Ev_{opt} + E\Big(\epsilon_\Upsilon - \epsilon_\Psi - \Delta u^B - d_a^B - \Delta_f^B\Big) \tag{3.20}$$

with

$$F = \begin{bmatrix} 0_{(n-l)\times(n-l)} & I_{(n-l)\times(n-l)} \\ 0_{(n-l)\times(n-l)} & 0_{(n-l)\times(n-l)} \end{bmatrix} \in \Re^{2(n-l)\times 2(n-l)} \tag{3.21}$$
$$E = \begin{bmatrix} 0_{(n-l)\times(n-l)} \\ I_{(n-l)\times(n-l)} \end{bmatrix} \in \Re^{2(n-l)\times(n-l)}.$$

Definition 8. A continuously differentiable function $V(\zeta) : \Re^{2(n-l)} \to \Re$ is an exponentially stabilizing CLF for the system (3.20) if $\epsilon_\Upsilon = \epsilon_\Psi = \Delta u = d_a = \Delta_f = 0$ and there exist a set of controls $\mathcal{V}$ and positive scalars $\alpha_Q, a_1, a_2 > 0$ such that [4]

$$a_1\|\zeta\|^2 \leq V(\zeta) \leq a_2\|\zeta\|^2, \tag{3.22}$$
$$\inf_{v_{opt}\in\mathcal{V}} [\mathcal{L}_F V(\zeta) + \mathcal{L}_E V(\zeta) v_{opt}] \leq -\alpha_Q V(\zeta),$$

where $\mathcal{L}_F V(\zeta) = \frac{\partial V(\zeta)}{\partial \zeta} F\zeta$ and $\mathcal{L}_E V(\zeta) = \frac{\partial V(\zeta)}{\partial \zeta} E$ are the Lie derivatives of $V(\zeta)$ with respect to F and E, respectively.

Motivated by the desire to achieve exponential convergence of the error trajectory ζ to zero in the absence of ϵ_Υ, ϵ_Ψ, Δu, d_a, and Δ_f through a CLF-based controller, let us select the following

Lyapunov function

$$V(\zeta) = \zeta^T P \zeta, \;\; \lambda_{min}(P)\|\zeta\|^2 \leq V(\zeta) \leq \lambda_{max}(P)\|\zeta\|^2, \tag{3.23}$$

where $\lambda_{min}(.)$ and $\lambda_{max}(.)$ denote minimum and maximum eigenvalues of a matrix; and $P = P^T \in \Re^{2(n-l)\times 2(n-l)} > 0$ is the solution of CARE $F^T P + PF - PEE^T P + Q = 0$ with $Q = Q^T \in \Re^{2(n-l)\times 2(n-l)} > 0$.

To achieve exponential convergence of $V(\zeta)$ to zero, we seek a set of all stabilizing optimal signals v_{opt} to satisfy the following CLF constraint

$$\psi_0(\zeta) + \psi_1^T(\zeta) v_{opt} \leq 0 \tag{3.24}$$

with

$$\psi_0(\zeta) = L_F V(\zeta) + \alpha_Q V(\zeta), \qquad \psi_1(\zeta) = L_E^T V(\zeta), \tag{3.25}$$

and

$$L_F V(\zeta) = \zeta^T (PF + F^T P)\zeta, \;\; L_E V(\zeta) = 2\zeta^T P E, \tag{3.26}$$

where $\psi_1(\zeta)$ is a $n-l$-denominational vector, and $L_F V(\zeta)$ and $\psi_0(\zeta)$ are both scalars.

One candidate of v_{opt} to satisfy the condition (3.24) is the PWMNC law (2.39) using which it follows that

$$\left\| \begin{matrix} e(t) \\ \dot{e}(t) \end{matrix} \right\| \leq \sqrt{\frac{\lambda_{max}(P)}{\lambda_{min}(P)}} \left\| \begin{matrix} e(0) \\ \dot{e}(0) \end{matrix} \right\| e^{-\frac{\alpha}{2}t}, \tag{3.27}$$

which leads to exponential convergence of $\big(e(t), \dot{e}(t)\big)$ at a rate of $\frac{\alpha}{2}$.

By noting that the PWMNC can be expressed as a convex optimization problem, the QP-CLF controller has been recently introduced in which the CLF constraint is encoded in a QP to ensure stability in a pointwise optimal fashion [4]. Although this controller derives ζ to zero in the absence of unknown disturbances ϵ_Υ, ϵ_Ψ, Δu, d_a, and Δ_f, the errors converge to a neighborhood of the origin in the presence of these terms, where the size of the neighborhood is dependent on the scale of the unknown terms. To avoid the performance degradation of the QP-CLF controller in the presence of the terms ϵ_Υ, ϵ_Ψ, Δu, d_a, and Δ_f, the next part presents an intelligent robust CLF (IRCLF) to robustify the closed-loop system against the above-mentioned unknown terms without knowing their bounds.

C. Intelligent robust CLF (IRCLF)

One of the main disadvantages of the QP-CLF controller is that its performance is degraded for system (3.20) with unknown terms ϵ_Υ, ϵ_Ψ, Δu^B, d_a^B, and Δ_f^B. In the following, an IRCLF is introduced which uses the RCLF and a projection-based adaptation mechanism to deal with the given issues without knowing the bounds of the unknown terms.

We begin by robustifying the CLF through defining the following robust term

$$R(\zeta) = K_r\|\zeta^T PE\|,\ K_r > 0 \tag{3.28}$$

and $D = \epsilon_\Upsilon - \epsilon_\Psi - \Delta u^B - d_a^B - \Delta_f^B$ as the lumped disturbance.

Definition 9. Given the system (3.20), the function $V(\zeta)$ is an exponentially stabilizing RCLF if there exist a set of controls $\mathcal{V}$ and positive scalars $K_r, \rho > 0$ such that $K_r = 2\bar{D} + \rho$ and

$$\begin{gathered} a_1\|\zeta\|^2 \leq V(\zeta) \leq a_2\|\zeta\|^2, \\ \inf_{v_{opt}\in\mathcal{V}} [\mathcal{L}_F V(\zeta) + R(\zeta) + \mathcal{L}_E V(\zeta) v_{opt}] \leq -\alpha_Q V(\zeta), \end{gathered} \tag{3.29}$$

where $\bar{D} = \bar{\epsilon}_\Upsilon + \bar{\epsilon}_\Psi + \overline{\Delta u} + \bar{d} + \overline{\Delta_f}$ is the bound of the lumped disturbance such that $\|D\| \leq \bar{D}$.

Let us take the time derivative of $V(\zeta)$ along the system trajectory (3.20) to have

$$\dot{V}(\zeta) = L_F V(\zeta) + L_E V(\zeta)\big(v_{opt} + D\big). \tag{3.30}$$

To achieve exponential convergence of $V(\zeta)$ to zero, i.e., $\dot{V}(\zeta) \leq \alpha_Q V(\zeta)$, a class of controls

v_{opt} is sought to hold the following RCLF constraint

$$\psi_{0_r}(\zeta) + \psi_1^T(\zeta)v_{opt} \leq 0 \;\text{ with }\; \psi_{0_r}(\zeta) = \psi_0(\zeta) + R(\zeta). \tag{3.31}$$

The above RCLF constraint holds by using the PWMNC in terms of $\psi_{0_r}(\zeta)$ yielding

$$v_{opt}(\psi_{0_r}(\zeta), \psi_1(\zeta)) \tag{3.32}$$

if the robust gain K_r is selected as

$$K_r = 2\bar{D} + \rho. \tag{3.33}$$

Again, when the signal v_{opt} is generated by an equivalent QP optimization problem, a QP-RCLF controller is emerged. Although such a controller is able to drive the error ζ to zero even in the presence of D, the main drawback of this approach is that the bound of the lumped disturbance is required to tune the robust gain K_r. Since $\bar{D}$ is unknown, the minimal stabilizing value for the robust gain K_r is not known. Thus, if this gain is not correctly selected, it may not be able to properly compensate for D or may increase the control effort when $\psi_{0_r}(\zeta) > 0$.

To relieve the engineer of the need to define the robust gain K_r correctly and enhance the optimality of the controller without knowing the bound of disturbances, the gain K_r can be automatically updated using an adaptation mechanism. To design such adaption law while providing robustness and preventing the parameter drift, the following projection-based robust gain adaptation mechanism is suggested

$$\dot{K}_r = K_{r_0}\text{Proj}\Big(K_r, \|\zeta^T PE\|\Big), \tag{3.34}$$

where $\text{Proj}(K_r, \|\zeta^T PE\|)$ is defined as

$$\text{Proj} = \begin{cases} \|\zeta^T PE\| - \frac{(\nabla g(K_r))^2}{\|\nabla g(K_r)\|^2}\|\zeta^T PE\| g(K_r), & \text{if } \; g(K_r) > 0 \text{ and } \|\zeta^T PE\|\nabla g(K_r) > 0 \\ \|\zeta^T PE\|, & \text{otherwise} \end{cases}, \tag{3.35}$$

where $g(K_r) = \frac{\|K_r\|^2 - K_{r_{max}}^2}{\nu_{K_r} K_{r_{max}}^2} : \Re \longrightarrow \Re$ is a smooth convex function; $K_{r_{max}}$ is a prescribed upper bound of K_r to ensure that the robust gain does not exceed $K_{r_{max}}$; $\nu_{K_r} > 0$ is the projection tolerance; and $\nabla g(K_r) = \frac{\partial g(K_r)}{\partial K_r} \in \Re$ is the derivative of $g(K_r)$ w.r.t. K_r evaluated at K_r.

The adaptation mechanism (3.35) guarantees the boundedness of $K_r(t)$ by $K_{r_{max}}\sqrt{1+\nu_{K_r}}$ (no concern about the drift issue on the robust gain K_r) such that

$$\begin{aligned} &\text{if } |K_r(0)| \leq K_{r_{max}} \text{ and } g(K_r) \leq 1, \\ &\text{then } |K_r(t)| \leq K_{r_{max}}\sqrt{1+\nu_{K_r}}, \ \forall t \geq 0. \end{aligned} \tag{3.36}$$

Thus, the robust term (3.28) along with the adaptation mechanism (3.34) constructs the IRCLF structure for which the following properties are met: (i) when $\psi_{0_r}(\zeta) \leq 0$, $v_{opt}(\psi_{0_r}(\zeta), \psi_1(\zeta))$ and in turn $R(\zeta)$ are off, emerging a robust mechanism in a pointwise optimal fashion; (ii) even if $\psi_{0_r}(\zeta) > 0$, K_r increases as needed (unlike the robust controllers with constant gain); (iii) there is no need to know the bound of the unknown terms; (iv) it prevents the parameter drift in UUB case; and (v) it bounds K_r as desired.

Remark 14 (Adaptive QP-RCLF presented in [31])**.** To handle the control map uncertainty, one approach is to consider $U\Delta B$ as an extra disturbance (ϵ_B) acting on Eq. (3.11). By doing so, the acceleration equations (3.11) can be rewritten as

$$\ddot{q}_a = YP + B_0 u^* + \epsilon_B + \Delta u^B + d_a^B + \Delta_f^B. \tag{3.37}$$

Utilizing the same control law (3.17), the adaptive component v_{ad} uses the regressor matrix Y to estimate the parameter vector P such that $v_{ad} = Y(q, \dot{q}, \widehat{\ddot{q}}_u, \widehat{\ddot{q}}_a, u)\widehat{P}$. This way, the error dynamics (3.20) are given as

$$\dot{\zeta} = F\zeta + Ev_{opt} + E(D - \epsilon_B). \tag{3.38}$$

Given the system (3.38), the same discussion from Eq. (3.21) to Eq. (3.31) can be followed. However, under this approach, the robust term has to compensate for one more disturbance, which can result in a higher control effort. Furthermore, since in this case, ΔB is not desired to be estimated, a proper dynamic estimation is not achieved and in turn, it may negatively impact the system's performance. This method with constant robust gain can be found in [31].

Remark 15 (Robust term)**.** It should be pointed out that $R(\zeta)$ compensates for D in a pointwise optimal fashion, such that when $\psi_{0_r}(\zeta) \leq 0$, the system is stable and the robust term is not actively enforced.

With the formulation of IRCLF in hand, it can be assured that the unknown terms, associated with the acceleration estimation error, the parameter estimation error, and other disturbances, are automatically compensated. Now, it is time to estimate the unknown system dynamics through the derivation of a parameter adaptation mechanism. This will be developed in the next part.

D. Estimator structure

This part is devoted to derive a parameter adaptation mechanism that can identify the unknown system dynamics by estimating the parameter vector Υ. A proper dynamic estimation plays a role in decreasing the error ϵ_Υ, consequently, generating the smaller K_r by the IRCLF and in turn enhancing the control optimality of the proposed controller. For this purpose, we extend the CL adaptive mechanism [21] for simultaneous estimation of the system's parameters and control map as a unified parameter vector Υ. Let us define the following update law, in which both instantaneous (first term) and recorded information (second term) of the positions, velocities, control inputs, and estimated accelerations are utilized

$$\dot{\widehat{\Upsilon}} = -\eta_1 \widehat{\Psi}^T E^T P \zeta - \eta_2 \sum_{i=1}^{m} \widehat{\Psi}_i^T \widehat{\epsilon}_{\Upsilon_i}, \tag{3.39}$$

where $\eta_i \in \Re^{(r+n-l)\times(r+n-l)}$ for $i = 1, 2$ are two diagonal matrices whose entries are positive; m is the number of the recorded data points; and $\widehat{\Psi}_i$ and $\widehat{\epsilon}_{\Upsilon_i}$ are realized at the i-th recorded data for $i \in [1, 2, ..., m]$.

Since the true system dynamics $\Psi\Upsilon$ are not known, the residual ϵ_{Υ_i} is not realizable. Alternatively, the estimates of ϵ_{Υ_i} can be computed as

$$\widehat{\epsilon}_{\Upsilon_i} = \widehat{\Psi}_i \widehat{\Upsilon} - (\widehat{\Psi\Upsilon})_i \ \text{ with } \ (\widehat{\Psi\Upsilon})_i = \widehat{\ddot{q}}_{a_i} - B_0 u_i^*, \tag{3.40}$$

where $\widehat{\ddot{q}}_{a_i}$ is the i-th recorded acceleration that is estimated by an optimal fixed-point smoother (OFPS) algorithm [29, 30] applying for the linear system (3.9).

Remark 16 (Recording data points)**.** To achieve the best estimation of $\Psi\Upsilon$ and, consequently, the smallest possible disturbance ϵ_Υ, the storing algorithm only keeps those points that are sufficiently different from the last point recorded [22]. This way, for $m \geq \frac{r+n-l}{n-l}$, the history stack $H = [\widehat{\Psi}_i^T, ..., \widehat{\Psi}_m^T] \in \Re^{r+n-l \times m(n-l)}$ will have $\text{rank}(H) = r + n - l$ and in turn provide full-rank updates for the most accurate estimation.

Thus, using the adaptation law (3.39) along with the above recording data policy and the acceleration estimation, the unknown dynamics $\xi = \Psi\Upsilon$ can be estimated as $\widehat{\xi} = \widehat{\Psi}\widehat{\Upsilon}$ such that $\widetilde{\xi} = \Psi\Upsilon - \widehat{\Psi}\widehat{\Upsilon}$ converges to a small neighborhood of the origin. To this end, we can utilize the the adaptive signal $v_{ad} = \widehat{\Psi}\widehat{\Upsilon}$ for use in the main control law (3.17). Because the ultimate goal of this work is to develop a multi-objective controller, the next part will synthesize a QP which uses all the predefined components, i.e., control law, IRCLF, and parameter adaptation, to ensures active space stabilization and robustness in a pointwise optimal fashion.

Remark 17 (Acceleration estimation)**.** Note that the estimate of the acceleration is improved using the OFPS algorithm over the ordinary Kalman filter, but it enforces a constant time delay. For the second term of the adaptation law of Eq. (3.39) (CL part), the acceleration information is estimated by the OFPS to provide more accurate estimation. In this term, the acceleration is only computed when the history stack H is updated and it is not required at the current time. Thus, the delay from the OFPS only postpones the history stack to be full ranked and does not impact the tracking error at the current time [21]. However, since the first term of the adaptation law (traditional part) uses the current acceleration information, tracking performance will be affected by delayed acceleration if the OFPS algorithm is used. That is why, the acceleration used in the first term is provided by the Kalman filter.

E. QP-IRCLF controller

In this part, the pointwise optimal signal $v_{opt}(\psi_{0_r}(\zeta), \psi_1(\zeta))$ is generated in the closed-loop form by the following online QP as a convex optimization problem

$$\begin{aligned} \mathbf{v}^*_{\mathbf{opt}} =& \underset{h}{\text{argmin}} \quad \mathbf{v}^{\mathbf{T}}_{\mathbf{opt}}\mathbf{v}_{\mathbf{opt}} + \mathbf{h}^{\mathbf{T}}_{\mathbf{cont}} l_{cont} \mathbf{h}_{\mathbf{cont}} + l_{rclf} \mathbf{h}_{\mathbf{rclf}}{}^2 \\ \text{s.t.}\ & \text{RCLF (Eq. (3.31))} : \psi_{0_r}(\zeta) + \psi_1^T(\zeta)\mathbf{v}_{\mathbf{opt}} \leq \mathbf{h}_{\mathbf{rclf}} \\ & \text{CB}_1 : \mathbf{v}_{\mathbf{opt}} - \ddot{q}^d_a + v_{ad} + B_0 \underline{u} \leq \mathbf{h}_{\mathbf{cont}} \\ & \text{CB}_2 : -\mathbf{v}_{\mathbf{opt}} + \ddot{q}^d_a - v_{ad} - B_0 \bar{u} \leq \mathbf{h}_{\mathbf{cont}}, \end{aligned} \tag{3.41}$$

where $h = (\mathbf{h}_{\mathbf{rclf}}, \mathbf{h}_{\mathbf{cont}}, \mathbf{v}_{\mathbf{opt}}) \in \Re^{2(n-l)+1}$ is the vector of the optimization variables; the control input u^* in (3.17) is enforced to satisfy $\underline{u} \leq u^* \leq \bar{u}$; and $l_{rclf} \in \Re$ and $l_{cont} \in \Re^{(n-l)\times(n-l)}$ are the penalty coefficients to relax the IRCLF constraint and the control bounds, respectively.

The reason behind assigning such coefficients is that the control bounds and the IRCLF constraint may not be jointly realizable for different applications. Under this condition, a trade off should be made between the performance and optimality by choosing the convenient penalty coefficients l_{rclf} and l_{cont}. Next subsection will perform a stability analysis to ensure that all system's solutions are uniformly ultimately bounded under the proposed adaptive QP-IRCLF controller.

3.4.3 Stability analysis

Subsection 3.4.2 has formulated the proposed control scheme. The goal of this subsection is to formally prove the convergence / UUB of system's solutions when the proposed controller is applied. For this purpose, let us define the following Lyapunov function candidate

$$W(\zeta, \widetilde{\Upsilon}, \widetilde{K}_r) = V(\zeta) + \frac{1}{2}\widetilde{\Upsilon}^T\eta^{-1}\widetilde{\Upsilon} + \frac{1}{2K_{r_0}}\widetilde{K}_r^2, \tag{3.42}$$

where assume that $\eta_1 = \eta_2 = 2\eta$ and define $\widetilde{K}_r = K_r - K_r^*$ with K_r^* as the ideal robust gain. Throughout this subsection, we make the following assumption.

Assumption 4 (Stable zero dynamics)**.** The zero dynamics of the system (3.1) are stable.

Theorem 3. *Consider the Lyapunov function (3.42), the control law (3.17), the adaptation laws (3.34) and (3.39), and the unified QP-IRCLF controller (3.41). Under the Assumptions 3 and 4, Property 5, and applying the recording policy in Remark 16 and the Lemma 1, uniform ultimate boundedness of* $(\widetilde{\Upsilon}, \zeta, \widetilde{K}_r)$ *is guaranteed for all* $\Upsilon \in \Re^{r+n-l}$ *and any* $\zeta(0) \in \Re^{2(n-l)}$ *without knowing the bounds of the unknown disturbances.*

Proof. We begin by taking the time derivative of the Lyapunov function (3.42) to have

$$\dot{W} = 2\zeta^T P\dot{\zeta} + \widetilde{\Upsilon}^T\eta^{-1}\dot{\widetilde{\Upsilon}} + \frac{1}{K_{r_0}}\dot{K}_r\widetilde{K}_r. \tag{3.43}$$

Substituting the error dynamics (3.20), the update law (3.39), and the robust gain adaptation mechanism (3.34) in case that $g(K_r) > 0$ and $\|\zeta^T P_\gamma E\|\nabla g(K_r) > 0$ into Eq. (3.43) yields

$$\begin{aligned}\dot{W} =& 2\zeta^T PF\zeta + 2\zeta^T PE\left(v_{opt} + \epsilon_\Upsilon - \epsilon_\Psi - \Delta u^B - d_a^B - \Delta_f^B\right) - 2\widetilde{\Upsilon}^T\widehat{\Psi}^T E^T P\zeta \\ &- 2\widetilde{\Upsilon}^T\sum_{i=1}^{m}\widehat{\Psi}_i^T\widehat{\epsilon}_{\Upsilon_i} - 2\widetilde{\Upsilon}^T\eta^{-1}\dot{\Upsilon} + \widetilde{K}_r\left(\|\zeta^T PE\| - \frac{(\nabla g(K_r))^2}{\|\nabla g(K_r)\|^2}\|\zeta^T PE\|g(K_r)\right).\end{aligned} \tag{3.44}$$

Noting that $\epsilon_\Upsilon = \widehat{\Psi}\widetilde{\Upsilon}$ and $\widehat{\epsilon}_{\Upsilon_i} = \widehat{\Psi}_i\widetilde{\Upsilon} - \epsilon_{\Psi_i}$, defining $H_1 = 2\sum_{i=1}^{m}\widehat{\Psi}_i^T\widehat{\Psi}_i$, and canceling the similar parts, we have

$$\begin{aligned}\dot{W} =&2\zeta^T PF\zeta + 2\zeta^T PE\left(v_{opt} - \epsilon_\Psi - \Delta u^B - d_a^B - \Delta_f^B\right) - \widetilde{\Upsilon}^T H_1 \widetilde{\Upsilon} \\ &+ 2\widetilde{\Upsilon}^T \sum_{i=1}^{m} \widehat{\Psi}_i^T \epsilon_{\Psi_i} - 2\widetilde{\Upsilon}^T \eta^{-1}\dot{\Upsilon} + \widetilde{K}_r\left(\|\zeta^T PE\| - \frac{(\nabla g(K_r))^2}{\|\nabla g(K_r)\|^2}\|\zeta^T PE\| g(K_r)\right).\end{aligned} \tag{3.45}$$

Recall that the QP solution coincides with the solution of the PWMNC $v_{opt}(\psi_{0_r}(\zeta), \psi_1(\zeta))$ in the closed-loop form. Thus, replacing v_{opt} with the first term of (2.39) yields

$$\begin{aligned}\dot{W} =&2\zeta^T PF\zeta - \psi_1^T(\zeta)\left(\frac{\psi_{0_r}(\zeta)\psi_1(\zeta)}{\psi_1^T(\zeta)\psi_1(\zeta)}\right) - \widetilde{\Upsilon}^T H_1 \widetilde{\Upsilon} + 2\widetilde{\Upsilon}^T \sum_{i=1}^{m} \widehat{\Psi}_i^T \epsilon_{\Psi_i} - 2\widetilde{\Upsilon}^T \eta^{-1}\dot{\Upsilon} \\ &- 2\zeta^T PE\left(\epsilon_\Psi + \Delta u^B + d_a^B + \Delta_f^B\right) + \widetilde{K}_r\|\zeta^T PE\| - \widetilde{K}_r\frac{(\nabla g(K_r))^2}{\|\nabla g(K_r)\|^2}\|\zeta^T PE\| g(K_r).\end{aligned} \tag{3.46}$$

Note that

$$-\widetilde{K}_r\frac{(\nabla g(K_r))^2}{\|\nabla g(K_r)\|^2}\|\zeta^T PE\| g(K_r) \le 0 \tag{3.47}$$

and expand ψ_{0_r} to have

$$\begin{aligned}\dot{W} =&-\alpha_Q\zeta^T P\zeta - K_r^*\|\zeta^T PE\| - \widetilde{\Upsilon}^T H_1 \widetilde{\Upsilon} + 2\widetilde{\Upsilon}^T \sum_{i=1}^{m} \widehat{\Psi}_i^T \epsilon_{\Psi_i} - 2\widetilde{\Upsilon}^T \eta^{-1}\dot{\Upsilon} \\ &- 2\zeta^T PE\left(\epsilon_\Psi + \Delta u^B + d_a^B + \Delta_f^B\right).\end{aligned} \tag{3.48}$$

Considering the bounds on terms $\dot{\Upsilon}$, ϵ_Ψ, Δu^B, d_a^B, and Δ_f^B, it follows that:

$$\begin{aligned}\dot{W} \le&-\alpha_Q\lambda_{min}(P)\|\zeta\|^2 - \lambda_{min}(H_1)\|\widetilde{\Upsilon}\|^2 + 2\|\widetilde{\Upsilon}\|\|\sum_{i=1}^{m} \widehat{\Psi}_i\epsilon_{\Psi_i}\| + 2\|\widetilde{\Upsilon}\|\|\eta^{-1}\|\bar{\Upsilon} \\ &-\left(K_r^* - 2\left(\bar{\epsilon}_\Psi + \overline{\Delta u} + \bar{d} + \overline{\Delta_f}\right)\right)\|\zeta\|\|PE\|.\end{aligned} \tag{3.49}$$

At this stage, we assume the following.

Assumption 5 (Matching assumption)**.** Assume that

$$\exists K_r^* : K_r^* = 2(\bar{\epsilon}_\Psi + \overline{\Delta u} + \bar{d} + \overline{\Delta_f}). \tag{3.50}$$

Th above assumption assumes only the existence of K_r^* so that true knowledge of the ideal gain is not required. Due to Assumption 5, the last term in Eq. (3.49) vanishes and we have

$$\dot{W} \leq -\alpha_Q \lambda_{min}(P)\|\zeta\|^2 - \lambda_{min}(H_1)\|\widetilde{\Upsilon}\|^2 + 2\|\widetilde{\Upsilon}\| \left(\| \sum_{i=1}^{m} \widehat{\Psi}_i \epsilon_{\Psi_i} \| + \|\eta^{-1}\|\bar{\Upsilon} \right). \tag{3.51}$$

Let us define two positive scalars ϵ_b and $\bar{\eta}$ such that $\| \sum_{i=1}^{m} \widehat{\Psi}_i \epsilon_{\Psi_i} \| \leq \epsilon_b$ and $\|\eta^{-1}\| \leq \bar{\eta}$, which follows the following

$$\dot{W} \leq -\alpha_Q \lambda_{min}(P)\|\zeta\|^2 - \lambda_{min}(H_1)\|\widetilde{\Upsilon}\|^2 + C\|\widetilde{\Upsilon}\|, \tag{3.52}$$

where $C = 2(\epsilon_b + \bar{\Upsilon}\bar{\eta})$.

Hence, $\dot{W} < 0$ outside the compact set

$$\Omega = \left\{ \left(\zeta, \widetilde{\Upsilon}, \widetilde{K}_r\right) \in \Re^{2(n-l)} \times \Re^{r+n-l} \times \Re : \|\zeta\| \leq B_\zeta \wedge \|\widetilde{\Upsilon}\| \leq B_{\widetilde{\Upsilon}} \wedge \|\widetilde{K}_r\| \leq B_{\widetilde{K}_r} \right\}, \tag{3.53}$$

where

$$\begin{aligned} B_\zeta &= \sqrt{\frac{C\|\widetilde{\Upsilon}\| - \lambda_{min}(H_1)\|\widetilde{\Upsilon}\|^2}{\alpha_Q \lambda_{min}(P)}} \\ B_{\widetilde{\Upsilon}} &= \frac{C + \sqrt{C^2 - 4\alpha_Q \lambda_{min}(P)\lambda_{min}(H_1)\|\zeta\|^2}}{2\lambda_{min}(H_1)} \\ B_{\widetilde{K}_r} &= 2K_{r_{max}}\sqrt{1 + \nu_{K_r}}. \end{aligned} \tag{3.54}$$

Hence, all trajectories $(\zeta, \widetilde{\Upsilon}, \widetilde{K}_r)$ enter the set Ω in finite time T and remain there $\forall\ t \geq T$. This proves UUB of all signals in the closed-loop dynamics.

The above proof holds even if the projection operator does not alter the term $\|\zeta^T PE\|$. In this case, the second term of (3.35) is utilized in Eq. (3.44) and the same results can be similarly achieved. The above proof of Theorem 3 holds even in case that $\psi_{0_r}(\zeta) \leq 0$, from which it follows that $2\zeta^T PF\zeta \leq -\alpha_Q \zeta^T P\zeta - K_r\|\zeta^T PE\|$ (according to Eq. (3.31)) and the optimal signal v_{opt} vanishes (due to (2.39)). Using these properties, Eq. (3.45) reduces to Eq. (3.48) and following the same argument, the proof is similar to that above, resulting in the UUB of all signals. □

Remark 18 (Ultimate bounds)**.** According to Eq. (3.54), the ultimate bounds on ζ and $\widetilde{\Upsilon}$ are dependent on the acceleration estimation error ϵ_Ψ and the bound on the derivative of the control map defect ΔB.

Remark 19 (Tracking performance)**.** The ultimate bound on the tracking error ζ can be decreased by increasing the design parameter α_Q.

Special Case. Asymptotic Convergence: Theorem 3 proved the UUB of all signals under the proposed adaptive QP-IRCLF controller. However, asymptotic convergence (stronger form of stability) of the tracking and estimation errors $(\zeta, \widetilde{\Upsilon})$ to the origin can be also achieved if the acceleration estimation is perfect and the elements of ΔB are constant.

Theorem 4. *Apply the recording policy in Remark 16 and assume that Assumptions 3 and 4 hold. Given the Lyapunov function (3.42), and laws (3.17), (3.34), (3.39), and (3.41), if the acceleration estimation error is zero and the elements of ΔB are constant, asymptotic convergence of $(\widetilde{\Upsilon}, \zeta)$ to the origin is guaranteed for any initial condition $\zeta(0)$, and all unknown system parameters, unmodeled dynamics, and disturbances without knowing their bounds a priori.*

Before proving this theorem, let us first define *uniform continuity* and state the Barbalat lemma [81].

Definition 10 (Uniform continuity)**.** A function $h(t) : \Re \rightarrow \Re$ is said to be *uniformly continuous* on $[0, \infty]$ if

$$\forall\, \epsilon > 0,\ \exists\, \delta(\epsilon) > 0,\ \forall\, t_1 \geq 0,\ \forall\, t \geq 0, |t - t_1| < \delta \rightarrow |h(t) - h(t_1)| < \epsilon. \tag{3.55}$$

Definition 11 (Barbalat lemma)**.** If $h(t)$ is uniformly continuous for all $t \geq 0$ and if the limit of the integral $\lim_{t\to\infty} \int_0^t h(\tau)d\tau$ exists and is finite, then $\lim_{t\to\infty} h(t) = 0$.

Proof. The assumption of zero acceleration estimation error and constant ΔB immediately follows that $\epsilon_{\Psi_i} = \bar{\Upsilon} = 0$, which reduces Eq. (3.49) to have

$$\dot{W} \leq -\alpha_Q \lambda_{min}(P)\|\zeta\|^2 - \lambda_{min}(H_1)\|\widetilde{\Upsilon}\|^2, \tag{3.56}$$

implying negative semi-definiteness of $\dot{W}$.

Let us define the following uniformly continuous function

$$h(t) = \alpha_Q \lambda_{min}(P)\|\zeta\|^2 + \lambda_{min}(H_1)\|\tilde{\Upsilon}\|^2 \geq 0 \tag{3.57}$$

to have $\dot{W}(t) \leq -h(t)$ of which integrating form 0 to ∞ yields

$$W(0) - W(\infty) \geq \lim_{t\to\infty} \int_0^t h(\tau)d\tau. \tag{3.58}$$

Since $\dot{W}(t) \leq 0$, the term $W(0) - W(\infty)$ is positive and finite, from which it follows that $\lim_{t\to\infty} \int_0^t h(\tau)d\tau$ is also positive ($h(t)$ is positive) and finite. Hence, due to the Barbalat lemma, it follows that

$$\lim_{t\to\infty} h(t) = \lim_{t\to\infty} \left(\alpha_Q \lambda_{min}(P)\|\zeta\|^2 + \lambda_{min}(H_1)\|\widetilde{\Upsilon}\|^2\right) = 0. \tag{3.59}$$

With the results of Remark 16 in hand, H_1 is positive definite and in turn $\lambda_{min}(H_1) > 0$. On the other hand, since $\lambda_{min}(P) > 0$ and $\alpha_Q > 0$, Eq. (3.59) implies that $(\zeta, \widetilde{\Upsilon}) \to 0$. This proves asymptotic convergence of the tracking and estimation errors $(\zeta, \widetilde{\Upsilon})$ to zero in the closed-loop dynamics while $\widetilde{K}_r$ is also UUB due to the boundedness of K_r by $K_{r_{max}}\sqrt{1 + \nu_{K_r}}$. □

Remark 20 (Uniform continuity of function $h(t)$)**.** To prove the uniform continuity of the function $h(t)$ presented in (3.57), the boundedness of its time derivative has to be shown; for this purpose,

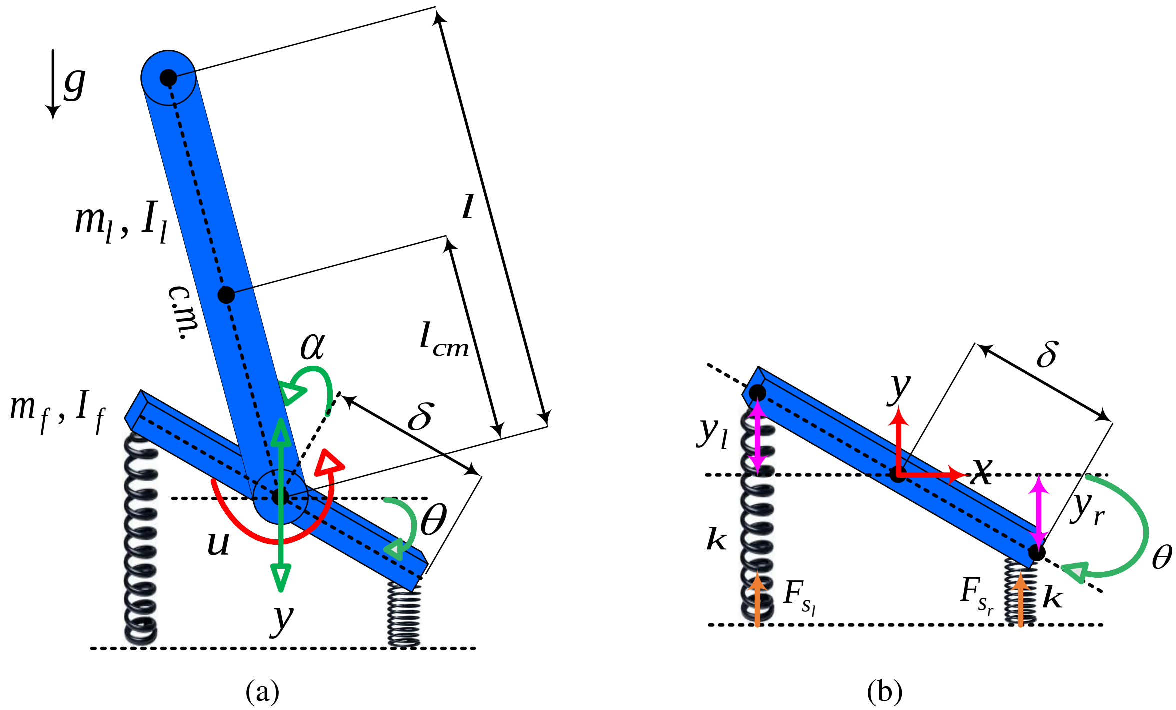

Figure 3.1: (a) The foot-leg model, and (b) foot and soft ground

the following discussion can be made. In view of Eqs. (3.42) and (3.56), it can be inferred that $W > 0$ and $\dot{W} \leq 0$ implying that all variables ζ, $\widetilde{\Upsilon}$, and $\widetilde{K}_r$ are bounded. From the boundedness of ζ and due to Assumption 4, since the reference trajectory q_a^d and its derivative are bounded, then q and $\dot{q}$ are bounded. This along with the boundedness of v_{opt} (by enforcing control bounds in QP optimization) and the assumption of all the disturbances being bounded concludes the boundedness of $\dot{\zeta}$. On the other hand, since $\dot{\Upsilon}$, ζ, and the acceleration estimation error are all bounded, it follows that $\dot{\tilde{\Upsilon}}$ is bounded. Taken altogether, since all the variables $\zeta, \tilde{\Upsilon}, \dot{\zeta}$, and $\dot{\tilde{\Upsilon}}$ are bounded, then

$$\dot{h}(t) = 2\alpha_Q \lambda_{min}(P)\zeta^T\dot{\zeta} + 2\lambda_{min}(H_1)\tilde{\Upsilon}^T\dot{\tilde{\Upsilon}} \tag{3.60}$$

is bounded which follows that $h(t)$ is uniformly continuous.

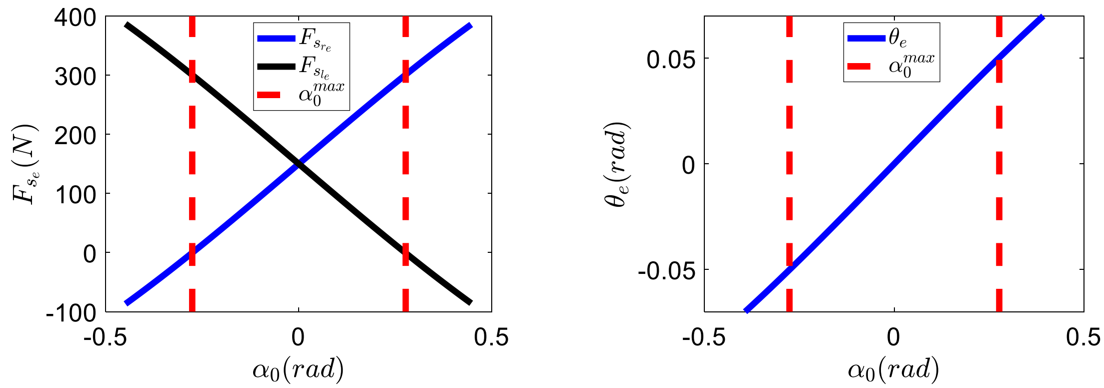

Figure 3.2: The quasi-static spring forces (left) and foot angle (right) with the stabilization range (no negative forces) indicated by red dashed lines.

3.5 Simulation results

In this section, simulation studies are carried out to validate the effectiveness of the proposed adaptive QP-IRCLF. A comprehensive comparison is then conducted between our control strategy with an adaptive QP-RCLF (Remark 14 from [31]) and the baseline non-adaptive QP-RCLF on two illustrative underactuated robotic systems: a foot-leg model on deformable ground shown in Fig. 3.1 and the overhead crane system shown in Fig. 3.5. The proposed controller is applied for both systems through the laws (3.17), (3.34), (3.39), and (3.41) while utilizing the recording policy in Remark 16 and the estimated system's acceleration. The design parameters of all controllers are tuned such that they can achieve their best performance in different simulation conditions.

3.5.1 Example 1. the foot-leg model on deformable ground

A. Modeling and initialization

The model is a foot plus a leg resting on two unidirectional springs to represent the soft ground as shown in Fig. 3.1(a). The springs are located at the ends of the feet so that they can only exert a pushing force, but cannot create a pulling force. Thus, the simulation with pulling force will be considered as the *instability condition* of the system. We assume that the foot-leg system can only

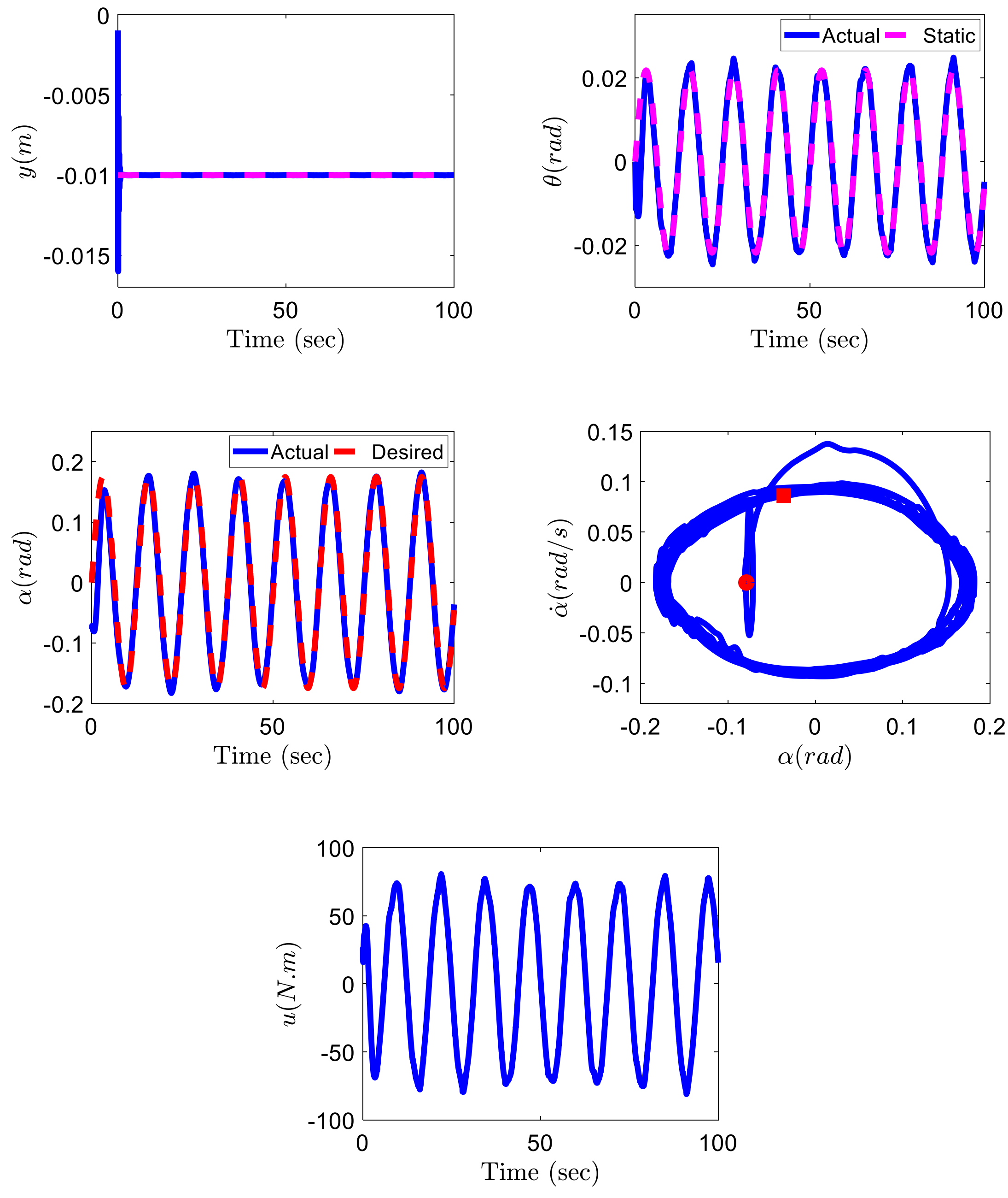

(a) Condition 1: Initial condition mismatch, and 40% uncertainty in parameters and control map

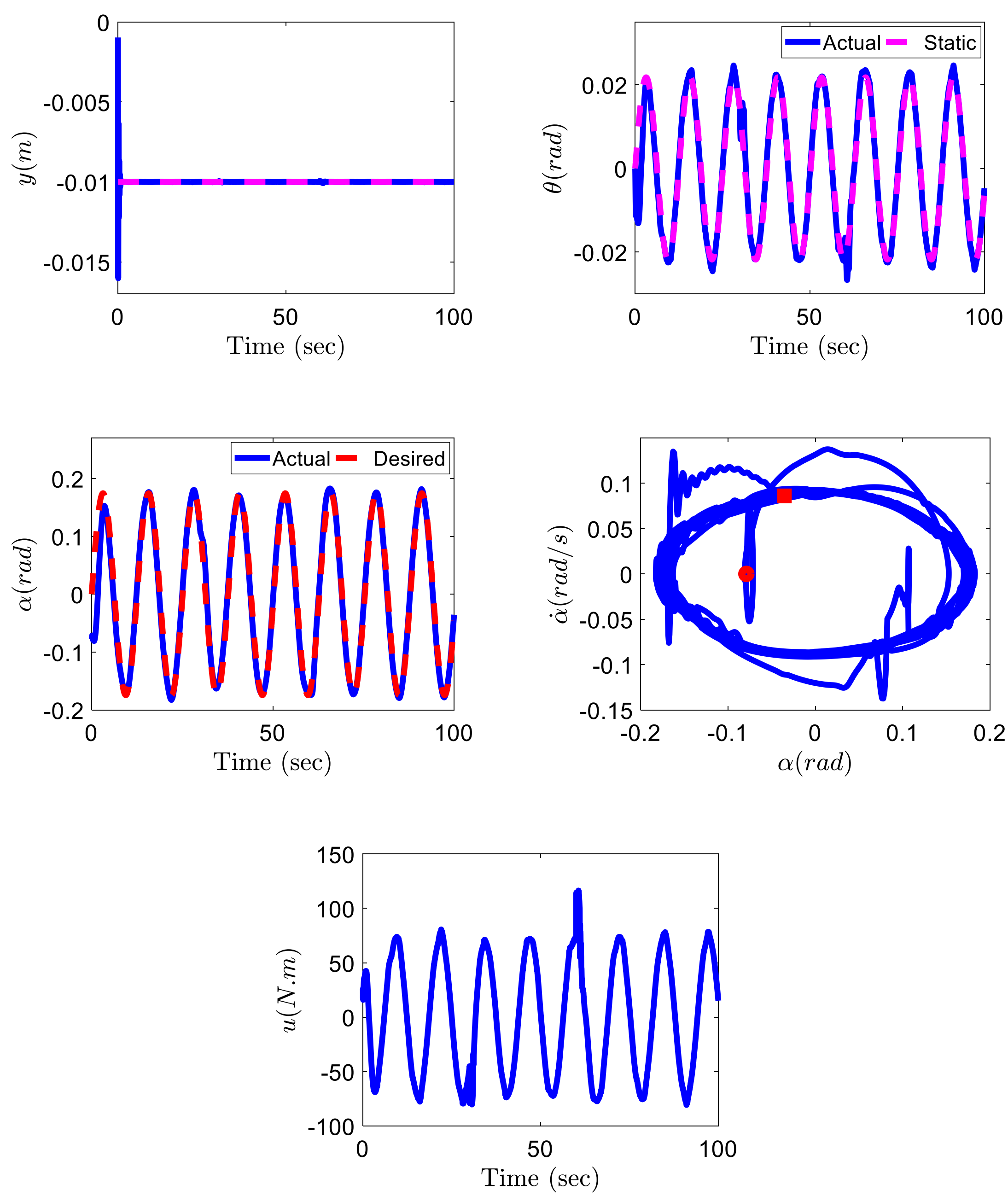

(b) Condition 2: Initial condition mismatch, 40% uncertainty in parameters and control map, and applied disturbances

Figure 3.3: The passive state space solutions (y, θ), active space tracking, phase portrait, and ankle torque under Condition 1 and Condition 2. The desired leg angle and the quasi-static trajectories are indicated by the red and magenta dashed lines, respectively. The red square and circle show the starting and the end points, respectively.

move up and down (no horizontal motion). The horizontal position of the foot is also assumed to be at zero and coincides with the center of the foot (which is where the ankle will lie for simplicity). Thus, the proposed model has a prismatic-revolute-revolute (PRR) joint structure as illustrated in Fig. 3.1(a). The foot-leg system can be modeled as a three DoF robot ($n = 3$) and its equations of motion are derived using the Euler-Lagrange formula as

$$M(q)\ddot{q} + C(q, \dot{q})\dot{q} + G(q) = \tau_{ext} + \tau, \tag{3.61}$$

where $q = [y, \theta, \alpha]^T \in \Re^3$ is the vector of the generalized coordinates with y as the vertical displacement, θ as the foot angle, and α as the leg angle; $M(q)$, $C(q, \dot{q})$, $G(q)$ are the inertia matrix, the Coriolis and Centripetal matrix, and gravity vector, respectively; the system has only one actuator at the ankle so $\tau = [0, 0, u]^T$ with u as the ankle torque; and $\tau_{ext} = J^T(q)F_s$ is the effect of the combined spring forces $F_s = [F_{s_r}, F_{s_l}]^T$ stemming from the soft ground on each joint, where the Jacobian matrix J is defined as

$$J(q) = \begin{bmatrix} 1 & -\delta\text{cos}(\theta) & 0 \\ 1 & \delta\text{cos}(\theta) & 0 \end{bmatrix}. \tag{3.62}$$

The ground force's components are modeled as $F_{s_r} = -ky_r$ and $F_{s_l} = -ky_l$ for which we define $y_r = y - \delta\text{sin}(\theta)$ and $y_l = y + \delta\text{sin}(\theta)$. Due to the structure (3.1), let us define $\Phi(q) = G(q) - \tau_{ext}$, which comprises both gravity and ground reaction force effects. Then, the partitioned form (3.2) of system (3.61) in the lower actuated form is given as

$$M_{uu} = \begin{bmatrix} m_f + m_l & -l_{cm}m_l\text{sin}(\theta+\alpha) \\ -l_{cm}m_l\text{sin}(\theta+\alpha) & m_l l_{cm}^2 + I_f + I_l \end{bmatrix}, \; M_{au} = \begin{bmatrix} -l_{cm}m_l\text{sin}(\theta+\alpha) & m_l l_{cm}^2 + I_l \end{bmatrix},$$

$$M_{aa} = m_l l_{cm}^2 + I_l, \;\; M_{ua} = \begin{bmatrix} -l_{cm}m_l\text{sin}(\theta+\alpha) \\ m_l l_{cm}^2 + I_l \end{bmatrix}, \;\; C_a = [0, 0, 0]$$

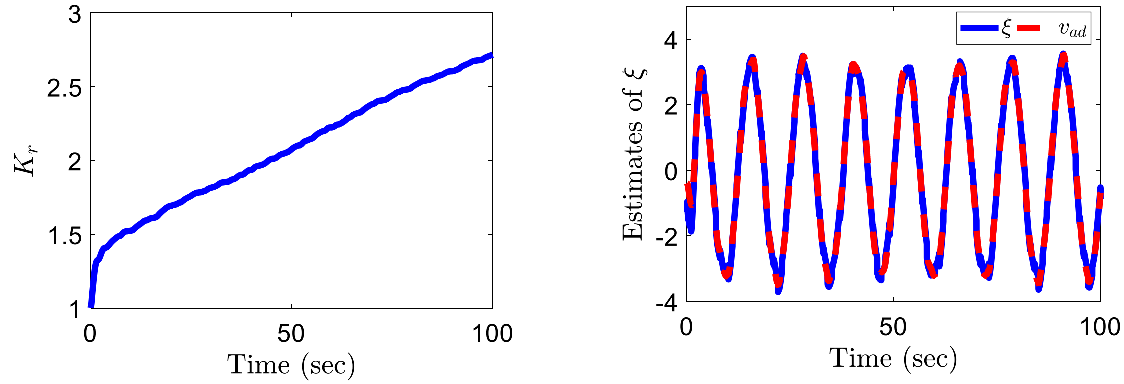

(a) Condition 1

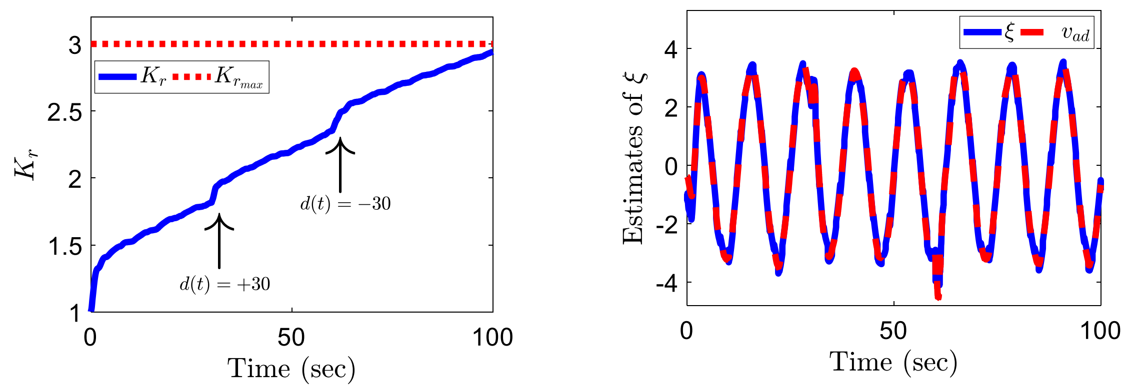

(b) Condition 2

Figure 3.4: The robust gain evolution and the dynamic estimation ξ under Conditions 1 and 2, where the red dotted line indicates the prescribed upper bound of the robust gain.

$$C_u = \begin{bmatrix} 0 & -l_{cm} m_l \cos(\theta+\alpha)(\dot{\theta}+2\dot{\alpha}) & -l_{cm} m_l \cos(\theta+\alpha)\dot{\alpha} \\ 0 & 0 & 0 \end{bmatrix}, \tag{3.63}$$

$$\Phi_u = \begin{bmatrix} g(m_f+m_l)+2ky \\ k\delta^2 \sin(2\theta) - g l_{cm} m_l \sin(\theta+\alpha) \end{bmatrix}, \; \Phi_a = -g l_{cm} m_l \sin(\theta+\alpha),$$

where I_l and I_f are the moments of inertia of the leg and foot about the ankle joint, respectively; m_l and l_{cm} are the mass and length of the leg to the center of mass; m_f is the mass of the foot; δ is the length between the ankle joint and the tip of the foot; and k is the spring stiffness.

As seen from (3.63), the foot-leg model is an underactuated system with only one DoA, which follows that $l = 2$ and $n - l = 1$. The task is to apply the proposed controller for this system to track the desired trajectory $\alpha^d(t) = A\text{sin}(2\pi f t)$ over 100 sec, while avoiding the ground reaction force to be negative. It follows that the simulation fails and the foot-leg system falls over (an instability condition) if $F_{s_r} < 0$ and/or $F_{s_l} < 0$. To avoid this concern, the range of motion for the leg angle α, i.e., *stabilization range*, should be computed using the quasi-static equilibrium (QSE) of the system for which no pulling force is generated. For this purpose, we begin by deriving the QSEs (y_e, θ_e) from $\Phi(q) = 0$ for a fixed α_0, which are the solutions of

$$\begin{aligned} & g(m_f + m_l) + 2ky_e = 0 \\ & k\delta^2\text{sin}(2\theta_e) - gl_{cm}m_l\text{sin}(\theta_e + \alpha_0) = 0. \end{aligned} \tag{3.64}$$

We then evaluate the forces at QSEs as

$$\begin{aligned} F_{s_{r_e}} &= -k(y_e - \delta\text{sin}(\theta_e)) \\ F_{s_{l_e}} &= -k(y_e + \delta\text{sin}(\theta_e)). \end{aligned} \tag{3.65}$$

By plotting $F_{s_{r_e}}$, $F_{s_{l_e}}$, and θ_e versus α_0 (as illustrated in Fig. 3.2), it can bee seen that the system does not fall over for $\alpha \in [-0.27, +0.27]$ (rad). In other words, the stabilization leg angle must lie within the given range to have the only pushing non-negative forces. Therefore, the desired $\alpha^d(t)$ should be assigned for $-0.27 \leq A(rad) \leq +0.27$, based on which we choose $A = 0.175$ (rad) and $f = \frac{1}{4\pi}$ $(Hertz)$ during the simulation.

B. Design parameters and controller set up

For the sake of having a fair comparison, the design parameters of all controllers (proposed, adaptive QP-RCLF, and baseline QP-RCLF) are chosen to be the same as $Q = l_{cont} = \text{diag}(1,1)$, $l_{rclf} = 10$, $\bar{u} = 150$, $\underline{u} = -150$, $K_{r_0} = 1$, $K_r(0) = 1$, $K_{r_{max}} = 3$, $\nu_{K_r} = 0.1$, $\eta_1 = \eta_2 =$

diag$(1, 1, 0.01)$, and $m = 3$[1]. The proposed controller and the adaptive QP-RCLF both use $\alpha_Q = 1$. However since the simulation with this α_Q fails for the baseline non-adaptive QP-RCLF, the convergence coefficient is selected to be $60\alpha_Q$ to have a reasonable tracking performance for this controller.

The active space of the system (3.63) can be written in the form of (3.12) to obtain

$$\ddot{\alpha} = \Psi\Upsilon + b_0 u \tag{3.66}$$

with $\Psi = [Y, u]$ and $\Upsilon = [P, \Delta b]^T$ including the regressor matrix and parameter vector

$$\begin{aligned} Y =& [-\hat{\ddot{\theta}}, \sin(\theta + \alpha)(g + \hat{\ddot{y}})] \\ P =& [1, \frac{m_l l_{cm}}{J_l + m_l l_{cm}^2}], \end{aligned} \tag{3.67}$$

where $b_0 = \frac{1}{J_l + m_l l_{cm}^2}$ is the base control coefficient with $\Delta b = b - b_0$ as the unknown part of b.

The objective is to control the active space (leg joint), while the passive space (other joints) stays bounded and the ground reaction forces remain positive (to prevent the system falls over). To evaluate the performance of different controllers, the simulation is carried out under the following two different conditions:

Condition 1 (Initial condition mismatch; and 40% parameter uncertainty)**.** In this condition, the initial conditions are randomly chosen as $q(0) = [0, 0, -0.0785]^T$ and $\dot{q}(0) = 0$, and all parameters are perturbed equally and at the same time by 40%.

Condition 2 (Initial condition mismatch; 40% parameter uncertainty; and disturbance)**.** In this condition, in addition to Condition 1, two unexpected pushes are also randomly applied to the leg joint at $t = 30$ and 60 (sec) with magnitudes of $+30$ and -30 $(N.m)$, respectively.

[1]Since for the foot-leg system, $r = 2$ and $n - l = 1$, then the number of the recorded data points should be selected as $m \geq 3$ for use in the recording policy in Remark 16.

C. Simulation results

Simulation results are shown in Figs. 3.3 and 3.4 with the proposed adaptive QP-IRCLF under Conditions 1 and 2. Figure. 3.3(a) confirms that under Conditions 1, the leg joint position nicely tracks its desired trajectory, while the passive joint positions (y, θ) stay bounded and converge to their quasi-static trajectories. This figure also demonstrates the phase portrait of the leg joint, showing convergence of the controller to a stable limit periodic orbit. In order to evaluate the adaptation mechanism (3.34), Condition 2 is applied to the system to test the robustness of the proposed controller. It can be seen in Fig. 3.3(b) that tracking of the leg joint is maintained while the other joints stay stable. This figure also shows that the portrait deviates at the disturbance encounters, but then smoothly converges to the cycle. These observations confirm a strong robustness of the proposed controller as it can tolerate the disturbance and parameter uncertainties simultaneously.

Figure 3.4 depicts the evolution of K_r generated by the proposed adaptation law (3.34) under Conditions 1 and 2. It can be observed in Fig. 3.4(a) that the robust gain is able to adapt itself based upon the scale of parameter uncertainties and the initial conditions in such a way that stabilization of the leg joint is maintained under Condition 1. In addition, under Condition 2, K_r can become adjusted at the disturbance exposure (Figure 3.4(b)) to maintain the tracking performance, while the boundedness of K_r is always guaranteed by $K_{r_{max}}\sqrt{1+\nu_{K_r}} \approx 3.15$ (the parameter drift will never happen). Figure 3.4 also illustrates that under both conditions, the adaptive signal v_{ad} appropriately estimates the augmented dynamic ξ such that the estimation error converges to a small neighborhood around the origin. These findings reveal that our proposed control approach is able to provide an appropriate dynamic estimation under both Conditions 1 and 2. Taken altogether, the results in Figs. 3.3 and 3.4 support the claim of Theorem 3 in which UUB of all system's solutions $(\zeta, \widetilde{\xi}, K_r)$ is guaranteed.

To show the superiority of the proposed controller over the adaptive QP-RCLF and the baseline QP-RCLF, a numerical comparison is performed under both Conditions 1 and 2 through Table 3.1. This table lists root mean square error (RMSE) of the active joint tracking (sum of position and velocity) RMSE_t, RMS value of the ankle torque $\mathrm{RMS}_{\mathrm{u}}$, absolute peak torque value $u_{\max}$, RMSE of

Table 3.1: Comparison results for different controllers under both conditions (Condition 1 / Condition 2) for 100 sec simulation on the foot-leg system, where the negative values in red show that the ground forces are negative (the robot falls over).

	Proposed	Adaptive QP-RCLF	Baseline
RMSE_t (rad)	0.037 / 0.040	0.065 / 0.090	0.114 / 0.120
$u_{\max}$ (N.m)	81 / 115	89 / 145	139 / 168
$\mathrm{RMS}_{\mathrm{u}}$ (N.m)	52 / 53	62 / 65	83 / 84
$F_{s_r}^{max}$ (N)	356 / 354	361 / 421	462 / 462
$F_{s_l}^{max}$ (N)	369 / 369	369 / 478	471 / 492
$F_{s_r}^{min}$ (N)	20 / 20	20 / -63	-39 / -67
$F_{s_l}^{min}$ (N)	20 / 20	20 / 1	-38 / -38
RMSE_ξ	0.172 / 0.175	1.315 / 1.00	-

dynamic estimation RMSE_ξ, and maximum and minimum values of the spring force components for 100 sec simulation. It can be inferred from Table 3.1 that under Condition 1, the proposed controller (i) improves tracking by 43% and 67%; (ii) decreases $u_{\max}$ by 9% and 41%; (iii) reduces the control cost by 16% and 37%, all compared with the adaptive QP-RCLF and the baseline method, respectively. This table also shows that the baseline controller is not able to maintain the stability criteria under this condition such that $F_{s_r}^{min}, F_{s_l}^{min} < 0$, which implies that the robot falls down under this controller. The quantitative results also reveal that our controller improves the dynamic estimation by 86% over the adaptive QP-RCLF. These improvements obtained by the proposed controller are mainly due to the estimation and control of the augmented dynamic ξ along with the derivation of the IRCLF component and dynamic estimator. Recall that these results are obtained where the coupling effects between the passive and active subspaces are taken into consideration for the control design by estimating the system's acceleration. Overall, these results provide strong evidence that the proposed control methodology outperforms other two controllers regarding the all design requirements when Condition 1 is applied.

The strong robustness of our proposed controller can be significantly highlighted when Condition 2 is applied for which the quantitative results are reported in Table 3.1. The first thing that catches our attention is that neither adaptive QP-RCLF nor baseline QP-RCLF is able to maintain the stability criteria under this condition (negative ground forces), which implies that the robot

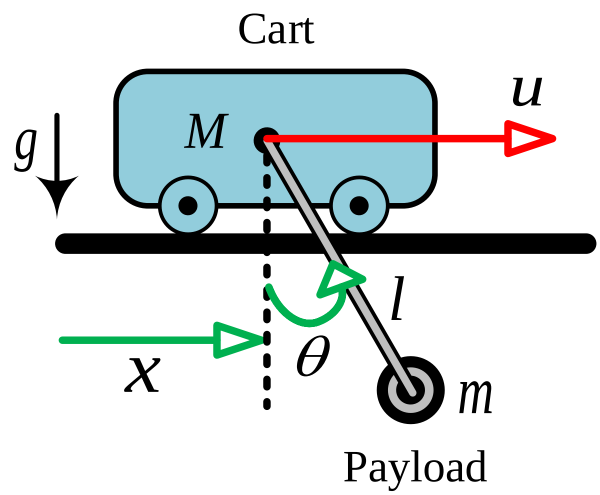

Figure 3.5: The overhead crane system

falls down when these controllers are applied. However, the proposed controller can nicely tolerate the pushes and remain stable. Regarding the other design specifications, the numerical results reveal that the proposed controller (i) enhances the tracking performance by 56% and 67%; (ii) decreases $u_{\max}$ by 20% and 31%; and (iii) improves $\mathrm{RMS_u}$ by 19% and 37%, all compared with the adaptive QP-RCLF and the baseline QP-RCLF, respectively. Our approach also improves RMSE_ξ by 83% compared with the adaptive QP-RCLF. These findings are consistent with previous results in Condition 1 showing the benefits of our approach over the other two controllers. Taken altogether, the results here confirm the strong robustness of our control methodology under both model uncertainties and disturbances.

3.5.2 Example 2. the overhead crane model

A. Modeling and initialization

The overhead crane, shown in Fig. 3.5, is a two DoF system which consists of a cart and a payload suspended with a massless rope from the cart. For this system, the partitioned structure (3.2) in the “upper actuated” form is given as

$$
\begin{aligned}
M_{aa} = m + M,\ M_{au} = ml\text{cos}(\theta),\ M_{ua} = M_{au},\ M_{uu} = ml^2 \\
C_a = [-ml\dot{\theta}\text{sin}(\theta), 0],\ C_u = [0, 0],\ \Phi_a = 0,\ \Phi_u = mgl\text{sin}(\theta),
\end{aligned}
\tag{3.68}
$$

where x and θ are the cart position and the payload angle respectively such that $q = [x, \theta]^T$ (m, rad); m and M are the masses of the cart and the payload; l is the length of the rope; and the system has only one actuator at the cart so that $\tau = [u, 0]^T$. The task is to control the cart position to track the desired trajectory $y_d = 0.8\text{sin}(t)$ over 100 sec simulation.

B. Design parameters and controller set up

In this example, the design parameters are tuned as $Q = l_{cont} = \text{diag}(1, 1)$, $l_{rclf} = 10$, $\bar{u} = 40$, $\underline{u} = -40$, $K_{r_0} = 1$, $K_r(0) = 1$, $K_{r_{max}} = 4$, $\nu_{K_r} = 0.1$, $\eta_1 = \eta_2 = \text{diag}(0.1, 0.01)$, and $m = 2$[2]. Unlike the proposed controller that uses $\alpha_Q = 1$, the convergence coefficients of the adaptive QP-RCLF and the baseline QP-RCLF are chosen to be $5\alpha_Q$ and $20\alpha_Q$, respectively. The reason why we choose such larger gains is that these two controllers are not able to maintain tracking with $\alpha_Q = 1$. The active space of the overhead crane (3.68) can be stated in the form of (3.12) to obtain

$$
\ddot{x} = \Psi\Upsilon + b_0 u, \tag{3.69}
$$

where the regressor, the parameter, and the base control coefficient can be derived as

$$
\begin{aligned}
Y =& \dot{\theta}^2\text{sin}(\theta) - \hat{\ddot{\theta}}\text{cos}(\theta) \\
P =& \frac{ml}{m + M} \\
b_0 =& \frac{1}{m + M}.
\end{aligned}
\tag{3.70}
$$

Again, to evaluate the controllers, the following two conditions are considered:

[2]Since for the overhead crane system, $r = 1$ and $n - l = 1$, we should pick $m \geq 2$ for use in the recording policy in Remark 16.

Condition 3 (Initial condition mismatch; and 100% parameter uncertainty)**.** In this condition, the initial conditions are $q(0) = [0.4, -\frac{\pi}{10}]^T$ and $\dot{q}(0) = 0$, and all parameters are deviated by 100%.

Condition 4 (Initial condition mismatch; 100% parameter uncertainty; and disturbance)**.** In this condition, Condition 3 holds while disturbances $d(t) = +20, -20$ $(N.m)$ are applied to the system at $t = 30, 60$ (sec), respectively.

C. Simulation results

Figure 3.6 illustrates simulation results obtained by applying the proposed controller to the overhead crane system under Conditions 3 and 4. Under both conditions, the cart position rapidly converges to its desired trajectory, as indicated in Fig 3.6. As also shown in this figure, the boundedness of the payload angle is always satisfied for both conditions. In addition, it can be seen in Fig 3.6 that the overhead crane control is very low force. This figure also demonstrates how the robust gains evolve under different conditions towards maintaining the tracking performance. In particular, Fig. 3.6(b) shows that when Condition 4 is applied, the gain K_r updates itself twice at $t = 30$ and $t = 60$ (sec) to compensate for the unexpected disturbances. Finally, as demonstrated in Fig. 3.6, the adaptive signal v_{ad} nicely estimates the actual unknown dynamic ξ. These results confirm that under our proposed controller, tracking error, dynamic estimation error, and the robust gain are all bounded, which is in agreement with Theorem 3 in which UUB of all system's solutions is guaranteed.

Table 3.2 provides a numerical evaluation of different controllers applied to the overhead crane system under Conditions 3 and 4. A cursory glance at Table 3.2 reveals that when Condition 3 is applied our controller (i) enhances tracking performance by 50% and 60%; (ii) reduces u_{max} by 25% and 58%; and (iii) improves RMS$_u$ by 9% and 11%, all compared with the adaptive QP-RCLF and the baseline QP-RCLF, respectively. With proposed controller, the estimation performance is also improved by 20% over the adaptive QP-RCLF. Table 3.2 also confirms the benefits of our proposed controller over the other two controllers when Condition 4 is imposed to the system. Under this condition, the proposed controller (i) enhances tracking by 62% and 65%; (ii) reduces u_{max}

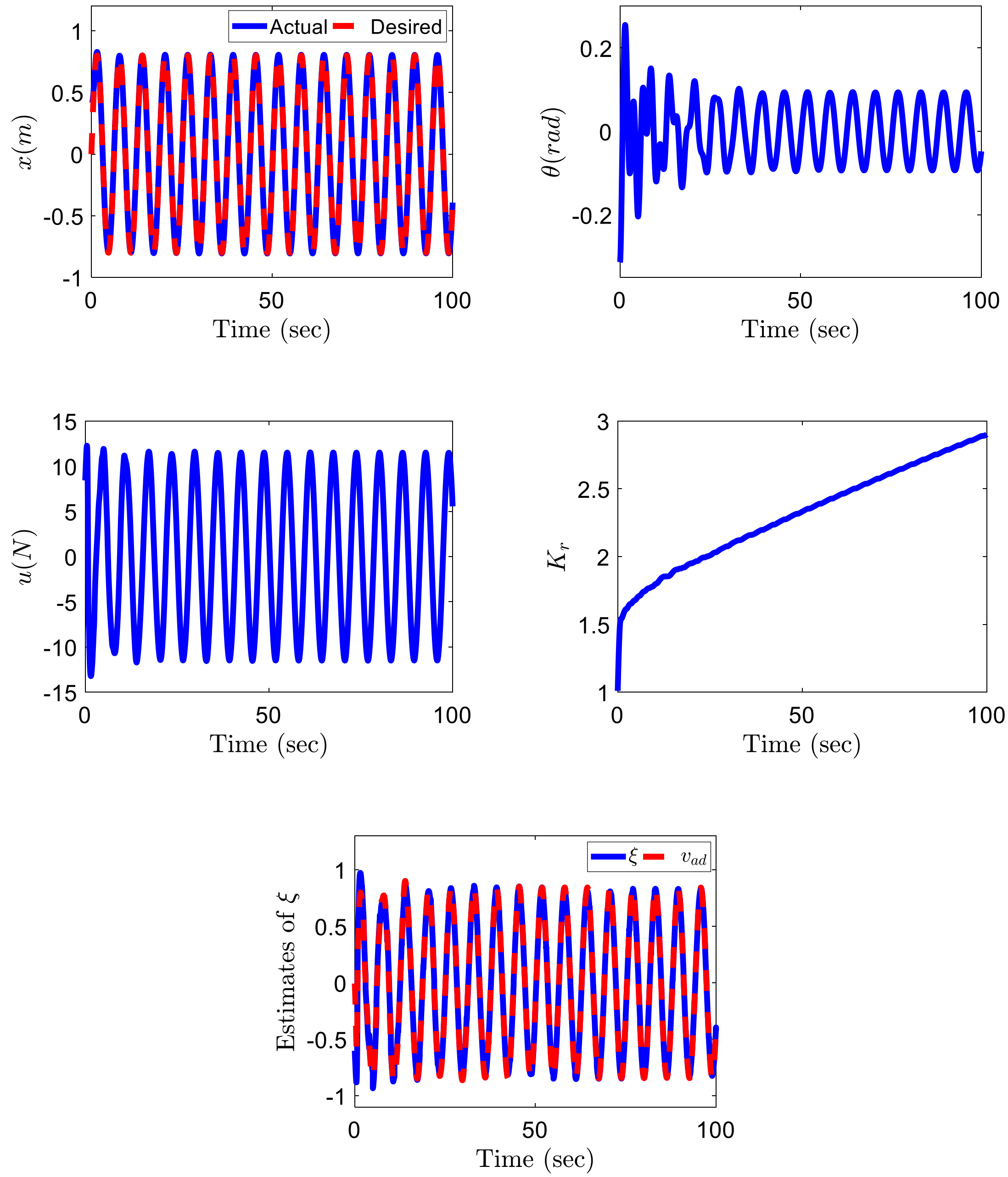

(a) Condition 3: Initial condition mismatch, and 100% parameter uncertainty in parameters and control coefficient

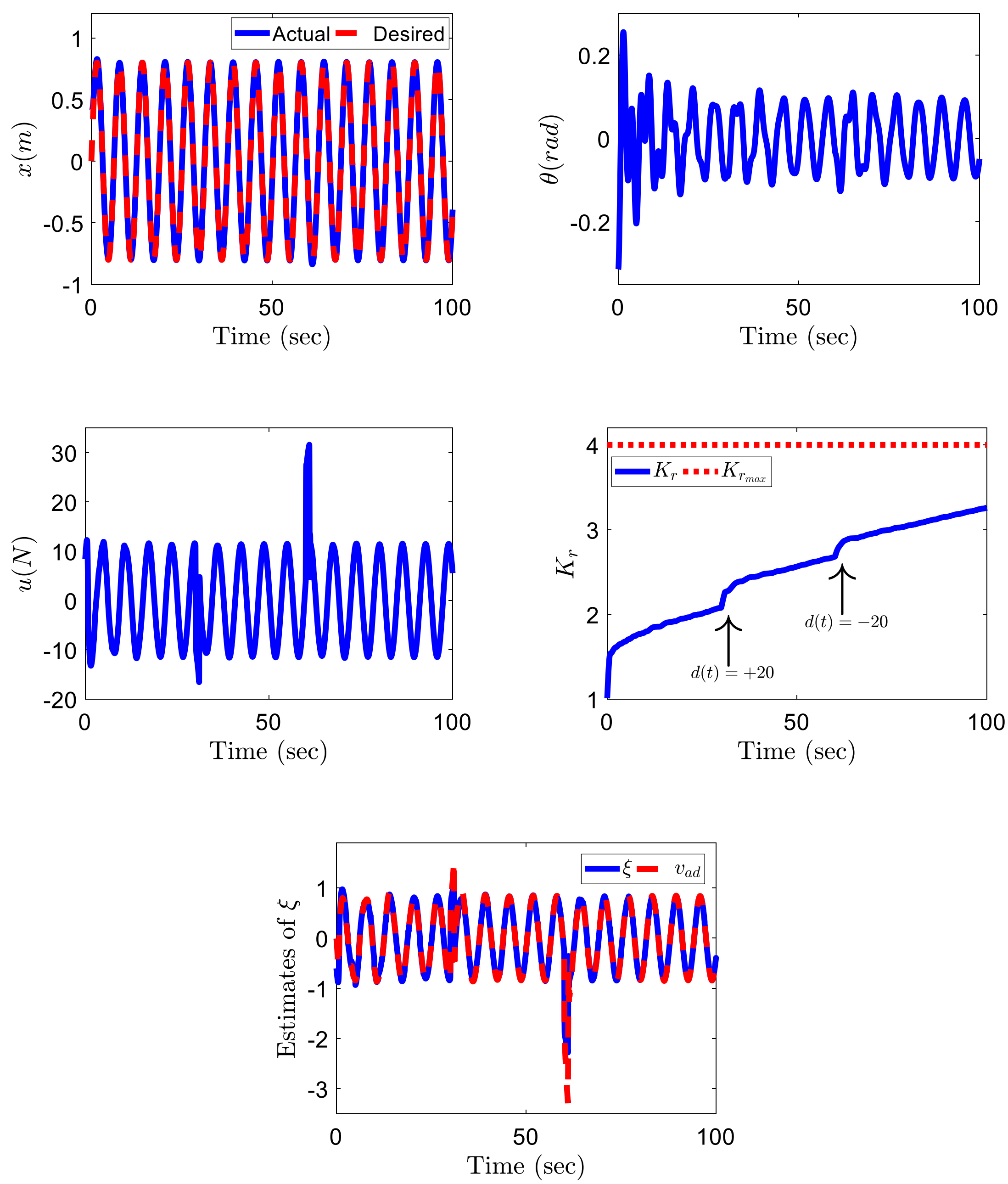

(b) Condition 4: Initial condition mismatch, 100% parameter uncertainty in parameters and control coefficient, and applied disturbances

Figure 3.6: The active space tracking (cart position), passive state space solution θ (payload angle), control force, robust gain evolution, and dynamic estimation ξ under Conditions 3 and 4, where the red dotted line indicates the prescribed upper bound of the robust gain.

Table 3.2: Comparison results for different controllers under both conditions (Condition 3 / Condition 4) for 100 sec simulation on the overhead crane system.

	Proposed	Adaptive QP-RCLF	Baseline
RMSE_t (rad)	0.067 / 0.070	0.135 / 0.184	0.170 / 0.200
$u_{\max}$ (N)	13 / 31	18 / 37	32 / 40
$\mathrm{RMS_u}$ (N)	8.13 / 8.60	8.95 / 9.45	9.20 / 10.00
RMSE_ξ	0.048 / 0.093	0.060 / 1.340	-
$\theta_{\max}$ (rad)	0.313 / 0.313	0.313 / 0.320	0.314 / 0.315

by 14% and 20%; and (iii) enhances RMS_u by 9% and 14%, all compared with the adaptive QP-RCLF and the baseline QP-RCLF, respectively. In addition, our controller improves the estimation performance by 9% compared with the adaptive QP-RCLF. It can be also seen in Table 3.2 that the peak payload angle θ_{max} is relatively the same under all controllers.

According to both examples together, the results provide convincing evidence for the claim that our proposed control scheme can outperform the adaptive QP-RCLF and the baseline QP-RCLF controllers in the presence of model uncertainties and unknown disturbances.

3.6 Conclusions and next chapter

This chapter presented a robust QP-based adaptive control approach for the active space stabilization of underactuated robotic systems. The unified multi-objective controller was able to identify the model uncertainties and robustify the closed-loop system against unmodeled dynamics and disturbances in an optimal control fashion without the need for knowing the bounds of these unknown terms. UUB of all system's solutions was proven through Theorems 3 and 4 by using Lyapunov and Barbalat arguments. To demonstrate these results, the proposed technique was implemented in simulations on two underactuated robotic systems through which the soundness of our method was validated. Comparisons with existing controllers (the baseline and adaptive QP-RCLF controllers) confirmed the benefits of our approach with regard to different design objectives.

The controller developed in this chapter can be slightly modified for fully-actuated systems. The presented approach can be implemented for a wide range of underactuated robotic systems when only the active space stabilization is required. However, there is a variety of underactuated applications with the objective of stabilizing the passive space (the space that cannot be actuated directly) while guaranteeing the boundedness of other solutions. This naturally encourages us to extend the presented approach for such systems in the presence of unmatched uncertainties while providing a formal disturbance-to-error stability analysis. This goal will be formulated in the next chapter.

CHAPTER 4

PASSIVE (NON-COLLOCATED) SPACE CONTROL AND SAFETY OF UNDERACTUATED SYSTEMS

This chapter extends and encompasses the QP-CLBF approach whose direct application to uncertain nonlinear dynamical systems with model uncertainties and disturbances could potentially degrade the performance of closed-loop systems and violate safety-critical constraints. In this chapter, we present a novel robust quadratic program-based adaptive approach for non-collocated control of a class of underactuated robotic systems with diagonal inertia matrices through which exponential disturbance-to-error (eDE) stability of all system solutions is ensured. We begin by developing a backstepping design technique based on which a neural network-based adaptive control is designed to approximate unknown nonlinear functions. To compensate uncanceled uncertainties, including modeling approximation error, chained error effects between coordinates, and time-varying disturbances, virtual inputs are designed whose gains are evolved by projection-based adaptation mechanisms. To construct a three-term control law, including feedforward, adaptive, and optimal terms, a QP optimization problem is synthesized to compute a family of optimal stabilizing signals while encoding time-varying robust CLF (TVRCLF) and CBF (TVRCBF), and control bounds as constraints. In contrast with existing QP-CLBF, our control technique with proposed TVRCLF and TVRCBF significantly improves control objectives, and strictly guarantee safety by automatically compensating unknown uncertainties without the need for knowing their bounds *a priori*. The eDES of all system errors is proven using Lyapunov stability arguments for both collocated and no-collocated coordinates. Simulations and comparisons to a baseline QP-CLBF-based feedback linearization (QP-CLBF/FL) on a single-link flexible-joint robot verify the benefits of the proposed control approach.

4.1 Background

In recent years, researchers have become increasingly interested in controlling of underactuated robotic systems due to their redundant applications such as aerial and underwater vehicles [82, 83], flexible-joint robots [84, 85], and walking robots [86, 87]. A challenging control problem with underactuated robots is that they have fewer degrees of actuation (DoA) than degrees of freedom (DoF). This, coupled with the existence of modeling uncertainties and disturbances makes such problem even more complex. The control of underactuated robots can be generally categorized into two different problems: *collocated* and *non-collocated* control, where the former controls the "actuated" degrees of freedom whose dimension is the same as the number of torque inputs and the latter stabilizes the remaining "passive" degrees [88, 89]. Over the years, an enormous amount of control strategies has been developed based on sliding modes [67, 90, 91], fuzzy logic [75, 92], adaptive controls [73, 93], and backstepping techniques [84, 94] for the collocated and non-collocated control of underactuated robots.

As we know, the QP-CLBF approach satisfies a large and diverse set of objectives for nonlinear dynamical systems through which both stabilization and safety can be ensured in an optimal fashion [5, 95]. However, as mentioned, the main drawback of QP-CLBF is that the existence of modeling inaccuracies degrades the performance of closed-loop systems and causes the violation of safety-critical constraints. Although the robust QP-CLBFs presented in [96, 78] could robustify the system against unmodeled dynamics and disturbances, the underlying assumption for those approaches is that the bound of unknown terms should be known *a priori*, which is not a practical assumption. It should be pointed out that under high gain control parameters, stabilization and safety may be achieved for the above approaches, however, this results in increasing the control efforts and restricting the safe sets.

4.2 Contributions

The shortcomings above along with the desire of extending the applications of QP-CLBF controller [5] motivates us to introduce a unified implementable control framework for the non-collocated control of underactuated robots. This chapter focuses on the control problem of the n DoF-one DoA underactuated robots with diagonal inertia matrices whose applications include, but not limited to, flexible-joint robots [84], moment gyroscopes [97], beam-ball systems [68], magnetic suspensions [98], and servo systems [99]. Note that clearly, the complexity of non-collocated control problem reduces for systems with non-diagonal inertia matrices as the control inputs can directly reach through the dynamics to stabilize the variables of interest. The main idea behind this work is that strict safety performance and accurate control objectives are achieved for underactuated robots with diagonal inertia matrices under a novel robust quadratic program-based adaptive control approach, that can ensure stability from bounded model inaccuracies and disturbances existing in the dynamics to all system solutions.

The goals of this chapter are, therefore, four-fold:

1. Drive non-collocated coordinate to a desired trajectory in an optimal fashion in the presence of modeling uncertainties and disturbances without knowing their bounds *a priori* (Theorem 6)

2. Prove exponential disturbance-to-error (eDE) stability of both collocated and non-collocated degrees of freedom (Theorem 6)

3. Guarantee strict safety for collocated coordinate against uncanceled terms with unknown bounds (Theorem 5)

4. Demonstrate benefits of the proposed controller over an existing QP-CLBF-based feedback linearization (QP-CLBF/FL) method (Section 4.7)

To the best of our knowledge, to date, no study has focused on developing a formal robust quadratic program-based adaptive approach to non-collocated control and safety of underactuated robots under which the above goals are satisfied.

To address the first goal, we begin by developing a $2n$-step backstepping design procedure for an uncertain strict-feedback form of the n DoF-one DoA underactuated robots with diagonal inertia matrices. Utilizing this recursive method, a radial basis function neural network (RBFNN)-based adaptive control is designed to approximate the unknown nonlinear functions. To achieve a proper estimation while being robust to disturbances, recorded data is concurrently used with instantaneous data to derive the neural network's weights. Modeling approximation error, chained errors between the system's states stemming from the backstepping design, and time-varying disturbances are compensated by designing virtual inputs whose gains are evolved by projection-based adaptation laws. With the estimates of unknown functions in hand, a three-term control law, including feed-forward, adaptive, and optimal terms, is suggested whose optimal term (stabilizing signal) is the solution of a QP optimization problem subject to a time-varying robust CLF (TVR-CLF). The novel TVRCLF along with the backstepping design ensures driving non-collocated coordinate to a desired trajectory while a time-varying robust gain compensates for the uncanceled terms without knowing their bounds *a priori*.

With the second goal in mind, a $2n$-step stability analysis is performed to guarantee eDES of all collocated and non-collocated coordinates for any bounded disturbances. For this purpose, Lyapunov arguments are investigated to derive the ultimate bounds of system's errors with respect to disturbances. To satisfy the third goal, a novel time-varying robust CBF (TVRCBF) is introduced whose gain is automatically updated in such a way that safety requirements are strictly satisfied for collocated coordinate of the system. By combining TVRCBF, TVRCLF, and torque bounds as optimization constraints encoded to a QP, an optimal balance is sought between non-collocated control, collocated safety, and torque requirements. Simulations and comparisons to a QP-CLBF/FL method on a single-link flexible-joint robot—an underactuated system with two DoF and one DoA—are carried out to validate the soundness and benefits of the proposed control methodology. The structure of this chapter is as follows. Section 4.3 presents the system description and problem statement. Section 4.4 revisits basic preliminaries and definitions. Section 4.5

formulates the proposed robust quadratic program-based adaptive controller. Section 4.6 provides the stability analysis. Section 4.7 presents the simulation and comparison results. Section 4.8 concludes the chapter and suggests for the future work.

4.3 System description and problem statement

In this section, we begin by describing a class of underactuated systems and then present our problem statement. Consider a class of n DoF-one DoA underactuated robotic systems with diagonal inertia matrices described by the following equations of motion (EoM):

$$M(q)\ddot{q} + C(q,\dot{q})\dot{q} + G(q) = u + d(t), \tag{4.1}$$

where $q = [q_{nc}, q_c]^T \in \Re^n$ is the vector of generalized coordinates in which $q_{nc} = [q_1, ..q_{n-1}] \in \Re^{n-1}$ and $q_c = q_n$ belong to the non-collocated (passive) and collocated (active) spaces, respectively; $u = [0_{1\times n-1}, u_c]^T$ is the control vector with u_c as the collocated space's torque; $d(t) = [d_1(t), ..., d_n(t)]^T$ is the vector of unknown disturbances acting on both collocated and non-collocated spaces; $M(q) = \text{diag}(m_{11}, \ldots, m_{nn}) \in \Re^{n\times n}$ is the diagonal inertia matrix; $C(q,\dot{q}) = [c_1, \ldots, c_n]^T \in \Re^{n\times n}$ is the Coriolis and Centripetal matrix with $c_i^T \in \Re^n$; and $G(q) = [g_1, \ldots, g_n]^T \in \Re^n$ is the gravity vector.

Assumption 6. The unknown disturbance $d(t)$ is uniformly bounded for all $t \geq 0$.

Let us define the state vector $z = [q_1, \dot{q}_1, ..., q_n, \dot{q}_n]^T \in \Re^{2n}$ to obtain the following strict-feedback form of the system (4.1)

$$\begin{aligned}
&\dot{z}_i = z_{i+1}, && i = 1, 3, \ldots, 2n-3 \\
&\dot{z}_i = z_{i+1} + f_{k_{i/2}}(z) + f_{un_{i/2}}(z) + d_{m_{i/2}}(t), && i = 2, 4, \ldots, 2n-2 \\
&\dot{z}_{2n-1} = z_{2n}, \qquad \dot{z}_{2n} = f_{k_n}(z) + f_{un_n}(z) + d_{m_n}(t) + b_0 u_n,
\end{aligned} \tag{4.2}$$

where the control coefficient $b = \frac{1}{m_{nn}}$ is assumed to be separable into the known term b_0 and unknown state-dependent term $\Delta b(z)$. The functions $f_{k_i}(z)$ and $f_{k_n}(z)$ are known with nominal system parameters, and the functions $f_{un_i}(z)$ and $f_{un_n}(z)$ are unknown such that they can be expressed in the following forms

$$\begin{aligned} f_{k_i}(z) &= -\frac{1}{m_{ii}}\left(c_i\dot{q} + g_i\right) - z_{2i+1}, && 1 \leq i \leq n-1 \\ f_{k_n}(z) &= -\frac{1}{m_{nn}}\left(c_n\dot{q} + g_n\right) \end{aligned} \tag{4.3}$$

and

$$\begin{aligned} f_{un_i}(z) &= \Delta f_i(z), & d_{m_i}(t) =& \frac{d_i(t)}{m_{ii}}, \quad 1 \leq i \leq n-1 \\ f_{un_n}(z) &= \Delta f_n(z) + \Delta b(z)u_n, & d_{m_n}(t) =& \frac{d_n(t)}{m_{nn}}, \end{aligned} \tag{4.4}$$

where the functions $\Delta f_i(z)$ and $\Delta f_n(z)$ stem from the parameter uncertainties and unmodeled dynamics. Due to Assumption 6, the above disturbances are bounded such that $|d_{m_i}| \leq \bar{d}_{m_i}$ and $|d_{m_n}| \leq \bar{d}_{m_n}$ for some $\bar{d}_{m_i}, \bar{d}_{m_n} > 0$.

This chapter is aimed at extending the applications of QP-CLBF controller to non-collocated control of underactuated robotic systems while enhancing the existing functionalities of this method with regard to stabilization and safety in the presence of model uncertainties and disturbances. The objective of this chapter is to design a robust quadratic program-based adaptive controller, mainly, based on backstepping technique and quadratic programs, for the system (4.2) such that (i) the non-collocated variable z_1 follows a desired trajectory z_1^d, (ii) all system errors are exponential disturbance-to-error stable (eDES), and (iii) the collocated variable z_{2n-1} is enforced to stay in the specified safe set $\underline{z}_{2n-1} \leq z_{2n-1} \leq \bar{z}_{2n-1}$. In the next section, basic preliminaries and definitions will be revisited to meet the demands for the later control design stages.

Assumption 7. The desired trajectory z_1^d is of *class* $\mathcal{C}^{2n}$.

4.4 Basic preliminaries and definitions

This section provides an overview of basic preliminaries and definitions [100, 26, 101] that will be later used when developing the proposed algorithm.

Definition 12. A continuous function $\alpha_1 : [0, a) \longrightarrow \mathbb{R}^+$ for some $a > 0$ belongs to *class* $\mathcal{K}$ if it is strictly increasing and $\alpha_1(0) = 0$. A continuous function $\alpha_2 : \mathbb{R}^+ \longrightarrow \mathbb{R}^+$ belongs to *class* $\mathcal{K}_\infty$ if it is strictly increasing, $\alpha_2(0) = 0$, and $\lim\limits_{r \longrightarrow \infty} \alpha_2(r) \longrightarrow \infty$. A continuous function $\alpha_3 : (-b, c) \longrightarrow (-\infty, \infty)$ for some $b, c > 0$ belongs to a extended *class* $\mathcal{K}$ if it is strictly increasing and $\alpha_3(0) = 0$. A continuous function $\alpha_4 : \mathbb{R}^+ \times \mathbb{R}^+ \longrightarrow \mathbb{R}^+$ belongs to *class* $\mathcal{KL}$ if $\alpha_4(r, t)$ is *class* $\mathcal{K}_\infty$ for each t and $\lim\limits_{t \longrightarrow \infty} \alpha_4(s, t) \longrightarrow 0$.

Definition 13 (eISS)**.** Consider the system $\dot{x}(t) = f(x(t), u(t))$, where $x \in \Re^n$ and $u \in \Re^m$ are the state and input vectors, and $f : \mathbb{R}^n \times \mathbb{R}^m \longrightarrow \mathbb{R}^n$ is locally Lipschitz with $f(0, 0) = 0$. This system is exponential input-to-state stable (eISS) if there exist $\alpha_2 \in \mathcal{K}_\infty$, $\alpha_4 \in \mathcal{KL}$, and some positive constant λ such that

$$|x(t)| \leq \alpha_4(|x(0)|, t)e^{-\lambda t} + \alpha_2(\|u\|_\infty),\ \forall x(0), \forall u, \forall t \geq 0. \tag{4.5}$$

Definition 14. An eISS system holds the asymptotic gain (AG) property if there exists $\alpha_2 \in \mathcal{K}_\infty$ such that $\overline{\lim\limits_{t \longrightarrow \infty}} |x(t, x(0), u)| \leq \alpha_2(\|u\|_\infty),\ \forall x(0), \forall u$. An eISS system is zero stable (ZS) if there exists $\alpha_4 \in \mathcal{KL}$ such that $|x(t, x(0), 0)| \leq \alpha_4(|x(0)|, t)e^{-\lambda t},\ \forall x(0), \forall t \geq 0$. The system is eISS if and only if it is AG and ZS.

Definition 15 (eISS-LF)**.** Consider the system $\dot{x} = f(x(t), u(t))$. A continuously differentiable function $V(x) : \mathbb{R}^n \longrightarrow \mathbb{R}^+$ is an eISS-Lyapunov function (eISS-LF) if there exist $\alpha_2 \in \mathcal{K}_\infty$ and some constant $\lambda > 0$ such that

$$\dot{V}(x) \leq -\lambda V(x) + \alpha_2(\|u\|_\infty),\ \forall x, \forall u. \tag{4.6}$$

Definition 16 (Projection operator)**.** The projection operator for two vectors $\mathscr{X}, \mathscr{Y} \in \mathbb{R}^n$ is defined as

$$\text{Proj}(\mathscr{X}, \mathscr{Y}) = \begin{cases} \mathscr{Y} - \frac{\nabla g(\mathscr{X})(\nabla g(\mathscr{X}))^T}{\|\nabla g(\mathscr{X})\|^2}\mathscr{Y} g(\mathscr{X}), & \text{if } g(\mathscr{X}) > 0 \ \wedge \ \mathscr{Y}^T \nabla g(\mathscr{X}) > 0 \\ \mathscr{Y}, & \text{otherwise} \end{cases}, \tag{4.7}$$

where $g(\mathscr{X}) = \frac{\mathscr{X}^T\mathscr{X} - \mathscr{X}_{max}^2}{\nu_{\mathscr{X}}\mathscr{X}_{max}^2} : \mathbb{R}^n \longrightarrow \mathbb{R}$ is a smooth convex function; $\mathscr{X}_{max}$ is the norm bound enforced on $\mathscr{X}$; and $\nu_{\mathscr{X}} > 0$ is the projection tolerance. The projection operator has the following properties: (i) it guarantees forward invariance of set $\mathcal{D} = \{\mathscr{X} \in \Re^n : \|\mathscr{X}\| \leq \mathscr{X}_{max}\sqrt{1+\nu_{\mathscr{X}}}\}$ for $g(\mathscr{X}) \leq 1$ and (ii) $-\tilde{\mathscr{X}}^T(\mathscr{Y} - \text{Proj}(\mathscr{X}, \mathscr{Y}, g)) \leq 0$, where $\tilde{\mathscr{X}} = \mathscr{X} - \mathscr{X}^*$ with $\mathscr{X}^*$ as the true value of $\mathscr{X}$.

Definition 17 (eISSs-ZCBF)**.** Consider the system $\dot{x} = f(x) + g(x)(u + D(x,t))$ with state $x \in \Re^n$, input $u \in \Re^m$, unknown disturbance $D(x,t) \in \Re^m$, and the locally Lipschitz functions $f : \mathbb{R}^n \longrightarrow \mathbb{R}^n$ and $g : \mathbb{R}^n \longrightarrow \mathbb{R}^n \times \mathbb{R}^m$. Define the set $\mathcal{C} = \{x \in \Re^n : \ h(x) \geq 0\}$ for which $h : \Re^n \to \Re$ is an r-times continuously differentiable function with relative degree r. Given the system above, the function $h(x)$ is an exponential input-to-state safe zeroing control barrier function (eISSs-ZCBF) for the set $\mathcal{C}$, if there exist $\alpha_1 \in \mathcal{K}$, a set of controls $\mathcal{V}_2$, gains $K^T \in \Re^r$ with proper positive elements k_i for $i = 1, ..., r$, and bound $\bar{D}$ to have $\|D(x,t)\| \leq \bar{D}$ such that

$$\sup_{u \in \mathcal{V}_2} \left[\mathcal{L}_f^r h(x) + \mathcal{L}_g \mathcal{L}_f^{r-1} h(x) u\right] \geq -KH(x) - \alpha_1\left(\|D(x,t)\|\right), \tag{4.8}$$

where $H(x) = [\mathcal{L}_f^{r-1}h(x), \ldots, \mathcal{L}_f h(x), h(x)]^T \in \Re^r$.

In case that $D(x,t) = 0$ (i.e., $\alpha_1\left(\|D(x,t)\|\right) = 0$), $h(x)$ is an exponential ZCBF (eZCBF) from which it follows that the forward invariance of set $\mathcal{C}$ is always guaranteed.

In the next section, we formulate our proposed multi-objective robust quadratic program-based adaptive control methodology to meet the objectives listed in Section 4.3.

4.5 Proposed robust quadratic program-based adaptive controller

With the above definitions in hand, this section, which deals with the formulation of our proposed controller, is organized into five distinct subsections. Subsection 4.5.1 designs a backstepping technique based on which virtual inputs and main control law are formulated. Projection-based adaptation mechanisms are also derived to compensate uncanceled dynamics with unknown bounds. Subsection 4.5.2 introduces a TVRCLF using which a robust stabilizing signal is generated for the system in the presence of unknown disturbances. Subsection 4.5.3 develops an adaptive control based on RBFNNs to approximate unknown functions, and inform virtual inputs and control law about them. Subsection 4.5.4 suggests a TVRZCBF under which strict safety requirements are ensured. Subsection 4.5.5 finally constructs a QP by unifying all the design components above to generate the optimal stabilizing control in a pointwise fashion.

4.5.1 Virtual inputs, control law, and error dynamics

In this section, an adaptive backstepping design approach is developed for the system (4.2). The design procedure includes $2n$ steps and uses the following coordinate transformations

$$e_1 = z_1 - z_1^d \text{ and } e_i = z_i - z_i^d \text{ for } i = 2, \ldots, 2n, \tag{4.9}$$

where z_1^d is a predefined desired trajectory; e_1 is the non-collocated tracking error; e_i for $i = 2, \ldots, 2n$ is the intermediate system error; and z_i^d for $i = 2, \ldots, 2n$ is the virtual input to be designed later.

Step 1: Using the transformation (4.9) along with the system (4.2), one obtains

$$\dot{e}_1 = \dot{z}_1 - \dot{z}_1^d = z_2 - \dot{z}_1^d = e_2 + z_2^d - \dot{z}_1^d. \tag{4.10}$$

By choosing the virtual input

$$z_2^d = \dot{z}_1^d - k_1 e_1 - k_{r_1}(t)\text{tanh}(\frac{e_1}{a_1}), \tag{4.11}$$

the error dynamics (4.10) can be written as

$$\dot{e}_1 = -k_1 e_1 + e_2 - k_{r_1}(t)\text{tanh}(\frac{e_1}{a_1}), \tag{4.12}$$

where $k_1, a_1 > 0$ are some parameters to be designed later; $\tanh(.)$ is the hyperbolic tangent function; and $k_{r_1}(t)$ is the time-varying robust gain whose adaptation law is suggested as

$$\dot{k}_{r_1} = l_1 \left(\text{Proj}\left(k_{r_1}, e_1 \text{tanh}(\frac{e_1}{a_1}) \right) - \sigma_1 k_{r_1} \right) \tag{4.13}$$

with scalars $l_1, \sigma_1 > 0$ and Proj(.,.) defined in Definition 16. This shows that for any bounded error e_2, the trajectory e_1 converges to a neighborhood of the origin exponentially at a rate of $k_1 > 0$.

Step 2: Using Eqs. (4.9) and (4.2), one has

$$\dot{e}_2 = \dot{z}_2 - \dot{z}_2^d = z_3 + f_{k_1} + f_{un_1} + d_{m_1}(t) - \dot{z}_2^d = e_3 + z_3^d + f_{k_1} + f_{un_1} + d_{m_1}(t) - \dot{z}_2^d, \tag{4.14}$$

where $\dot{z}_2^d$ is known and can be computed by taking the time derivative of (4.11).

By picking the virtual input

$$z_3^d = \dot{z}_2^d - f_{k_1} - \hat{f}_{un_1} - k_2 e_2 - k_{r_2}(t)\text{tanh}(\frac{e_2}{a_2}), \tag{4.15}$$

the system (4.14) becomes

$$\dot{e}_2 = -k_2 e_2 + e_3 + (f_{un_1} - \hat{f}_{un_1}) + d_{m_1}(t) - k_{r_2}(t)\text{tanh}(\frac{e_2}{a_2}), \tag{4.16}$$

where $k_2, a_2 > 0$ and $k_{r_2}(t)$ is updated by

$$\dot{k}_{r_2} = l_2 \left(\text{Proj} \left(k_{r_2}, e_2 \text{tanh}(\frac{e_2}{a_2}) \right) - \sigma_2 k_{r_2} \right) \tag{4.17}$$

with $l_2, \sigma_2 > 0$. In view of (4.16), e_2 exponentially converges to a neighborhood of the origin with convergence rate $k_2 > 0$ for any bounded signals e_3, $f_{un_1} - \hat{f}_{un_1}$, and $d_{m_1}(t)$.

Step i ($i = 3, 5, \ldots, 2n-3$)**:** With the virtual inputs derived from Step 1 to Step $i-1$ in hand, the adaptive backstepping design procedure at i-th step for $i = 3, 5, \ldots, 2n-3$ is presented as follows:

Utilizing Eqs. (4.9) and (4.2), one can obtain

$$\dot{e}_i = \dot{z}_i - \dot{z}_i^d = z_{i+1} - \dot{z}_i^d = e_{i+1} + z_{i+1}^d - \dot{z}_i^d. \tag{4.18}$$

Let us split $\dot{z}_i^d$ into the known term $\dot{z}_{i_k}^d$ and the unknown term $\dot{z}_{i_u}^d$, and define $f_{un_{n+i-2}} = -\dot{z}_{i_u}^d$ to obtain

$$\dot{e}_i = e_{i+1} + z_{i+1}^d + f_{un_{n+i-2}} - \dot{z}_{i_k}^d, \tag{4.19}$$

for which selecting

$$z_{i+1}^d = -k_i e_i + \dot{z}_{i_k}^d - \hat{f}_{un_{n+i-2}} - k_{r_i}(t) \text{tanh}(\frac{e_i}{a_i}) \tag{4.20}$$

results in

$$\dot{e}_i = -k_i e_i + e_{i+1} + (f_{un_{n+i-2}} - \hat{f}_{un_{n+i-2}}) - k_{r_i}(t) \text{tanh}(\frac{e_i}{a_i}), \tag{4.21}$$

where $k_i, a_i > 0$ and $k_{r_i}(t)$ is updated by the following adaptation law

$$\dot{k}_{r_i} = l_i \left(\text{Proj} \left(k_{r_i}, e_i \text{tanh}(\frac{e_i}{a_i}) \right) - \sigma_i k_{r_i} \right) \tag{4.22}$$

with $l_i, \sigma_i > 0$. Referring to (4.21), for any bounded variables e_{i+1} and $f_{un_{n+i-2}} - \hat{f}_{un_{n+i-2}}$, e_i exponentially converges to a neighborhood of the origin at a rate of $k_i > 0$.

Step i ($i = 4, 6, \ldots, 2n-2$)**:** The design procedure for i-th step with $i = 4, 6, \ldots, 2n-2$ is slightly different from the previous step as presented as follows:

Once again, referring to Eqs. (4.9) and (4.2), one can write

$$\dot{e}_i = \dot{z}_i - \dot{z}_i^d = z_{i+1} + f_{k_{i/2}} + f_{un_{i/2}} + d_{m_{i/2}}(t) - \dot{z}_i^d = e_{i+1} + z_{i+1}^d + f_{k_{i/2}} + f_{un_{i/2}} + d_{m_{i/2}}(t) - \dot{z}_i^d. \quad (4.23)$$

By defining $\dot{z}_i^d = \dot{z}_{i_k}^d + \dot{z}_{i_u}^d$ and $f_{un_{n+i-2}} = f_{un_{i/2}} - \dot{z}_{i_u}^d$, one has

$$\dot{e}_i = e_{i+1} + z_{i+1}^d + f_{k_{i/2}} + f_{un_{n+i-2}} + d_{m_{i/2}}(t) - \dot{z}_{i_k}^d, \quad (4.24)$$

for which picking

$$z_{i+1}^d = -k_i e_i + \dot{z}_{i_k}^d - f_{k_{i/2}} - \hat{f}_{un_{n+i-2}} - k_{r_i}(t)\tanh(\frac{e_i}{a_i}) \quad (4.25)$$

yields

$$\dot{e}_i = -k_i e_i + e_{i+1} + (f_{un_{n+i-2}} - \hat{f}_{un_{n+i-2}}) + d_{m_{i/2}}(t) - k_{r_i}(t)\tanh(\frac{e_i}{a_i}), \quad (4.26)$$

in which $k_{r_i}(t)$ can be updated by (4.22). Again, Eq. (4.26) implies that for any bounded variables e_{i+1}, $f_{un_{n+i-2}} - \hat{f}_{un_{n+i-2}}$, and $d_{m_{i/2}}(t)$, e_i is exponentially convergent into a ball of the origin while the rate of convergence is $k_i > 0$.

Step $2n-1$**:** With having the virtual input z_{n-1}^d from Step $2n-2$, and using Eqs. (4.9) and (4.2), one can write

$$\dot{e}_{2n-1} = e_{2n} + z_{2n}^d - \dot{z}_{2n-1}^d \quad (4.27)$$

for which splitting $\dot{z}_{2n-1}^d$ into terms $\dot{z}_{2n-1_u}^d$ and $\dot{z}_{2n-1_k}^d$ while defining $f_{un_{3n-3}} = -\dot{z}_{2n-1_u}^d$ results in

$$\dot{e}_{2n-1} = e_{2n} + z_{2n}^d + f_{un_{3n-3}} - \dot{z}_{2n-1_k}^d. \quad (4.28)$$

Let us select

$$z_{2n}^{d} = -k_{2n-1}e_{2n-1} + \dot{z}_{2n-1_k}^{d} - \hat{f}_{un_{3n-3}} - k_{r_{2n-1}}(t)\text{tanh}(\frac{e_{2n-1}}{a_{2n-1}}) \tag{4.29}$$

using which (4.28) becomes

$$\dot{e}_{2n-1} = -k_{2n-1}e_{2n-1} + e_{2n} + (f_{un_{3n-3}} - \hat{f}_{un_{3n-3}}) - k_{r_{2n-1}}(t)\text{tanh}(\frac{e_{2n-1}}{a_{2n-1}}), \tag{4.30}$$

where $k_{2n-1}, a_{2n-1} > 0$ and $k_{r_{2n-1}}(t)$ is evolved by

$$\dot{k}_{r_{2n-1}} = l_{2n-1}\left(\text{Proj}\left(k_{r_{2n-1}}, e_{2n-1}\text{tanh}(\frac{e_{2n-1}}{a_{2n-1}})\right) - \sigma_{2n-1}k_{r_{2n-1}}\right) \tag{4.31}$$

with $l_{2n-1}, \sigma_{2n-1} > 0$. This shows that if e_{2n} and $f_{un_{3n-3}} - \hat{f}_{un_{3n-3}}$ are bounded, then exponential convergence of e_{2n-1} into a ball of the origin is ensured with the rate of convergence $k_{2n-1} > 0$.

Step $2n$**:** Utilizing the virtual input designed from the previous step (Step $2n-1$), this final step is devoted to compute the collocated control torque u_n.

In view of Eqs. (4.9) and (4.2), one writes

$$\dot{e}_{2n} = \dot{z}_{2n} - \dot{z}_{2n}^{d} = f_{k_n} + f_{un_n} + d_{m_n}(t) + b_0u_n - \dot{z}_{2n}^{d}. \tag{4.32}$$

Letting $\dot{z}_{2n}^{d} = \dot{z}_{2n_k}^{d} + \dot{z}_{2n_u}^{d}$ and $f_{un_{3n-2}} = f_{un_n} - \dot{z}_{2n_u}^{d}$ leads to

$$\dot{e}_{2n} = f_{k_n} + f_{un_{3n-2}} + d_{m_n}(t) + b_0u_n - \dot{z}_{2n_k}^{d}. \tag{4.33}$$

Pick the main control law as

$$u_n = \frac{1}{b_0}(\dot{z}_{2n_k}^{d} - f_{k_n} - \hat{f}_{un_{3n-2}} + v_{opt}) \tag{4.34}$$

using which the system (4.33) becomes

$$\dot{e}_{2n} = v_{opt} + (f_{un_{3n-2}} - \hat{f}_{un_{3n-2}}) + d_{m_n}(t), \tag{4.35}$$

which follows that a stabilizing control signal v_{opt} can provide exponential convergence of e_{2n} to a neighborhood around the origin for any bounded estimation error $f_{un_{3n-2}} - \hat{f}_{un_{3n-2}}$ and disturbance $d_{m_n}(t)$.

In the next section, the stabilizing control signal v_{opt} will be computed in an optimal fashion to guarantee the stability of the error dynamics (4.35).

4.5.2 Time-varying robust control Lyapunov function (TVRCLF)

While traditional CLF-based controllers [5, 8] ensure the stability of nonlinear systems, their performance is degraded under unknown modeling errors and disturbances. Robust CLF-based approaches [78, 101] enhance the performance of those controllers by incorporating a robust component whose "constant" gain should be manually tuned to compensate for unknown terms. However since the bound of these terms is unknown, improper selection of the gains causes either undesirable tracking performance or aggressive control effort. In this section, a TVRCLF is introduced to ensure exponential disturbance-to-error (eDE) stability of the system (4.35) (from the disturbance $(f_{un_{3n-2}} - \hat{f}_{un_{3n-2}}) + d_{m_n}(t)$ to the error e_{2n}). An adaptive law is designed to tune the robust gain automatically in such a way that all disturbances are rejected without knowing their bounds *a priori* .

For this purpose, we begin by presenting the following definition.

Definition 18. Given the system (4.35), the function $V(e_{2n})$ is an exponentially stabilizing TVRCLF if there exist a set of controls $\mathcal{V}$ and positive scalars $\lambda, a_1, a_2 > 0$ such that

$$a_1|e_{2n}|^2 \leq V(e_{2n}) \leq a_2|e_{2n}|^2, \tag{4.36}$$
$$\inf_{v_{opt}\in\mathcal{V}} [\mathcal{R}_{clf}(e_{2n}) + e_{2n}v_{opt}] \leq -\lambda V(e_{2n}),$$

where $\mathcal{R}_{clf}(e_{2n})$ is the time-varying robust component that can automatically compensate for the uncanceled terms.

Let us pick the Lyapunov function $V(e_{2n}) = \frac{1}{2}e_{2n}^2$ whose time derivative along the error dynamics of the collocated space is

$$\dot{V}(e_{2n}) = e_{2n}v_{opt} + e_{2n}\Big((f_{un_{3n-2}} - \hat{f}_{un_{3n-2}}) + d_{m_n}(t)\Big). \tag{4.37}$$

By picking $v_{opt} = -\frac{\lambda}{2}e_{2n}$, one has

$$\dot{V}(e_{2n}) = -\frac{\lambda}{2}e_{2n}^2 + e_{2n}\Big((f_{un_{3n-2}} - \hat{f}_{un_{3n-2}}) + d_{m_n}(t)\Big) \tag{4.38}$$

which reduces to

$$\dot{V}(e_{2n}) \leq -\lambda V(e_{2n}) + |e_{2n}||(f_{un_{3n-2}} - \hat{f}_{un_{3n-2}}) + d_{m_n}(t)|. \tag{4.39}$$

Due to Definition 15, $V(e_{2n})$ is an eDES-LF (with exponential rate λ) in the error dynamics $\dot{e}_{2n}$ such that the ultimate bound of the error trajectory e_{2n} is

$$\left(\frac{2|(f_{un_{3n-2}} - \hat{f}_{un_{3n-2}}) + d_{m_n}(t)|}{\lambda}\right)^{1/2}. \tag{4.40}$$

Due to Definition 7, to find a balance between the stabilization and control optimality, the stabilizing signal v_{opt} can be generated by the following PWMNC law [27]

$$v_{opt}\big(\phi_0(e_{2n}), \phi_1(e_{2n})\big) = \begin{cases} -\frac{\phi_0(e_{2n})}{\phi_1(e_{2n})} & \text{if } \phi_0(e_{2n}) > 0 \\ 0 & \text{if } \phi_0(e_{2n}) \leq 0 \end{cases} \tag{4.41}$$

for which $\phi_0(e_{2n})$ and $\phi_1(e_{2n})$ are defined as

$$\phi_0(e_{2n}) = \lambda V(e_{2n}) + \mathcal{R}_{clf}(e_{2n}), \quad \phi_1(e_{2n}) = e_{2n} \tag{4.42}$$

with the robust component

$$\mathcal{R}_{clf}(e_{2n}) = k_{r_{2n}}(t)e_{2n}\text{tanh}(\frac{e_{2n}}{a_{2n}}), \tag{4.43}$$

where $a_{2n} > 0$. Note that the law (4.41) applies for all $e_{2n} \in V^{-1}(c_v, \infty)$ and never divides by zero as the set

$$v_{opt}(e_{2n}) = \{v_{opt} : \phi_0(e_{2n}) + \phi_1(e_{2n})v_{opt} \leq 0\} \tag{4.44}$$

is *nonempty* for $e_{2n} \in V^{-1}(c_v, \infty)$. Hence, the law (4.41) is implementable for all $V(e_{2n}) > c_v$.

The time-varying robust gain $k_{r_{2n}}(t)$ can be updated by the following law to compensate for the uncanceled term $(f_{un_{3n-2}} - \hat{f}_{un_{3n-2}}) + d_{m_n}(t)$

$$\dot{k}_{r_{2n}} = l_{2n}\left(\text{Proj}\left(k_{r_{2n}}, e_{2n}\text{tanh}(\frac{e_{2n}}{a_{2n}})\right) - \sigma_{2n}k_{r_{2n}}\right), \tag{4.45}$$

where $l_{2n}, \sigma_{2n} > 0$.

The solution of the PWMNC (4.41) can also be generated by a QP while incorporating the following TVRCLF constraint in the optimization problem to ensure eDE stability for the error dynamics $\dot{e}_{2n}$:

$$\phi_0(e_{2n}) + \phi_1(e_{2n})v_{opt} \leq 0. \tag{TVRCLF}$$

Noting that the time-varying disturbance $d_{m_i}(t)$ for $i = 1, \ldots, n$ is compensated by the adaptation mechanism

$$\dot{k}_{r_i} = l_i\left(\text{Proj}\left(k_{r_i}, e_i\text{tanh}(\frac{e_i}{a_i})\right) - \sigma_i k_{r_i}\right), \quad i = 1, \ldots, 2n, \tag{4.46}$$

the next step will concentrate on designing adaptation mechanisms to estimate the unknown functions $f_{un_1}, f_{un_{3n-3}}, f_{un_{3n-2}}$, and $f_{un_{n+i-2}}$ for $i = 3, 4, \ldots, 2n-1$.

4.5.3 Unknown nonlinear function estimation

To implement the virtual inputs z_3^d, z_{2n}^d, and z_{i+1}^d for $i = 3, 4, \ldots, 2n-1$, and the main control law u_n, the estimate of the unknown functions $f_{un_1}, f_{un_{3n-3}}, f_{un_{3n-2}}$, and $f_{un_{n+i-2}}$ for $i = 3, 4, \ldots, 2n-1$ is required. In this section, we begin by revisiting the radial basis function neural networks (RBFNNs) [102] to approximate these unknown functions and then develop adaptation mechanisms to estimate the approximated models.

The continuous function $f_{un}(z) : \mathbb{R}^{2n} \longrightarrow \mathbb{R}$ can be modeled as

$$f_{un}(z) = P_f^T \Phi_f(z) + \epsilon_f(z) \tag{4.47}$$

for which the true weight vector $P \in \Re^{n_f+1}$ and the basis function $\Phi(z) \in \Re^{n_f+1}$ are defined as

$$P = [p_0, p_1, p_2, \ldots, p_{n_f}]^T \text{ and } \Phi(z) = [b_w, \Phi_1(z), \Phi_2(z), \ldots, \Phi_{n_f}(z)]^T \tag{4.48}$$

with the bias $b_w > 0$ and the Φ' elements given by the Gaussian kernels

$$\Phi_i(z) = e^{-\frac{\|z-z_{c_i}\|}{\eta_i^2}}, \quad i = 1, \ldots, n_f, \tag{4.49}$$

where n_f is the number of nodes in the RBFNN; and z_{c_i} and η_i represent the center of the receptive field and the width of the Gaussian kernel, respectively.

Remark 21. The error $\epsilon_f(z)$ shrinks down for n_f to be sufficiently large which follows that the function $f_{un}(z)$ can be approximated by $f_{un}(z) = P_f^T \Phi_f(z)$. There also exists a positive constant $\bar{\epsilon}_f$ such that $|\epsilon_f(z)| \leq \bar{\epsilon}_f$.

Due to Remark 21, the unknown functions $f_{un_1}, f_{un_{3n-3}}, f_{un_{3n-2}}$, and $f_{un_{n+i-2}}$ for $i = 3, 4, \ldots, 2n-1$ can be approximated as

$$\hat{f}_{un_1}(z) = \hat{P}_{f_1}^T \Phi_{f_1}(z), \qquad \hat{f}_{un_{n+i-2}}(z) = \hat{P}_{f_{n+i-2}}^T \Phi_{f_{n+i-2}}(z), \tag{4.50}$$
$$\hat{f}_{un_{3n-3}}(z) = \hat{P}_{f_{3n-3}}^T \Phi_{f_{3n-3}}(z), \qquad \hat{f}_{un_{3n-2}}(z) = \hat{P}_{f_{3n-2}}^T \Phi_{f_{3n-2}}(z)$$

in which the weight vectors are updated by the following adaptation mechanisms

$$\begin{aligned}
\dot{\hat{P}}_{f_1} &= \Gamma_{f_1}^{-1}\left(\Phi_{f_1}(z)e_2 + \sum_{j=1}^{m_1} \Phi_{f_{1_j}}(z)\delta_{f_{1_j}}^T(z) - \sigma_{f_1}\hat{P}_{f_1}\right) \\
\dot{\hat{P}}_{f_{n+i-2}} &= \Gamma_{f_{n+i-2}}^{-1}\left(\Phi_{f_{n+i-2}}(z)e_i + \sum_{j=1}^{m_{n+i-2}} \Phi_{f_{n+i-2_j}}(z)\delta_{f_{n+i-2_j}}^T(z) - \sigma_{f_{n+i-2}}\hat{P}_{f_{n+i-2}}\right), \ \ i = 3, 4, \ldots, 2n-1 \\
\dot{\hat{P}}_{f_{3n-3}} &= \Gamma_{f_{3n-3}}^{-1}\left(\Phi_{f_{3n-3}}(z)e_{2n-1} + \sum_{j=1}^{m_{3n-3}} \Phi_{f_{3n-3_j}}(z)\delta_{f_{3n-3_j}}^T(z) - \sigma_{f_{3n-3}}\hat{P}_{f_{3n-3}}\right) \\
\dot{\hat{P}}_{f_{3n-2}} &= \Gamma_{f_{3n-2}}^{-1}\left(\Phi_{f_{3n-2}}(z)e_{2n} + \sum_{j=1}^{m_{3n-2}} \Phi_{f_{3n-2_j}}(z)\delta_{f_{3n-2_j}}^T(z) - \sigma_{f_{3n-2}}\hat{P}_{f_{3n-2}}\right),
\end{aligned} \tag{4.51}$$

where m_1, m_{n+i-1}, m_{3n-3}, and m_{3n-2} are the numbers of the recorded data points; $\Gamma_{f_1}^{-1} \in \Re^{(n_{f_1}+1)\times(n_{f_1}+1)}$, $\Gamma_{f_{n+i-2}}^{-1} \in \Re^{(n_{f_{n+i-2}}+1)\times(n_{f_{n+i-2}}+1)}$, $\Gamma_{f_{3n-3}}^{-1} \in \Re^{(n_{f_{3n-3}}+1)\times(n_{f_{3n-3}}+1)}$, and $\Gamma_{f_{3n-2}}^{-1} \in \Re^{(n_{f_{3n-2}}+1)\times(n_{f_{3n-2}}+1)}$ are positive definite diagonal matrices; and σ_{f_1}, $\sigma_{f_{n+i-1}}$, $\sigma_{f_{3n-3}}$, and $\sigma_{f_{3n-2}}$ are positive scalars.

The laws presented in (4.51) use recorded data concurrently with instantaneous data to render a proper estimation while being robust to disturbances. These three-term adaptation mechanisms unify (i) a traditional term which derives the parameter adaptation based upon the instantaneous system's errors [11] (first term), (ii) a concurrent learning (CL) term which enhances the estimation performance by exploiting recorded information [103] (second term), and a σ-modification term to robustify the adaptation against disturbances [104] (third term).

To implement the second term (CL) of (4.51), the discrepancy between unknown real functions and their estimates, evaluated at j-th recorded data point, is defined as

$$\begin{aligned} \delta_{f_{1_j}} =& f_{un_{1_j}} - \hat{f}_{un_{1_j}}, & \delta_{f_{n+i-2_j}} =& f_{un_{n+i-2_j}} - \hat{f}_{un_{n+i-2_j}}, \\ \delta_{f_{3n-3_j}} =& f_{un_{3n-3_j}} - \hat{f}_{un_{3n-3_j}}, & \delta_{f_{3n-2_j}} =& f_{un_{3n-2_j}} - \hat{f}_{un_{3n-2_j}} \end{aligned} \tag{4.52}$$

for which the unknown real functions are identified as follows

$$\begin{aligned} f_{un_{1_j}} &= \hat{\dot{e}}_2 + \nu_{1_j}, & \nu_{1_j} &= -f_{k_{1_j}} - z_{3_j} + \dot{z}^d_{2_j} & & \\ f_{un_{n+i-2_j}} &= \hat{\dot{e}}_i + \nu_{n+i-2_j}, & \nu_{n+i-2_j} &= -e_{i+1_j} - z^d_{i+1_j} + \dot{z}^d_{i_{k_j}}, & i &= 3, \ldots, 2n-3 \\ f_{un_{n+i-2_j}} &= \hat{\dot{e}}_i + \nu_{n+i-2_j}, & \nu_{n+i-2_j} &= -e_{i+1_j} - z^d_{i+1_j} + \dot{z}^d_{i_{k_j}} - f_{k_{i/2}}, & i &= 4, \ldots, 2n-2 \\ f_{un_{3n-3_j}} &= \hat{\dot{e}}_{2n-1} + \nu_{3n-3_j}, & \nu_{3n-3_j} &= -e_{2n} - z^d_{2n_j} + \dot{z}^d_{2n-1_{k_j}} & & \\ f_{un_{3n-2_j}} &= \hat{\dot{e}}_{2n} + \nu_{3n-2_j}, & \nu_{3n-2_j} &= -f_{k_{n_j}} - b_0 u_{n_j} + \dot{z}^d_{2n_{k_j}} & & \end{aligned} \tag{4.53}$$

in which $\hat{\dot{e}}_2$, $\hat{\dot{e}}_i$, $\hat{\dot{e}}_{2n-1}$, and $\hat{\dot{e}}_{2n}$ are estimated by an optimal fixed-point smoother (OFPS) [30]. Note that (4.53) is derived by using Eqs. (4.14), (4.19), (4.24), (4.28), (4.33) while assuming that the disturbances $d_{m_1}(t)$, $d_{m_{i/2}}(t)$, and $d_{m_n}(t)$ are properly compensated by the proposed robust gain adaptation mechanisms (4.46).

At this point, the error dynamics can be rewritten as

$$\begin{aligned} \dot{e}_1 &= -k_1 e_1 + e_2 - k_{r_1}(t)\tanh(\frac{e_1}{a_1}) \\ \dot{e}_2 &= -k_2 e_2 + e_3 + \tilde{P}^T_{f_1}\Phi_{f_1}(z) + \epsilon_{f_1}(z) + d_{m_1}(t) - k_{r_2}(t)\tanh(\frac{e_2}{a_2}) \\ \dot{e}_i &= -k_i e_i + e_{i+1} + \tilde{P}^T_{f_{n+i-2}}\Phi_{f_{n+i-2}}(z) + \epsilon_{f_{n+i-2}}(z) - k_{r_i}(t)\tanh(\frac{e_i}{a_i}), \quad i = 3, \ldots, 2n-3 \\ \dot{e}_i &= -k_i e_i + e_{i+1} + \tilde{P}^T_{f_{n+i-2}}\Phi_{f_{n+i-2}}(z) + \epsilon_{f_{n+i-2}}(z) + d_{m_{i/2}}(t) - k_{r_i}(t)\tanh(\frac{e_i}{a_i}), \quad i = 4, \ldots, 2n-2 \\ \dot{e}_{2n-1} &= -k_{2n-1} e_{2n-1} + e_{2n} + \tilde{P}^T_{f_{3n-3}}\Phi_{f_{3n-3}}(z) + \epsilon_{f_{3n-3}}(z) - k_{r_{2n-1}}(t)\tanh(\frac{e_{2n-1}}{a_{2n-1}}) \\ \dot{e}_{2n} &= v_{opt} + \tilde{P}^T_{f_{3n-2}}\Phi_{f_{3n-2}}(z) + \epsilon_{f_{3n-2}}(z) + d_{m_n}(t), \end{aligned} \tag{4.54}$$

where $\tilde{P}_f = P_f - \hat{P}_f$ and $\epsilon_f(z)$ are the estimation and approximation errors, respectively.

Remark 22. In this work, the RBF neural network $\hat{P}_f^T \Phi_f(z)$ for each unknown function defined in (4.50) contains n_f nodes with centers uniformly randomly distributed in the interval $[z_{1_{min}}, z_{1_{max}}] \times \cdots \times [z_{i_{min}}, z_{i_{max}}] \times \cdots \times [z_{2n_{min}}, z_{2n_{max}}]$ for $i = 1, \ldots, 2n$.

Remark 23. To achieve a proper estimation of the weight vector P_f, let us define the matrix $Z = [\Phi_{f_1}(z), \ldots, \Phi_{f_m}(z)] \in \Re^{(n_f+1)\times m}$ which stores those basis functions that are sufficiently different from the last point stored. Under this storing algorithm, if z_1^d is such that $\Phi_f(z)$ is *exciting* [105] over a finite interval, then $\text{rank}(Z) = n_f + 1$ and in turn, $H = ZZ^T \in \Re^{(n_f+1)\times(n_f+1)}$ is guaranteed to be a positive definite matrix [103].

Remark 24. The number of recorded data points should be selected in such a way that $m \geq n_f + 1$ holds. If a larger m is picked, the matrix Z may store a richer recorded data stack depending on the level of excitation of $\Phi_f(z)$. This results in a larger $\lambda_{min}(Z)$ and in turn a larger exponential Lyapunov convergence rate. In should be pointed out that determining the maximum value of m is not easy to decide a priori, but could be limited due to the computation complexity and memory restriction.

The next section will develop a time-varying control barrier function using which the collocated variable z_{2n-1} is strictly enforced to lie in a safe set.

4.5.4 Time-varying robust control barrier function (TVRCBF)

As aimed in the previous sections, the proposed robust quadratic program-based adaptive controller drives the non-collocated variable z_1 to z_1^d while providing eDE stability of all system solutions. In this section, we aim to enforce the collocated position z_{2n-1} to remain in a predefined safe set using the concept of control barrier functions (CBFs) [5]. This subsection consists of two parts. Part A provides a brief introduction to eISSs-ZCBF (Definition 15) for applying to the collocated position safety. The impact of unknown disturbances on the safety constraint violation is then evaluated and our proposed solution is suggested in Part B to ensure a strict safety for the collocated coordinate z_{2n-1}.

A. Exponential disturbance-to-state safe zeroing control barrier function (eDSSs-ZCBF):

The goal is to seek a family of the stabilizing signal v_{opt} to maintain the collocated position z_{2n-1} in the following safe set

$$\mathcal{C} = \{z \in \Re^{2n} : h_i(z) \geq 0,\ i = 1, 2\} \tag{4.55}$$

with $h_i(z)$ for $i = 1, 2$ as a two-times continuously differentiable function with relative degree two that is defined as

$$h_1(z) = z_{2n-1} - \underline{z}_{2n-1},\ \ h_2(z) = \bar{z}_{2n-1} - z_{2n-1}, \tag{4.56}$$

where $\underline{z}_{2n-1}$ and $\bar{z}_{2n-1}$ are the minimum and maximum threshold values for the collocated position z_{2n-1}, respectively.

For this purpose, we begin by substituting the main control law (4.34) (derived in Step $2n$) into the system (4.2) to obtain

$$\dot{z}_{2n} = \mathcal{K}_1(z) + \mathcal{K}_2(z)(v_{opt} + D(z, t)), \tag{4.57}$$

where $\mathcal{K}_1(z) = \dot{z}^d_{2n_k} - \hat{f}_{un_{3n-2}}(z)$, $\mathcal{K}_2(z) = 1$, and $D(z, t) = f_{un_n}(z) + d_{m_n}(t)$.

For the system (4.57), the following ZCBF certificate can be considered such that $h_i(z)$ becomes an eDSSs-ZCBF due to Definition 16

$$\mathcal{L}^2_{\mathcal{K}_1} h(z) + \mathcal{L}_{\mathcal{K}_2}\mathcal{L}_{\mathcal{K}_1} h(z) v_{opt} \geq -\alpha h_a(z), \tag{4.58}$$

where $\alpha = [\alpha_1, \alpha_2]$ and $h_a(z) = [\mathcal{L}_{\mathcal{K}_1} h(z), h(z)]^T$ with $\alpha_1, \alpha_2 > 0$.

Lemma 2. Given the system (4.57), the set $\mathcal{C}$, and the ZCBF certificate (4.58), the function $h(z)$ is an eDSSs-ZCBF with the ultimate violation bound $B_{b_1} = |\mathcal{L}_{\mathcal{K}_2}\mathcal{L}_{\mathcal{K}_1} h(z)| \|D(z, t)\|_\infty$.

Proof. Adding term $\mathcal{L}_{\mathcal{K}_2}\mathcal{L}_{\mathcal{K}_1} h(z) D(z, t)$ to both sides of the barrier certificate (4.58) yields

$$\mathcal{L}^2_{\mathcal{K}_1} h(z) + \mathcal{L}_{\mathcal{K}_2}\mathcal{L}_{\mathcal{K}_1} h(z) \left(v_{opt} + D(z, t)\right) \geq -\alpha h_a(z) + \mathcal{L}_{\mathcal{K}_2}\mathcal{L}_{\mathcal{K}_1} h(z) D(z, t) \tag{4.59}$$

for which utilizing the system dynamics $\dot{z}_{2n-1}$ and $\dot{z}_{2n}$ results in

$$\ddot{h} + \alpha_1 \dot{h} + \alpha_2 h \geq \mathcal{L}_{\mathcal{K}_2}\mathcal{L}_{\mathcal{K}_1} h(z) D(z,t) \geq -|\mathcal{L}_{\mathcal{K}_2}\mathcal{L}_{\mathcal{K}_1} h(z)| \|D(z,t)\|_\infty : B_{b_1}. \tag{4.60}$$

This, in turn, implies that $h_i(z)$ for $i = 1, 2$ is an eDSSs-ZCBF for which the violation of the collocated position z_{2n-1} from the safe set $\mathcal{C}$ is bounded in a neighborhood of the set boundary, where the size of the neighborhood is B_{b_1}. □

Utilizing the barrier certificate suggested in Lemma 2 leads to safety constraint violation whose ultimate bound depends on the scale of $D(z,t)$. In the next part, we will propose a time-varying robust control barrier certificate using which an accurate safety-critical system is obtained.

B. Exponential time-varying robust ZCBF (eTVRZCBF):

While robust CBF techniques [96, 78] are able to shrink down the violation ultimate bound, they assume that the bound of disturbances is known, which is not the case in real-world applications; hence, the barrier gains should be heuristically tuned by engineers. Consequently, improper selection of these gains leads to either the degradation of safety performance or the restriction of safe set. This part is devoted to present a TVRZCBF certificate to automatically compensate for the unknown disturbance $D(z,t)$ without the need for knowing its bounds *a priori*. This, in turn, provides an accurate safety for the collocated position z_{2n-1} to be restricted to always lie within its prespecified bounds.

To achieve this goal, we begin by estimating the unknown disturbance $D(z,t)$ by using the system (4.2) as presented as follows

$$\hat{D}(z,t) = \hat{\dot{z}}_{2n} + \nu_n \;\text{ with }\; \nu_n = -(f_{k_n} + b_0 u_n), \tag{4.61}$$

where the joint acceleration $\hat{\dot{z}}_{2n}$ can be estimated by a Kalman filter (KF) algorithm [30].

Assumption 8. Assume that the KF provides a bounded acceleration estimation error which follows that there exists a positive scalar $\bar{\epsilon}_D$ for $\epsilon_D = D(z,t) - \hat{D}(z,t)$ such that $|\epsilon_D| \leq \bar{\epsilon}_D$.

With the estimate of the disturbance $D(z,t)$ in hand, the following TVRZCBF certificate is suggested

$$\mathcal{L}^2_{\mathcal{K}_1}h(z) + \mathcal{L}_{\mathcal{K}_2}\mathcal{L}_{\mathcal{K}_1}h(z)v_{opt} + \mathcal{L}_{\mathcal{K}_2}\mathcal{L}_{\mathcal{K}_1}h(z)\hat{D}(t) + \mathcal{R}_{cbf}(h(z)) \geq -\alpha h_a(z), \qquad \text{(TVRZCBF)}$$

in which $\mathcal{R}_{cbf}(h(z))$ is a time-varying robust component that is defined by

$$\mathcal{R}_{cbf}(h(z)) = -K_b|\mathcal{L}_{\mathcal{K}_2}\mathcal{L}_{\mathcal{K}_1}h(z)| \tag{4.62}$$

whose robust gain is evolved by the kernel function

$$K_b(h(z)) = K_{b_0}\left(1 - e^{-\frac{\|h(z)\|^2}{2\rho^2}}\right) \tag{4.63}$$

with the tuning gain $K_{b_0} > 0$ and the kernel size $\rho > 0$.

Theorem 5. *Given the system (4.57), the set $\mathcal{C}$, and the TVRZCBF certificate (TVRZCBF) along with the time-varying robust component (4.62) and the robust gain (4.63), if the vector α is properly selected, then the forward invariance of set $\mathcal{C}$ is guaranteed and the function $h(z)$ is an exponential TVRZCBF (eTVRZCBF).*

Proof. By adding the term $\mathcal{L}_{\mathcal{K}_2}\mathcal{L}_{\mathcal{K}_1}h(z)D(z,t)$ to both sides of the TVRZCBF certificate (TVRZCBF), one has

$$\begin{aligned}\mathcal{L}^2_{\mathcal{K}_1}h(z) + \mathcal{L}_{\mathcal{K}_2}\mathcal{L}_{\mathcal{K}_1}h(z)\left(v_{opt} + D(z,t)\right) + \mathcal{L}_{\mathcal{K}_2}\mathcal{L}_{\mathcal{K}_1}h(z)\hat{D}(z,t) - K_b|\mathcal{L}_{\mathcal{K}_2}\mathcal{L}_{\mathcal{K}_1}h(z)| \geq \\ -\alpha h_a(z) + \mathcal{L}_{\mathcal{K}_2}\mathcal{L}_{\mathcal{K}_1}h(z)D(z,t)\end{aligned} \tag{4.64}$$

for which noting that

$$\ddot{h} = \mathcal{L}^2_{\mathcal{K}_1}h(z) + \mathcal{L}_{\mathcal{K}_2}\mathcal{L}_{\mathcal{K}_1}h(z)\left(v_{opt} + D(z,t)\right) \quad \text{and}$$
$$\mathcal{L}_{\mathcal{K}_2}\mathcal{L}_{\mathcal{K}_1}h(z)(D(z,t) - \hat{D}(z,t)) \geq -|\mathcal{L}_{\mathcal{K}_2}\mathcal{L}_{\mathcal{K}_1}h(z)||D(z,t) - \hat{D}(z,t)| \geq -|\mathcal{L}_{\mathcal{K}_2}\mathcal{L}_{\mathcal{K}_1}h(z)|\bar{\epsilon}_D,$$

one obtains

$$\ddot{h} + \alpha_1 \dot{h} + \alpha_2 h \geq -|\mathcal{L}_{\mathcal{K}_2}\mathcal{L}_{\mathcal{K}_1} h(z)|(K_b - \bar{\epsilon}_D). \tag{4.65}$$

In view of (4.65), if $\epsilon_D = 0$, then $h(z) \to 0$ based on which $K_b(h(z)) = 0$; hence, it follows that the right hand side of (4.65) is zero which implies that $h(z)$ is an eTVRZCBF under a proper selection of α. On the other hand, the existence of $\epsilon_D \neq 0$ causes violation/restriction of the safe set $\mathcal{C}$ resulting in the function $h(z)$ to be nonzero. For $h(z) \neq 0$, the robust component $\mathcal{R}_{cbf}$ measures the distance between the variable z_{2n-1} and its allowable threshold, and tunes the robust gain K_b to automatically compensate for the source of this error that is $\epsilon_D \neq 0$. Hence, the mechanism (4.63) applies to the system until the disturbance ϵ_D is fully compensated, resulting in the strict forward invariance of set $\mathcal{C}$. □

Remark 25. Utilizing the TVRZCBF certificate (TVRZCBF), the collocated position z_{2n-1} is always enforced to lie within its prescribed threshold values in the presence of the unknown disturbance $D(z,t)$ without the need for knowing its bound *a priori* (in contrast with existing robust CBFs, there is no any ultimate violation/restriction bound).

Remark 26. Under the proposed TVRZCBF, the forward invariance of set $\mathcal{C}$ is ensured. However, under robust ZCBFs with constant robust gain K_{cons}, the function $h(z)$ is an eDSSs-ZCBF for which the ultimate violation bound is $K_{cons} - |D(z,t)|$. Since the disturbance $D(z,t)$ is not known, its bound is not given and in turn, the robust ZCBF with an improper selection of K_{cons} can cause violation/restriction of the safe set.

4.5.5 QP structure

In this section, the stabilizing signal v_{opt} is computed by constructing an online QP optimization problem while satisfying the TVRCLF constraint (TVRCLF), the TVRZCBF constraint (TVRZCBF), and some required torque bounds:

$$\begin{aligned}
\mathbf{U}^* = &\underset{\mathbf{U}=(\boldsymbol{\rho}_\mathbf{r},\boldsymbol{\rho}_\mathbf{c},\mathbf{v}_\mathbf{opt})^T\in\Re^3}{\operatorname{argmin}} \quad \mathbf{v}_\mathbf{opt}^2 + \sigma_c\boldsymbol{\rho}_\mathbf{c}^2 + \sigma_r\boldsymbol{\rho}_\mathbf{r}^2 \qquad (4.66)\\
\text{s.t.}\ &\mathrm{TVRCLF}: \phi_1(e_{2n})\mathbf{v}_\mathbf{opt} - \boldsymbol{\rho}_\mathbf{r} \le -\phi_0(e_{2n})\\
&\mathrm{TVRZCBF}_1: +\mathbf{v}_\mathbf{opt} \le +H_1 + \alpha_1 h_2(z) - \alpha_2 z_{2n} - K_b(h_2(z))\\
&\mathrm{TVRZCBF}_2: -\mathbf{v}_\mathbf{opt} \le -H_1 + \alpha_1 h_1(z) + \alpha_2 z_{2n} - K_b(h_1(z))\\
&\mathrm{CB}_1: +\mathbf{v}_\mathbf{opt} - b_0\boldsymbol{\rho}_\mathbf{c} \le b_0\bar{u}_n + H_2\\
&\mathrm{CB}_2: -\mathbf{v}_\mathbf{opt} - b_0\boldsymbol{\rho}_\mathbf{c} \le b_0\bar{u}_n - H_2
\end{aligned}$$

where $K_b(h_i)$ is the robust gain evaluated at $h_i(z)$ for $i = 1, 2$, and the functions H_1 and H_2 are defined as

$$H_1 = \hat{f}_{un_{3n-2}} - \hat{D} - \dot{z}^d_{2n_k} \text{ and } H_2 = \hat{f}_{un_{3n-2}} - \dot{z}^d_{2n_k} + f_{k_n}. \qquad (4.67)$$

Under the last two constraints, the control torque u_n is enforced to satisfy $-\bar{u}_n - \rho_c \le u_n \le +\bar{u}_n + \rho_c$; the user-defined coefficients $\sigma_r, \sigma_c > 0$ relax the TVRCLF constraint and torque bounds in case that all constraints are enforced simultaneously causing the infeasibility of the optimization.

Remark 27. The above QP is feasible if the constraints are not in conflict with each other, which depends on the application that this optimization problem is applied to.

With the computed stabilizing signal v_{opt} in hand, the next section provides a detailed stability analysis through which the eDE stability of all system errors is proven.

4.6 Stability analysis

This section is concerned with proving the eDE stability of all system solutions, including the non-collocated tracking and collocated intermediate errors, the weight estimation error, and the robust gain estimation error, in the presence of unknown terms stemming from model uncertainties and disturbances. Throughout this section, we make the following assumption.

Assumption 9 (Matching assumption)**.** Assume that there exist some scalars

$$k^*_{r_{2n}}, k^*_{r_{2n-1}}, \dots, k^*_{r_i}, \dots k^*_{r_2}, k^*_{r_1} > 0 \tag{4.68}$$

such that

$$\begin{aligned} k^*_{r_{2n}} &= \bar{\epsilon}_{f_{3n-2}} + \bar{d}_{m_n} && \quad (4.69)\\ k^*_{r_{2n-1}} &= \bar{\epsilon}_{f_{3n-3}} + B_{2n} \\ k^*_{r_i} &= B_{i+1} + \bar{\epsilon}_{f_{n+i-2}} + \bar{d}_{m_{i/2}}, && i = 4, 6, \dots, 2n-2 \\ k^*_{r_i} &= B_{i+1} + \bar{\epsilon}_{f_{n+i-2}}, && i = 3, 5, \dots, 2n-3 \\ k^*_{r_2} &= B_3 + \bar{\epsilon}_{f_1} + \bar{d}_{m_1} \\ k^*_{r_1} &= B_2, \end{aligned}$$

where $\bar{\epsilon}_f > 0$ is the upper bound of the approximation error (Remark 21); $k^*_r > 0$ is the true value of the robust gain k_r; and $B_{2n}, \dots, B_i, \dots, B_2 > 0$ denote the ultimate bounds of the intermediate errors $e_{2n}, \dots, e_i, \dots, e_2$, respectively. Note that the above assumption assumes only the existence of k^*_r so that true knowledge of the ideal gain is not required.

Theorem 6. *Given the virtual inputs (4.11), (4.15), (4.20), (4.25), and (4.29), the main control law (4.34), the weight adaptation law (4.51), the robust adaptation mechanism (4.46), and the optimization problem (4.66) inducing the TVRCLF (TVRCLF) and TVRZCBF (TVRZCBF) constraints, all the system solutions are eDES for any bounded disturbances and any initial conditions.*

Proof. The proof is comprised of $2n$ steps beginning from the $2n$-th step.

Step $2n$: Consider the following candidate eDES-LF

$$V_{2n}(e_{2n}, \tilde{P}_{f_{3n-2}}, \tilde{k}_{r_{2n}}) = \frac{1}{2}\left(e^2_{2n} + \tilde{P}^T_{f_{3n-2}} \Gamma_{f_{3n-2}} \tilde{P}_{f_{3n-2}} + \frac{1}{l_{2n}} \tilde{k}^2_{r_{2n}}\right) \tag{4.70}$$

such that

$$\frac{1}{2}\min\left(1,\lambda_{\min}(\Gamma_{f_{3n-2}}),\frac{1}{l_{2n}}\right)\|\xi_{2n}\|^2\leq V_{2n}\leq\frac{1}{2}\max\left(1,\lambda_{\max}(\Gamma_{f_{3n-2}}),\frac{1}{l_{2n}}\right)\|\xi_{2n}\|^2, \quad (4.71)$$

where $\xi_{2n}=[e_{2n},\tilde{P}_{f_{3n-2}},\tilde{k}_{r_{2n}}]^T\in\Re^{n_{f_{3n-2}}+3}$ and $\tilde{k}_{r_{2n}}=k_{r_{2n}}-k^*_{r_{2n}}$ with the true value $k^*_{r_{2n}}$.

Taking the time derivative of V_{2n} along the error dynamics $\dot{e}_{2n}$ given by Eq. (4.54) yields

$$\dot{V}_{2n}=e_{2n}v_{opt}+e_{2n}\tilde{P}^T_{f_{3n-2}}\Phi_{f_{3n-2}}+e_{2n}\epsilon_{f_{3n-2}}+e_{2n}d_{m_n}(t)-\tilde{P}^T_{f_{3n-2}}\Gamma_{f_{3n-2}}\dot{\hat{P}}_{f_{3n-2}}+\frac{1}{l_{2n}}\tilde{k}_{r_{2n}}\dot{k}_{r_{2n}}. \quad (4.72)$$

By substituting the PWMNC law (4.41) (in case of $\phi_0>0$) and the weight adaptation law (4.51) into (4.72), one has

$$\begin{aligned}\dot{V}_{2n}=&-\frac{\lambda}{2}e_{2n}^2-k_{r_{2n}}e_{2n}\tanh(\frac{e_{2n}}{a_{2n}})-\tilde{P}^T_{f_{3n-2}}H_{3n-2}\tilde{P}_{f_{3n-2}}+\tilde{P}^T_{f_{3n-2}}\sigma_{f_{3n-2}}\hat{P}_{f_{3n-2}} \quad (4.73)\\&+e_{2n}\left(\epsilon_{f_{3n-2}}+d_{m_n}(t)\right)+\frac{1}{l_{2n}}\tilde{k}_{r_{2n}}\dot{k}_{r_{2n}},\end{aligned}$$

where $H_{3n-2}=\sum_{j=1}^{m_{3n-2}}\Phi_{f_{3n-2_j}}\Phi^T_{f_{3n-2_j}}>0$.

By adding and subtracting the term $e_{2n}\tanh(\frac{e_{2n}}{a_{2n}})\left(\bar{\epsilon}_{f_{3n-2}}+\bar{d}_{m_n}\right)$, we have

$$\begin{aligned}\dot{V}_{2n}\leq&-\frac{\lambda}{2}|e_{2n}|^2-k_{r_{2n}}e_{2n}\tanh(\frac{e_{2n}}{a_{2n}})-\left(\lambda_{\min}(H_{3n-2})+\sigma_{f_{3n-2}}\right)\|\tilde{P}_{f_{3n-2}}\|^2+\frac{1}{l_{2n}}\tilde{k}_{r_{2n}}\dot{k}_{r_{2n}} \quad (4.74)\\&+\left(\bar{\epsilon}_{f_{3n-2}}+\bar{d}_{m_n}\right)\left(|e_{2n}|-e_{2n}\tanh(\frac{e_{2n}}{a_{2n}})\right)+e_{2n}\tanh(\frac{e_{2n}}{a_{2n}})\left(\bar{\epsilon}_{f_{3n-2}}+\bar{d}_{m_n}\right)\\&+\sigma_{f_{3n-2}}\|\tilde{P}_{f_{3n-2}}\|\|P_{f_{3n-2}}\|.\end{aligned}$$

Substituting the robust adaptation law (4.45), and noting that $k^*_{r_{2n}}=\bar{\epsilon}_{f_{3n-2}}+\bar{d}_{m_n}$ (due to Assumption 9) and $|e_{2n}|-e_{2n}\tanh(\frac{e_{2n}}{a_{2n}})\leq c_{2n}a_{2n}$ for some scalar $c_{2n}>0$ yields

$$\dot{V}_{2n} \leq -\frac{\lambda}{2}|e_{2n}|^2 - \left(\lambda_{\min}(H_{3n-2}) + \sigma_{f_{3n-2}}\right)\|\tilde{P}_{f_{3n-2}}\|^2 - (\tilde{k}_{r_{2n}} + \bar{\epsilon}_{f_{3n-2}} + \bar{d}_{m_n})e_{2n}\tanh(\frac{e_{2n}}{a_{2n}}) \quad (4.75)$$
$$+ \tilde{k}_{r_{2n}}\mathrm{Proj}(k_{r_{2n}}, e_{2n}\tanh(\frac{e_{2n}}{a_{2n}})) - \tilde{k}_{r_{2n}}\sigma_{2n}(\tilde{k}_{r_{2n}} + \bar{\epsilon}_{f_{3n-2}} + \bar{d}_{m_n}) + \left(\bar{\epsilon}_{f_{3n-2}} + \bar{d}_{m_n}\right)c_{2n}a_{2n}$$
$$+ e_{2n}\tanh(\frac{e_{2n}}{a_{2n}})\left(\bar{\epsilon}_{f_{3n-2}} + \bar{d}_{m_n}\right) + \sigma_{f_{3n-2}}\|\tilde{P}_{f_{3n-2}}\|\|P_{f_{3n-2}}\|.$$

By applying the projection operator (Definition 16) and canceling the similar terms, one can obtain

$$\dot{V}_{2n} \leq -\frac{\lambda}{2}|e_{2n}|^2 - \left(\lambda_{\min}(H_{3n-2}) + \sigma_{f_{3n-2}}\right)\|\tilde{P}_{f_{3n-2}}\|^2 - \sigma_{2n}|\tilde{k}_{r_{2n}}|^2 + E_{2n}, \quad (4.76)$$

where

$$E_{2n} = \left(\bar{\epsilon}_{f_{3n-2}} + \bar{d}_{m_n}\right)\left(c_{2n}a_{2n} + \sigma_{2n}|\tilde{k}_{r_{2n}}|\right) + \sigma_{f_{3n-2}}\|\tilde{P}_{f_{3n-2}}\|\|P_{f_{3n-2}}\|. \quad (4.77)$$

Using the property (4.71), one obtains

$$\dot{V}_{2n}(e_{2n}, \tilde{P}_{f_{3n-2}}, \tilde{k}_{r_{2n}}) \leq -\kappa_{2n}V_{2n}(e_{2n}, \tilde{P}_{f_{3n-2}}, \tilde{k}_{r_{2n}}) + E_{2n} \quad (4.78)$$

with exponential Lyapunov converge rate

$$\kappa_{2n} = \frac{\min\left(\lambda, 2\lambda_{\min}(H_{3n-2}) + 2\sigma_{f_{3n-2}}, 2\sigma_{2n}\right)}{\max\left(1, \lambda_{\max}(\Gamma_{f_{3n-2}}), \frac{1}{l_{2n}}\right)}. \quad (4.79)$$

Due to Definition 15, V_{2n} is an eDES-LF in the error dynamics $\dot{e}_{2n}$. By applying the Comparison lemma [26] (Lemma 3.4), we have

$$V_{2n}(e_{2n}, \tilde{P}_{f_{3n-2}}, \tilde{k}_{r_{2n}}) \leq V_{2n}(e_{2n}(0), \tilde{P}_{f_{3n-2}}(0), \tilde{k}_{r_{2n}}(0))e^{-\kappa_{2n}t} + \frac{E_{2n}}{\kappa_{2n}} \quad (4.80)$$

from which

$$\|\xi_{2n}\| \leq \left[\frac{\max\left(1, \lambda_{\max}(\Gamma_{f_{3n-2}}), \frac{1}{l_{2n}}\right)}{\min\left(1, \lambda_{\min}(\Gamma_{f_{3n-2}}), \frac{1}{l_{2n}}\right)}\right]^{\frac{1}{2}} \|\xi_{2n}(0)\| e^{-\frac{\kappa_{2n}}{2}t} + \left[\frac{2E_{2n}}{\kappa_{2n}\min\left(1, \lambda_{\min}(\Gamma_{f_{3n-2}}), \frac{1}{l_{2n}}\right)}\right]^{\frac{1}{2}}. \tag{4.81}$$

In view of (4.81) and Definition 14, the system is ZS for $E_{2n} = 0$ and it holds the AG property if $\|\xi_{2n}(0)\| = 0$, which follows that the system is eDES.

Selecting $\kappa_{2n} = \kappa_{2n_1} + \kappa_{2n_2}$ with $\kappa_{2n_1}, \kappa_{2n_2} > 0$, Eq. (4.78) becomes

$$\dot{V}_{2n}(e_{2n}, \tilde{P}_{f_{3n-2}}, \tilde{k}_{r_{2n}}) \leq -\kappa_{2n_1} V_{2n}(e_{2n}, \tilde{P}_{f_{3n-2}}, \tilde{k}_{r_{2n}}) \tag{4.82}$$

if

$$-\frac{\kappa_{2n_2}}{2}|e_{2n}|^2 - \frac{\kappa_{2n_2}}{2}\lambda_{\min}(\Gamma_{f_{3n-2}})\|\tilde{P}_{f_{3n-2}}\|^2 - \frac{\kappa_{2n_2}}{2l_{2n}}|\tilde{k}_{r_{2n}}|^2 + E_{2n} \leq 0 \tag{4.83}$$

which results in the following ultimate bound for e_{2n}

$$|e_{2n}| \leq \sqrt{\frac{2E_{2n}}{\kappa_{2n_2}} - \lambda_{\min}(\Gamma_{f_{3n-2}})\|\tilde{P}_{f_{3n-2}}\|^2 - \frac{1}{l_{2n}}|\tilde{k}_{r_{2n}}|^2} : B_{2n}. \tag{4.84}$$

Remark 28. Note that when $\phi_0 \leq 0$, the stabilizing signal is inactivated due to the law (4.41) (i.e., $v_{opt} = 0$); hence, the first term of (4.72) vanishes. However since the condition $\phi_0 \leq 0$ has the property of $k_{r_{2n}} e_{2n} \tanh(\frac{e_{2n}}{a_{2n}}) \leq -\frac{\lambda}{2} e_{2n}^2$, the same result can be obtained in (4.76), which in turn, provides the same bound B_{2n} as derived in (4.84).

Step $2n-1$: Let us define

$$V_{2n-1}(e_{2n-1}, \tilde{P}_{f_{3n-3}}, \tilde{k}_{r_{2n-1}}) = \frac{1}{2}\left(e_{2n-1}^2 + \tilde{P}_{f_{3n-3}}^T \Gamma_{f_{3n-3}} \tilde{P}_{f_{3n-3}} + \frac{1}{l_{2n-1}}\tilde{k}_{r_{2n-1}}^2\right) \tag{4.85}$$

with

$$\frac{1}{2}\min\left(1, \lambda_{\min}(\Gamma_{f_{3n-3}}), \frac{1}{l_{2n-1}}\right) \|\xi_{2n-1}\|^2 \leq V_{2n-1} \leq \frac{1}{2}\max\left(1, \lambda_{\max}(\Gamma_{f_{3n-3}}), \frac{1}{l_{2n-1}}\right) \|\xi_{2n-1}\|^2, \tag{4.86}$$

where $\xi_{2n-1} = [e_{2n-1}, \tilde{P}_{f_{3n-3}}, \tilde{k}_{r_{2n-1}}]^T \in \Re^{n_{f_{3n-3}}+3}$ and $\tilde{k}_{r_{2n-1}} = k_{r_{2n-1}} - k^*_{r_{2n-1}}$.

Taking the time derivative of (4.85) along the dynamics (4.54), (4.31), and (4.51), adding and subtracting the term $e_{2n-1}\tanh(\frac{e_{2n-1}}{a_{2n-1}})(B_{2n} + \bar{\epsilon}_{f_{3n-3}})$, noting that $k^*_{r_{2n-1}} = B_{2n} + \bar{\epsilon}_{f_{3n-3}}$ due to Assumption 9, and recalling that $|e_{2n-1}| - e_{2n-1}\tanh(\frac{e_{2n-1}}{a_{2n-1}}) \leq c_{2n-1}a_{2n-1}$ for some $c_{2n-1} > 0$, one has

$$\begin{aligned}\dot{V}_{2n-1} \leq & - k_{2n-1}|e_{2n-1}|^2 - \left(\lambda_{\min}(H_{3n-3}) + \sigma_{f_{3n-3}}\right) \|\tilde{P}_{f_{3n-3}}\|^2 + c_{2n-1}a_{2n-1}(B_{2n} + \bar{\epsilon}_{f_{3n-3}}) \\ & - (\tilde{k}_{r_{2n-1}} + B_{2n} + \bar{\epsilon}_{f_{3n-3}})e_{2n-1}\tanh(\frac{e_{2n-1}}{a_{2n-1}}) + \tilde{k}_{r_{2n-1}}\text{Proj}(k_{r_{2n-1}}, e_{2n-1}\tanh(\frac{e_{2n-1}}{a_{2n-1}})) \\ & - \tilde{k}_{r_{2n-1}}\sigma_{2n-1}(\tilde{k}_{r_{2n-1}} + B_{2n} + \bar{\epsilon}_{f_{3n-3}}) + e_{2n-1}\tanh(\frac{e_{2n-1}}{a_{2n-1}})(B_{2n} + \bar{\epsilon}_{f_{3n-3}}) \\ & + \sigma_{f_{3n-3}}\|\tilde{P}_{f_{3n-3}}\|\|P_{f_{3n-3}}\|,\end{aligned} \tag{4.87}$$

where $H_{3n-3} = \sum_{j=1}^{m_{3n-3}} \Phi_{f_{3n-3_j}} \Phi^T_{f_{3n-3_j}} > 0$. Apply the projection operator, defined in Definition 16, to have

$$\dot{V}_{2n-1} \leq -k_{2n-1}|e_{2n-1}|^2 - \left(\lambda_{\min}(H_{3n-3}) + \sigma_{f_{3n-3}}\right) \|\tilde{P}_{f_{3n-3}}\|^2 - \sigma_{2n-1}|\tilde{k}_{r_{2n-1}}|^2 + E_{2n-1} \tag{4.88}$$

with

$$E_{2n-1} = (B_{2n} + \bar{\epsilon}_{f_{3n-3}})(c_{2n-1}a_{2n-1} + |\tilde{k}_{r_{2n-1}}|\sigma_{2n-1}) + \sigma_{f_{3n-3}}\|\tilde{P}_{f_{3n-3}}\|\|P_{f_{3n-3}}\|, \tag{4.89}$$

from which it follows that

$$\dot{V}_{2n-1} \leq -\kappa_{2n-1} V_{2n-1} + E_{2n-1} \quad \text{with} \tag{4.90}$$
$$\kappa_{2n-1} = \frac{\text{min}\left(2k_{2n-1}, 2\lambda_{\text{min}}(H_{3n-3}) + 2\sigma_{f_{3n-3}}, 2\sigma_{2n-1}\right)}{\text{max}\left(1, \lambda_{\text{max}}(\Gamma_{f_{3n-3}}), \frac{1}{l_{2n-1}}\right)}.$$

Referring to Definition 15, V_{2n-1} is an eDES-LF in the error dynamics $\dot{e}_{2n-1}$. Use the Comparison lemma to obtain

$$V_{2n-1} \leq V_{2n-1}(0)e^{-\kappa_{2n-1}t} + \frac{E_{2n-1}}{\kappa_{2n-1}} \tag{4.91}$$

from which, one can write

$$\|\xi_{2n-1}\| \leq \left[\frac{\text{max}\left(1, \lambda_{\text{max}}(\Gamma_{f_{3n-3}}), \frac{1}{l_{2n-1}}\right)}{\text{min}\left(1, \lambda_{\text{min}}(\Gamma_{f_{3n-3}}), \frac{1}{l_{2n-1}}\right)}\right]^{\frac{1}{2}} \|\xi_{2n-1}(0)\| e^{-\frac{\kappa_{2n-1}}{2}t} + \left[\frac{2E_{2n-1}}{\kappa_{2n-1}\text{min}\left(1, \lambda_{\text{min}}(\Gamma_{f_{3n-3}}), \frac{1}{l_{2n-1}}\right)}\right]^{\frac{1}{2}}. \tag{4.92}$$

Equation (4.92) shows that the system is ZS for $E_{2n-1} = 0$ and the AG property holds for $\|\xi_{2n-1}(0)\| = 0$, which implies that the system is eDES. By selecting $\kappa_{2n-1} = \kappa_{2n-1_1} + \kappa_{2n-1_2}$ with $\kappa_{2n-1_1}, \kappa_{2n-1_2} > 0$, Eq. (4.90) reduces to $\dot{V}_{2n-1} \leq -\kappa_{2n-1_1} V_{2n-1}$ if

$$-\frac{\kappa_{2n-1_2}}{2}|e_{2n-1}|^2 - \frac{\kappa_{2n-1_2}}{2}\lambda_{\text{min}}(\Gamma_{f_{3n-3}})\|\tilde{P}_{f_{3n-3}}\|^2 - \frac{\kappa_{2n-1_2}}{2l_{2n-1}}|\tilde{k}_{r_{2n-1}}|^2 + E_{2n-1} \leq 0 \tag{4.93}$$

from which the ultimate bound of e_{2n-1} is

$$|e_{2n-1}| \leq \sqrt{\frac{2E_{2n-1}}{\kappa_{2n-1_2}} - \lambda_{\text{min}}(\Gamma_{f_{3n-3}})\|\tilde{P}_{f_{3n-3}}\|^2 - \frac{1}{l_{2n-1}}|\tilde{k}_{r_{2n-1}}|^2} : B_{2n-1}. \tag{4.94}$$

Step i ($i = 4, 6, \ldots, 2n-2$)**:** With the ultimate bounds derived from Step $2n$ to Step $i+1$ in hand, the eDE stability at i-th step is proven as follows:

Define $\xi_i = [e_i, \tilde{P}_{f_{n+i-2}}, \tilde{k}_{r_i}]^T \in \Re^{n_{f_{n+i-2}}+3}$ with $\tilde{k}_{r_i} = k_{r_i} - k^*_{r_i}$, and consider

$$V_i(e_i, \tilde{P}_{f_{n+i-2}}, \tilde{k}_{r_i}) = \frac{1}{2}\left(e_i^2 + \tilde{P}^T_{f_{n+i-2}}\Gamma_{f_{n+i-2}}\tilde{P}_{f_{n+i-2}} + \frac{1}{2l_i}\tilde{k}^2_{r_i}\right) \quad \text{with} \tag{4.95}$$

$$\frac{1}{2}\text{min}\left(1, \lambda_{\text{min}}(\Gamma_{f_{n+i-2}}), \frac{1}{l_i}\right)\|\xi_i\|^2 \leq V_i \leq \frac{1}{2}\text{max}\left(1, \lambda_{\text{max}}(\Gamma_{f_{n+i-2}}), \frac{1}{l_i}\right)\|\xi_i\|^2.$$

Take the time derivative of (4.95) along the dynamics $\dot{e}_i$ to have

$$\begin{aligned}\dot{V}_i = &- k_i e_i^2 + e_i e_{i+1} + e_i \tilde{P}^T_{f_{n+i-2}}\Phi_{f_{n+i-2}} + e_i\left(\epsilon_{f_{n+i-2}} + d_{m_{i/2}}(t)\right) \\ &- e_i k_{r_i}\text{tanh}(\frac{e_i}{a_i}) - \tilde{P}^T_{f_{n+i-2}}\Gamma_{f_{n+i-2}}\dot{\hat{P}}_{f_{n+i-2}} + \frac{1}{l_i}\tilde{k}_{r_i}\dot{k}_{r_i}.\end{aligned} \tag{4.96}$$

Use the adaptation laws (4.51) and (4.22), add and subtract $e_i\text{tanh}(\frac{e_i}{a_i})(B_{i+1} + \bar{\epsilon}_{f_{n+i-2}} + \bar{d}_{m_{i/2}})$, assume that $k^*_{r_i} = B_{i+1} + \bar{\epsilon}_{f_{n+i-2}} + \bar{d}_{m_{i/2}}$ (Assumption 9), and note that $|e_i| - e_i\text{tanh}(\frac{e_i}{a_i}) \leq c_i a_i$ for some $c_i > 0$ to write

$$\begin{aligned}\dot{V}_i \leq &- k_i|e_i|^2 - \left(\lambda_{\text{min}}(H_{n+i-2}) + \sigma_{f_{n+i-2}}\right)\|\tilde{P}_{f_{n+i-2}}\|^2 + c_i a_i(B_{i+1} + \bar{\epsilon}_{f_{n+i-2}} + \bar{d}_{m_{i/2}}) \\ &- (\tilde{k}_{r_i} + B_{i+1} + \bar{\epsilon}_{f_{n+i-2}} + \bar{d}_{m_{i/2}})e_i\text{tanh}(\frac{e_i}{a_i}) - \tilde{k}_{r_i}\sigma_i(\tilde{k}_{r_i} + B_{i+1} + \bar{\epsilon}_{f_{n+i-2}} + \bar{d}_{m_{i/2}}) \\ &+ \tilde{k}_{r_i}\text{Proj}(k_{r_i}, e_i\text{tanh}(\frac{e_i}{a_i})) + e_i\text{tanh}(\frac{e_i}{a_i})(B_{i+1} + \bar{\epsilon}_{f_{n+i-2}} + \bar{d}_{m_{i/2}}) + \sigma_{f_{n+i-2}}\|\tilde{P}_{f_{n+i-2}}\|\|P_{f_{n+i-2}}\|,\end{aligned} \tag{4.97}$$

where $H_{n+i-2} = \sum_{j=1}^{m_{n+i-2}}\Phi_{f_{n+i-2_j}}\Phi^T_{f_{n+i-2_j}} > 0$. Note that B_{i+1} is the ultimate bound of e_{i+1} calculated at the $i+1$-th step, which depends on the chained bounds from Step $2n$ to Step $i+2$ such that $|e_{i+1}| \leq B_{i+1}(B_{2n}, \ldots, B_{i+2})$.

Once again, applying the projection operator (Definition 16) yields

$$\dot{V}_i \leq -k_i|e_i|^2 - \left(\lambda_{\text{min}}(H_{n+i-2}) + \sigma_{f_{n+i-2}}\right)\|\tilde{P}_{f_{n+i-2}}\|^2 - \sigma_i|\tilde{k}_{r_i}|^2 + E_i, \tag{4.98}$$

where

$$E_i = (B_{i+1} + \bar{\epsilon}_{f_{n+i-2}} + \bar{d}_{m_{i/2}})(c_i a_i + \sigma_i|\tilde{k}_{r_i}|) + \sigma_{f_{n+i-2}}\|\tilde{P}_{f_{n+i-2}}\|\|P_{f_{n+i-2}}\|.$$

This can be then written as

$$\dot{V}_i \leq -\kappa_i V_i + E_i \quad \text{with} \tag{4.99}$$
$$\kappa_i = \frac{\min\left(2k_i, 2\lambda_{\min}(H_{n+i-2}) + 2\sigma_{f_{n+i-2}}, 2\sigma_i\right)}{\max\left(1, \lambda_{\max}(\Gamma_{f_{n+i-2}}), \frac{1}{l_i}\right)}.$$

This shows that V_i is an eDES-LF in the error dynamics $\dot{e}_i$. Use Comparison lemma to obtain $V_i \leq V_i(0)e^{-\kappa_i t} + \frac{E_i}{\kappa_i}$ based on which, one has

$$\|\xi_i\| \leq \left[\frac{\max\left(1, \lambda_{\max}(\Gamma_{f_{n+i-2}}), \frac{1}{l_i}\right)}{\min\left(1, \lambda_{\min}(\Gamma_{f_{n+i-2}}), \frac{1}{l_i}\right)}\right]^{\frac{1}{2}} \|\xi_i(0)\| e^{-\frac{\kappa_i}{2}t} + \left[\frac{2E_i}{\kappa_i \min\left(1, \lambda_{\min}(\Gamma_{f_{n+i-2}}), \frac{1}{l_i}\right)}\right]^{\frac{1}{2}}, \tag{4.100}$$

which follows that the system is ZS for $E_i = 0$ and the AG property holds for $\|\xi_i(0)\| = 0$, implying that the system is eDES. Defining $\kappa_i = \kappa_{i_1} + \kappa_{i_2}$ with $\kappa_{i_1}, \kappa_{i_2} > 0$ such that the following relation holds

$$-\frac{\kappa_{i_2}}{2}|e_i|^2 - \frac{\kappa_{i_2}}{2}\lambda_{\min}(\Gamma_{f_{n+i-2}})\|\tilde{P}_{f_{n+i-2}}\|^2 - \frac{\kappa_{i_2}}{2l_i}|\tilde{k}_{r_i}|^2 + E_i \leq 0 \tag{4.101}$$

yields $\dot{V}_i \leq -\kappa_{i_1} V_i$ from which the ultimate bound of e_i is derived as

$$|e_i| \leq \sqrt{\frac{2E_i}{\kappa_{i_2}} - \lambda_{\min}(\Gamma_{f_{n+i-2}})\|\tilde{P}_{f_{n+i-2}}\|^2 - \frac{1}{l_i}|\tilde{k}_{r_i}|^2} : B_i. \tag{4.102}$$

Step i ($i = 3, 5, \ldots, 2n-3$)**:** This step includes the following steps.

1. Take the time derivative of the Lyapunov function (4.95) along the dynamics $\dot{e}_i$, and the adaptation laws (4.51) and (4.22), for $i = 3, 5, \ldots, 2n-3$.

2. Add and subtract the term $e_i \tanh(\frac{e_i}{a_i})(B_{i+1} + \bar{\epsilon}_{f_{n+i-2}})$ in Step 1 while applying the Assumption 9.

3. Apply the projection operator, stated in Definition 16, to obtain (4.98) with

$$E_i = (B_{i+1} + \bar{\epsilon}_{f_{n+i-2}})(c_i a_i + \sigma_i|\tilde{k}_{r_i}|) + \sigma_{f_{n+i-2}}\|\tilde{P}_{f_{n+i-2}}\|\|P_{f_{n+i-2}}\|. \tag{4.103}$$

4. Use the disturbance E_i from the Step 3 to obtain $\dot{V}_i$, $\|\xi_i\|$, $|e_i|$ as derived in (4.99), (4.100), and (4.102), respectively.

5. By following the Steps 1-4, it is proven that V_i is an eDES-LF in the error dynamics $\dot{e}_i$ for $i = 3, 5, \ldots, 2n-3$ and the system is eDES.

Step 2: Let us define

$$V_2(e_2, \tilde{P}_{f_1}, \tilde{k}_{r_2}) = \frac{1}{2}\left(e_2^2 + \tilde{P}_{f_1}^T \Gamma_{f_1} \tilde{P}_{f_1} + \frac{1}{l_2}\tilde{k}_{r_2}^2\right) \text{ with} \tag{4.104}$$

$$\frac{1}{2}\text{min}\left(1, \lambda_{\text{min}}(\Gamma_{f_1}), \frac{1}{l_2}\right)\|\xi_2\|^2 \leq V_2 \leq \frac{1}{2}\text{max}\left(1, \lambda_{\text{max}}(\Gamma_{f_1}), \frac{1}{l_2}\right)\|\xi_2\|^2, \tag{4.105}$$

where $\xi_2 = [e_2, \tilde{P}_{f_1}, \tilde{k}_{r_2}]^T \in \Re^{n_{f_1}+3}$ and $\tilde{k}_{r_2} = k_{r_2} - k_{r_2}^*$.

Take the time derivative of V_2 along the dynamics $\dot{e}_2$, $\dot{\hat{P}}_{f_1}$, and $\dot{k}_{r_2}$, add and subtract the term $e_2\text{tanh}(\frac{e_2}{a_2})(B_3 + \bar{\epsilon}_{f_1} + \bar{d}_{m_1})$, assume that $k_{r_2}^* = B_3 + \bar{\epsilon}_{f_1} + \bar{d}_{m_1}$ (Assumption 9), note that $|e_2| - e_2\text{tanh}(\frac{e_2}{a_2}) \leq c_2 a_2$ for some $c_2 > 0$, and apply the projection operator (Definition 16) to obtain

$$\dot{V}_2 \leq -\kappa_2 V_2 + E_2 \tag{4.106}$$

with

$$\begin{aligned} E_2 =& (B_3 + \bar{\epsilon}_{f_1} + \bar{d}_{m_1})(c_2 a_2 + \sigma_2|\tilde{k}_{r_2}|) + \sigma_{f_1}\|\tilde{P}_{f_1}\|\|P_{f_1}\|, \\ \kappa_2 =& \frac{\text{min}\,(2k_2, 2\lambda_{\text{min}}(H_1) + 2\sigma_{f_1}, 2\sigma_2)}{\text{max}\left(1, \lambda_{\text{max}}(\Gamma_{f_1}), \frac{1}{l_2}\right)}, \text{ and} \\ H_1 =& \sum_{j=1}^{m_1} \Phi_{f_{1_j}} \Phi_{f_{1_j}}^T > 0, \end{aligned} \tag{4.107}$$

where B_3 is the ultimate bound of e_3 calculated in Step 3.

In view of (4.106), the Lyapunov function V_2 is an eDES-LF in the error dynamics $\dot{e}_2$. Employing Comparison lemma, we have $V_2 \leq V_2(0)e^{-\kappa_2 t} + \frac{E_2}{\kappa_2}$ using which, one obtains

$$\|\xi_2\| \leq \left[\frac{\max\left(1, \lambda_{\max}(\Gamma_{f_1}), \frac{1}{l_2}\right)}{\min\left(1, \lambda_{\min}(\Gamma_{f_1}), \frac{1}{l_2}\right)}\right]^{\frac{1}{2}} \|\xi_2(0)\| e^{-\frac{\kappa_2}{2}t} + \left[\frac{2E_2}{\kappa_2 \min\left(1, \lambda_{\min}(\Gamma_{f_1}), \frac{1}{l_2}\right)}\right]^{\frac{1}{2}} \tag{4.108}$$

from which it follows that the system is ZS for $E_2 = 0$ and the AG property holds for $\|\xi_2(0)\| = 0$; it further implies that the system is eDES. By picking $\kappa_2 = \kappa_{2_1} + \kappa_{2_2}$ with $\kappa_{2_1}, \kappa_{2_2} > 0$, Eq. (4.106) becomes $\dot{V}_2 \leq -\kappa_{2_1} V_2$ if

$$-\frac{\kappa_{2_2}}{2}|e_2|^2 - \frac{\kappa_{2_2}}{2}\lambda_{\min}(\Gamma_{f_1})\|\tilde{P}_{f_1}\|^2 - \frac{\kappa_{2_2}}{2l_2}|\tilde{k}_{r_2}|^2 + E_2 \leq 0 \tag{4.109}$$

using which

$$|e_2| \leq \sqrt{\frac{2E_2}{\kappa_{2_2}} - \lambda_{\min}(\Gamma_{f_1})\|\tilde{P}_{f_1}\|^2 - \frac{1}{l_2}|\tilde{k}_{r_2}|^2} : B_2. \tag{4.110}$$

Step 1: In the final step, the ultimate bound of the main tracking error e_1 is calculated which shows how accurate the non-collocated variable z_1 can track the desired trajectory z_1^d.

Let us select

$$V_1(e_1, \tilde{k}_{r_1}) = \frac{1}{2}\left(e_1^2 + \frac{1}{l_1}\tilde{k}_{r_1}^2\right) \quad \text{with} \tag{4.111}$$
$$\frac{1}{2}\min\left(1, \frac{1}{l_1}\right)\|\xi_1\|^2 \leq V_1 \leq \frac{1}{2}\max\left(1, \frac{1}{l_1}\right)\|\xi_1\|^2,$$

where $\xi_1 = [e_1, \tilde{k}_{r_1}]^T \in \Re^2$ with $\tilde{k}_{r_1} = k_{r_1} - k_{r_1}^*$.

By taking the time derivative of V_1 along the dynamics $\dot{e}_1$ and the robust gain adaptation law $\dot{k}_{r_1}$, one has

$$\dot{V}_1 = -k_1 e_1^2 + e_1 e_2 - e_1 k_{r_1}(t)\text{tanh}(\frac{e_1}{a_1}) + \tilde{k}_{r_1}\text{Proj}(k_{r_1}, e_1\text{tanh}(\frac{e_1}{a_1})) - \tilde{k}_{r_1}\sigma_1 k_{r_1}. \tag{4.112}$$

By adding and subtracting the term $e_1\text{tanh}(\frac{e_1}{a_1})B_2$, applying the projection operator (Definition 16), noting that $k_{r_1}^* = B_2$ (Assumption 9), and recalling that $|e_1| - e_1\text{tanh}(\frac{e_1}{a_1}) \leq c_1 a_1$ for some $c_1 > 0$, we have

$$\dot{V}_1 \leq -k_1|e_1|^2 - \sigma_1|\tilde{k}_{r_1}|^2 + B_2(c_1 a_1 + \sigma_1|\tilde{k}_{r_1}|), \tag{4.113}$$

which can be written as

$$\begin{aligned} \dot{V}_1 \leq& -\kappa_1 V_1 + E_1 \ \text{ with} \\ E_1 =& B_2(c_1 a_1 + \sigma_1|\tilde{k}_{r_1}|) \ \text{ and} \\ \kappa_1 =& \frac{\text{min}\,(2k_1, 2\sigma_1)}{\text{max}\left(1, \frac{1}{l_1}\right)} \end{aligned} \tag{4.114}$$

form which it follows that V_1 is an eDES-LF in the error dynamics $\dot{e}_1$. Once again, by using Comparison lemma, one writes

$$\|\xi_1\| \leq \left[\frac{\text{max}\left(1, \frac{1}{l_1})\right)}{\text{min}\left(1, \frac{1}{l_1}\right)}\right]^{\frac{1}{2}} \|\xi_1(0)\| e^{-\frac{\kappa_1}{2}t} + \left[\frac{2E_1}{\kappa_1 \text{min}\left(1, \frac{1}{l_1}\right)}\right]^{\frac{1}{2}} \tag{4.115}$$

which shows that the system is eDES because it is ZS for $E_1 = 0$ (i.e., $B_2 = 0$) and the AG property holds for $\|\xi_1(0)\| = 0$.

Similarly, by selecting $\kappa_1 = \kappa_{1_1} + \kappa_{1_2}$ for $\kappa_{1_1}, \kappa_{1_2} > 0$, Eq. (4.114) becomes $\dot{V}_1 \leq -\kappa_{1_1} V_1$ if $-\frac{\kappa_{1_2}}{2}|e_1|^2 - \frac{\kappa_{1_2}}{2l_1}|\tilde{k}_{r_1}|^2 + E_1 \leq 0$ using which the ultimate bound of e_1 is

$$|e_1| \leq \sqrt{\frac{2E_1}{\kappa_{1_2}} - \frac{1}{l_1}|\tilde{k}_{r_1}|^2} : B_1. \tag{4.116}$$

Taken altogether, this section confirms that all system errors are eDES and specifically, the non-collocated tracking error e_1 is bounded in a neighborhood around the origin whose size is B_1. □

Remark 29. The ultimate bound of the non-collocated tracking error e_1 is dependent on the ultimate bounds of the other collocated and non-collocated intermediate errors; this, in turn, implies that B_1 depends on $B_2, B_3, \ldots, B_{2n}$.

Remark 30. The weight and robust gain adaptation mechanisms (4.51) and (4.46) contribute to the system in following different ways.

1. The weight adaptation law (4.51) identifies the approximated model of the unknown function f_{un} by estimating the weight vector P_f, while is able to compensate neither the modeling and chained errors nor time-varying disturbances.

2. The robust adaptation law (4.46) compensates the modeling approximation error ϵ_f, the chained error effect B_i, and the unknown disturbance $d_m(t)$. In other words, this adaptation mechanism mitigates the discrepancy between the actual and approximated models as well as the chained errors from one coordinate to another and unknown disturbances.

3. Under the existing backstepping-based adaptive controllers, if the number of nodes in the RBFNN is chosen to be sufficiently large such that $n_f \to \infty$, the unknown function f_{un} is properly approximated and in turn, the modeling approximation error vanishes. Although this results in the smaller ultimate bound B_1 (lower tracking error e_1), the problem deals with a high-dimensional weight vector, which in turn, causes a computationally demanding estimation process. This further increases the computational time and is less suitable for real-time control algorithms. In contrast with the existing backstepping adaptive approaches, however, in this chapter, a reasonable number of nodes is selected to compromise the computational complexity and effectiveness, while the modeling approximation and chain errors, and disturbances are automatically compensated by the robust gain adaptation mechanisms without knowing the bounds of the aforementioned unknown terms *a priori*.

Remark 31. To achieve better attenuation of the modeling approximation and the chain errors, and the time-varying disturbances, the smaller value of the width a_i for $i = 1, ..., 2n$ can be selected. However, it should be pointed out that if $a_i \to 0$, then tanh$(.)$ becomes discontinuous and the virtual inputs and the main control law are not implementable.

With the main results of Theorems 5 and 6 in hand, the next section will implement the proposed control methodology on an illustrative underactuated robotic system. The benefits of our approach will also be confirmed over the baseline QP-CLBF/FL.

4.7 Simulation results

This section is devoted to demonstrate the soundness of the proposed control approach on an underactuated robot of class (4.1). Comparisons to a baseline QP-CLBF-based feedback linearization (QP-CLBF/FL) [106, 5] method are then carried out to verify the benefits of our proposed controller. The baseline QP-CLBF/FL linearizes the system using coordinate transformations, as described in [106], for which the stabilizing control is provided by employing a QP while encoding the baseline CLF and CBF constraints [5]. A single-link flexible-joint robot rotating in the vertical plane is chosen in which the link is driven by a motor through a torsional spring while ignoring the viscous damping. This robot is a two DoF-one DoA system whose model is described by the following EoM:

$$M(q)\ddot{q} + G(q) = u + d(t), \tag{4.117}$$

where $q = [q_1, q_2]^T \in \Re^2$ in which q_1 (rad) is the link angular displacement (non-collocated coordinate) and q_2 (rad) is the motor angular displacement (collocated coordinate); $u = [0, u_2]^T$ with u_2 $(N.m)$ as the motor torque; $d(t) = [d_1(t), d_2(t)]^T$ is the vector of time-varying disturbances; $M(q) = \text{diag}(I, J) \in \Re^{2\times 2}$ is the inertia matrix with I and J as the link and motor inertias, respectively; and $G(q) = [MgL\text{sin}(q_1) + K(q_1 - q_2), -K(q_1 - q_2)]^T \in \Re^2$ is the gravity vector in which M is the link mass, L is the center of mass, K is the torsional spring stiffness, and g is the gravity constant.

In view of (4.2), it is obtained that the state vector is $z = [q_1, \dot{q}_1, q_2, \dot{q}_2]^T \in \Re^4$, the known functions with nominal system parameters are

$$f_{k_1}(z) = -\frac{1}{I}(MgL\sin(z_1) + K(z_1 - z_3)) - z_3 \quad \text{and} \tag{4.118}$$
$$f_{k_2}(z) = \frac{1}{J}(K(z_1 - z_3)),$$

b_0 is our best guess about the control coefficient $b = \frac{1}{J}$, and the unknown disturbances are $d_{m_1}(t) = \frac{d_1(t)}{I}$ and $d_{m_2}(t) = \frac{d_2(t)}{J}$. The time-varying disturbances are considered to be $d_1(t) = 3 + 3\sin(8t)$ and $d_2(t) = 3 + 5\sin(5t)$ while including some Gaussian random noise with strength 0.3. Due to the presence of parameter uncertainties, there exist unknown functions $f_{un_i}(z)$ for $i = 1, 2$ as defined in (4.4). The control objectives are (i) to drive the link angular displacement z_1 from a randomly-selected initial condition to the desired displacement $z_1^d = \frac{pi}{4}\sin(2t)$ while the system and intermediate errors are all eDES and (ii) to enforce the motor angular displacement to stay in the safe set $-\frac{2\pi}{5}(rad) \leq z_3 \leq +\frac{2\pi}{5}(rad)$.

For doing so, we begin by estimating the unknown functions $f_{un_1}(z)$, $f_{un_3}(z)$, and $f_{un_4}(z)$ (defined in (4.4), and Steps 2 and $2n$, respectively) through the laws (4.50) and (4.51). To compute the robust gain k_{r_i} for $i = 1, \ldots, 4$ and the optimal signal v_{opt}, the adaptation mechanism (4.46) is applied and the optimization problem (4.66) is formulated while encoding the TVRCLF and TVRZCBF constraints (the torque bounds are selected in such a way that the motor torque is not saturated by them). Utilizing the estimates $\hat{f}_{un_1}(z)$, $\hat{f}_{un_3}(z)$, and $\hat{f}_{un_4}(z)$, the robust gains k_{r_i}, and the stabilizing signal v_{opt}, the virtual inputs (z_2^d, z_3^d, and z_4^d) and the motor torque u_2 are computed by laws (4.11), (4.15), (4.29), and (4.34). To ensure accurate safety for the motor angular displacement z_3, the proposed TVRZCBF is applied through Theorem 5 while picking two relative degree 2 barrier functions $h_1 = z_3 + \frac{2\pi}{5}$ and $h_2 = \frac{2\pi}{5} - z_3$. Design parameters of both proposed and baseline controllers are tuned to achieve the best tradeoff between the non-collocated tracking accuracy and the collocated safety performance.

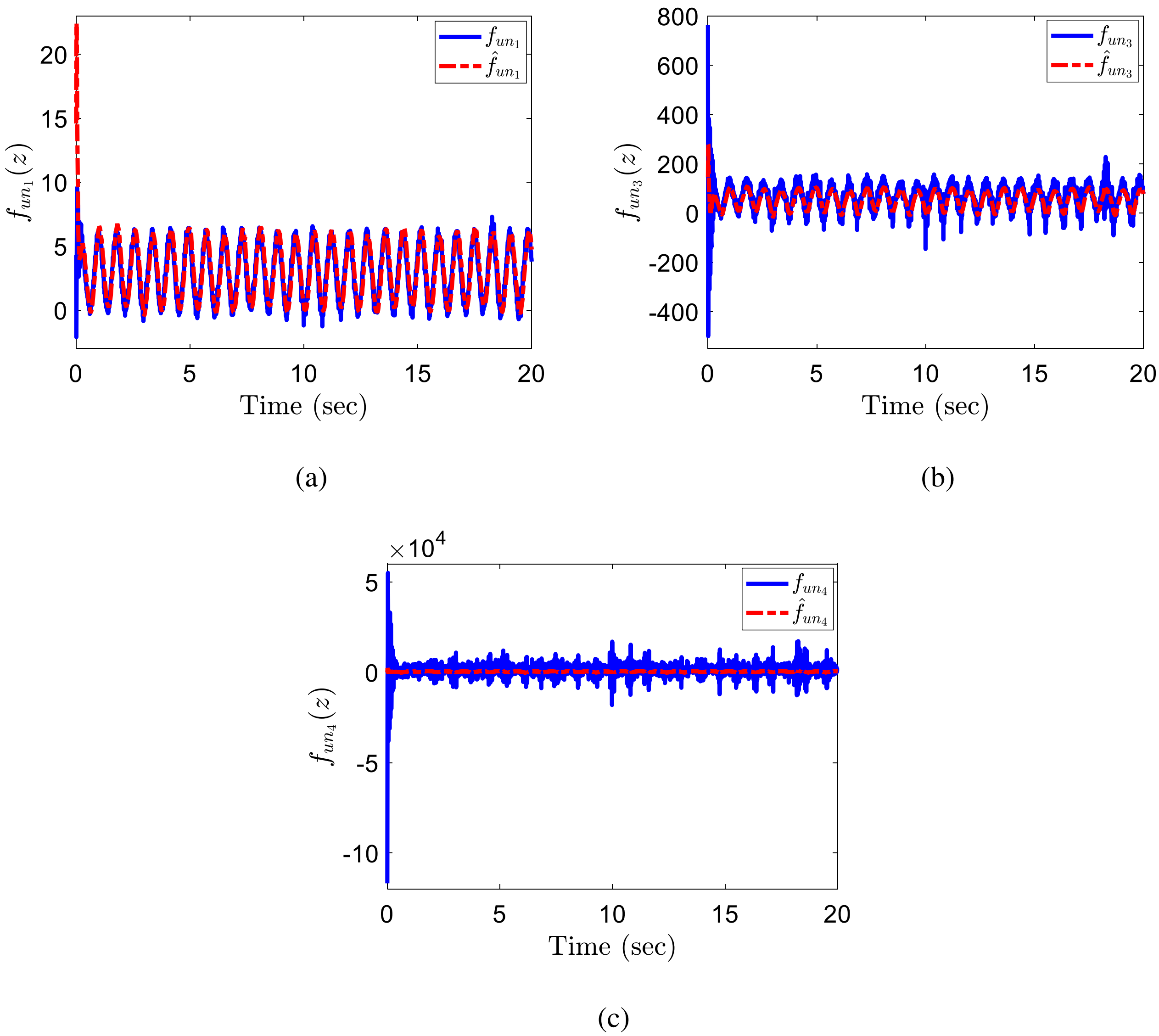

Figure 4.1: Results of the proposed controller for the estimates of unknown functions (a) f_{un_1}, (b) f_{un_3}, and (c) f_{un_4}.

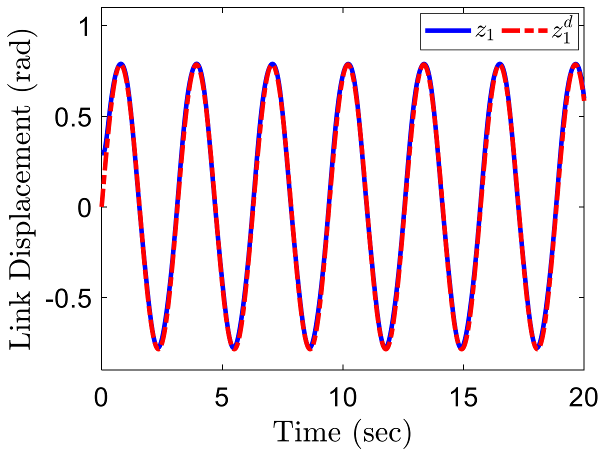

(a)

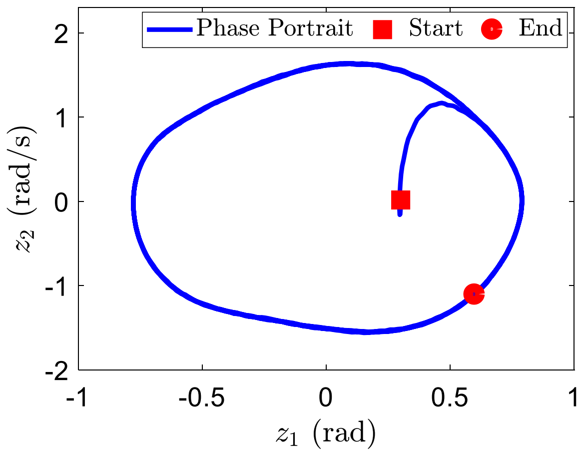

(b)

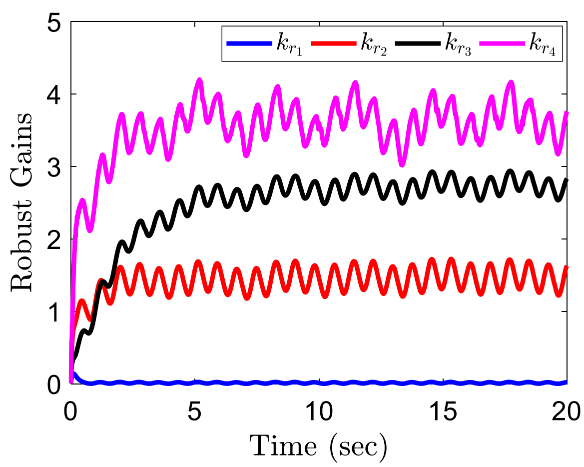

(c)

Figure 4.2: Results of the proposed controller, including (a) the link angular displacement tracking performance, (b) the phase portrait whose consistency indicates stale limit cycle for the robot link, and (c) the evolution of robust gains.

4.7.1 Verification of the proposed controller

Figure 4.1(a)-(c) illustrate the estimates of the unknown functions $f_{un_1}(z)$, $f_{un_3}(z)$, and $f_{un_4}(z)$ while utilizing the model (4.50) and the weight adaptation mechanism (4.51). It can be seen that all three unknown functions are properly identified. Figure 4.2(a) compares the link angular displacement z_1 of the flexible-joint robot with the desired trajectory z_1^d when the proposed controller is applied. As observed in this figure, z_1 is not distinguishable for z_1^d, implying that the non-collocated link displacement tracking error e_1 is bounded in a small neighborhood around the origin whose size can be realized by B_1 described in (4.116). Figure 4.2(b) demonstrates phase portrait for the link over 20 sec simulation time from which it is observed that the controller converges to a stable limit periodic orbit. Such great tracking performance and consistent portrait for the robot link stem from the combined effect of the proper unknown function estimation (see Fig 4.1), the proposed TVRCLF, and the robust gains k_{r_i} for $i = 1, \ldots, 4$ whose evolution is demonstrated in Fig 4.2(c). Observe that in contrast with the robust gains k_{r_i} for $i = 1, \ldots, 3$, the gain k_{r_1}, which affects on the error dynamics e_1 presented in (4.54), takes much lower magnitude. The reason for this is that the ultimate bound of the link displacement tracking error (see (4.116)) depends on the chained errors from the other collocated and non-collocated spaces whose effects are already compensated by the robust gains k_{r_i} for $i = 1, \ldots, 3$. It is also worth noting that due to the noise effects and the sinusoidal nature of z_1^d, these gains are fluctuating around their true values as listed in (4.68). Taken altogether, these results support the claim of Theorem 6 in which eDES of all system's errors is guaranteed.

Figure 4.3(a) and (b) depict the results of the proposed TVRZCBF through which the collocated motor angular displacement is restricted to stay in its prescribed upper and lower bounds. Figure 4.3(a) demonstrates the positiveness of the barrier functions h_1 and h_2, implying the forward invariance of the safe set (4.55). While Theorem 5 formally guarantees, these results provide a perfect safety for the variable z_3 under the TVRZCBF whose non-negative gains are evolved based upon the mechanism (4.63) (see Fig. 4.3(b)). These results confirm that with the proposed time-varying control barrier technique, safety is strictly achieved in the presence of unknown disturbances without the need for knowing their bounds *a priori*.

4.7.2 Comparison results

This section provides convincing evidence demonstrating the superiority of our proposed control methodology over the baseline QP-CBLF/FL. Figure 4.4(a) illustrates the tracking error of the non-collocated link angular displacement obtained by applying both controllers. It is clearly observed that the tracking performance is significantly improved under the proposed controller. Figure 4.4(b) shows the safety performance for the collocated motor angular displacement under both controllers. It can be seen that in contrast with the baseline QP-CBLF/FL under which the motor displacement violates the safe set (indicated by magenta dashed line in Fig. 4.4(b)), the variable z_3 is perfectly bounded in the set with our proposed controller. This is in agreement with both Theorems 5 and 6, which guarantees perfect safety of the collocated variable z_3 and eDE stability of the non-collocated tracking error e_1, respectively.

To highlight the benefits of our proposed controller over the baseline method, a numerical comparison is performed whose results are incorporated in Table 4.1. This table lists the RMS value of link displacement tracking error, the RMS value of the motor torque, and the absolute peak motor displacement value. It can be inferred from Table 4.1 that the proposed controller improves the tracking error by 67% and reduces the motor torque by 93%. This table also shows that unlike the baseline QP-CBLF/FL that violates the safe set by 42%, perfect safety is rendered under the proposed controller. These improvements obtained by the proposed controller are mainly due to the unknown function estimation and the robust gain adaptation, along with the derivations of TVR-CLF and TVRZCBF, whose results are presented in Theorems 5 and 6. These findings support our claim that the baseline QP-CBLF/FL is not able to properly balance safety and stability for non-collocated control of underactuated robots with unknown dynamics and time-varying disturbances; hence, the proposed controller is required to apply for such control problem as a remedy to mitigate the issues of the existing QP-CBLF/FL.

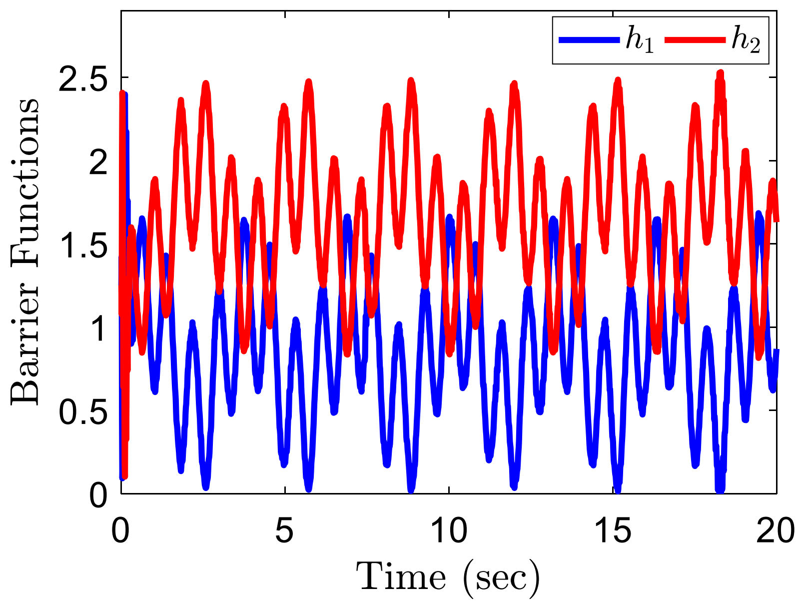

(a)

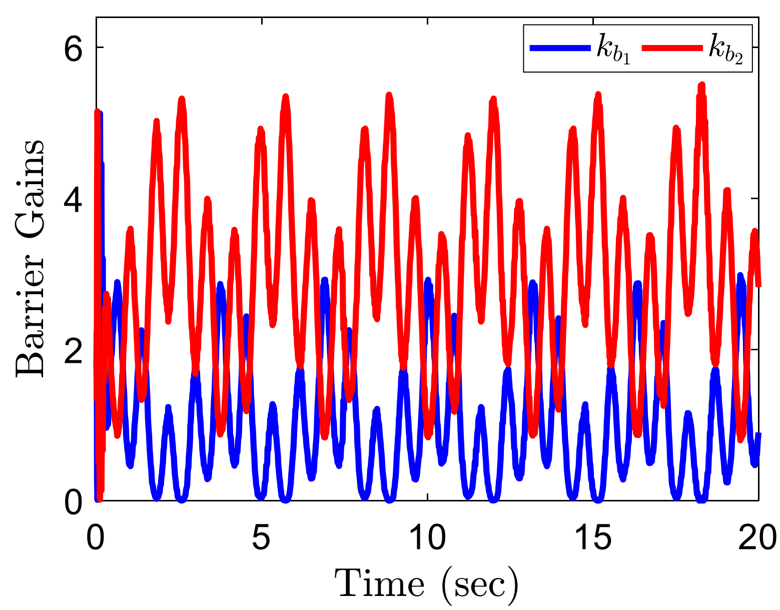

(b)

Figure 4.3: Results of the proposed controller, including (a) the barrier functions h_1 and h_2 with positive values indicating perfect safety, and (b) the evolution of barrier gains.

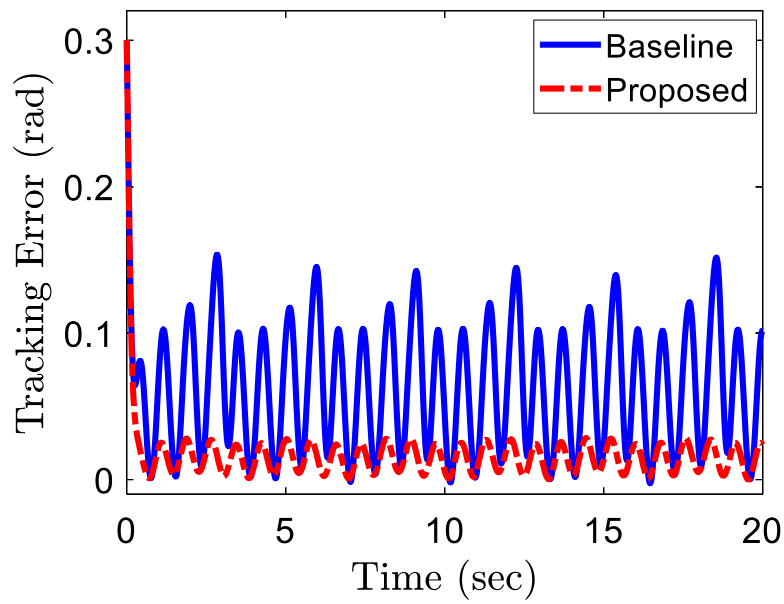

(a)

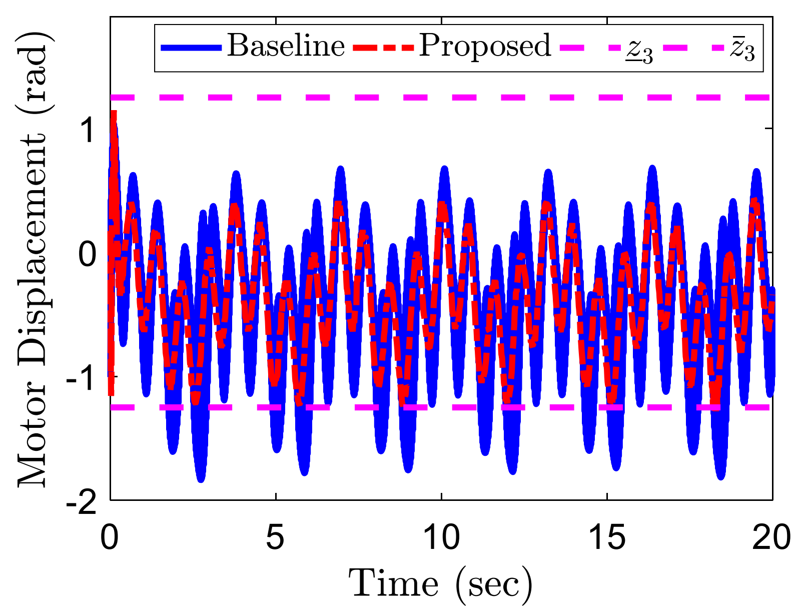

(b)

Figure 4.4: Comparison results between the proposed scheme and the baseline QP-CLBF/FL, including (a) the link angular displacement tracking error e_1 and (b) the safety performance of motor angular displacement z_3.

Table 4.1: Comparison results of different controllers for 20 sec simulation on the single-link flexible-joint robot, where RMS is a function that returns the root mean square of a signal. The best value of each metric is underlined.

Controller	$\mathrm{RMS_{e_1}}$ (rad)	$\mathrm{RMS_{u_2}}$ (N.m)	$\lvert z_3\rvert_{\max}$ (rad)
Proposed	<u>0.026</u>	<u>133</u>	<u>1.250</u>
Baseline	0.078	2000	1.780

4.8 Discussions and conclusions

The direct application of recently-developed QP-CLBF approach [5, 95] to non-collocated control of underactuated robots with model uncertainties and disturbances degrades the performance of closed-loop systems and leads to the violation of safety-critical constraints. Although existing robust QP-CLBFs [96, 78] are able to mitigate the above issues, perfect stabilization and safety cannot still be guaranteed against disturbances whose bounds are unknown. Even assuming that under high gain design parameters, the above objectives are satisfied, heuristic methods of parameter tuning could potentially cause increasing the control efforts and restricting the safe sets. Motivated by resolving the above issues and the desire of introducing a novel controller, this chapter presented a robust quadratic program-based adaptive control approach for extending the applications of QP-CLBF to non-collocated control of a class of n DoF-one DoA underactuated robots with diagonal inertia matrices.

Beginning with the design of a backstepping technique for the given system, that includes $2n$ steps, we developed neural network-based adaptation mechanisms to estimating unknown nonlinear functions. To compensate remaining uncanceled terms, virtual inputs were derived whose gains are automatically adjusted by projection-based adaptation laws. A three-term control law, including feed-forward, adaptive, and stabilizing terms, was suggested whose latter term is generated in an optimal fashion by synthesizing a QP subject to TVRCLF and TVRCBF constraints as well as torque bounds. The explicit motivation for the introduction of these time-varying terms was to achieve accurate non-collocated tracking and perfect collocated safety in the presence of unknown disturbances without requiring their bounds for use in the control design. We proved eDE stability of all system errors and the forward invariance of safe sets through Theorems 5 and 6. To demonstrate these results, simulation studies were carried out on an illustrative underactuated system: a single-link flexible-joint robot. The results confirmed the soundness of the proposed technique by achieving accurate link displacement tracking while enforcing the motor displacement to lie in its safe set. Comparisons with a baseline QP-CLBF/FL provided evidence that our proposed controller significantly enhances tracking error by 67% and reduces the control torque by 93% over QP-CLBF/FL. In contrast with QP-CLBF/FL under which the safety violation was 42%, the proposed scheme could achieve safety-critical requirements strictly. This provides convincing evidence of applicability of our proposed approach as an alternative for QP-CLBF/FL to be applied to the class of underactuated robots studied in this work. Future studies will have to continue extending the present technique to non-collocated control of "stochastic" robotic applications.

CHAPTER 5

ADAPTIVE QP-CLBF WITH EXPONENTIAL SOLUTIONS

This chapter presents an adaptive QP-CLBF approach for a class of nonlinear systems in the presence of parameter uncertainties and unknown control coefficient. We begin by presenting a filtering-based concurrent learning (FCL) adaptive technique to guarantee simultaneous exponential convergence of system parameters and control coefficient. The proposed FCL extends and encompasses the baseline CL technique, which was developed to achieve exponential convergence of either system parameters exclusively or control coefficient. The proposed FCL adaptive method is then unified with a modified version of the QP-CLBF to achieve exponential convergence of system parameters, control coefficient, state variables, and control barrier functions. The main contribution of this chapter is that all results are exponential in the presence of modeling error associated with both parameter uncertainty and unknown control coefficient. This is formally proved by employing a Lyapunov argument. Soundness of the proposed approach is finally demonstrated on two illustrative examples: a mass-damper system and an underwater vehicle. Simulation results show that the proposed control methodology achieves exponential results with regard to trajectory tracking, parameter estimation, and safety.

5.1 Background

The previous chapters provided convincing evidence supporting the claim that although QP-CLBF can guarantee stability and safety, model uncertainties may degrade the stabilization of a closed-loop system and lead to violation of safety-critical constraints. As discussed, robustness of this approach has been extensively researched and different robust QP-CLBFs have been recently formulated for nonlinear dynamical systems [107, 108, 96, 78]. Although for systems with uncertainties, robust QP-CLBFs can drive system errors and violation of the safety-critical constraints to small neighborhoods around the origin, they are not still convergent to zero. In many physical systems, model uncertainty arises from “both” unknown system parameters and control coefficient[1]. This adds more complexity to control of nonlinear systems and may deteriorate the performance of robust QP-CLBFs regarding stability and safety.

Recall that Slotine’s adaptive control techniques (TEB-based and TEB/PEB-based) [11, 12] utilize only instantaneous data for adaptation and require *PE* conditions for the system states to guarantee parameter convergence. However, as comprehensively studied, CL approach [21, 28] is able to guarantee exponential convergence of both tracking and parameter errors while requiring a *finite excitation condition* which is a weaker condition than *PE*. Most TEB-based, TEB/PEB-based, and CL-based adaptive techniques have focused mainly on estimating the system parameters, so limited research has been done investigating the impact of both parameter uncertainties and unknown control coefficient in nonlinear control systems [21, 11, 84, 31, 35]. To the best of our knowledge, to date, no study has looked specifically at the exponential convergence of both parameter uncertainties and control coefficient at the same time.

5.2 Contributions

In this chapter, an adaptive QP-based control technique is formulated to guarantee simultaneous exponential convergence of system parameters and control coefficient, while providing exponential convergence of tracking error and safety-critical constraints. In particular, this work basically extends the QP-CLBF controller (which degrades the stability and safety in the presence of model uncertainties) and the CL technique (which has not been developed to guarantee exponential convergence of both system parameters and control coefficient) to the n^{th}-order single-input single-output (SISO) nonlinear systems (multi-input multi-output (MIMO) systems are beyond the scope of this work).

[1] Parametric uncertainty can arise from “control coefficient” and “system parameters”. The former determines how an input affects system states, while the latter determine how current states affect states change.

The main contributions of this chapter are fourfold:

1. The introduction of a new adaptation technique to guarantee simultaneous exponential convergence of system parameters and control coefficient

2. The design of an adaptive QP-CLBF controller to achieve exponential convergence of system errors while strictly avoiding the violation of safety constraints

3. Formal convergence analysis using a Lyapunov stability argument

4. Validation of the proposed controller on two illustrative nonlinear systems: a mass-damper system and an underwater vehicle

In this chapter, the n^{th}-order SISO nonlinear system is first transformed into an "isolated form" through which control input is separated alone on one side of a dynamical model. The main control law is suggested which uses two quantities: the estimate of unknown parameters and the nth derivative of state. The former is driven by a proposed filtering-based CL (FCL) adaptive technique and the latter is provided by an optimal estimation utilizing the QP solution. The FCL extends the baseline CL by exploiting a filtered version of the system's basis function and a prediction error in the input signal. We then show that this formulation can encompass the CL for simultaneous exponential convergence of system parameters and control coefficient errors. The results of QP-based CLFs and QP-based CBFs are revisited and they are then modified based upon the suggested control law. The negative impact of model inaccuracies (associated with parameter uncertainties and unknown control coefficient) is then discussed. The CBFs and CLFs are then unified with the FCL via QP to emerge an adaptive QP-CLBF, providing exponential results of all system solutions. The soundness of the proposed control technique is finally verified on two nonlinear systems: a mass-damper system and an underwater vehicle. Simulation results show that our approach can exponentially drive trajectory tracking, parameter estimation, and safety errors to zero.

The chapter is organized as follows. Section 5.3 presents the problem statement and the control law. Section 5.4 revisits the QP-based CLFs and CBFs, and discuss the impact of uncertainties on them. Section 5.5 derives the FCL, formulates the proposed adaptive QP-CLBF, and presents the stability analysis. Section 5.6 presents the simulation results. Section 5.7 concludes the chapter and suggests for the future work.

5.3 Problem statement and control law

This section comprises two subsections. In the first subsection, we begin by introducing a class of nonlinear systems with parameter uncertainties and unknown control coefficient. Utilizing an isolated form of the system, the remainder of this subsection describes the problem statement. Based upon the isolated form, the second subsection is devoted to construct the main control law to achieve our design objectives.

5.3.1 Problem statement

Consider the following affine form of an n^{th}-order SISO nonlinear system

$$x^{(n)} = f(X) + g(X)u, \tag{5.1}$$

where $x^{(n)}$ is the nth derivative of x; $u \in \Re$ is the control signal; and $X = [x, \dot{x}, ..., x^{(n-1)}]^T \in \Re^n$ is the state vector. Functions $f(X) \in \Re$ and $g(X) \in \Re$ are unknown continuous nonlinear system functions that can be linearly parameterized as

$$f(X) = a^T \phi(X) \ \text{ and } \ g(X) = b\varphi(X), \tag{5.2}$$

where $\phi(X) \in \Re^r$ and $\varphi(X) \in \Re$ are known functions; $a = [a_1, a_2, ..., a_r]^T \in \Re^r$ is the system's base parameters; and $b \in \Re$ is the control coefficient. The vector a is a vector of unknown parameters and the control coefficient b is an unknown constant of known sign.

Assumption 10. Assume that only the state vector X is measurable, but not the nth derivative of x, i.e., $x^{(n)}$.

To satisfy the needs of the later design structure, the nonlinear system (5.1) along with the definitions in (5.2) is transformed into the following "isolated form[2]"

$$\Theta^T Y(x^{(n)}, \phi(X)) = \varphi(X)u \tag{5.3}$$

with the parameter vector Θ and the basis function $Y(x^{(n)}, \phi(X))$ as

$$\Theta = \frac{1}{b}\begin{bmatrix} 1 \\ a \end{bmatrix} \in \Re^{r+1}, \quad Y = \begin{bmatrix} x^{(n)} \\ -\phi(X) \end{bmatrix} \in \Re^{r+1}. \tag{5.4}$$

Referring to Eq. (5.4), the $r+1$-dimensional parameter vector Θ contains the unknown system parameters and the unknown control coefficient. The basis function Y cannot be directly used for the controller, as based on Assumption 10, it contains the unmeasurable quantity $x^{(n)}$. Thus, both Θ and $x^{(n)}$ are required to be estimated for use in the control algorithm. The control objective is to synthesize a quadratic program-based adaptive controller to guarantee exponential convergence of tracking error, parameter error, and control coefficient error in an optimal fashion without the need for the nth derivative of x while also enforcing safety-critical constraints. The next subsection introduces a quadratic program-based adaptive control law to achieve the above-mentioned objectives.

5.3.2 Control law

With the goal of controlling the variable x, we define the tracking error as $e = x - x_d(t)$, where $x_d(t)$ represents the desired trajectory to be of **class** $\mathcal{C}^n$. Let us define the estimate of $x^{(n)}$ as

$$\widehat{x^{(n)}} = x_d^{(n)}(t) + v_{opt}, \tag{5.5}$$

[2] An isolated form separates the term $\varphi(X)u$ alone on one side of the dynamical system (5.1).

where $v_{opt} \in \Re$ is a pointwise optimal signal that will later be generated by a QP optimization problem. Using the definitions of $\widehat{x^{(n)}}$ and e, Eq. (5.3) can be expressed as

$$\frac{1}{b}e^{(n)} - \frac{1}{b}v_{opt} + \Theta^T \widehat{Y}(\widehat{x^{(n)}}, \phi(X)) = \varphi(X)u. \tag{5.6}$$

Define control law $u \in \Re$ as

$$u = \frac{1}{\varphi(X)} \widehat{\Theta}^T \widehat{Y}(\widehat{x^{(n)}}, \phi(X)), \tag{5.7}$$

where $\widehat{\Theta}$ is an estimate of Θ, $\varphi(X)$ is assumed to be nonsingular, i.e., $\varphi(X) \neq 0$, and the estimates of the basis function Y are defined as

$$\widehat{Y}(\widehat{x^{(n)}}, \phi(X)) = [\widehat{x^{(n)}}, -\phi^T(X)]^T. \tag{5.8}$$

Substituting Eq. (5.7) into Eq. (5.6) yields

$$e^{(n)} = v_{opt} + b\widetilde{\Theta}^T \widehat{Y}(\widehat{x^{(n)}}, \phi(X)), \tag{5.9}$$

where $\widetilde{\Theta} = \widehat{\Theta} - \Theta$ is the estimation error.

Define $\xi = [e, \dot{e}, ..., e^{(n-1)}] \in \Re^n$ and rewrite Eq. (5.9) as

$$\dot{\xi} = F\xi + G\left(v_{opt} + D(\widetilde{\Theta})\right), \tag{5.10}$$

where $D(\widetilde{\Theta}) = b\widetilde{\Theta}^T \widehat{Y}(\widehat{x^{(n)}}, \phi(X))$ and

$$F = \begin{bmatrix} 0 & I \\ 0 & 0 \end{bmatrix} \in \Re^{n \times n}, \quad G = \begin{bmatrix} 0 \\ 1 \end{bmatrix} \in \Re^{n \times 1}. \tag{5.11}$$

With the error dynamics (5.10) in hand and with the goal of extending the QP-CLBF controller in a way that its results are exponentially convergent, the next section revisits and modifies the

QP-CLBF, and discusses the impact of the uncertainty term $D(\widetilde{\Theta})$ on the stability and safety.

5.4 Impact of uncertainties on QP-CLF and QP-CBF

The use of QP-CLBF [5] can ensure safety through CBFs and control objectives via CLFs for systems without uncertainties. However, under this controller, stability and safety are degraded for systems with uncertainties. In this section, we will first briefly revisit definitions and results relating to QP-CLFs and QP-CBFs for the nonlinear system in Eq. (5.1). We then discuss the effects of uncertainties on the performance of these controllers and finally suggest our solutions to tackle such effects.

5.4.1 QP-CLF

In this section, we aim to design a controller to stabilize the error dynamics (5.10). We begin by considering the special case of $D(\widetilde{\Theta}) = 0$ using which the error dynamics (5.10) become

$$\dot{\xi} = F\xi + Gv_{opt}. \tag{5.12}$$

Definition 19. A continuously differentiable function $V(\xi) : \Re^n \rightarrow \Re$ is an exponentially stabilizing control Lyapunov function (eCLF) for the error dynamics (5.12) if there exist a set of controls $\mathcal{V}_1$ and positive scalars $\eta, a_1, a_2 > 0$ such that [4]

$$\begin{aligned} a_1\|\xi\|^2 \leq V(\xi) \leq a_2\|\xi\|^2, \\ \inf_{v_{opt}\in\mathcal{V}_1} [\mathcal{L}_F V(\xi) + \mathcal{L}_G V(\xi)v_{opt}] \leq -\eta V(\xi), \end{aligned} \tag{5.13}$$

where $\mathcal{L}_F V(\xi) = \frac{\partial V(\xi)}{\partial \xi}F\xi$ and $\mathcal{L}_G V(\xi) = \frac{\partial V(\xi)}{\partial \xi}G$ are the Lie derivatives of $V(\xi)$ with respect to F and G, respectively.

To formulate a CLF-based controller in the absence of the uncertainty term $D(\widetilde{\Theta})$, choose a candidate Lyapunov function

$$V(\xi) = \xi^T P \xi, \tag{5.14}$$

where given F and G by (5.11) , $P = P^T > 0$ is the solution of the CARE $F^T P + PF - PGG^T P + Q = 0$ with $Q = Q^T > 0$.

The time derivative of V along the trajectory of Eq. (5.12) yields

$$\dot{V}(\xi) = \mathcal{L}_F V(\xi) + \mathcal{L}_G V(\xi) v_{opt} \tag{5.15}$$

with

$$\mathcal{L}_F V(\xi) = \xi^T (PF + F^T P)\xi \text{ and } \mathcal{L}_G V(\xi) = 2\xi^T PG. \tag{5.16}$$

To guarantee exponential convergence of ξ to zero, a family of v_{opt} is sought to satisfy the following CLF constraint

$$\Phi_0(\xi) + \Phi_1(\xi) v_{opt} \leq 0 \tag{5.17}$$

for which

$$\Phi_0(\xi) = \mathcal{L}_F V(\xi) + \eta V \text{ and } \Phi_1(\xi) = \mathcal{L}_G V(\xi), \tag{5.18}$$

where η is a positive constant. Note that the CLF constraint (5.17) is equivalent to the inequality constraint $\dot{V}(\xi) \leq -\eta V(\xi)$ to guarantee that the Lyapunov function (5.14) is exponentially convergent.

To meet the inequality constraint of Eq. (5.17), one candidate for v_{opt} is the following PWMNC law

$$v_{opt} = \begin{cases} -\frac{\Phi_0(\xi)}{\Phi_1(\xi)} & \text{if } \Phi_0(\xi) > 0 \\ 0 & \text{if } \Phi_0(\xi) \leq 0 \end{cases}. \tag{5.19}$$

The optimal signal v_{opt} can be alternatively generated pointwise in time by using a quadratic program while including the CLF constraint of Eq. (5.17). This formulation of the QP-CLF [3] ensures exponential convergence of ξ to zero and in turn according to Definition 19, $V(\xi)$ is a valid eCLF.

We now turn to the general case in which $D(\widetilde{\Theta}) \neq 0$ for the dynamics given by (5.10). Due to the existence of $D(\widetilde{\Theta})$, applying either the baseline QP-CLF or its robust modifications [78, 10] does not result in an exponential convergence of the solutions to zero. In this case, using such controllers only provides UUB of $V(\xi)$ with exponential convergence rate η from which it follows that

$$\dot{V}(\xi) \leq -\eta V(\xi) + z_1\left(\|\widetilde{\Theta}\|\right), \tag{5.20}$$

where $z_1 \in \mathcal{K}_\infty$[3]. Equation (5.20) implies that under the controllers presented in [3, 78, 10], if $D(\widetilde{\Theta}) \neq 0$, then the tracking error ξ converges to a neighborhood around the origin for which the ultimate bound is dependent on the uncertainty stemming from the unknown system parameters and control coefficient.

In Section 5.5.1, we will propose an adaptive controller that can provide simultaneous exponential convergence of system parameters and control coefficient. This implies that $\widetilde{\Theta}$ exponentially converges to zero and in turn according to Eq. (5.20), exponential convergence of ξ is guaranteed.

5.4.2 QP-CBF

In this section, the goal is to establish safety requirements for the system (5.1) through which the system states are restricted to stay in a *safety set*. For this purpose, we seek a family of the optimal signals v_{opt} to keep the state vector X in the following safety set

$$\mathcal{C} = \{X \in \Re^n : \ h(X) \geq 0\}, \tag{5.21}$$

[3]A continuous function $z_1 : [0, \infty) \longrightarrow [0, \infty)$ belongs to a class-$\mathcal{K}_\infty$ function if it is strictly increasing, $z_1(0) = 0$, and $\lim_{q \longrightarrow \infty} z_1(q) \longrightarrow \infty$.

where $h : \Re^n \to \Re$ is an r_h-times continuously differentiable function with relative degree r_h[4].

For this purpose, let us define the following companion form by applying the control law (5.7) to the system (5.3)

$$\dot{X} = F_b(X, x_d^{(n)}) + G_b\left(v_{opt} + D(\widetilde{\Theta})\right), \tag{5.22}$$

where

$$\begin{aligned} F_b &= [x_2, \ldots, x_n, x_d^{(n)}]^T \in \Re^n \;\text{ and} \\ G_b &= [0_{(n-1)\times 1}, 1]^T \in \Re^n. \end{aligned} \tag{5.23}$$

Once again for the case of $D(\widetilde{\Theta}) = 0$, from (5.22) we obtain

$$\dot{X} = F_b(X, x_d^{(n)}) + G_b v_{opt}. \tag{5.24}$$

Definition 20. Given the system (5.24), the function $h(X)$ is an exponentially zeroing barrier function (eZCBF) for the set $\mathcal{C}$, if there exists a set of controls $\mathcal{V}_2$ and gains $K^T \in \Re^{r_h}$ with positive elements k_i for $i = 1, ..., r_h$, such that [109]

$$\sup_{v_{opt}\in\mathcal{V}_2} \left[\mathcal{L}_{F_b}^{r_h} h(X) + \mathcal{L}_{G_b}\mathcal{L}_{F_b}^{r_h-1} h(X) v_{opt}\right] \geq -KH(X) \tag{5.25}$$

with

$$H(X) = [\mathcal{L}_{F_b}^{r_h-1} h(X), \ldots, \mathcal{L}_{F_b} h(X), h(X)]^T \in \Re^{r_h}. \tag{5.26}$$

The existence of such $h(X)$ renders a family of v_{opt} (generated by a QP while incorporating the CBF constraint of Eq. (5.25)) that guarantees forward invariance of set $\mathcal{C}$ i.e., if $h(X_0) \geq 0$, then $h(X(t)) \geq 0, \forall t$. With a proper selection of k_i [109], if $D(\widetilde{\Theta}) = 0$, then $h(X)$ exponentially

[4]The function $h(X)$ has relative degree r_h, if r_h-times time derivative of $h(X)$ has to be taken in order to appear the optimal signal v_{opt}.

converges to zero. However, similar to what we discussed regarding the effect of uncertainties on QP-CLF, the existence of $D(\widetilde{\Theta})$ causes violation/restriction of the safe set $\mathcal{C}$; whereby, the problem has to be generalized for the system (5.22), where $D(\widetilde{\Theta}) \neq 0$.

Again, in this case, under either the baseline QP-CBF [109, 23] or its robust versions [96, 25], $h(X)$ does not vanish in the set boundary but converges to a neighborhood around it from which the inequality (5.25) becomes

$$h^{(r_h)}(X) + k_1 h^{(r_h-1)}(X) + \cdots + k_{r_h} h(X) \geq -z_2 \left(\|\widetilde{\Theta}\| \right), \tag{5.27}$$

where $z_2 \in \mathcal{K}$[5]. Equation (5.27) implies that under the methods presented in [109, 23, 96, 25], $D(\widetilde{\Theta}) \neq 0$ leads to safety constraint violation in which the ultimate violation bound depends on the scale of $\widetilde{\Theta}$. In the next section, we will introduce our proposed adaptive technique to guarantee exponential convergence of both system parameters and control coefficient, and in turn driving the CBF to zero. This will help avoid the barrier violation while using the same CBF certificate of Eq. (5.25).

Remark 32. Although the existing robust QP-CLBF [96, 25, 78, 10, 31, 35] can provide convergence of CLF and CBF to smaller ultimate bounds for the system Eq. (5.1), the results are still UUB and the exponential convergence cannot be achieved against the parameter uncertainty and unknown control coefficient.

With the goal of developing an adaptive QP-CLBF with exponential results, the next section is devoted to unifying the QP-CLBF with FCL technique for systems with parameter uncertainty and unknown control coefficient.

5.5 Unified adaptive QP-CLBF

Section 5.4 has discussed the effect of parameter uncertainty and unknown control coefficient on the QP-CLF and QP-CBF. According to the inequities (5.20) and (5.27), the results are not

[5]A continuous function $z_2 : [0, a) \longrightarrow [0, \infty)$ belongs to a class-$\mathcal{K}$ function if it is strictly increasing and $z_1(0) = 0$.

exponential in the presence of $\widetilde{\Theta}$. This section has two principle objectives. The first is to design a filtering-based concurrent learning (FCL) adaptive controller to guarantee exponential convergence of both system parameters a and control coefficient b in the system (5.2). The second objective is to synthesize a QP optimization w.r.t. the CLF and CBF constraints, which uses the parameter estimates derived by the FCL to guarantee exponential convergence of the tracking error ξ and the barrier function $h(X)$ to zero. The solution of this optimization, v_{opt}, will be then used in the control law (5.7) and finally applied to system Eq. (5.1).

5.5.1 Filtering-based CL (FCL)

As mentioned earlier, exponential convergence of QP-CLF and QP-CBF requires driving $D(\widetilde{\Theta})$ exponentially to zero. This section extends the CL adaptive control [21] which was developed to guarantee exponential convergence of tracking and system parameter estimation errors to zero. In the CL technique, stored data is concurrently used with the online data to achieve exponential convergence of the solutions without the need for *PE* conditions on the system states; instead the finite exciting condition is required.

However, this technique has two main disadvantages. The first one is that the formulation relies on the estimates of $x^{(n)}$; if they are not accurate, the solutions converge to an ultimate bound whose size is dependent on the estimation error of $x^{(n)}$ [110, 111]. The second one is that this technique is not formulated to achieve simultaneous exponential convergence of system parameters and control coefficient, even if $x^{(n)}$ is perfectly estimated. Motivated by these issues related to the baseline CL, this section extends the CL and develops a new technique that can guarantee exponential convergence of both system parameter and control coefficient, and also removes the need for the numerical estimation of $x^{(n)}$ using a fixed-point smoother.

Due to the presence of the unavailable quantity $x^{(n)}$ in Eq. (5.4), Eq. (5.3) cannot be directly used for the parameter estimation. To cope with this issue, the filtering technique [81] is employed. Let us filter both sides of Eq. (5.3) by a first-order stable filter $c/(s+c)$ with s as the Laplace variable and $c > 0$ as a known constant number. In the time domain, this filtering can be done by convolving both sides of Eq. (5.3) by the impulse response of the filter i.e., $w(t) = ce^{-ct}$:

$$\int_0^t w(t-\tau)\Theta^T Y(x^{(n)}, \phi(X))d\tau = \int_0^t w(t-\tau)\varphi(X)ud\tau \tag{5.28}$$

which can be expanded as

$$\int_0^t w(t-\tau)\left[\frac{1}{b}x^{(n)} - \frac{a}{b}\phi(X)\right]d\tau = \int_0^t w(t-\tau)\varphi(X)ud\tau. \tag{5.29}$$

Exploiting the partial integration, the first term on the left-hand side of Eq. (5.29) becomes

$$\begin{aligned}\frac{1}{b}\int_0^t w(t-\tau)x^{(n)}d\tau =& +\frac{1}{b}\Big[w(t-\tau)x^{(n-1)}\Big|_0^t - \int_0^t \frac{d}{d\tau}(w(t-\tau))x^{(n-1)}d\tau\Big] \\ =&\frac{1}{b}\Big[w(0)x^{(n-1)}(t) - w(t)x^{(n-1)}(0) - \int_0^t \frac{d}{d\tau}(w(t-\tau))x^{(n-1)}(\tau)d\tau\Big].\end{aligned} \tag{5.30}$$

Substituting Eq. (5.30) into Eq. (5.29), the left-hand side of Eq. (5.29) can be written as

$$z(t) = \Theta^T Y_f(X) \tag{5.31}$$

with

$$Y_f = \begin{bmatrix} w(0)x^{(n-1)}(t) - w(t)x^{(n-1)}(0) - \int_0^t \frac{d}{d\tau}(w(t-\tau))x^{(n-1)}(\tau)d\tau \\ -\int_0^t w(t-\tau)\phi(X(\tau))d\tau \end{bmatrix}, \tag{5.32}$$

where $Y_f \in \Re^{r+1}$ is the filtered version of Y; and $z(t)$ is the filtered version of the right-hand side of Eq. (5.29). Thus, signal $z(t)$ can be computed from the right-hand side of Eq. (5.29)

$$z(t) = \int_0^t w(t-\tau)\varphi(X)ud\tau. \tag{5.33}$$

The estimate of $z(t)$ can be then defined as

$$\hat{z}(t) = \widehat{\Theta}^T Y_f(X). \tag{5.34}$$

With the computed signals Y_f, $z(t)$, and $\hat{z}(t)$, and the matrix P as the solution of CARE in hand, the following filtering-based concurrent learning (FCL) parameter adaptation mechanism is suggested as

$$\dot{\widehat{\Theta}} = -\gamma \left(\widehat{Y} \xi^T P G \mathrm{sgn}(b) + \sum_{i=1}^{m} Y_f(X_i) \delta_i^T \right), \tag{5.35}$$

where $\gamma \in \Re^{r+1 \times r+1} > 0$ is the adaptation convergence rate; m is the number of stored data points; X_i is the i-th recorded state vector; and δ is the prediction error that is computed as

$$\delta(t) = \hat{z}(t) - z(t) = \widetilde{\Theta}^T Y_f(X) \tag{5.36}$$

with $Y_f(X_i)$ and δ_i are both realized for the i-th store data.

The above adaptation law comprises two terms. The first term is a TEB adaptation law, which updates the parameters based upon the error trajectory ξ. The second term is a PEB adaptation mechanism, that enhances the parameter estimation by using the prediction error signal δ and the filtered vector $Y_f(X)$ realized for i-th stored data with $i = [1, 2, \ldots, m]$.

To guarantee the exponential convergence of the parameter error $\widetilde{\Theta}$ to zero, the following recording policy is used for δ and Y_f.

Recording policy. Let define matrix $Z = [Y_f(X_1), \ldots, Y_f(X_m)] \in \Re^{r+1 \times m}$, which only stores the filtered vectors $Y_f(X_i)$ that are sufficiently different from the last filtered vector stored [21]. In order to store such vectors, if

$$\frac{\|Y_f(X(t)) - Y_{f_L}\|^2}{\|Y_f(X(t))\|} \geq \epsilon_p \tag{5.37}$$

for a given positive scalar ϵ_p, then the filtered vector $Y_f(X(t))$ is eligible to be stored in the matrix Z, where Y_{f_L} represents the last filtered vector stored.

Using this policy, if x_d is such that $Y_f(X)$ is exciting over a finite interval i.e., if there exist positive constants T and α such that for an interval $[t, t+T]$ and $t \geq t_0$,

$$\int_t^{t+T} Y_f(X(\tau))Y_f^T(X(\tau))d\tau \geq \alpha I, \tag{5.38}$$

then all $r+1$ columns of the matrix are linearly independent, rank$(Z) = r+1$, and in turn the parameter estimation error exponentially converges to zero, i.e., $\widetilde{\Theta} \to 0$.

Remark 33. The main differences between the FCL adaptation law, presented in Eq. (5.35), and the CL mechanism, presented in [21], are two-fold. (i) The adaptation law (5.35) uses the prediction error $\delta(t)$ in its second term which does not require an estimate of $x^{(n)}$. On the contrary, the CL mechanism requires the estimates of $x^{(n)}$ that is provided by a fixed-point smoother. Thus, under the baseline CL, if these estimates are not accurate, $\widetilde{\Theta}$ does not converge to zero, but stays bounded to a neighborhood of the origin [110, 111]. (ii) The second term of Eq. (5.35) records the filtered basis of the system $Y_f(X)$ which allows the FCL to achieve simultaneous convergence of a and b, whereas the baseline CL collects the original basis.

5.5.2 Adaptive QP-CLBF

With the formulation of the FCL in hand, the goal of this subsection is to unify safety, stability, and adaptation through a QP optimization to formulate a multi-objective controller. The appeal of FCL adaptation law lies in the use of the same CLF and CBF constraints presented in Eq. (5.20) and (5.27) even in the presence of the system parameters and control coefficient. Relying on Eq. (5.35) that can provide exponential convergence of $D(\widetilde{\Theta})$ to zero (will be proved in Section 5.5.3), exponential convergence of $V(\xi)$ and $h(X)$ can be achieved.

The PWMNC in (5.19) can be equivalently formulated by the following optimization problem w.r.t the constraints (5.20) and (5.27) to find the optimal signal v_{opt}

$$\begin{aligned} \mathbf{v}^*_{\mathbf{opt}} = &\underset{\mathbf{v_{opt}} \in \Re}{\text{argmin}} \quad \mathbf{v_{opt}}^2 \\ &\text{s.t.} \ \ \Phi_1(\xi)\mathbf{v_{opt}} \leq -\Phi_0(\xi) \\ &\qquad \mathcal{L}_{F_1}^{r_h} h(X) + \mathcal{L}_{G_1}\mathcal{L}_{F_1}^{r_h-1} h(X)\mathbf{v_{opt}} \geq -KH(X) \\ &\qquad + \widehat{b}^{-1}\varphi^{-1}(X)\mathbf{v_{opt}} \leq \bar{u} - \widehat{\Theta}^T Y^d \left(x_d^{(n)}, \phi(X), \varphi(X)\right) \\ &\qquad - \widehat{b}^{-1}\varphi^{-1}(X)\mathbf{v_{opt}} \leq \bar{u} + \widehat{\Theta}^T Y^d \left(x_d^{(n)}, \phi(X), \varphi(X)\right) \end{aligned} \tag{5.39}$$

where $Y^d = \varphi^{-1}(X)[x_d^{(n)}, -\phi(X)]^T$; the first constraint ensures exponential convergence of ξ to zero; the second one guarantees exponential convergence of $h(X)$ (with a proper selection of gain K); and the last two constraints enforce the control input u to be bounded as $-\bar{u} \leq u \leq +\bar{u}$. The next subsection provides a formal stability analysis to show simultaneous exponential convergence of $\widetilde{\Theta}$, ξ, and $h(X)$ to zero.

Remark 34. The last two constraints encoded in the QP optimization problem (5.39) apply control bounds to the system such that the optimal control value can be found with respect to these bounds. It should be pointed out that under these constraints, the control input may hit its prescribed bounds, causing input saturation phenomenon. Since dealing with this phenomenon is beyond the scope of this work, the control bounds are selected in such a way that the control input will not be saturated by them.

5.5.3 Stability analysis

To show the global exponential convergence of the system solutions $(\xi, \widetilde{\Theta})$, let us define the following Lyapunov function

$$W(\xi, \widetilde{\Theta}) = V(\xi) + V_\Theta(\widetilde{\Theta}) \tag{5.40}$$

with

$$V_\Theta(\widetilde{\Theta}) = \widetilde{\Theta}^T \gamma^{-1} |b| \widetilde{\Theta}, \tag{5.41}$$

which benefits from the following bounding property

$$\min\left(\lambda_{\min}(P), \lambda_{\min}(|b|\gamma^{-1})\right) \|\zeta\|^2 \leq V(\zeta) \leq \max\left(\lambda_{\max}(P), \lambda_{\max}(|b|\gamma^{-1})\right) \|\zeta\|^2, \tag{5.42}$$

where $\lambda_{\min}(.)$ and $\lambda_{\max}(.)$ denote the minimum and the maximum eigenvalues of a matrix, and $\zeta = [\xi^T, \widetilde{\Theta}^T]^T \in \Re^{n+r+1}$.

Theorem 7. *Consider the Lyapunov function (5.40), the control law (5.7), the estimate of $x^{(n)}$ in Eq. (5.5), the optimization problem (5.39), and the adaptation mechanism (5.35). Under the Assumption 10 and applying the Recording Policy, the global exponential convergence of ζ is guaranteed for unknown system parameters, unknown control coefficient, and any $\xi(0)$.*

Proof. The time derivative of W along the trajectory of Eq. (5.10) is

$$\dot{W}(\zeta) = 2\xi^T PF\xi + 2\xi^T PG\left(v_{opt} + b\widetilde{\Theta}^T\widehat{Y}\right) + 2\widetilde{\Theta}^T\gamma^{-1}|b|\dot{\widehat{\Theta}}. \tag{5.43}$$

Using the definitions of $\mathcal{L}_F V(\xi)$ and $\Phi_1(\xi)$, Eq. (5.43) becomes

$$\dot{W}(\zeta) = \mathcal{L}_F V(\xi) + \Phi_1(\xi)\left(v_{opt} + b\widetilde{\Theta}^T\widehat{Y}\right) + 2\widetilde{\Theta}^T\gamma^{-1}|b|\dot{\widehat{\Theta}}. \tag{5.44}$$

Upon substitution of $\mathcal{L}_F V(\xi)$ from Eq. (5.16) and v_{opt} from Eq. (5.19) for $\Phi_0(\xi) > 0$, Eq. (5.44) becomes

$$\dot{W}(\zeta) = -\eta\xi^T P\xi + 2\xi^T PGb\widetilde{\Theta}^T\widehat{Y} + 2\widetilde{\Theta}^T\gamma^{-1}|b|\dot{\widehat{\Theta}}. \tag{5.45}$$

Substituting the adaptation law (5.35) and the prediction error (5.36) into Eq. (5.45) yields

$$\dot{W}(\zeta) = -\eta\xi^T P\xi - \widetilde{\Theta}^T H\widetilde{\Theta}, \tag{5.46}$$

where

$$H = 2|b|\sum_{i=1}^{m} Y_f(X_i)Y_f^T(X_i) = 2|b|ZZ^T \tag{5.47}$$

is a positive definite matrix due to the full rankness of matrix Z, which is guaranteed by applying the Recording Policy on the filtered vector $Y_f(X)$.

Then, Eq. (5.46) can be reduced to

$$\begin{aligned}\dot{W}(\zeta) \leq -\eta\lambda_{\min}(P)\|\xi\|^2 - \lambda_{\min}(H)\|\widetilde{\Theta}^2 &\leq -\min\Big(\eta\lambda_{\min}(P), \lambda_{\min}(H)\Big)\|\zeta\|^2 \\ &\leq -\underbrace{\frac{\min\Big(\eta\lambda_{\min}(P), \lambda_{\min}(H)\Big)}{\max\Big(\lambda_{\max}(P), \lambda_{\max}(|b|\gamma^{-1})\Big)}}_{\beta>0} W(\zeta)\end{aligned} \tag{5.48}$$

from which it follows that

$$W(\zeta(t)) \leq W(\zeta(0))e^{-\beta t}. \tag{5.49}$$

Employing the Rayleigh-Ritz inequality, Eq. (5.49) provides

$$\|\zeta(t)\| \leq \underbrace{\sqrt{\frac{\max\left(\lambda_{\max}(P), \lambda_{\max}(|b|\gamma^{-1})\right)}{\min\left(\lambda_{\min}(P), \lambda_{\min}(|b|\gamma^{-1})\right)}}}_{A>0}\|\zeta(0)\|e^{-\frac{\beta}{2}t} \tag{5.50}$$

which leads to

$$\left\|\begin{matrix}\xi(t) \\ \widetilde{\Theta}(t)\end{matrix}\right\| \leq A\left\|\begin{matrix}\xi(0) \\ \widetilde{\Theta}(0)\end{matrix}\right\| e^{-\frac{\beta}{2}t}. \tag{5.51}$$

This shows that the system solutions $(\xi(t), \widetilde{\Theta}(t))$ converge to zero exponentially at a rate of $\frac{\beta}{2}$, and since $W(\zeta)$ is radially unbounded, the results are also global. $\square$

Remark 35. Th above proof implies that the estimation error of both system parameters a and the control coefficient b converges to zero at the exponential rate $\frac{\beta}{2}$, i.e., $\hat{a} \to a$ and $\hat{b} \to b$.

Remark 36. The exponential convergence of $\widetilde{\Theta}$ to zero results in an exponential convergence of the eZCBF $h(X)$ to zero, providing an accurate safety-critical system.

Table 5.1: Physical parameters used in the simulation results.

System	Parameter	Value	Units
Mass-damper system	m	7	kg
	f_0	0.1	N
	f_1	5	$\frac{Ns}{m}$
	f_2	0.25	$\frac{Ns^2}{m^2}$
Underwater vehicle	m	7	kg
	c	3	$\frac{Ns^2}{m^2}$

5.6 Simulation results

In this section, we illustrate the effectiveness of our proposed control strategy through simulations on two illustrative examples: (i) a first order mass-damper system and (ii) a second order underwater vehicle.

5.6.1 The mass-damper system

A mass-damper system moving in a straight line can be modeled by the following first order nonlinear system [5]

$$\dot{v} = a^T \phi(v) + bu, \tag{5.52}$$

where v (m/s) denotes the velocity of the system; u (N) is the force (control input); $b = \frac{1}{m}$ is the control coefficient with m (kg) as the mass of the system; and the vector of system's base parameters a and the known function $\phi(v)$ are given as

$$a = [a_1, a_2, a_3]^T = [\frac{f_0}{m}, \frac{f_1}{m}, \frac{f_2}{m}]^T \text{ and } \phi(v) = -[1, v, v^2], \tag{5.53}$$

where $f_0, f_1, f_2 > 0$ are the friction coefficients. Physical parameters of the mass-damper system are listed in Table 5.1.

By comparing the mass-damper dynamics (5.52) with Eqs. (5.1)-(5.4), we can easily obtain that $n = 1$, $r = 3$, and $\varphi = 1$. The control objectives are (i) to drive the mass-damper system's velocity v from a randomly-selected initial condition $v_0 = 0.5$ (m/s) to the desired velocity $v_d = \sin(t)$,

(ii) to estimate the system parameters a and the unknown control coefficient b starting from a randomly-selected initial condition $(a_0, b_0) = (1.5, 1.5, 1.5, 1.5)$, (iii) to enforce the input force constraint $-20N \leq u \leq 20N$, and (iv) to enforce the velocity constraint $\underline{v} \leq v \leq \bar{v}$ by defining the following eZCBFs

$$h_1 = \bar{v} - v \text{ and } h_2 = v - \underline{v} \tag{5.54}$$

with $\bar{v} = +0.7\ (m/s)$ and $\underline{v} = -0.7\ (m/s)$. Note that the eZCBFs in Eq. (5.54) are both velocity-based and relative degree 1, i.e., $r_h = 1$. Exponential convergence of all items (i)-(iv) is desired when applying the proposed adaptive QP-CLBF through the laws (5.5), (5.7), (5.17), (5.18), (5.25), (5.32)-(5.36), and (5.39).

Case 1. In this case, the proposed controller is applied while the CBF constraint is not actively enforced in Eq. (5.39). By doing so, exponential convergence of tracking and estimation errors is sought while the mass-damper system's velocity is not restricted. From left to the right, Fig. 5.1 depicts the mass-damper system's velocity tracking, the estimated base parameters a and b, the input force u as well as the optimal signal v_{opt}, and the Lyapunov function W with its derivative $\dot{W}$. As illustrated in Figs. 5.1(a) and 5.1(b), the mass-damper system's velocity accurately tracks the desired velocity, and the system parameters a and the control coefficient b reach their ideal values in 20 sec. Once a and b converge, the optimal signal v_{opt} converges to zero and the input force is properly minimized (Fig. 5.1(c)). Figure 5.1(d) shows that the Lyapunov function W exponentially converges to zero, implying that all the results are exponential and achieved simultaneously as proven in Theorem 7.

Case 2. In order to enforce the velocity constraint, in this case all the constraints are activated in Eq. (5.39). The forward invariance of the safe set (whose CBF is defined in Eq. (5.54)) is illustrated in Fig. 5.2(a) by the mass-damper system's velocity v restricted between the prescribed upper and lower bounds, and the positiveness of eZCBFs h_1 and h_2. Due to the limits on the velocity, a sluggish convergence of the system parameters a_i for $i = 1, 2, 3$ and the control coefficient b is observed in Fig. 5.2(b) while also slightly fluctuating around their true values. This case shows that the proposed control strategy is able to achieve exponential convergence of all system solutions in the presence of the unknown system parameters and the unknown control coefficient while the mass-damper system's velocity is constrained.

5.6.2 The underwater vehicle

An underwater vehicle moving in a straight line can be modeled by the following second order nonlinear system [81]

$$\ddot{x} = a^T \phi(x, \dot{x}) + bu, \tag{5.55}$$

where x (m) and $\dot{x}$ (m/s) represent the position and the velocity of the vehicle; u (N) is the propeller force (control input); $b = \frac{1}{m}$ is the control coefficient, in which m (kg) is the mass of the vehicle; and the system base parameter a and the known function $\phi(x, \dot{x})$ are

$$a = \frac{c}{m} \text{ and } \phi(x, \dot{x}) = -\dot{x}^2 \text{sign}(\dot{x}), \tag{5.56}$$

where $c > 0$ is the drag coefficient. The base parameters of the vehicle are listed in Table 5.1.

In view of Eqs. (5.1)-(5.4), it can be figured out that $n = 2$, $r = 1$, $\varphi = 1$, and $X = [x, \dot{x}]^T$. For this system, the control tasks are (i) to obtain convergence of the state vector X from a randomly-selected initial condition $X_0 = [0.5, 0]^T$ to the desired trajectory X_d with $x_d = \sin(t)$, (ii) to achieve convergence of (a, b) starting from a randomly-selected initial condition $(a_0, b_0) = (1.5, 1)$ to their actual values, (iii) to bound the propeller force as $-20N \leq u \leq 20N$, and (iv) to enforce the constraint $\underline{x} \leq x \leq \bar{x}$ on the vehicle's position x by defining two relative degree 2 eZCBFs (position-based constraints i.e., $r_h = 2$) as

$$h_1 = \bar{x} - x \text{ and } h_2 = x - \underline{x}, \tag{5.57}$$

where $\bar{x} = +0.7$ and $\underline{x} = -0.7$. Again, we will apply our proposed approach comprises the laws (5.5), (5.7), (5.17), (5.18), (5.25), (5.32)-(5.36), and (5.39) to obtain exponential convergence of all above-mentioned items (i)-(iv).

Case 3. In this case, exponential convergence of the system solutions (ξ, a, b), guaranteed by Theorem 7, is verified while the CBF constraint (5.57) is not taken into account. As indicated in Fig. 5.3(a), the actual position of the vehicle converges to the desired position. The convergence of the system parameter a and the control coefficient b to the true values can be seen in Fig. 5.3(b). The propeller force and the optimal signal v_{opt} obtained from the QP optimization are illustrated in Fig. 5.3(c). In addition, it can be seen in Fig. 5.3(d) that the Lyapunov function converges to zero. While Theorem 7 formally guarantees, Fig. 5.3 verifies that all solutions are exponential and converge in 10 sec.

Case 4. To enforce the vehicle's position to be bounded between $\underline{x} = -0.7$ and $\bar{x} = +0.7$, the relative-degree two safety constraint (5.57) is activated in this case. Fig. 5.4(a) shows the position x that is restricted by its upper and lower bounds. This figure also shows non-negativity of the functions h_1 and h_2 demonstrating enforcement of the position-based constraints. Fig. 5.4(b) illustrates exponential convergence of the system parameters a and the control coefficient b to their actual values (due to Theorem 7) in spite that the vehicle's position is restricted. Therefore, as the estimation error converges to zero, h_1 and h_2 vanish in the set boundary and an accurate safety is obtained.

5.7 Conclusions and future works

The baseline QP-CLBF controller can only guarantee accurate safety and stability for systems without uncertainties. Existing robust QP-CLBFs are able to enhance the performance of the baseline approach but still cannot drive the system errors to zero. In this chapter, an adaptive QP-CLBF controller has been proposed for a class of nonlinear systems with parameter uncertainty and unknown control coefficient, that can provide exponential results. We have introduced an extension of the CL adaptive approach, which was not developed for simultaneous estimation of system parameters and control coefficient, to guarantee exponential convergence of all parameter errors to zero simultaneously. This was achieved by introducing a filtering-based CL, called FCL technique, that allows for simultaneous exponential convergence of system parameters and control coefficient without the need for numerical estimation of state derivatives using a fixed-point smoother. An adaptive QP-CLBF controller has been then formulated by synthesizing a QP subject to CLF and CBF constraints while using the parameter estimates derived by the FCL technique to ensure accurate safety and stability for systems with uncertainties. It has been proved using a Lyapunov argument that under the proposed scheme, simultaneous exponential convergence of all system parameter error, control coefficient error, tracking error, and safety-critical constraints to zero can be achieved. Simulation results have shown the soundness of the proposed scheme on two illustrative examples: a first order mass-damper system and a second order underwater vehicle.

This chapter has formulated the adaptive QP-CLBF controller for n^{th}-order SISO nonlinear systems. Although the proposed controller can be applied to a variety of mechanical and robotic systems, there are numerous MIMO applications of the presented approach that have been excluded from the scope of this thesis. This naturally motivates us to conduct our future direction towards extending the proposed scheme for the uncertain MIMO nonlinear systems.

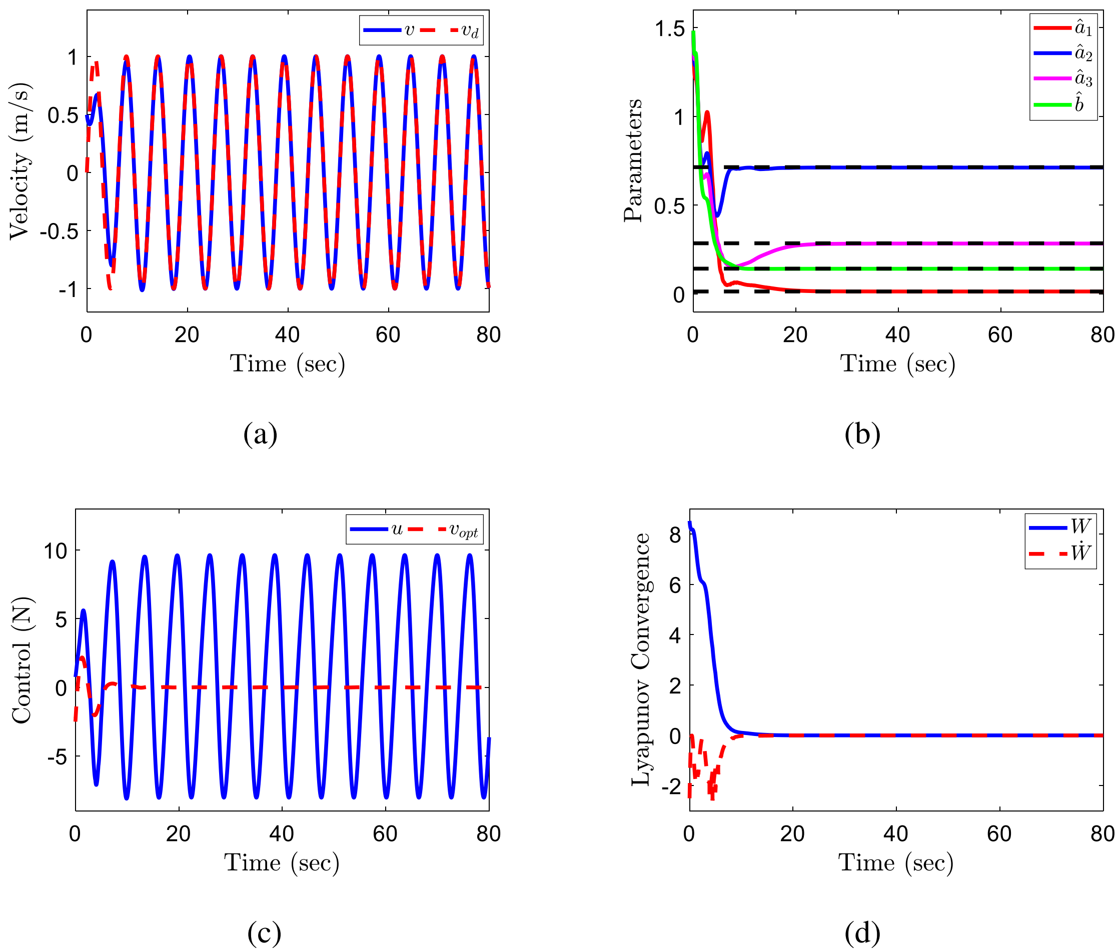

Figure 5.1: Results of the proposed controller applying for the mass-damper system in Case 1, including (a) the velocity v tracking, (b) the estimates of the system parameters a and the control coefficient b with their actual values indicated by black dashed lines, (c) the input force u and the pointwise optimal signal v_{opt}, and (d) the Lyapunov function and its derivative.

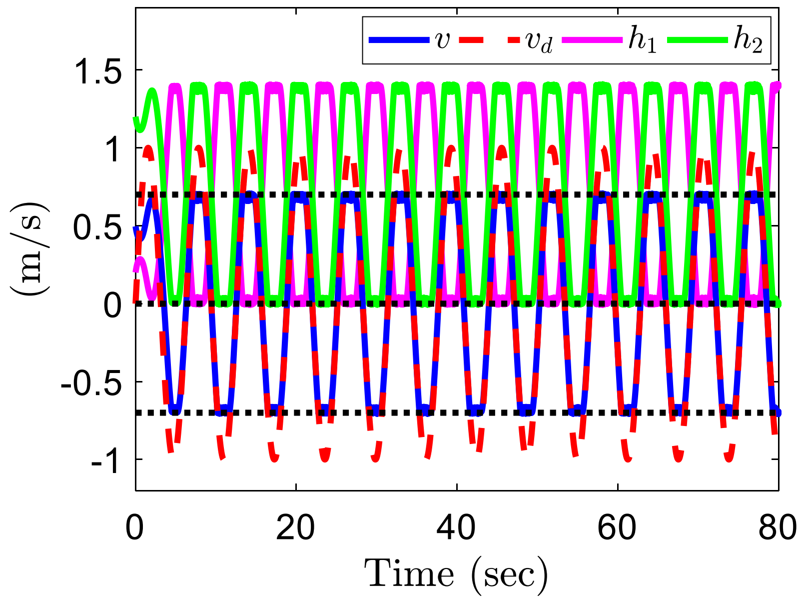

(a)

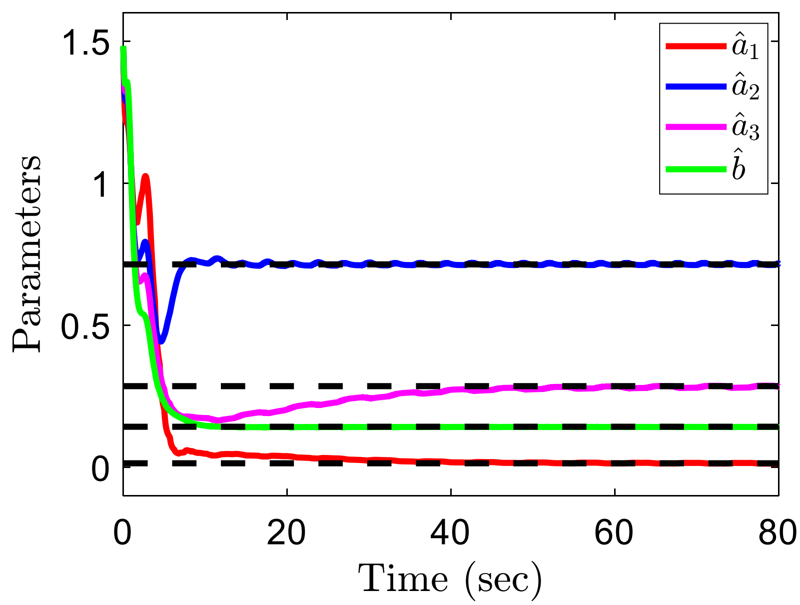

(b)

Figure 5.2: Results of the proposed controller applying for the mass-damper system in Case 2, including (a) the velocity v with its upper and lower bounds indicated by black dotted lines as well as the eZCBFs with positive values indicating satisfaction and (b) the estimates of the system parameters a and the control coefficient b with their actual values indicated by black dashed lines.

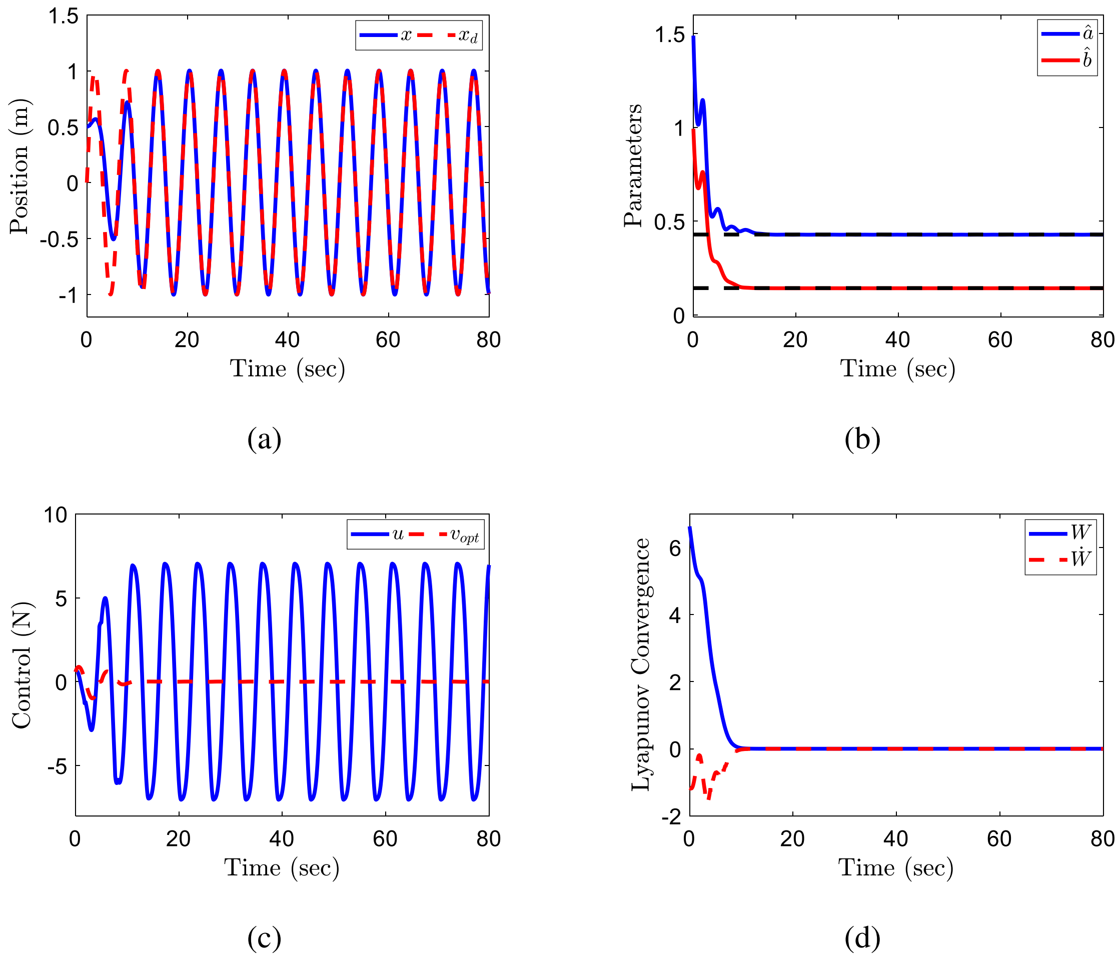

Figure 5.3: Results of the proposed controller applying for the underwater vehicle in Case 3, including (a) the position x tracking, (b) the estimates of the system parameters a and the control coefficient b with their actual values indicated by black dashed lines, (c) the propeller force u and the optimal signal v_{opt}, and (d) the Lyapunov function and its derivative.

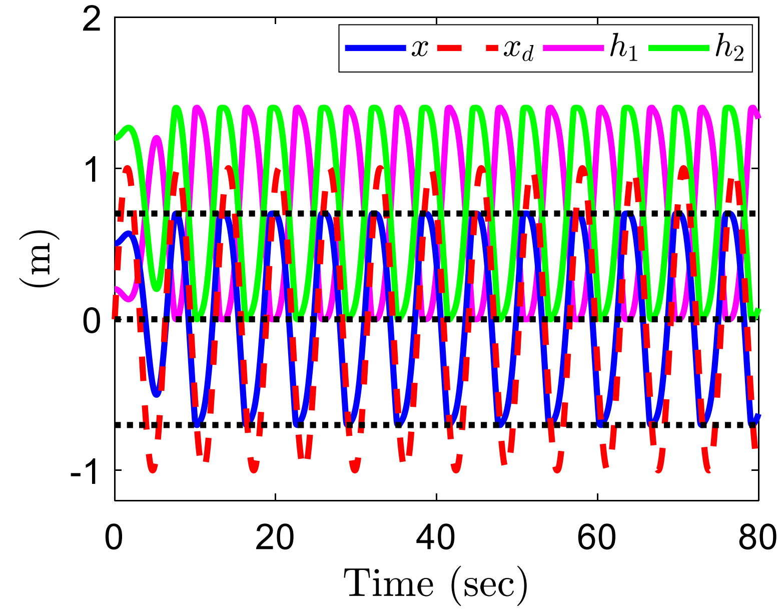

(a)

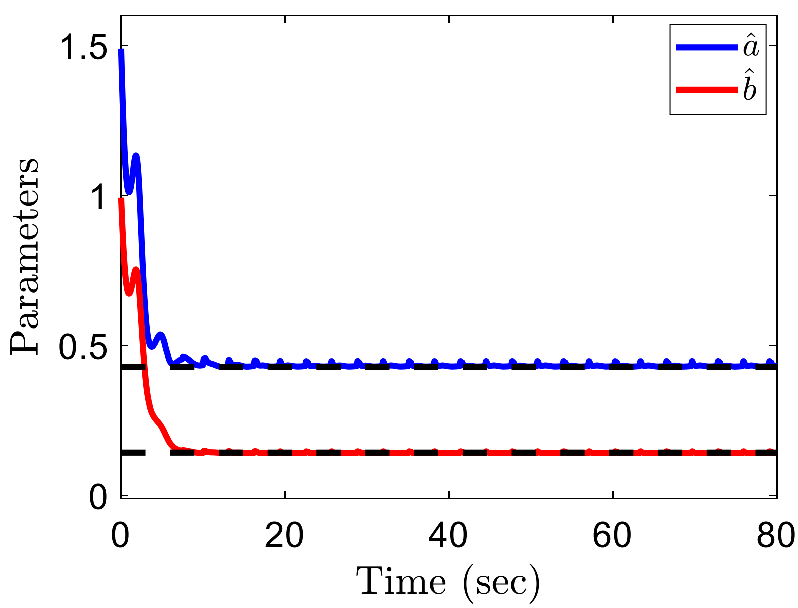

(b)

Figure 5.4: Results of the proposed controller applying for the underwater vehicle in Case 4, including (a) the position x with its upper and lower bounds indicated by black dotted lines as well as the eZCBFs with positive values indicating satisfaction and (b) the estimates of the system parameters a and the control coefficient b with their actual values indicated by black dashed lines.

CHAPTER 6

DISCUSSION, CONCLUSIONS, AND FUTURE WORKS

6.1 Discussion and conclusions

The QP-CLBF controllers are widely used for nonlinear systems, wherein they have the advantage that they can balance stability and safety in a pointwise optimal fashion. However, they are not amenable to guarantee the performance of closed-loop systems and satisfy safety-critical constraints in the presence of parameter uncertainties, unmodeled dynamics, and disturbances. This motivated the results presented in this thesis. We proposed five different control approaches towards unifying adaptation, robustness, CLFs, and CBFs into a QP framework that can enhance the existing functionalities of QP-CLBFs to achieve better control objectives and safety performance. The proposed control schemes extend the applications of QP-CLBFs to uncertain fully actuated and underactuated systems that include structured and unstructured uncertainties as well as system-environment interactions. This could allow for reliable implementation of the proposed controllers that their soundness is formally proven on real-world systems whose dynamics models are fully/partially unknown and that involve significant contact with the environment.

In this thesis, we formulated five different robust quadratic program-based adaptive controllers for fully actuated and underactuated systems, the contribution of each problem can be summarized as follows:

Control of fully actuated nonlinear systems with structured uncertainties. A two-layer controller is presented for fully actuated nonlinear systems whose dynamics can be expressed linearly in terms of the unknown parameter. In the inner layer, the unknown system dynamics are identified by an adaptive control and the estimates are sent to the outer later in which a QP is synthesized utilizing an RCLF constraint and control bounds. The RCLF is responsible for compensating uncanceled dynamics and disturbances. The UUB of all system solutions are proven and the benefits of the unified controller over the baseline QP-CLF are demonstrated through simulation.

Control and safety of fully actuated nonlinear systems with unstructured uncertainties. A two-layer three-term (adaptive, optimal, and feed-forward) control strategy is formulated for fully actuated nonlinear systems with unstructured uncertainties and time-varying disturbances. The unknown dynamics of the system are estimated by a neuro-adaptive approach to inform the adaptive term. The pointwise optimal term is generated by a QP while incorporating three inequality constraints RCLF, CBF, and control bounds. A robust term robustifies the proposed controller to disturbances and uncanceled uncertainties. The end result is a single controller that can balance stabilization and safety in the presence of modeling error and disturbances, while outperforming the baseline QP-CLBF and proving the UUB of all system signals.

Active space control of underactuated robotic systems. A multi-objective control scheme is presented for application to underactuated robotic systems that is able to achieve simultaneous objectives: active space control, system identification, and point-wise control optimality in the presence of unmodeled dynamics and disturbances. The system's accelerations are estimated as a remedy for nonlinear coupling between active and passive spaces, and as an alternative to the *direct measurement* and *substitution* methods for use in the control algorithm. The modeling uncertainty associated with both unknown system parameters and unknown control map is estimated. An IRCLF is presented to automatically compensate for acceleration estimation error, unmodeled dynamics, and disturbances without the need for their bounds *a priori*. Utilizing the IRCLF, a QP is synthesized to ensure the system stability with minimal control effort, while using the estimates of the unknown dynamics. Simulations and comparisons to the baseline QP-RCLF and an adaptive QP-RCLF on two different underactuated systems—a foot-leg model on the deformable ground and the overhead crane system—validate the superiority of our approach.

Passive space control and safety of underactuated robotic systems. A novel approach for non-collocated control of n DoF-one DoA underactuated robotic systems with diagonal inertia matrices is presented. By unifying a $2n$-step backstepping design procedure and RBFNNs, an adaptive control is designed to approximate the unknown nonlinear functions. Modeling approximation error, chained errors between the system's states stemming from the backstepping design, and time-varying disturbances are compensated by designing virtual inputs whose gains are evolved by projection-based adaptation laws. Novel TVRCLF and TVRCBF are presented to be encoded into a QP to balance stabilization and safety in the presence of unmodeled dynamics and disturbances without knowing their bounds *a priori*. The eDE stability of all system solutions is ensured and the benefits of our approach is confirmed over the baseline QP-CLBF/FL method on a single-link flexible-joint robot.

Control and safety of fully actuated systems with exponential results. A new adaptation technique, called FCL, is presented to guarantee simultaneous exponential convergence of system parameters and control coefficient. This technique extends and encompasses the traditional CL adaptive approach that suffers from the followings. CL formulation relies on the estimates of n-th derivative of state; if they are not accurate, the solutions converge to an ultimate bound whose size is dependent on the estimation error of $x^{(n)}$. CL is not formulated to achieve simultaneous exponential convergence of system parameters and control coefficient, even if $x^{(n)}$ is perfectly estimated. The FCL is unified with QP-CLBF to achieve exponential convergence of all system errors while strictly avoiding the violation of safety constraints. This is formally proven and the soundness of the proposed approach is demonstrated on two illustrative examples—a mass-damper system and an underwater vehicle.

6.2 Future works

With the proposed robust QP-based adaptive control approaches in hand, this thesis opens up the following possible directions for the future work.

Stabilization and safety of stochastic nonlinear systems. The presented approaches in this thesis can be implemented for a wide range of fully actuated and underactuated applications with deterministic nonlinear systems. However there is a variety of practical applications in which stochastic/random disturbances often exist that forbids the direct application of the presented approaches. Motivated by redundant applications with stochastic nonlinear systems, the future work would aim to reformulate CBF and CLF frameworks for such systems based upon which the proposed controllers can be extended, while providing a formal framework of boundedness in probability.

Control of multi-agent systems with uncertain dynamic network structure. In recent years, there has been an increasing interest in the consensus control design of multi-agent systems due to its multiple applications in formation control, rendezvous control, leader–follower problem, etc. In such problems, a graph is usually considered to model the information interaction among agents. One of the main challenges in such problems lies in the fact that consensus is not achievable if the connectivity of network/graph is destroyed during the missions. This, coupled with the existence of stochastic disturbances increases the complexity of consensus control of multi-agent systems. This naturally motivates us to extend the presented approaches to multi-agent system control while formally ensuring the consensus and convergence of all system solutions.

REFERENCES

[1] D. Mayne, J. Rawlings, C. Rao, and P. Scokaert, “Constrained model predictive control: Stability and optimality,” *Automatica*, vol. 36, no. 6, pp. 789 –814, 2000.

[2] J. W. Grizzle, G. Abba, and F. Plestan, “Asymptotically stable walking for biped robots: Analysis via systems with impulse effects,” *IEEE Transactions on Automatic Control*, vol. 46, no. 1, pp. 51–64, 2001.

[3] A. D. Ames and M. Powell, “Towards the unification of locomotion and manipulation through control lyapunov functions and quadratic programs,” *Control of Cyber-Physical Systems, Springer*, 219–240, 2013.

[4] A. D. Ames, K. Galloway, K. Sreenath, and J. W. Grizzle, “Rapidly exponentially stabilizing control lyapunov functions and hybrid zero dynamics,” *IEEE Transactions on Automatic Control*, vol. 59, no. 4, pp. 876–891, 2014.

[5] A. D. Ames, X. Xu, J. W. Grizzle, and P. Tabuada, “Control barrier function based quadratic programs for safety critical systems,” *IEEE Transactions on Automatic Control*, vol. 62, no. 8, pp. 3861–3876, 2017.

[6] H. Zhao, J. Horn, J. Reher, V. Paredes, and A. D. Ames, “Multicontact locomotion on transfemoral prostheses via hybrid system models and optimization-based control,” *IEEE Transactions on Automation Science and Engineering*, vol. 13, no. 2, pp. 502–513, 2016.

[7] H. Zhao, J. Horn, J. Reher, V. Paredes, and A. D. Ames, “First steps toward translating robotic walking to prostheses: A nonlinear optimization based control approach,” *Autonomous Robots*, vol. 41, no. 3, pp. 725–742, 2017.

[8] K. Galloway, K. Sreenath, A. D. Ames, and J. W. Grizzle, “Torque saturation in bipedal robotic walking through control lyapunov function-based quadratic programs,” *IEEE Access*, vol. 3, pp. 323–332, 2015.

[9] S. Kolathaya and A. D. Ames, “Exponential convergence of a unified clf controller for robotic systems under parameter uncertainty,” in *2014 American Control Conference*, 2014, pp. 3710–3715.

[10] S. Kolathaya and A. D. Ames, “Parameter to state stability of control lyapunov functions for hybrid system models of robots,” *Nonlinear Analysis: Hybrid Systems*, vol. 25, pp. 174 –191, 2017.

[11] J.-J. E. Slotine and J. A. Coetsee, “Adaptive sliding controller synthesis for non-linear systems,” *International Journal of Control*, vol. 43, no. 6, pp. 1631–1651, 1984.

[12] J.-J. E. Slotine and W. Li, “Composite adaptive control of robot manipulators,” *Automatica*, vol. 25, no. 4, pp. 509 –519, 1989.

[13] V. Azimi, D. Simon, and H. Richter, “Stable robust adaptive impedance control of a prosthetic leg,” in *Proceedings of the ASME 2015 Dynamic Systems and Control Conference*, 2015.

[14] V. Azimi, D. Simon, H. Richter, and S. A. Fakoorian, “Robust composite adaptive transfemoral prosthesis control with non-scalar boundary layer trajectories,” in *2016 American Control Conference (ACC)*, 2016, pp. 3002–3007.

[15] J.-J. E. Slotine and W. Li, “Adaptive manipulator control: A study case,” *IEEE Transactions on Automatic Control*, vol. 33, no. 11, pp. 995–1003, 1988.

[16] J. Yuan and Y. Stepanenko, “Composite adaptive control of flexible joint robots,” *Automatica*, vol. 29, no. 3, pp. 609 –619, 1993.

[17] V. Azimi, S. A. Fakoorian, T. T. Nguyen, and D. Simon, “Robust adaptive impedance control with application to a transfemoral prosthesis and test robot,” *J. Dyn. Sys., Meas., Control.*, vol. 12, no. 140, DS–17–1333, 2018.

[18] N. Hovakimyan and C. Cao, *L1 Adaptive Control Theory*. SIAM, 2010.

[19] H. Modares, F. L. Lewis, and M. B. N. Sistani, “Integral reinforcement learning and experience replay for adaptive optimal control of partially-unknown constrained-input continuous-time systems,” *Automatica*, vol. 50, no. 1, pp. 193–202, 2014.

[20] G. Chowdhary and E. N. Johnson, “Adaptive neural network flight control using both current and recorded data,” Georgia Institute of Technology, 2007.

[21] G. Chowdhary, M. Mühlegg, and E. Johnson, “Exponential parameter and tracking error convergence guarantees for adaptive controllers without persistency of excitation,” *International Journal of Control*, vol. 87, no. 8, pp. 1583–1603, 2014.

[22] C. Girish, Y. Tansel, M. Maximillian, and J. E. N., “Concurrent learning adaptive control of linear systems with exponentially convergent bounds,” *International Journal of Adaptive Control and Signal Processing*, vol. 27, no. 4, pp. 280–301,

[23] A. D. Ames, J. W. Grizzle, and P. Tabuada, “Control barrier function based quadratic programs with application to adaptive cruise control,” in *53rd IEEE Conference on Decision and Control*, 2014, pp. 6271–6278.

[24] Q. Nguyen and K. Sreenath, "Optimal robust safety-critical control for dynamic robotics," *International Journal of Robotics Research (IJRR)*, in review, 2016.

[25] X. Xu, P. Tabuada, J. W. Grizzle, and A. D. Ames, "Robustness of control barrier functions for safety critical control," *IFAC-PapersOnLine*, vol. 48, no. 27, pp. 54 –61, 2015.

[26] H. K. Khalil, *Nonlinear Systems, 3rd ed.* Prentice Hall, 2002.

[27] R. Freeman and P. Kokotovic, *Robust Nonlinear Control Design*. Birkhauser, 1996.

[28] G. Chowdhary and E. Johnson, "Concurrent learning for convergence in adaptive control without persistency of excitation," in *Decision and Control (CDC), 2010 49th IEEE Conference on*, IEEE, 2010, pp. 3674–3679.

[29] A. Gelb, *Applied optimal estimation*. MIT Press, 1974.

[30] D. Simon, *Optimal State Estimation: Kalman, H-infinity, and Nonlinear Approaches*. John Wiley & Sons, 2006.

[31] V. Azimi and P. A. Vela, "Performance reference adaptive control: A joint quadratic programming and adaptive control framework," in *2018 American Control Conference (ACC)*, 2018.

[32] K. Hornik, M. Stinchcombe, and H. White, "Multilayer feedforward networks are universal approximators," *Neural Networks*, vol. 2, no. 5, pp. 359 –366, 1989.

[33] F. Lewis, "Nonlinear network structures for feedback control," *Asian Journal of Control*, vol. 1, no. 4, pp. 205–228, 1999.

[34] G. V. Chowdhary and E. N. Johnson, "Theory and flight-test validation of a concurrent-learning adaptive controller," *Journal of Guidance Control and Dynamics*, vol. 34, no. 2, p. 592, 2011.

[35] V. Azimi and P. A. Vela, "Robust adaptive quadratic programming and safety performance of nonlinear systems with unstructured uncertainties," in *57th IEEE Conference on Decision and Control*, 2018.

[36] K.-D. Nguyen and H. Dankowicz, "Adaptive control of underactuated robots with unmodeled dynamics," *Robotics and Autonomous Systems*, vol. 64, pp. 84 –99, 2015.

[37] L. Consolini and M. Tosques, "On the VTOL exact tracking with bounded internal dynamics via a poincare map approach," *IEEE Transactions on Automatic Control*, vol. 52, no. 9, pp. 1757–1762, 2007.

[38] S. Farzan, A. Hu, E. Davies, and J. Rogers, "Modeling and control of brachiating robots traversing flexible cables," in *2018 IEEE International Conference on Robotics and Automation (ICRA)*, 2018, pp. 1645–1652.

[39] S. Farzan, A. Hu, E. Davies, and J. Rogers, "Feedback motion planning and control of brachiating robots traversing flexible cables," in *2019 American Control Conference (ACC)*, 2019, pp. 1323–1329.

[40] E. Davies, A. Garlow, S. Farzan, J. Rogers, and A. Hu, "Tarzan: Design, prototyping, and testing of a wire-borne brachiating robot," in *2018 IEEE/RSJ International Conference on Intelligent Robots and Systems (IROS)*, 2018, pp. 7609–7614.

[41] A. Ramezani, X. Shi, S. Chung, and S. Hutchinson, "Lagrangian modeling and flight control of articulated-winged bat robot," in *2015 IEEE/RSJ International Conference on Intelligent Robots and Systems (IROS)*, 2015, pp. 2867–2874.

[42] A. Ramezani, X. Shi, S.-J. Chung, and S. Hutchinson, "Nonlinear flight controller synthesis of a bat-inspired micro aerial vehicle," in *AIAA Guidance, Navigation, and Control Conference*. eprint: `https://arc.aiaa.org/doi/pdf/10.2514/6.2016-1376`.

[43] F. Plestan, J. W. Grizzle, E. R. Westervelt, and G. Abba, "Stable walking of a 7-dof biped robot," *IEEE Transactions on Robotics and Automation*, vol. 19, no. 4, pp. 653–668, 2003.

[44] D. Tlalolini, C. Chevallereau, and Y. Aoustin, "Human-like walking: Optimal motion of a bipedal robot with toe-rotation motion," *IEEE/ASME Transactions on Mechatronics*, vol. 16, no. 2, pp. 310–320, 2011.

[45] N. Wang, C. Qian, J. C. Sun, and Y. C. Liu, "Adaptive robust finite-time trajectory tracking control of fully actuated marine surface vehicles," *IEEE Transactions on Control Systems Technology*, vol. 24, no. 4, pp. 1454–1462, 2016.

[46] J.-J. E. Slotine and W. Li, "On the adaptive control of robot manipulators," *The International Journal of Robotics Research*, vol. 6, no. 3, pp. 49–59, 1987.

[47] B. Bischof, T. Glück, and A. Kugi, "Combined path following and compliance control for fully actuated rigid body systems in 3-d space," *IEEE Transactions on Control Systems Technology*, vol. 25, no. 5, pp. 1750–1760, 2017.

[48] S. Farzan and G. N. DeSouza, "From d-h to inverse kinematics: A fast numerical solution for general robotic manipulators using parallel processing," in *2013 IEEE/RSJ International Conference on Intelligent Robots and Systems*, 2013, pp. 2507–2513.

[49] S. Farzan and G. N. DeSouza, "A parallel evolutionary solution for the inverse kinematics of generic robotic manipulators," in *2014 IEEE Congress on Evolutionary Computation (CEC)*, 2014, pp. 358–365.

[50] V. Azimi, T. T. Nguyen, M. Sharifi, S. A. Fakoorian, and D. Simon, "Robust ground reaction force estimation and control of lower-limb prostheses: Theory and simulation," *IEEE Transactions on Systems, Man, and Cybernetics: Systems*, pp. 1–12, 2018.

[51] V. Azimi, T. Shu, H. Zhao, E. Ambrose, A. D. Ames, and D. Simon, "Robust control of a powered transfemoral prosthesis device with experimental verification," in *2017 American Control Conference (ACC)*, 2017, pp. 517–522.

[52] V. Azimi, T. Shu, H. Zhao, R. Gehlhar, D. Simon, and A. D. Ames, "Model-based adaptive control of transfemoral prostheses: Theory, simulation, and experiments," *IEEE Transactions on Systems, Man, and Cybernetics: Systems*, pp. 1–18, 2019.

[53] M. W. Spong, "The swing up control problem for the acrobot," *IEEE Control Systems*, vol. 15, no. 1, pp. 49–55, 1995.

[54] R. Fierro, F. L. Lewis, and A. Lowe, "Hybrid control for a class of underactuated mechanical systems," *IEEE Transactions on Systems, Man, and Cybernetics - Part A: Systems and Humans*, vol. 29, no. 6, pp. 649–654, 1999.

[55] R. Olfati-Saber, "Normal forms for underactuated mechanical systems with symmetry," *IEEE Transactions on Automatic Control*, vol. 47, no. 2, pp. 305–308, 2002.

[56] N. R. Gans and S. A. Hutchinson, "Visual servo velocity and pose control of a wheeled inverted pendulum through partial-feedback linearization," in *2006 IEEE/RSJ International Conference on Intelligent Robots and Systems*, 2006, pp. 3823–3828.

[57] I. Fantoni, R. Lozano, and M. W. Spong, "Energy based control of the pendubot," *IEEE Transactions on Automatic Control*, vol. 45, no. 4, pp. 725–729, 2000.

[58] K. Astrom and K. Furuta, "Swinging up a pendulum by energy control," *Automatica*, vol. 36, no. 2, pp. 287 –295, 2000.

[59] X. Z. Lai, J. H. She, S. X. Yang, and M. Wu, "Comprehensive unified control strategy for underactuated two-link manipulators," *IEEE Transactions on Systems, Man, and Cybernetics, Part B (Cybernetics)*, vol. 39, no. 2, pp. 389–398, 2009.

[60] M. W. Spong, J. K. Holm, and D. Lee, "Passivity-based control of bipedal locomotion," *IEEE Robotics Automation Magazine*, vol. 14, no. 2, pp. 30–40, 2007.

[61] P. Tsiotras and J. Luo, "Control of underactuated spacecraft with bounded inputs," *Automatica*, vol. 36, no. 8, pp. 1153 –1169, 2000.

[62] Z. Cao, Q. Xiao, R. Huang, and M. Zhou, "Robust neuro-optimal control of underactuated snake robots with experience replay," *IEEE Transactions on Neural Networks and Learning Systems*, vol. 29, no. 1, pp. 208–217, 2018.

[63] S. Kim and S. Kwon, "Nonlinear optimal control design for underactuated two-wheeled inverted pendulum mobile platform," *IEEE/ASME Transactions on Mechatronics*, vol. 22, no. 6, pp. 2803–2808, 2017.

[64] L. Barbazza, D. Zanotto, G. Rosati, and S. K. Agrawal, "Design and optimal control of an underactuated cable-driven micro-macro robot," *IEEE Robotics and Automation Letters*, vol. 2, no. 2, pp. 896–903, 2017.

[65] J. Huang, Z. H. Guan, T. Matsuno, T. Fukuda, and K. Sekiyama, "Sliding-mode velocity control of mobile-wheeled inverted-pendulum systems," *IEEE Transactions on Robotics*, vol. 26, no. 4, pp. 750–758, 2010.

[66] R. Xu and Ümit Özgüner, "Sliding mode control of a class of underactuated systems," *Automatica*, vol. 44, no. 1, pp. 233 –241, 2008.

[67] V. Sankaranarayanan and A. D. Mahindrakar, "Control of a class of underactuated mechanical systems using sliding modes," *IEEE Transactions on Robotics*, vol. 25, no. 2, pp. 459–467, 2009.

[68] I. Shah and F. U. Rehman, "Smooth second order sliding mode control of a class of underactuated mechanical systems," *IEEE Access*, vol. 6, pp. 7759–7771, 2018.

[69] T. Nguyen, V. Azimi, W. Su, and C. Edwards, "Improvement of control signals in output feedback sliding mode control of sampled-data systems," in *2017 American Control Conference (ACC)*, 2017, pp. 5762–5767.

[70] T. Nguyen, C. Edwards, V. Azimi, and W. Su, "Improving control effort in output feedback sliding mode control of sampled-data systems," *IET Control Theory Applications*, vol. 13, no. 13, pp. 2128–2137, 2019.

[71] T. Nguyen, C. Edwards, V. Azimi, and W.-C. Su, *On the control effort in output feedback sliding mode control of sampled-data systems*, 2019. arXiv: 1904.06489 [cs.SY].

[72] V. Azimi, D. Munther, M. Sharifi, and P. A. Vela, "Enhancing produce safety: State estimation-based robust adaptive control of a produce wash system," *Journal of Process Control*, vol. 86, pp. 1 –15, 2020.

[73] D. Pucci, F. Romano, and F. Nori, "Collocated adaptive control of underactuated mechanical systems," *IEEE Transactions on Robotics*, vol. 31, no. 6, pp. 1527–1536, 2015.

[74] M. Zhang, X. Ma, R. Song, X. Rong, G. Tian, X. Tian, and Y. Li, "Adaptive proportional-derivative sliding mode control law with improved transient performance for underactuated overhead crane systems," *IEEE/CAA Journal of Automatica Sinica*, vol. 5, no. 3, pp. 683–690, 2018.

[75] T. S. Wu, M. Karkoub, H. Wang, H. S. Chen, and T. H. Chen, "Robust tracking control of mimo underactuated nonlinear systems with dead-zone band and delayed uncertainty using an adaptive fuzzy control," *IEEE Transactions on Fuzzy Systems*, vol. 25, no. 4, pp. 905–918, 2017.

[76] X. Lin, J. Nie, Y. Jiao, K. Liang, and H. Li, "Adaptive fuzzy output feedback stabilization control for the underactuated surface vessel," *Applied Ocean Research*, vol. 74, pp. 40 –48, 2018.

[77] Y.-L. Gu and Y. Xu, "Under-actuated robot systems: Dynamic interaction and adaptive control," in *Proceedings of IEEE International Conference on Systems, Man and Cybernetics*, vol. 1, 1994, 958–963 vol.1.

[78] Q. Nguyen and K. Sreenath, "Optimal robust control for constrained nonlinear hybrid systems with application to bipedal locomotion," in *2016 American Control Conference (ACC)*, 2016, pp. 4807–4813.

[79] K. Reif, S. Gunther, E. Yaz, and R. Unbehauen, "Stochastic stability of the discrete-time extended kalman filter," *IEEE Transactions on Automatic Control*, vol. 44, no. 4, pp. 714–728, 1999.

[80] K. Reif, S. Gunther, E. Yaz, and R. Unbehauen, "Stochastic stability of the continuous-time extended kalman filter," *IEE Proceedings - Control Theory and Applications*, vol. 147, no. 1, pp. 45–52, 2000.

[81] J. Slotine and W. Li, *Applied Nonlinear Control*. Prentice Hall, 1991.

[82] R. Naldi, M. Furci, R. G. Sanfelice, and L. Marconi, "Robust global trajectory tracking for underactuated vtol aerial vehicles using inner-outer loop control paradigms," *IEEE Transactions on Automatic Control*, vol. 62, no. 1, pp. 97–112, 2017.

[83] C. P. Bechlioulis, G. C. Karras, S. Heshmati-Alamdari, and K. J. Kyriakopoulos, "Trajectory tracking with prescribed performance for underactuated underwater vehicles under model uncertainties and external disturbances," *IEEE Transactions on Control Systems Technology*, vol. 25, no. 2, pp. 429–440, 2017.

[84] A.-C. Huang and Y.-C. Chen, "Adaptive sliding control for single-link flexible-joint robot with mismatched uncertainties," *IEEE Transactions on Control Systems Technology*, vol. 12, no. 5, pp. 770–775, 2004.

[85] M. Jin, J. Lee, and N. G. Tsagarakis, "Model-free robust adaptive control of humanoid robots with flexible joints," *IEEE Transactions on Industrial Electronics*, vol. 64, no. 2, pp. 1706–1715, 2017.

[86] K. A. Hamed and R. D. Gregg, "Decentralized event-based controllers for robust stabilization of hybrid periodic orbits: Application to underactuated 3-d bipedal walking," *IEEE Transactions on Automatic Control*, vol. 64, no. 6, pp. 2266–2281, 2019.

[87] B. Brogliato, "Comments on "control of a planar underactuated biped on a complete walking cycle"," *IEEE Transactions on Automatic Control*, vol. 52, no. 5, pp. 961–964, 2007.

[88] M. W. Spong, "Underactuated mechanical systems," in *Control Problems in Robotics and Automation*, Springer Berlin Heidelberg, 1998, pp. 135–150.

[89] M. W. Spong, "Partial feedback linearization of underactuated mechanical systems," in *Proceedings of IEEE/RSJ International Conference on Intelligent Robots and Systems (IROS'94)*, vol. 1, 1994, 314–321 vol.1.

[90] J. Huang, S. Ri, T. Fukuda, and Y. Wang, "A disturbance observer based sliding mode control for a class of underactuated robotic system with mismatched uncertainties," *IEEE Transactions on Automatic Control*, vol. 64, no. 6, pp. 2480–2487, 2019.

[91] B. Lu, Y. Fang, and N. Sun, "Continuous sliding mode control strategy for a class of nonlinear underactuated systems," *IEEE Transactions on Automatic Control*, vol. 63, no. 10, pp. 3471–3478, 2018.

[92] E. Kayacan and R. Maslim, "Type-2 fuzzy logic trajectory tracking control of quadrotor vtol aircraft with elliptic membership functions," *IEEE/ASME Transactions on Mechatronics*, vol. 22, no. 1, pp. 339–348, 2017.

[93] J. Ghommam and M. Saad, "Adaptive leader–follower formation control of underactuated surface vessels under asymmetric range and bearing constraints," *IEEE Transactions on Vehicular Technology*, vol. 67, no. 2, pp. 852–865, 2018.

[94] K. D. Do, Z. P. Jiang, and J. Pan, "Underactuated ship global tracking under relaxed conditions," *IEEE Transactions on Automatic Control*, vol. 47, no. 9, pp. 1529–1536, 2002.

[95] A. D. Ames, S. Coogan, M. Egerstedt, G. Notomista, K. Sreenath, and P. Tabuada, "Control barrier functions: Theory and applications," in *2019 18th European Control Conference (ECC)*, 2019, pp. 3420–3431.

[96] S. Kolathaya and A. D. Ames, "Input-to-state safety with control barrier functions," *IEEE Control Systems Letters*, vol. 3, no. 1, pp. 108 –113, 2019.

[97] J. Montoya–Cháirez, V. Santibáñez, and J. Moreno–Valenzuela, “Adaptive control schemes applied to a control moment gyroscope of 2 degrees of freedom,” *Mechatronics*, vol. 57, pp. 73 –85, 2019.

[98] H. Yu, T. C. Yang, D. Rigas, and B. V. Jayawant, “Modelling and control of magnetic suspension systems,” in *Proceedings of the International Conference on Control Applications*, vol. 2, 2002, 944–949 vol.2.

[99] Y. Tan, J. Chang, and H. Tan, “Adaptive backstepping control and friction compensation for ac servo with inertia and load uncertainties,” *IEEE Transactions on Industrial Electronics*, vol. 50, no. 5, pp. 944–952, 2003.

[100] E. D. Sontag, *Input to State Stability: Basic Concepts and Results*. Springer Berlin Heidelberg, 2008, pp. 163–220.

[101] S. N. Yadukumar, “Input to state stabilizing control lyapunov functions for hybrid systems,” Ph.D. dissertation, Georgia Institute of Technology, 2016.

[102] R. M. Sanner and J. E. Slotine, “Gaussian networks for direct adaptive control,” *IEEE Transactions on Neural Networks*, vol. 3, no. 6, pp. 837–863, 1992.

[103] Z. Bell, A. Parikh, J. Nezvadovitz, and W. E. Dixon, “Adaptive control of a surface marine craft with parameter identification using integral concurrent learning,” in *2016 IEEE 55th Conference on Decision and Control (CDC)*, 2016, pp. 389–394.

[104] P. Ioannou and P. Kokotovic, *Adaptive systems with reduced models*. New York: Springer-Verlag, 1983.

[105] G. Tao, *Adaptive Control Design and Analysis*. Wiley, New York, 2003.

[106] M. Spong, S. Hutchinson, and M. Vidyasagar, *Robot Modeling and Control*. Wiley, 2005.

[107] L. Wang, E. A. Theodorou, and M. Egerstedt, “Safe learning of quadrotor dynamics using barrier certificates,” in *2018 IEEE International Conference on Robotics and Automation (ICRA)*, 2018, pp. 2460 –2465.

[108] R. Takano, H. Oyama, and M. Yamakita, “Application of robust control barrier function with stochastic disturbance model for discrete time systems,” *IFAC-PapersOnLine*, vol. 51, no. 31, pp. 46 –51, 2018, 5th IFAC Conference on Engine and Powertrain Control, Simulation and Modeling E-COSM 2018.

[109] Q. Nguyen and K. Sreenath, “Exponential control barrier functions for enforcing high relative-degree safety-critical constraints,” in *2016 American Control Conference (ACC)*, 2016, pp. 322 –328.

[110] M. Mühlegg, G. Chowdhary, and E. Johnson, "Concurrent learning adaptive control of linear systems with noisy measurements," in *AIAA Guidance, Navigation, and Control Conference*, 2012, pp. 1 –13.

[111] R. Kamalapurkar, B. Reish, G. Chowdhary, and W. E. Dixon, "Concurrent learning for parameter estimation using dynamic state-derivative estimators," *IEEE Transactions on Automatic Control*, vol. 62, no. 7, pp. 3594 –3601, 2017.